Organostibonates: Synthesis, Reactivity Studies and Investigating the Ligating Behavior of Organostibonate Pro-ligands towards Transition metals and Lanthanides

A Thesis
Submitted for the degree of
DOCTOR OF PHILOSOPHY

by

UPPARA UGANDHAR

(11CHPH05)

School of Chemistry
University of Hyderabad
Hyderabad 500 046
Telangana
India

December, 2020

This work is dedicated to

My Parents and My Son (Gautham)

"LIFE and TIME are the world's best teachers. LIFE teaches us to make good usage of TIME and TIME teaches us the value of LIFE"

Dr. A. P. J. Abdul Kalam

DECLARATION

I hereby declare that the matter embodied in the thesis entitled "***Organostibonates: Synthesis, Reactivity Studies and Investigating the Ligating Behavior of Organostibonate Pro-ligands towards Transition metals and Lanthanides***" is the result of investigation carried out by me in the School of Chemistry, University of Hyderabad, Hyderabad, India, under the supervision of **Prof. Viswanathan Baskar**.

In keeping with the general practice of reporting scientific observations, due acknowledgements have been made on the basis of the findings of other investigators. Any omission, which might have occurred by oversight or error, is regretted. This research work is free from Plagiarism. I hereby agree that my thesis can be deposited in Shodhganga/INFLIBNET. A report on plagiarism statistics from the University Librarian is enclosed.

V. Baskar

Prof. Viswanathan Baskar

(Supervisor)

V. BASKAR
Professor
School of Chemistry
University of Hyderabad
Hyderabad - 500 046.

U. Ugandhar

Uppara Ugandhar

(11CHPH05)

University of Hyderabad

December, 2020

CERTIFICATE

This is to certify that the thesis entitled "***Organostibonates: Synthesis, Reactivity Studies and Investigating the Ligating Behavior of Organostibonate Pro-ligands towards Transition metals and Lanthanides***" submitted by **Mr. Uppara Ugandhar** bearing registration number **11CHPH05** in partial fulfillment of the requirements for award of Doctor of Philosophy in the School of Chemistry is a bonafide work carried out by him under my supervision and guidance.

This thesis is free from plagiarism and has not been submitted previously in part or in full to this or any other University or Institution for award of any degree or diploma.

Parts of this thesis have been:

A. Published in the following publications:

1. U. Ugandhar and V. Baskar, *Dalton Trans.*, 2016, **45**, 6269.
2. M. S. R. Prabhu, U. Ugandhar and V. Baskar, *Dalton Trans.*, 2016, **45**, 6963.
3. U. Ugandhar, T. Navaneetha, Junaid Ali, S. Mondal, G. Vaitheeswaran and V. Baskar, *Inorg Chem.*, 2020, **59**, 6689.

B. Presented in the following Conferences:

1. Chemfest-2015

Further the student has passed the following courses towards fulfillment of course work Requirement for Ph.D.:

	Course. No	Title	Credits	Pass/Fail
1.	CY-801	Research Proposal	3	Pass
2.	CY-802	Chemistry Pedagogy	3	Pass
2.	CY-805	Instrumental Methods A	3	Pass
3.	CY-806	Instrumental Methods B	3	Pass

Prof. Viswanathan Baskar
(Thesis Supervisor)

V. BASKAR
Professor
School of Chemistry
University of Hyderabad
Hyderabad - 500 046.

Dean
School of Chemistry
University of Hyderabad

Dean
SCHOOL OF CHEMISTRY
University of Hyderabad
Hyderabad-500 046

University of Hyderabad
School of Chemistry
Ph. D. Coursework details

Name of the candidate: Ugandhar U

Name of the Supervisor: Dr. V. Bhaskar

Registration number: 11CHPH05

Course details:

Name of the course	Credits	Grade
1. CY-801 Research Proposal	3	B
2. CY-802 Chemistry Pedagogy	3	B+
3. CY-805 Instrumental Methods A	3	C
4. CY-806 Instrumental Methods B	3	C

Final Result: **Passed**

Dean

School of Chemistry

Dean
SCHOOL OF CHEMISTRY
University of Hyderabad
Hyderabad-500 046.

ACKNOWLEDGEMENT

The work presented in this thesis would not have been possible without my close association with many people. I take this opportunity to extend my sincere gratitude and appreciation to all those who made this Ph. D thesis possible.

First and foremost, I would like to extend my sincere gratitude to my research supervisor Prof. Viswanathan Baskar for introducing me to this exciting and fascinating field of science for his dedicated help, inspiration, advice, encouragement and constant support throughout my Ph. D tenure. He gave me moral support and guidance during my de registration time without his support I could not complete my de registration. His enthusiasm, integral view on research and providing high quality work, has made a deep impression on me. During our course of interaction in Ph. D course time, I have learnt extensively from him. I owe him lots of gratitude for having me shown this way of research. I am really glad to be associated with a person like Prof. Viswanathan Baskar in my life.

I would like to thank the former and present dean(s), School of Chemistry, for providing best research facilities and working atmosphere. I am thankful to all the faculty members of the School of Chemistry for their help, cooperation and encouragement at various stages.

I would like to express my sincere thanks to my doctoral committee members, Prof. K. Muralidharan and Prof. R. Balamurugan for their timely support.

My sincere thanks to all the teachers for their excellent teaching during my master's course. From their inspired and dedicated teaching, I have benefited much in my career. My special thanks to Prof. Samudranil Pal (M.Sc project supervisor), Prof. V. Baskar, Prof. K. C. Kumaraswamy, Prof. K. Muralidharan and Prof T. P. Radhakrishnan for the excellent teaching and inspiration in my M.Sc days.

I also thank all the non-teaching staff of the School of Chemistry for their assistance on various occasions. I would like to acknowledge DST funded National Single Crystal X-ray Diffraction Facility, UGC / UPE for providing the basic requirements and DST/UGC/CSIR for the financial support.

I sincerely thank to my senior labmates Dr. Anand Kumar Jami, Dr. P. V. V. N. Kishore, Dr. Sanathana Raj Prabu, Dr. N. Kumar, Dr. R. Amaleswari, for their generous help and moral support. I also thank to my juniors Dr. Junaid Ali, G. Narsimahulu, Suman Mondal, Navaneetha, Smruti and Calvin their assistance during the tenure of my work is gratefully acknowledged.

I thank all the research scholars of School of Chemistry, University of Hyderabad and friends which includes Dr. Kesav Rao. Dr. Sudheer, Dr. Satyanarayana, Dr. Suresh, Dr. Mohan, Dr. Kondareddy, Dr. Srujana, Dr. Gupta, Dr. Hari, Dr. Nandha Kishore, Dr. Swamy Maloth, Dr. Satheesh Kumar, Dr. Ramakrishna and so many others for the cheerful and enlivening atmosphere they maintained and for making my stay in the campus unforgettable

My special thanks to my M. Sc friends Dr. L. Srinivas Rao, Dr. G. G. K. Murthy, Dr. Anand, Nanaji, V. Satyanarayana, Dr. Y. Gurava Reddy, Swamy Madapa, Dr. A. Rajashekar, Venkateswarlu, Dr. Harinarayana, Srikanth, Dr. Krishna Reddy, Madhubabu, Dr. Suresh, Dr. B. Narasimha Rao and other friends who had made my M. Sc days memorable.

I would like to thankful to my degree classmates and Silver jubilee college friends Naresh, Subbarayudu, Srinivasulu, Nagaraju, Chennakeshava Reddy, Siddeswar, Rafi, Rajashekar, Madhusudhan, Chandh basha, Parushramudu, Jagadeesh, Durga Prasad, Sudhakar and other friends.

I express my heartfelt appreciation to dedicated teachers I got at different stages of my life. I will never forget Sudhakar sir, Prasad rao sir, Venugopal sir, Kiran sir, I still enjoy the happy moments I had with my school mates and college friend's Himam, Samsheer, Rangaswamy, Verabramham, Upendra, Venkataramana, Vali, Ramesh, Dhanunjaya, yellasubbadu, jagadeesh.

My heartfelt gratitude to my college lecture U. Kumara swamy sir who introduce me and inspire me to choose chemistry subject.

I would like to acknowledge to P. Raghurami reddy, P. Srinath reddy and P. Raghunandhan reddy (late) for their help in my initial stage of carrier.

I would like to give my heart felt appreciation to family members Ramya Krishna, Narayana, Beesamma, Laxmipathi, Vamshidhar, Kousalya, Kesav, Jayakrishna, Varun, Somagopal, Padmavathi, Vijaya, Charan, Sanvitha Sri and my special thanks to Devendra (anna) for his help.

Finally, I am gratefully indebted from the bottom of my heart to my parents **Shri. U. Sreeramulu** garu & Smt. **U. Mangamma** garu, without their sacrifice and mental support I would not have reached up to this stage. The way I grew up, the values I imbibed, the education I received and the person I am now is all of them.

I heartily thank my beloved brother **Dr. U. Venkataramudu** (ramu) who always inspires me for his scientific knowledge and he always support me in my Ph.D life. My special thanks to my sister U. Ramadevi (Susheela) whose unconditional love and affection has always been my strength.

I owe my deepest gratitude towards my wife **U. Mounika** (moni) for eternal support and understanding of my goals and aspirations. Her infallible love and support has always been my strength. Her patience and sacrifice will remain my inspiration throughout my life.

I am gratefully thanks to god for giving me such a cute and lovable son **U. Nandha Gautham**, he always gives me happiness when I am in stress and he has always been my strength.

I gratefully acknowledge to Council of Scientific and Industrial Research (CSIR) for providing me financial support and School of Chemistry, University of Hyderabad for providing best and world class facilities and peaceful environment to achieve my Ph. D degree.

University of Hyderabad **U. Ugandhar**

December, 2020

Name of the Student	**Uppara Ugandhar**
Roll Number	**11CHPH05**
School	**School of Chemistry**
Name of Thesis Supervisor	**Prof. V. Baskar**
Thesis title	***Organostibonates: Synthesis, Reactivity Studies and Investigating the Ligating Behavior of Organostibonate Pro-ligands towards Transition metals and Lanthanides***

SYNOPSIS

This thesis entitled "***Organostibonates: Synthesis, Reactivity Studies and Investigating the Ligating Behavior of Organostibonate Pro-ligands towards Transition metals and Lanthanides***". It is divided into five chapters and details of each chapter are given below

Chapter 1

Introduction

In the introduction chapter, detailed study of the historical background and synthesis of organostibonic acids are given in detail.Synthesis and structural characterization of organostibonic acids with main group elements, transition metals and different bases have also studied. Biological applications of organostibonic acids and some antimony compounds have been discussed in detail. Brief literature survey of organoantimony compounds and their reactivity studies have been discussed. In addition, this chapter also includes brief introduction to polyoxometalate(POMs) chemistry and the synthesis and structural properties of few literature reported antimony polyoxometalates.

Chapter 2

Monoorganoantimony (V) Phosphonates and PhosphoSelininates

The chapter deals with the synthesis and structural characterization of molecular oxo-hydroxo clusters based on monoorganoantimony(V) motifs which has been assembled by reactions of arylstibonic acids with protic ligands like *t*-butylphosphonic acid, phenylphosphonic acid,

phenylseleninic acid and *t*-butylsilanetriol. Interestingly reaction of arylstibonic acid with *t*-butylsilanetriol has led to the isolation of organoantimony(V) based molecular triangle stabilized by siloxane frameworks. Single crystal X-ray structural elucidation revealed the formation of $[(p\text{-iPr-}C_6H_4Sb)_4(OH)_4(t\text{-}BuPO_3)_6]$(**2.1**), $[(p\text{-}t\text{-Bu-}C_6H_4Sb)_4(O)_2(PhPO_3)_4(PhPO_3H)_4]$(**2.2**),$[(p\text{-iPr-}C_6H_4Sb)_4(O)_4(PhSeO_2)_2(t\text{-}BuPO_3)_4(t\text{-}BuPO_3H_2)_2]$(**2.3**), $[(p\text{-Me-}C_6H_4Sb)_4(O)_4(PhSeO_2)_2(t\text{-}BuPO_3)_4(t\text{-}BuPO_3H_2)_2]$(**2.4**) $[(p\text{-}t\text{-Bu-}C_6H_4Sb)_2(O)(PhSeO_2)_2(t\text{-}BuPO_3H)_4]$ (**2.5**) and $[(p\text{-iPr-}C_6H_4Sb)_3\{(t\text{-}BuSiO_2)_4(t\text{-}BuSiO_2OH)_2\}(\mu_3\text{-}O)(\mu\text{-}OH)_2]$ (**2.6**) respectively. ESI-MS studies revealed that the clusters maintain their structural integrity in solution too. Solution NMR studies (^1H, ^{31}P, ^{77}Se and ^{29}Si) show spectral patterns which correlates well with the observed solid state structures of **2.1-2.6**.

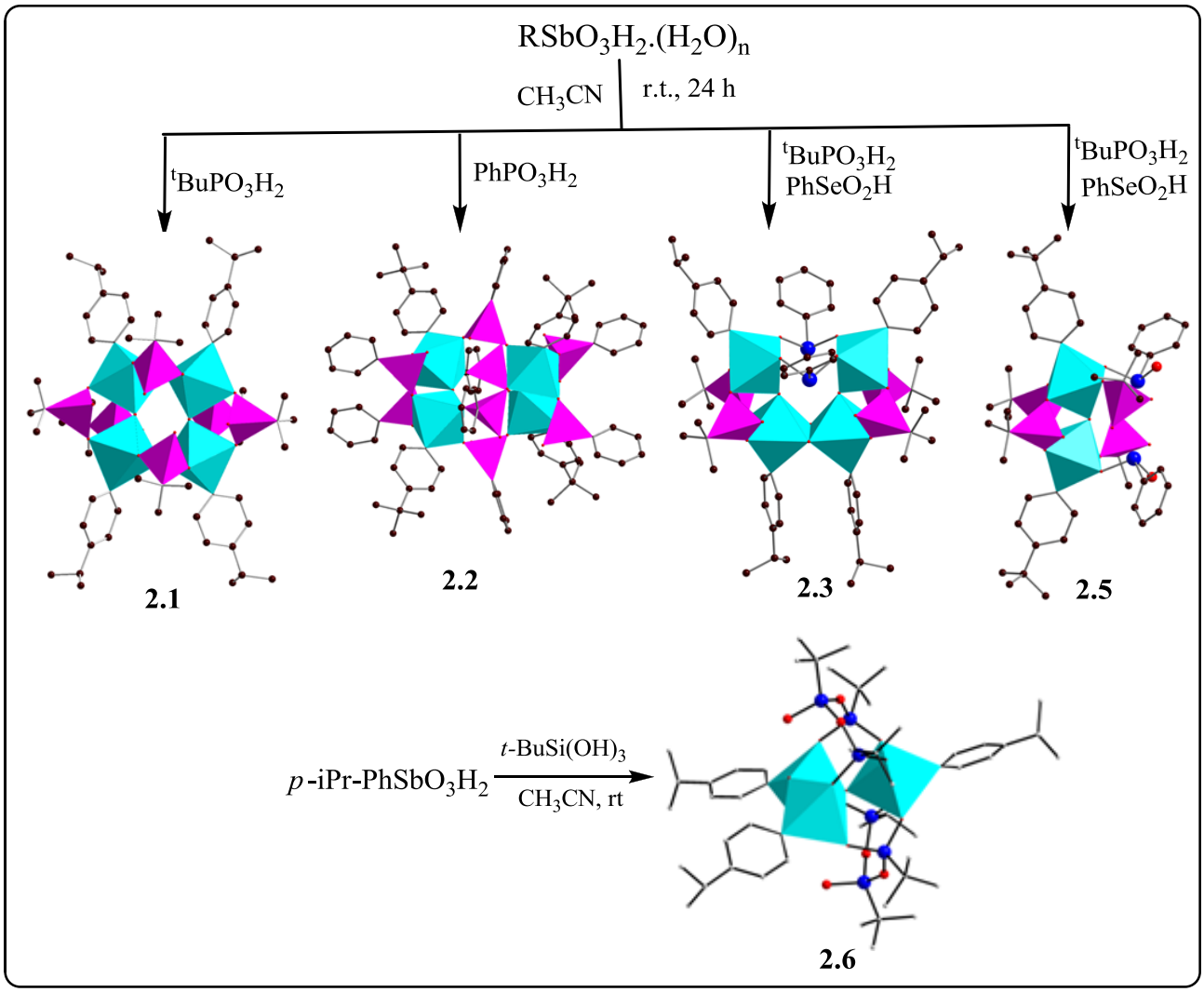

Figure 1: Synthetic scheme and solid state structures of Organostibonic acid- Phosphonate and phosphoselininatecomplexes

Chapter 3

Base Induced Assembly of Hexa-, Undeca- and TetradecanuclearPolyoxostibonates

The chapter deals with the isolation and structural characterization of novel organoantimony(V) based polyoxometalates. $(RSb)_4(OH)_4(t\text{-}BuPO_3)_6$ and $(RSb)_2(O)(t\text{-}BuPO_3H)_6$ independently in the presence of pyridine as a base under solvothermal conditions which affords hexanuclearorganoantimonate clusters $[(RSb)_6(\mu_3\text{-}O)_2(\mu_2\text{-}O)_6(t\text{-}BuPO_3)_4]$, [where R = *p*-iPr-$C_6H_4$ (**3.1**) and *p*-Cl-C_6H_4 (**3.2**)]. Further, reaction of organostibonic acids with diorganophosphinic acid (diclyclohexyl, diphenyl phosphinic acid) in presence of a tetraethyl ammonium hydroxide affords colorless products which on structural characterization reveals the formation of undecanuclear and tetradecanuclearpolyoxostibonates stabilized by phosphinates binding in the peripheral part of the POMs $Na_5(p\text{-}MeC_6H_4Sb)_{11}(O)_{28}\{(C_6H_{11})_2PO_2\}_2$ (**3.3**) and $Na_2(p\text{-}iPr\text{-}C_6H_4Sb)_{14}(O)_{28}(Ph_2PO_2)_8$ (**3.4**).

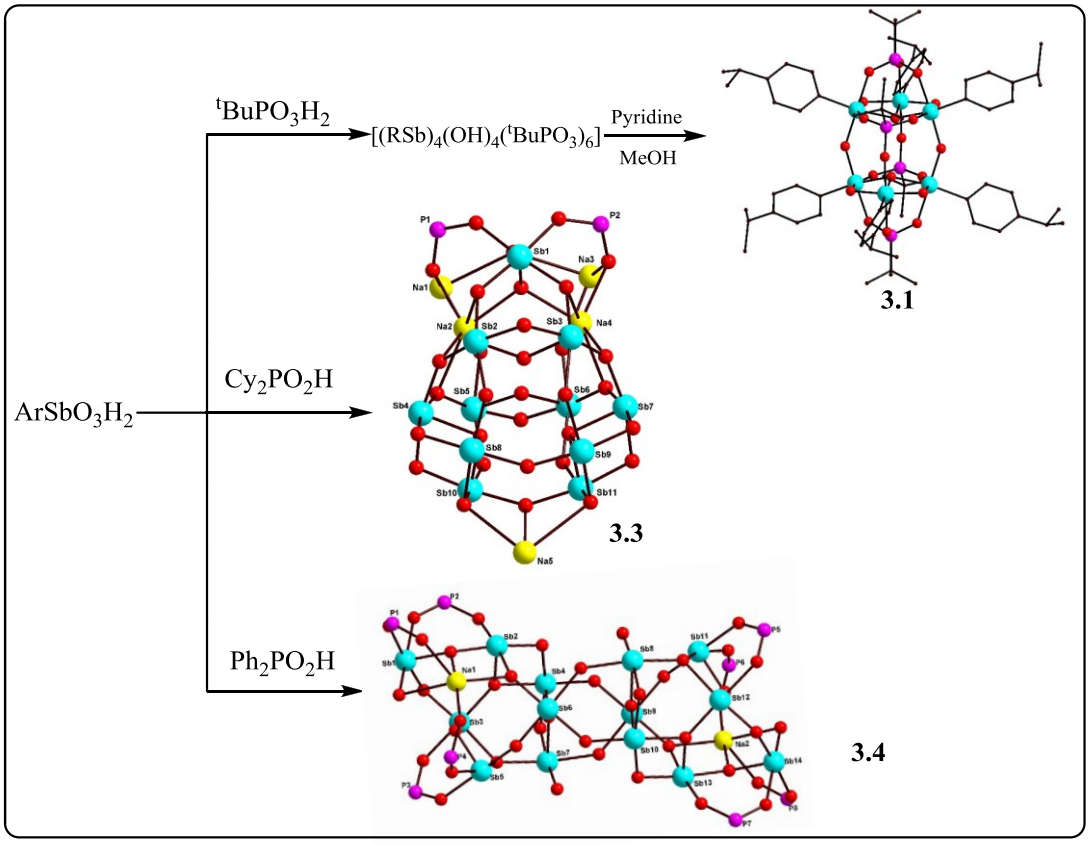

Figure 2: Synthetic scheme and solid state structures of Organostibonic- phosphinate complexes.

Chapter 4

Transition metal stibonate-phsophonate clusters:

Isolation of M_2Sb_4 (M= Mn, Co, Ni & Cu) Clusters

The chapter deals with the synthesis and structural characterization of arylstibonic acid-transition metal based molecular phosphonate clusters.Arylstibonic acid phosphonate pro-ligand, [(*p*-iPr-$C_6H_4Sb)_4(OH)_4$(*t*-$BuPO_3)_6$] was synthesized by condensation reaction of *p*-isopropylphenylstibonic acid ($ArSbO_3H_2$) with *t*-butylphosphonic acid. It contains four antimony centers forms a puckered eight-member Sb_4O_4 core held together by six *t*-butyl phosphonates. Reaction of transition metal acetate with antimonate-phosphonate pro-ligand [(*p*-iPr-$C_6H_4Sb)_4(OH)_4$(*t*-$BuPO_3)_6$] under solvothermal conditions in methanol, in the presence of pyridine as a base produced novel arylstibonic acid-transition metal based phosphonate clusters (compounds **4.1-4.4**). Single crystal structural elucidation revealed the formation of [M_2((*p*-iPr-$C_6H_4Sb)_4(\mu_3$-$O)_2(\mu_2$-$O)_2(\mu_2$-$OCH_3)_4$(*t*-$BuPO_3)_4(Py)_2.2CH_3OH$] {M= Mn(**4.1**), Co(**4.2**), Ni(**4.3**) and Cu(**4.4**)}.

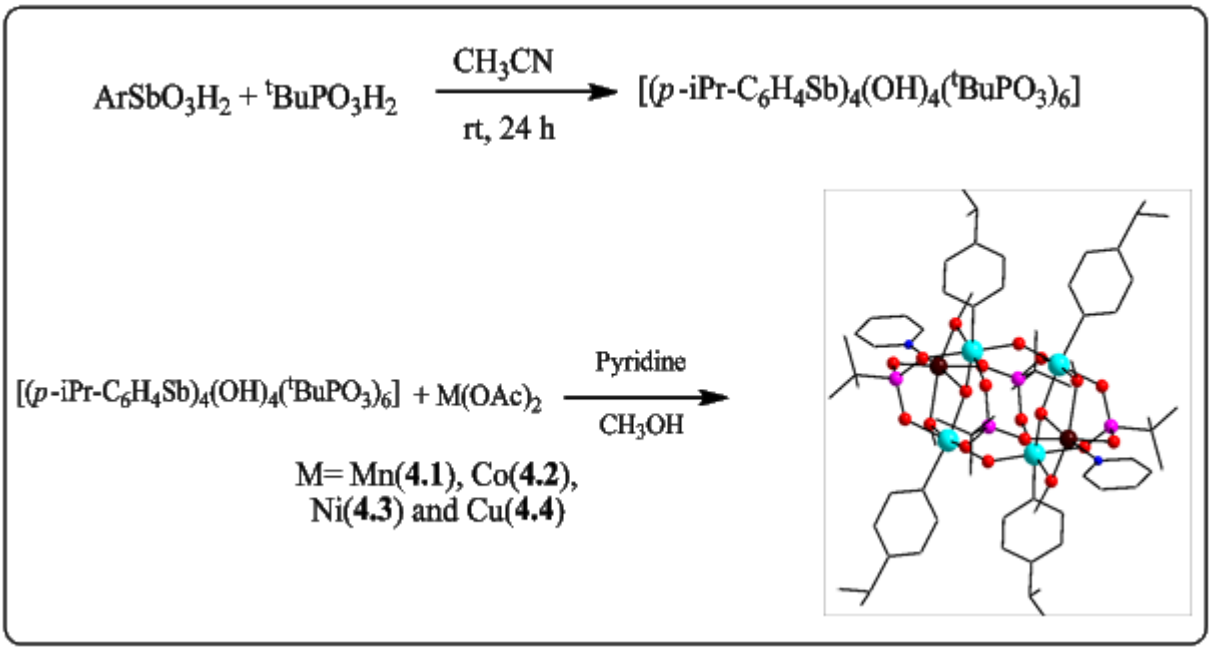

Figure 3: Synthetic scheme and solid state structures of Transition metal stibonate-phsophonate clusters

Chapter 5

Stibonate-Phosphonate Cluster Stabilizing Lanthanide ions (Ln = Pr, Gd & Dy)

The chapter deals with the synthesis, structures and magnetic properties of a family of lanthanide complexes containing antimonate-phosphonate ligands.Arylstibonic acid phosphonate pro-ligand, $[(p\text{-iPr-}C_6H_4Sb)_4(OH)_4(t\text{-}BuPO_3)_6]$ was synthesized by condensation reaction of *p*-isopropylphenylstibonic acid ($ArSbO_3H_2$) with *t*-butylphosphonic acid. Reaction of hydrated lanthanide acetate salt with antimonate-phosphonate pro-ligand $[(p\text{-iPr-}C_6H_4Sb)_4(OH)_4(t\text{-}BuPO_3)_6]$ under solvothermal conditions in methanol, in the presence of pyridine as a base produced two families of novel arylstibonic acid-lanthanide based metal phosphonate clusters. Single crystal structural elucidation revealed the formation of $[Pr_4(ArSb)_4(\mu_4\text{-}O)_2(\mu_2\text{-}OH)_2(\mu_2\text{-}OCH_3)_8(OCH_3)_4(t\text{-}BuPO_3H)_6(t\text{-}BuPO_3)_4]$ (**5.1**), $[Gd_4(ArSb)_4(\mu_4\text{-}O)_2(\mu_2\text{-}OH)_2(\mu_2\text{-}OCH_3)_8(OCH_3)_4(t\text{-}BuPO_3H)_6(t\text{-}BuPO_3)_4]$ (**5.2**) and $[Dy_{12}(ArSb)_{12}(\mu_3\text{-}OH)_6(\mu_2\text{-}OCH_3)_{12}(OCH_3)_{12}(t\text{-}BuPO_3H)_6(t\text{-}BuPO_3)_{18}\{(t\text{-}Bu)_2P_2O_5\}_6]$ (**5.3**). The clusters **5.1** and **5.2** are 1D coordination polymers whose repeating unit possesses tetramer motif. While two lanthanide ions in a tetramer are in eight-coordinate with triangular dodecahedron geometry, the other two antimony centers are in hexa-coordinate with octahedral geometry. In contrast to **5.1** and **5.2**, interestingly **5.3** possess novel twenty-four membered ring-type architecture, consist of six Dy(III) centers which are in eight-coordinate and present in square-antiprism geometry. While the other six Dy(III) centers which are in hexa-coordinate with octahedral geometry. Twelve antimony (V) centers are in hexa-coordinate with octahedral geometry. Interestingly rare di *t*-butylphosphonate $\{(t\text{-}Bu)_2P_2O_5\}$ ligand system is generated *in situ* by self-condensation of two *t*-butylphosphonic acids which help in stabilizing the Dy_{12} cluster. Preliminary magnetic moment studies (Dc and Ac) have been performed and the results are explained in detail.

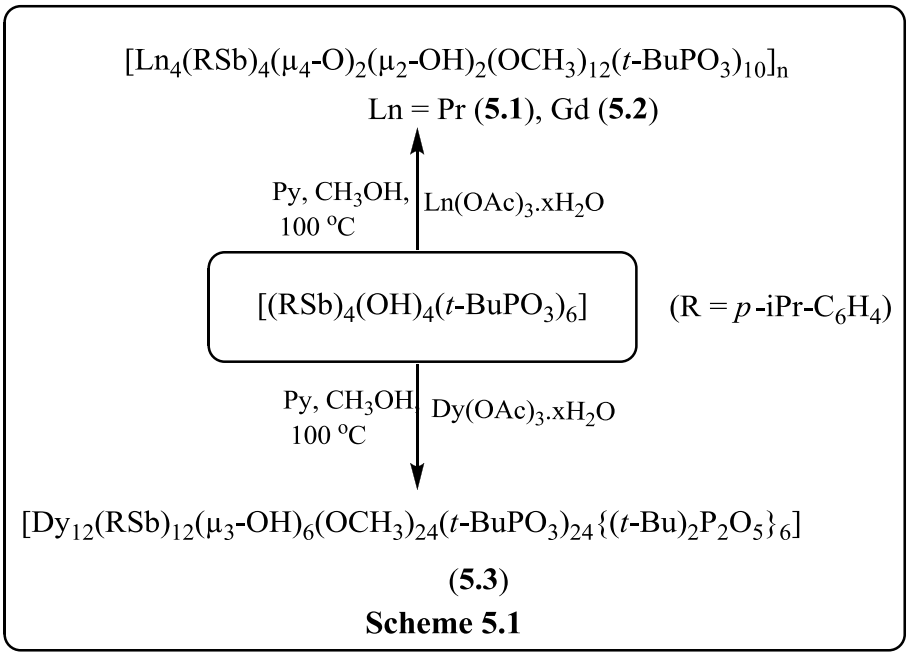

Scheme 5.1

Figure 4**:** Synthetic scheme of Arylstibonic acid-Lanthanide Based Metal Phosphonate Clusters

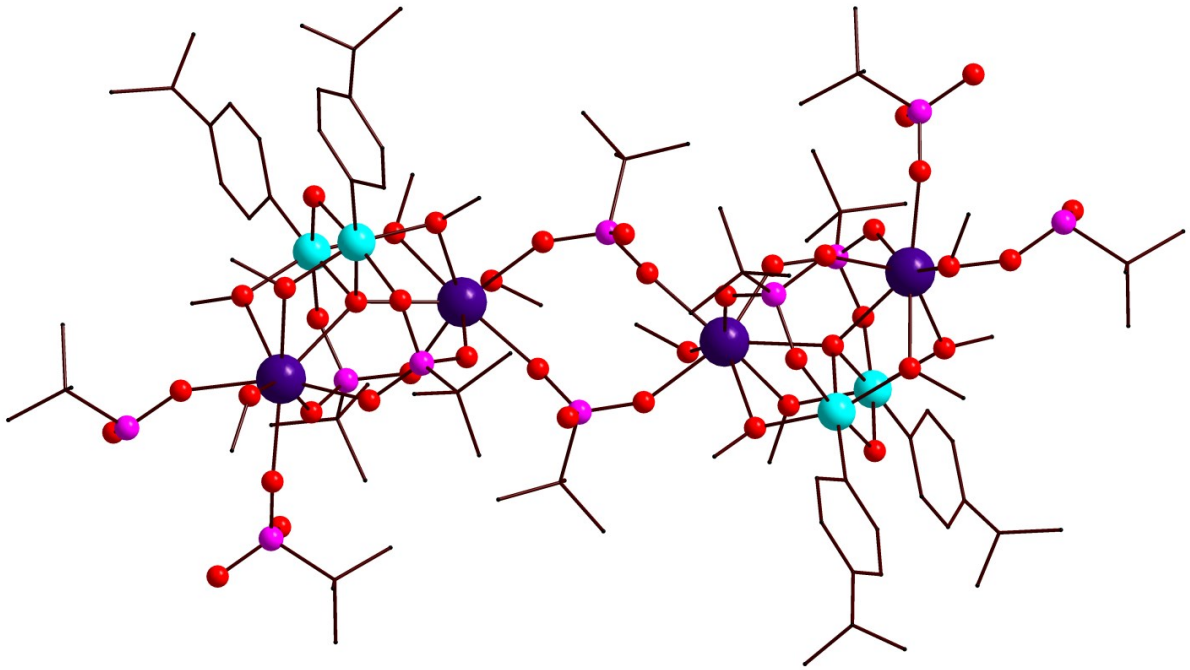

Figure 5: Solid state structure of **5.1**

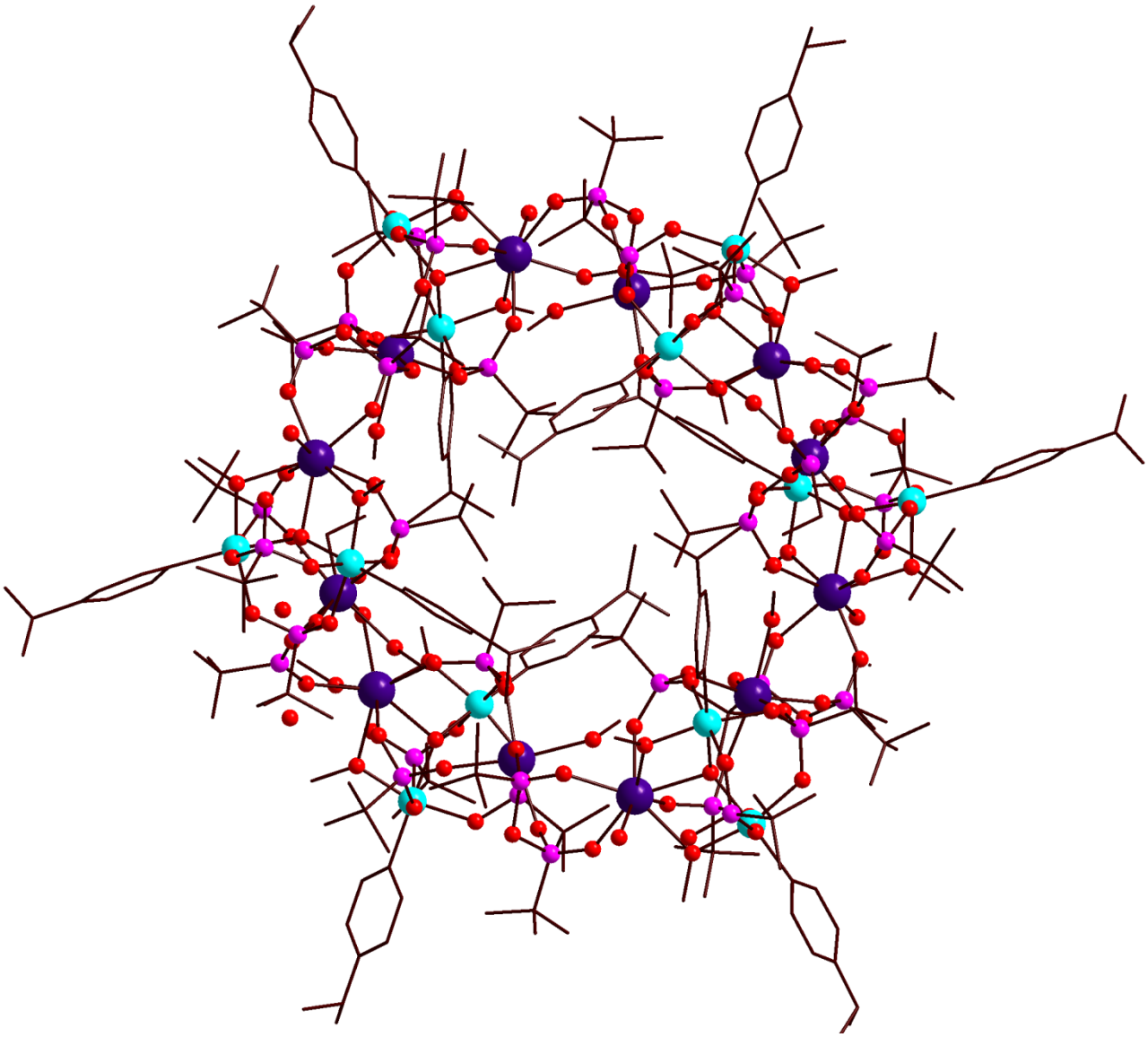

Figure 6: Solid state structure of **5.3**

CONTENTS

Declaration

Certificate

Acknowledgement

Synopsis

Contents

Chapter 1 Page No.

Introduction 1

1.1 General introduction to Antimony 1

1.2 Biological applications of Antimony 3

1.2.1 Biological applications of Arylstibonic acids 4

1.3 Introduction to Organostibonic acids 4

1.3.1 Preparation of organostibonic acids 5

1.3.2 Structure of organostibonic acids 6

1.3.3 Synthesis of first molecular arylstibonic acid 7

1.4 Reactions of arylstibonic acids 8

1.4.1 Arylstibonic acids with H_2SO4 and NaOH 8

1.4.2 Synthesis of reverse-keggin compounds 9

1.4.3 Synthesis of Polyoxostibonates 10-11

1.4.4 Synthesis of organostibonic acid-phosphonic acid pro-ligand 12-14

1.4.5 Reactions of arylstibonic acids with protic ligands 15

1.4.6 Synthesis of Organoantimony(V) Oxido Cubane cluster 16

1.4.7 Synthesis of Oxo-Centered Sb_3O triangle 17

1.4.8 Synthesis of adamantane type structures 18

1.4.9 Synthesis of mixed valent Sb(V)/(III) polyoxostibonates 19

1.5 Organoantimony (V) Compounds 20
1.5.1 Synthesis of organoantimony (V) halides 20
1.5.2 Synthesis of organoantimony(V) Oxides 21
1.6 Reactions of organoantimony(V) compounds 22
1.6.1 Reactions of Ph_3SbCl_2/Ph_2SbCl_3 with acetylacetone 22
1.6.2 Reactions of Ph_3SbCl_2/Ph_2SbCl_3 with Schiff base ligands 23
1.6.3 Reactions of Ph_3SbCl_2/Ph_2SbCl_3 with carboxylic acids 24-26
1.6.4 Reactions of Ph_3SbCl_2/Ph_2SbCl_3 with phosphinic acids 27-28
1.6.5 Reactions of Ph_3SbCl_2/Ph_2SbCl_3 with phenolic pyrazole 29
1.6.6 Reactions of Ph_3SbCl_2/Ph_2SbCl_3 with silane triols and diols 30
1.6.7 Reactions of Ph_3SbCl_2/Ph_2SbCl_3 with diorganotellurium oxides 31
1.6.8 Reaction of triphenylantimony (V) oxide with protic ligands 32-33
1.6.9 Reaction of triphenylantimony (V) oxide with diphenyltellurium oxide 34
1.6.10 Reactions of Ph_2SbCl_3 with silver acetate 35
1.7 Diorganoantimony based μ_4-peroxo complex 35
1.8 Quadruply and Triply bridged organoantimony(V) compounds 36
1.9 Hypervalency in Organoantimony (V) compounds 37
1.9.1 Synthesis of hypervalent antimoniated Schiff base 38
1.10 Polyoxometalates (POMs) 39
1.10.1 Synthesis of first crystalline organostibonic molybdate 40
1.10.2 Synthesis of Polyantimonate 41
1.10.3 Synthesis of Lanthanide Antimony(III) Oxohalides 42
1.10.4 Synthesis of Sb(V), Sb(V/III) and Sb(III) functionalized POMs 42-44
1.11 Motivation of present work 45
1.12 References 46-56

Chapter 2

Monoorganoantimony (V) Phosphonates and PhosphoSelininates

2.1 Introduction	59
2.2 Experimental Section	60
2.2.1 General Information	60
2.2.2 Instrumentation	60
2.2.3 Synthetic procedure for compounds 2.1-2.6	61
2.3 Results and Discussions	63-70
2.4 Conclusion	70
Crystallographic tables	71
2.5 Analytical and Spectroscopic data	77-85
2.6 References	86-88

Chapter 3

Base Induced Assembly of Hexa-, Undeca- and Tetradecanuclear Polyoxostibonates

3.1 Introduction	91
3..2 Experimental Section	92
3.2.1 General Information	92
3..2.2 Instrumentation	92
3.2.3a Synthetic procedure for compounds 3.1-3.2	93
3.2.3b Synthetic procedure for compounds 3.3-3.4	94
3.3 Results and Discussions	95-101
3.4 Conclusion	102
Crystallographic tables	103
3.5 Analytical and Spectroscopic data	108-112
3.6 References	113-116

Chapter 4

Transition metal stibonate-phsophonate clusters: Isolation of M_2Sb_4 (M= Mn, Co, Ni & Cu) Clusters

4.1 Introduction	119
4.2 Experimental Section	120
4.2.1 General Information	120
4.2.2 Instrumentation	120
4.2.3 Synthetic procedure for compounds 4.1-4.4	121
4.3 Results and Discussions	122-126
4.4 Conclusion	127
Crystallographic tables	128
4.5 Analytical and Spectroscopic data	132-133
4.6 References	134-137

Chapter 5

A First Example on Arylstibonic acid-Lanthanide Based Metal Phosphonate Clusters

5.1 Introduction	139
5.2 Experimental Section	141
5.2.1 General Information	141
5.2.2 Instrumentation	141
5.2.3 Synthetic procedure for compounds 5.1-5.3	142
5.3 Results and Discussions	142-149
5.4 Magnetic studies	150-151
5.5 Conclusion	151
Crystallographic tables	154
5.6 Analytical and Spectroscopic data	158-159
5.7 References	160-163

Abbreviations

i-Pr	Isopropyl
t-Bu	Tertiary butyl
Ph	Phenyl
Py	Pyridine
Cy	Cyclohexyl
POMs	Polyoxometalates
SMM	Single molecular magnet
Acac	Acetyl acetone
Mes	Mesityl
ACN	Acetonitrile
DCM	Dichloromethane
8-HQ	8-Hydroxy quinolone
3,5 DMPz	3, 5 dimethyl pyrazol
ESI-MS	Electron spray ionization mass spectrometry
XRD	X-ray diffraction
IR	Infra-Red Spectroscopy
NMR	Nuclear Magnetic Resonance Spectroscopy

INTRODUCTION

Chapter 1

The thesis work is mainly focused on the synthesis of soluble organostibonic acids and their reactivity studies towards protic ligands, main group elements, transition metals and lanthanide metals. Hence introduction chapter mainly focuses on organoantimony compounds and their biological applications, synthesis of different soluble organostibonic acids and their reactivity studies, a brief literature survey of various organoantimony(V) compounds and polyoxometalates (POMs).

1.1 Introduction:

Antimony (Sb) is a silver-white, brittle semimetal with flaky texture and an atomic number of 51. Antimony belongs to the nitrogen family [group 15 (VA) of periodic table], having electronegativity is 2.5, specific gravity is 6.68 and a melting point is 630.5 °C. Antimony has two stable isotopes ^{121}Sb and ^{123}Sb, with a natural abundance of 57.63 and 42.64 respectively. The periodic symbol of Sb has been derived from its Latin name *stibium*. Antimony generally behaves as a semimetal because its pure form is not malleable and shiny like true metals. Antimony hardness is 3 on Mohs scale, which is too soft to make hard objects, coins of antimony were issued in China province but due to poor durability soon minting was discontinued. Alchemy is a field of study where ancient scientists believed that antimony might help convert a lead into gold. The abundance of antimony is about 0.2 ppm in the earth's crust.[1] The antimony name was derived from the Greek words anti (opposed) and monos (solitude). Antimony in nature rarely occurs in its original metal form and it always shows a strong affinity towards sulfur and other metals (Cu, Pb and Ag) to form over 100 minerals. The major mineral of antimony is stibnite (Sb_2S_3) and it is used as a source for metallic antimony. Antimony was also found in lead, silver and copper ores in trace amounts and it was extracted from these ores by the process of smelting. China has a major source for antimony deposits.[2] Stibnite had soft nature, so it was used as black eye makeup in ancient times. Finely grounded stibnite powder is used as a bronzing for metals, black pigment and plaster casts. Antimony trioxides (Sb_2O_3) combine with halogenated particles and reduce the flame's speed, so Sb_2O_3 is used as a flame retardant

materials.[3] Antimony trioxide have been used in adhesives, plastics, decorative foams, textiles and building materials as a flame retardant. Antimony is mixed with lead to form a harder and stronger alloy, used in automobile lead-acid storage batteries, bullets, coverings for cables, tank linings, roofing sheets, chemical pumps and pipes. Its alloys are majorly used in industrial applications such as Babbitt metal (an alloy of Sb, Sn, Cu and Pb) useful as machine bearings due to its soft and slippery nature. With tin, antimony forms alloys such as Britannia metal and Pewter used for making utensils, cups, plates and pitches. Antimony alloy is also used in solder. Antimony has one of the specific characters as it expands when it cools and freezes. Type metal (an alloy of lead, antimony and tin) is used for printing newspapers; here, alloy fills every corner of costing mold used to prepare sharp type for printing. The semiconductor industry uses highly pure antimony (nearly 99.999 pure) in silicon wafers for making infrared detectors and diodes.[4] In nuclear reactors, antimony combine with beryllium and is used as a startup neutron source. Antimony sulfides are used as a combustion supporting material like striking surfaces of safety matches, tracer bullets and manufacture of detonators. Antimony has also been used in ceramics, glass making and as a vulcanizing agent in the rubber industry.[5] Sodium antimonite (NaO_3Sb) is used as a flame retardant to remove bubbles from the glass. The antimony chalcogenide materials (Sb_2S_3, Sb_2Te_3 nano rods, Sb_2Se_3 nano wires) are very interesting and fascinating applications in the field of electronics like in the manufacturing of television, cameras with photoconductor targets, electrochemical hydrogen storage, IR spectroscopy, thermoelectric and optoelectronic devices. For example, Sb_2S_3 has high Li intercalation capacity and Sb_2Se_3 display high electrochemical hydrogen storage.[6]

1.2 Biological applications:

Besides industrial applications, antimony is also widely used in medicine and cosmetics.[7, 8] Various antimony compounds have been used as drugs against pathogens, although several health hazards of these metals are well known. Organoantimony compounds such as sodium stibogluconate (pentostam) and meglumineantimonate (glucantime) have been used to treat leishmaniasis.[11] Intravenous administration of tartar emetic (potassium salt of antimonyl tartrate) has been used to treat kala-azar (visceral leishmaniasis) disease. Sodium salts of antimonyl tartrate were used instead of potassium salt for better results. Brahmachari *et al* synthesized pentavalent antimonial (urea stibamine) in the year 1920. Ehrlich discovers atoxyl or sodium salt

of a *p*-arsanilic acid drug and is used for treating sleeping sickness. Urea stibamine (urea salt of *p*-amino phenylstibonic acid) was a potential agent against kala-azar disease and it was used extensively during the 19th century.[9] Schmidt successfully synthesized stable pentavalent antimonial Solustibosan (sodium antimonyl gluconate) in the year 1936. Solustibosan is stable in water; it can be given intravenously, intramuscularly and subcutaneously.[10] Glucantime and Pentostam are two pentavalent antimonial drugs available commercially and they are used for treating both visceral and cutaneous leishmaniasis.[11] Potassium antimonyl tartrate [$K_2Sb_2(C_4H_2O_6)_2$] was previously used as a nauseant and expectorant; due to compound toxicity, it has been abandoned. Trivalent antimony (Sb^{3+}) is more toxic than pentavalent antimony (Sb^{5+}).[11b]

Organoantimony compounds exhibit significant anti-microbial activities[12] and also anti-tumor activities. Similar to cis-platin, some organoantimony compounds exhibit cytostatic activity.[13] However; the biological toxicity of Sb is much less when compared with Pt and Pd based anti-cancer substances. R. Kant *et al* reported organoantimony (III) amides may be used for the development of new drugs and also shows promising anti-cancer and anti-microbial activity.[14] T. Kaji *et al* reported selective cytotoxicity of vascular endothelial cells, which diminished when bismuth atom was displaced by antimony atom in tris[2-(N, N, dimethyl aminomethyl)phenyl] bismuthane TDPBi.[15] The group also investigated tris(pentafluorophenyl)stibane induced gene expression of MT-1A and MT-2A; they are subisoforms of Metallothionine (MT) in bovine endothelial cells.[16] Fahami *et al* synthesized various orgnoantimony compounds containing Schiff base ligands. These compounds show promising anti-microbial and anti-fungal activities.[17] U. Kortz *et al* investigated the structure-bioactivity relationship of three dimeric phenylantimony(III) heteropolytungstoarsenate. These polyoxoanions show significant anti-bacterial activity. The effective inhibitory bacterial activity of these polyoxoanions depends on the number of incorporated {$PhSb^{III}$} groups.[18] The group also reported three discrete organoantimony(III) heteropolytungstates might act as potential anti-microbial agents. It was suggested that by tuning the structure-bioactivity relationship of these polyoxoanions, they can be used as a biomedical agents. Besides biological inhibitor activity (anti-bacterial, antiviral, anti-tumor), these polyoxoanions can be used as a co-ligands for large biomolecules in crystallization.[19]

1.2.1 Biological applications of arylstibonic acids:

Organostibonic acid had a specific property to prevent basic leucine zipper (B-ZIP) proteins to DNA binding; hence organostibonic acids have been used as valuable anti-cancer agents. Charles Vinson *et al* investigated 25 different arylstibonic acids for their capability to restrict DNA binding of B-ZIP proteins.[20] Stivers *et al* reported various organostibonic acids for their effects on plasmid supercoil relaxation catalyzed by Human topoisomerase IB (*hTopo*). It was reported that arylstibonic acids show selectivity towards topoisomerase I inhibition in human beings and poxvirus (*vTopo*). They suggested that arylstibonic acids can be used as small molecules for elucidating the cellular functions of *hTopo*.[21] Arylstibonic acids are structurally similar to phosphotyrosine side chains in protein; hence sulphonic acid and carboxylic acid substituted arylstibonic acids were identified as potential inhibitors of the protein tyrosine phosphatase PTP-β and potential Cdc25 phosphatase inhibitors.[22] In addition, arylstibonic acids also inhibit CCAAT-enhancer-binding proteins.[23] The anti-HIV activity of arylstibonic acids has been reported by Shizuko Sei.[24] J. C. McKelvie *et al* investigated various arylstibonic acids for their capability to prevent *Yersinia pestis* DNA adenine methyltransferase (Dam) *in vitro* and they identified 4-stibono-benzenesulfonic acid as the most active organostibonic acid.[25]

1.3 Organostibonic acids:

The chemistry of organostibonic acids gained significant attention in recent years due to their biological activity.[20-25] Organostibonic acids act as potential anti-cancer agents, which inhibiting DNA binding[20] and also have been used as anti-microbial agents.[25] In the year 1910, Bart reaction was used to synthesize organoarsenic acids in which aromatic diazo compound reacts with arsenic trioxide (As_2O_3) in the presence of basic conditions to form organoarsenic acids with the spontaneous evolution of nitrogen gas. The similar method has been used for the preparation of organostibonic acids.[26] Further, Schmidt, Dunning and Reid modified this method to get better yield and purity of the organostibonic acids.[27] In the year 1940, Scheller prepared organoarsenic acids by adopting major changes to Bart reaction to improve the product's yield. In this method, aromatic amine was dissolved in an organic solvent and diazotize with concentrated aqueous sodium nitrite in the presence of arsenic trichloride. To assist the reaction cuprous salt Cu(I) catalyst and heat were also used during the course of reaction. Doak and Steinman synthesized organostibonic acids by using the Scheller reaction.[28] When compared to

arylstibonic acids, aliphatic stibonic acids are virtually nonexistent except for methanestibonic acid which has been reported.[29]

1.3.1 Preparation of organostibonic acids:

The para-substituted aniline (0.05 mol) was dissolved in ethanol (125 mL) and taken in a beaker with a magnetic stirrer surrounded by an ice bath. Concentrated sulfuric acid (0.05 mmol) and $SbCl_3$ (0.05 mol) were added after completely dissolved, the pink-colored thick solution formed after stirred for 30 min. A sodium nitrite (0.05 mol) solution was added to initiate diazotization, resulting in the formation of a thick red color solution. The mixture was stirred continuously for half an hour, then cuprous bromide (0.05 mol) catalyst was added (**Scheme 1**). To remove nitrogen gas the mixture was heated for some time. The obtained organostibonic acid was collected with the help of Buchner funnel, washed with distilled water and air-dried. The obtained organostibonic acid contains antimony trioxide as an impurity because arylstibonic acids are generally insoluble in water and common organic solvents; conventional recrystallization methods were not applicable. To purify the product, the crude stibonic acid was dissolved in concentrated hydrochloric acid (45 mL) and then pyridinium hydrochloride solution (5mL pyridine in 20 mL of concentrated HCl) was added under ice-bath condition. It turns to brown colored jelly type solid immediately; at this stage, the residue was kept for 12 h without disturbing. The jelly-like solid was removed by scratching and dried, after which it becomes brown colored powder. The obtained compound was collected on a Buchner funnel, washed with Conc., HCl, and dried. To a dilute sodium carbonate solution (1400 mL of 1% (w/v) solution) the dried compound was added and stirred for four hours then filtered. To this filtrate dilute 10%HCl was added dropwise with continuous stirring. The pure organostibonic acid was collected by filtration and washed with water and dilute HCl. This method is only applicable for the para and meta substituted anilines, not to ortho-substituted anilines. We have been successfully synthesized *p*-isopropylphenylstibonic acid, *p*-(*t*-butyl) phenylstibonic acid and *p*-2-butylphenylstibonic acid by following the procedure. When compared to earlier reported *p*-halostibonic acids, all these arylstibonic acids are readily dissolved in common organic solvents.

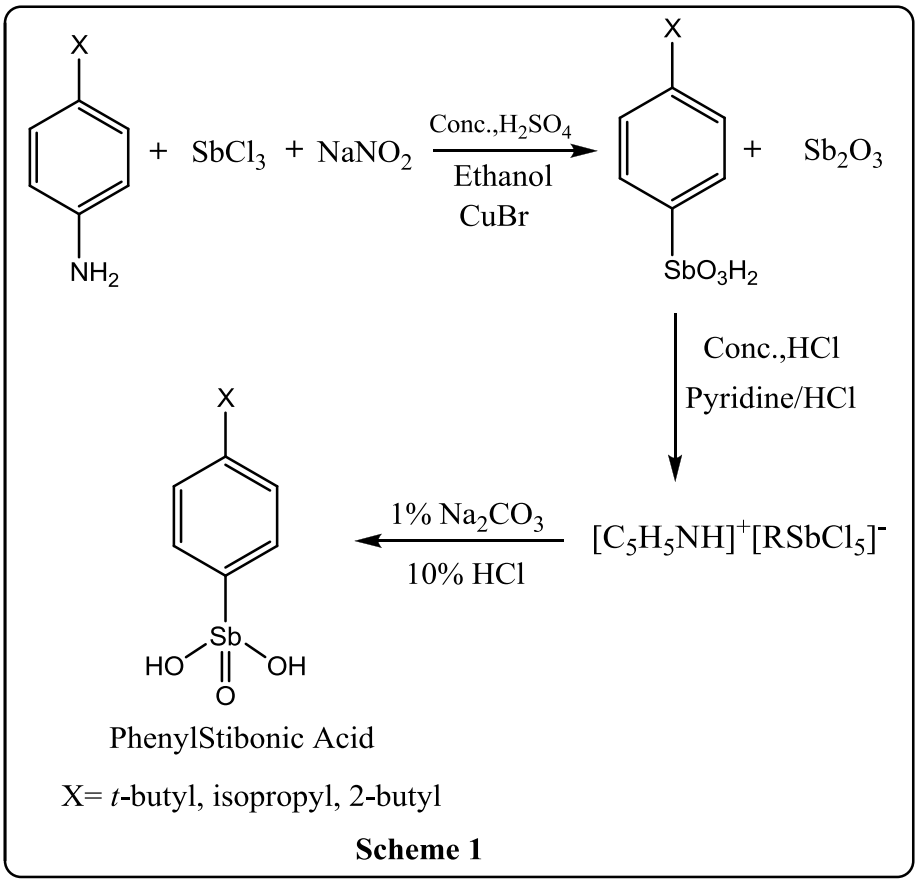

Scheme 1

1.3.2 Structure of Organostibonic acids:

The synthesis of organostibonic acids has known since last 100 years. Until now, the exact molecular structure of arylstibonic acid is unknown and the matter was a considerable debate. This has been due to their insoluble nature in water and organic solvents, decomposition on heating and hence lacks a distinct melting point. Due to different physical properties when compared to corresponding arsenic acids, Schmidt proposed arylstibonic acid exists as a trimer in solid state but in the alkaline condition, the trimer would dissociate into the monomeric form (**Figure 1**).[30] Depending on the preparation methods, different arylstibonic acids with a degree of associated water may vary. Based on molecular weight determinations, Macallum proposed a monomeric structure of organostibonic acid.[31] Schmidt's trimer conclusion was generally preferred over Macallum monomeric structure. Based on cryoscopic molecular weight determinations in benzene, acetic acid and formic acid, Doak suggested that arylstibonic acids exist as high molecular weight polymeric species $(ArSbO_3H_2)x.(H_2O)_n$ linked by hydrogen bonding. It was also suggested that arylstibonic acids behaved as pseudo-acids.[27] Based on ^{121}Sb

Mössbauer study, Bowen *et al* concluded that around antimony trigonal bipyramid geometry was present with bridging oxygen atoms are in epical positions.[32]

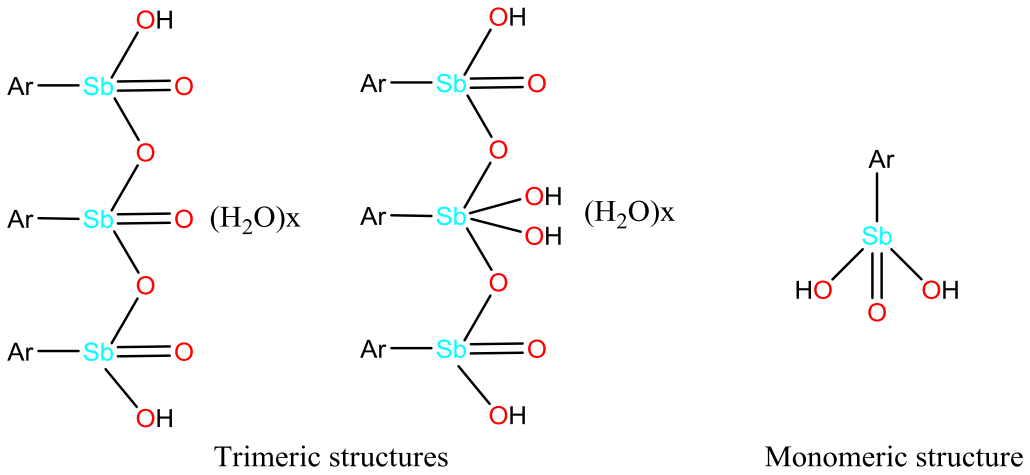

Figure 1: Schmidt proposed Arylstibonic acid structures

1.3.3 Synthesis of first molecular Organostibonic acid:

In a breakthrough work, Beckmann *et al* synthesized first molecular organostibonic acid [2, 6-$Mes_2C_6H_3Sb(O)(OH)_2]_2$ (**1**)(**Scheme 2**) by the controlled hydrolysis of 2, 6-$Mes_2C_6H_3SbCl_4$(Mes= mesityl) in alkaline conditions.[33] It exist as a dimer with a five-coordinate Sb and a Sb_2O_2 core, around antimony atom trigonal bipyramid geometry was present, it supported by earlier reports.[32] In this case, the bulky R groups (2,6-$Mes_2C_6H_3$) prevent higher aggregations; hence it crystallized as a dimer. Similarly, another controlled base hydrolysis of 2,6- $Mes_2C_6H_3Sb^{III}Cl_2$ in atmospheric conditions affords two different clusters [(2,6-$Mes_2C_6H_3Sb^{V})_2(ClSb^{III})_4(O)_8$] and [(2,6-$Mes_2C_6H_3Sb^{V})_4(ClSb^{III})_4(HOSb^{III})_2O_{14}$]. Here interestingly, from the Sb(III) starting precursor mixed-valent organoantimony (III/V) oxo clusters formation occurs.[34]

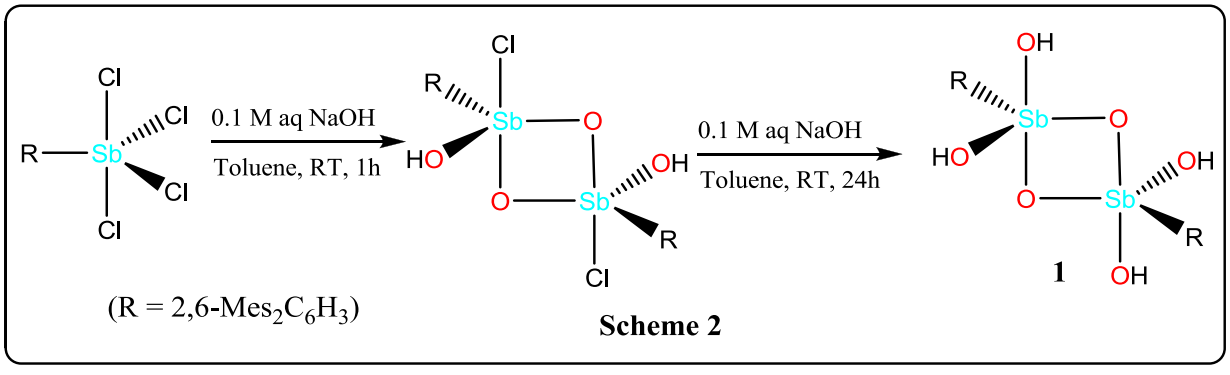

Scheme 2

1.4 Reactions of arylstibonic acids:

Methanestibonic acid was synthesized by the hydrolysis of tetraalkoxymethylstiborane or oxidation of dimethoxy methylstibine with H_2O_2 in dichloromethane and alcohol mixture solvent at low temperature. It was obtained as a colorless amorphous powder. Methanestibonic acid reacts with sodium hydroxide forms sodium salt $Na_2[MeSb(OH)_3O]_2.6H_2O$ and it reacts with 2, 3-dimethyl butane-2, 3-diol forms $\{MeSb[OC(Me)_2C(Me)_2O]_2\}$ were isolated and characterized.[35]

1.4.1 Arylstibonic acids with H_2SO_4 and NaOH:

The reaction of $[2,6\text{-}Mes_2C_6H_3Sb(O)(OH)_2]_2$ with H_2SO_4 and NaOH in a toluene/water solvent system results in the formation of $[2,\ 6\text{-}Mes_2C_6H_3Sb(O)(OH)_4(SO_4)]$ (**2**) and $[Na_2 2,6\text{-}Mes_2C_6H_3Sb(O)_4(OH)_{10}.2H_2O]$ (**3**) (**Scheme 3**). Here, a four-membered Sb_2O_2 ring opening occurs when treated with aqueous H_2SO_4 resulting in a six-membered heterocyclic ring. The amphoteric character of arylstibonic acids was confirmed while performing the reaction given below.[36]

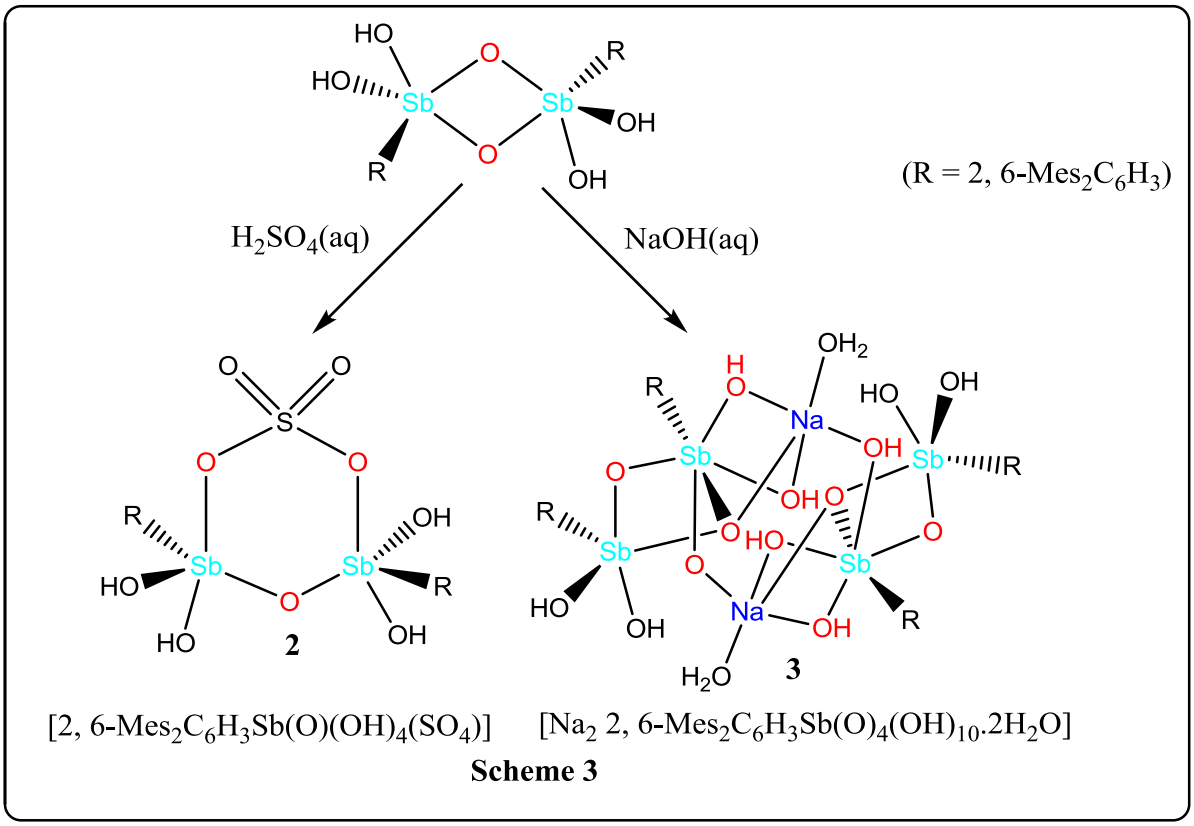

Scheme 3

1.4.2 Synthesis of reverse-Keggin compounds:

Polyoxometalates(POMs) of transition metal ions[92-98] have been known since the last two decades, whereas POMs which consists only main group elements are rare. The Keggin ion of general formula $[EM_{12}O_{40}]^{x-}$(where, E= p-block element Co, Fe, Cu, P, As, Sb, Bi, and M= d-block element Mo, W, V, Ti) was probably the most well-known POMs; here, at the center p-block element E was present and it is surrounded by twelve d-block elements. Reverse Keggin ion was obtained by the reaction of arylstibonic acid with various transition metal acetates in acetonitrile with pyridine or triethylamine as a base at 100 °C under hydrothermal conditions resulting in formation of novel dodecanuclear polyoxostibonates $\{[Mn(PhSb)_{12}O_{28}][Mn_4(H_2O)]\}$(**4**) (**Figure 2**). Here transition metal ions were encapsulated at the center of the Keggin. These POMs are termed as reverse Keggin ions as they are structurally similar to the well-known Keggin ion but with p-block and d-block elements, positions are reversed.

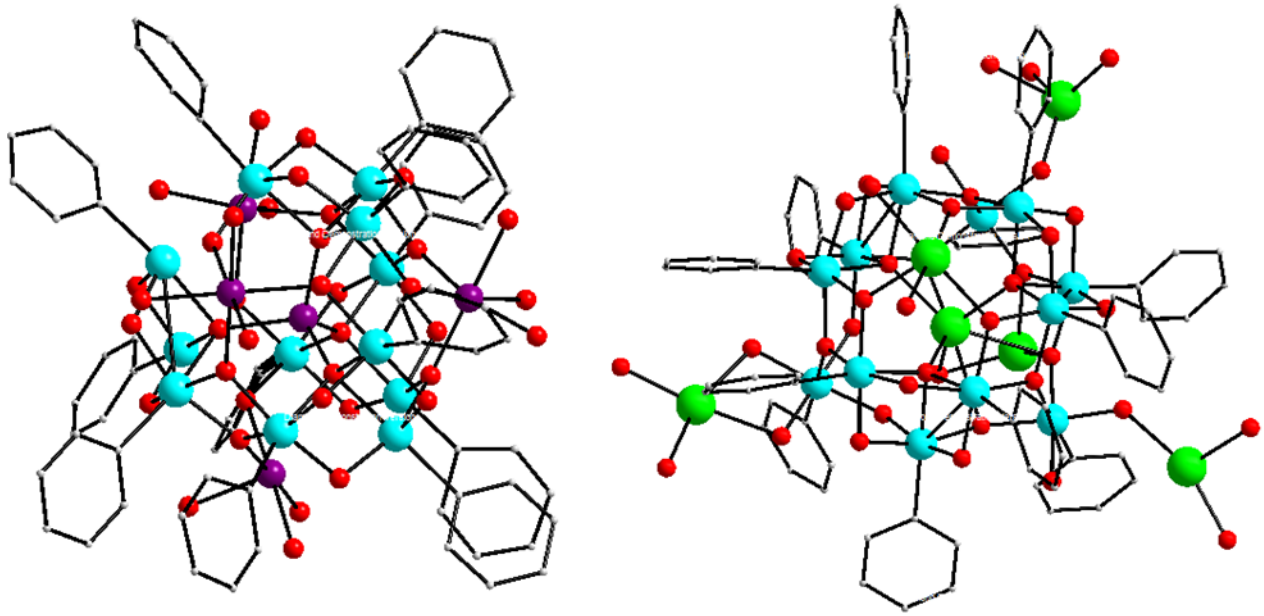

(a) **(b)**

Figure 2:Molecular structureof(a) $[Mn(PhSb)_{12}O_{28}Mn_4(H_2O)_6]$ (**4**) and (b) $\{Na_4(PhSb)_{16}O_{36}\}$cage (**5**); Color code: Cyan: Sb, Yellow: Na, Purple: Mn, Red: O.

The Keggin ion structure consist a central Mn(II) ion in tetrahedral geometry, which is surrounded by twelve organostibonic acid moieties, which are in an octahedral environment. Here in the presence of a base, arylstibonic acids self-condense to form the Sb_{12} POM framework. A similar reaction with nickel acetate forms polymeric nickel antimonate, which contains $\{Na_4(PhSb_{16})O_{36}\}$ cage (**5**) (**Figure 2**) as a repeating unit.[37]

1.4.3 Synthesis of Polyoxostibonates:

Nicholson's group synthesized a series of arylstibonic acids, like*p*-chlorophenylstibonic, *p*-tolylphenylstibonic, *p*-nitrophenylstibonic and α-Naphthylstibonic acid by using Scheller reaction. Further additional purification of arylstibonic acids has been done by ammonia/acetic acid diffusion method.[38b] The arylstibonic acids were dissolved in water/aqueous ammonia mixture in a plastic beaker and diffusing acetic acid into the solution in a closed desiccator to obtain sodium or potassium free arylstibonic acids. A plastic beaker was used to avoid leaching Na^+ ions from glassware, as arylstibonic acids had a strong affinity towards sodium ions. However, they found Na^+ ions are present in *p*-nitrophenylstibonic acid even after two diffusion purifications. They had extensively studied the solution behavior of various arylstibonic acids by using ESI-MS and found most of the arylstibonic acids exist as high molecular weight dodecanuclear aggregates $[H_8(RSb)_{12}O_{28}]$ in acetonitrile. It was also observed if pure arylstibonic acid solution is left standing in glassware or in the presence of a small amount of NaOH, sodium adducts of arylstibonic acids like $[NaH_5(RSb)_{12}O_{28}]^{2-}$, $[Na_3H_4(RSb)_{12}O_{28}]^{2-}$, $[Na_3H_3(RSb)_{12}O_{28}]^{2-}$ were obtained as found in ESI-MS spectra. This dodecanuclear polyoxostibonate cage has general formula is $[M_2H_{10-x}(RSb)_{12}O_{30}]^{x-}$ (**6**) (where M= K or Na) (**Figure 3**) and it behaves like inorganic cryptands and incorporating sodium ions or similar size cations in their cavities.[38]This dodecanuclear polyoxostibonate cage has two cation binding sites, the first cation present in ten coordination, while the second cation is in six coordination. They have also observed that the cation size plays a crucial role in templating the polyoxometalate formation. When arylstibonicacid is reacted with LiOH, results in the formation of dodecanuclear polyoxostibonate $[LiH_3(p\text{-}MeC_6H_4Sb)_{12}O_{28}]^{4-}$ (**7**) (**Figure 3**). Here Li^+ cation are fully enclosed with closed geometry. It may be due to the Li^+ ion being smaller in size than the Na^+ ion. The core of this structure $\{Sb_{12}O_{28}\}$ was similar to γ-Keggin ion geometry. The larger Ba^{2+} ion is introduced into the organostibonic acid structure resulted in the formation of tetradecanuclear

polyoxostibonate $[BaH_{10}(p\text{-}MeC_6H_4Sb)_{14}O_{34}].4H_2O$(**8**)(**Figure 4**).[39] A dramatic change was observed when Ba^{2+} cations were introduced, formingSb_{14} core with bowl-shape geometry and the barium cation encapsulated in the center with eleven coordination, whereas small Li^{+} cations forming Sb_{12} cage. Similarly organostibonic acids with Rb^{+} cation forms bowl-shape polyoxostibonate $[RbH_{11}(p\text{-}MeC_6H_4Sb)_{14}O_{34}]$.[40]

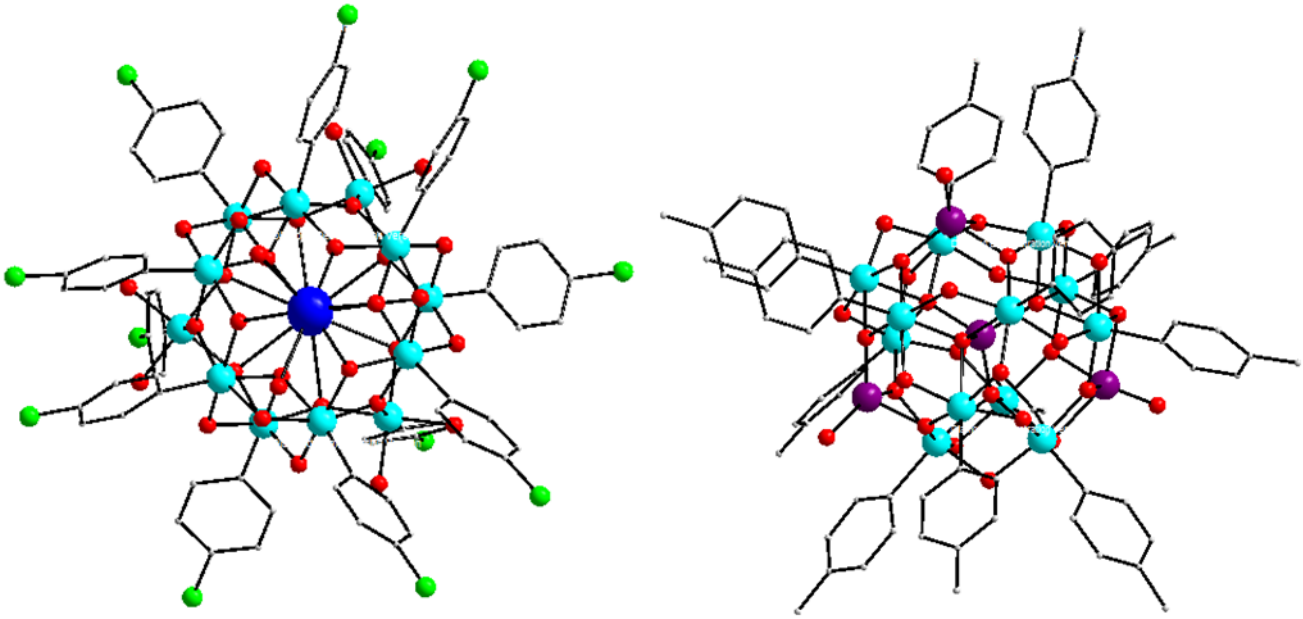

(a) **(b)**

Figure 3: Molecular structure of (a) $[K_2H_{10}(RSb)_{12}O_{30}]$(**6**) and (b) $[LiH_3(p\text{-}MeC_6H_4Sb)_{12}O_{28}]^{4-}$ (**7**) ; Color code: Cyan: Sb, Blue: K, Purple: Li, Green: Cl, Red: O.

When arylstibonic acids were reacted with transition metal (Co or Zn) chlorides in water/ammonia mixture, it resulted in the formation of dodecanuclear polyoxostibonate clusters $[Zn(p\text{-}ClC_6H_4Sb)_{12}O_{28}(ZnCl)_4]^{2-}$ (**9**) (**Figure 4**) in which Co^{2+} or Zn^{2+}cations occupy central tetrahedral sites; it looks like previously reported reverse Keggin ion.[32] These polyoxostibonates structures are similar to the ε-Keggin ion geometry. The Sb_{16} compound $[H_6(RSb)_{16}O_{36}]^{2-}$ is different when compare to Sb_{12} and Sb_{14} POMs and metal cations are not incorporate within its core. All traditional transition metal cations containing POMs were formed in acidic conditions, whereas interestingly, all these polyoxostibonates are formed in basic conditions. Based on ESI-MS studies of these polyoxostibonates in acetonitrile solvent reveals that structural integrity was retained in the solution too. Both Sb_{14} and Sb_{16} polyoxostibonates are unique in nature as there

are currently no structural similarities in W and Mo POMs chemistry. All these results suggest that arylstibonic acids under alkaline condition condensed itself, forming Sb_{12}, Sb_{14} and Sb_{16}polyoxostibonate clusters, which can act as inorganic cryptands for various alkali, alkaline earth and transition metal ions.[41]

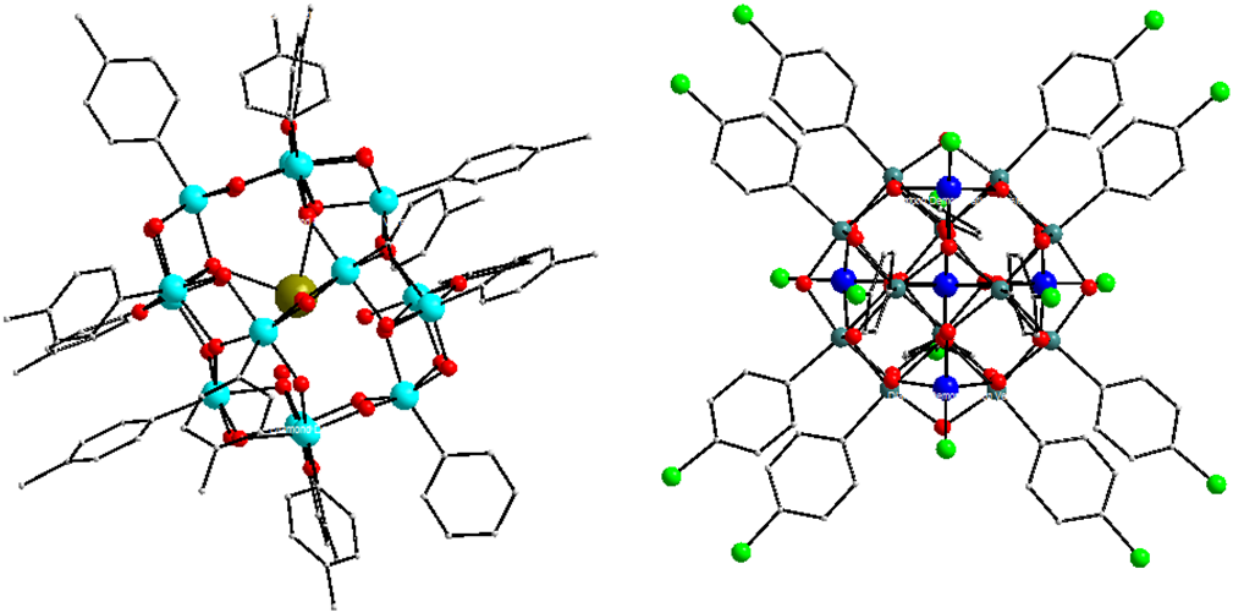

(a) **(b)**

Figure 4: Molecular structureofa) $[BaH_{10}(p\text{-}MeC_6H_4Sb)_{14}O_{34}]$ (**8**) and b) $[Zn(p\text{-}ClC_6H_4Sb)_{12}O_{28}(ZnCl)_4]^{2-}$ (**9**) ; Color code: Cyan: Sb, Grey: Ba, Blue: Zn, Green: Cl, Red: O.

1.4.4 Synthesis of Organostibonate phosphonic acid pro-ligand:

Phosphonic acids used as ligands do not form condensation products, while arylstibonic acids form polycondensation products. By mixing arylstibonic acids and phosphonic acids, the depolymerization of arylstibonic acid can lead to the formation of polydentate oxygen donor ligand systems. This main group metal phosphonate ligand system is very novel and it can act as a ligand to react with transition metals. Winpenny *et al* have been successfully synthesized organostibonic acid-phosphonic acid pro-ligands by the reaction of arylstibonic acids with phenyl phosphonic or *t*-butylphosphonicacids resulting in the formation of tetra/dinuclearorganoantimony phosphonate clusters.[42a] Several metal triangles like the manganese triangle, nickel triangle and chromium triangle are reported as pro-ligand to form

high nuclearity clusters.[43] Further, these arylstibonic acid phosphonate pro-ligand clusters can be used as a novel ligand platform for the assembling of polymetallic copper (II) and cobalt (II) complexes using solvothermal conditions.[42] Reactions of pro-ligand $[(ArSb)_4O_2(O_3PPh)_4(HO_3PPh)_4]$(**10**) (**Figure 5**) with $Co(OAc)_2$ with different bases under hydrothermal conditions forms different types of organoantimony cobalt clusters. With LiOMe/pyridine base, it forms $[Co_2(ArSb)_4O_4(PhPO_3)_4(OCH_3)_4(py)_2]$ (**11**) (**Figure 5**). While in the presence of pyrazine (pyz) as a base in methanol, it forms 1 Dimensional polymer $[Co_2(ArSb)_4O_4(PhPO_3)_4(OCH_3)_4(pyz)]_n$. With triethylamine/pyridine base in acetonitrile, it forms a tetranuclear cobalt cage $[Co_4(ArSb)_5O_9(PhPO_3)_6(py)_4]$.

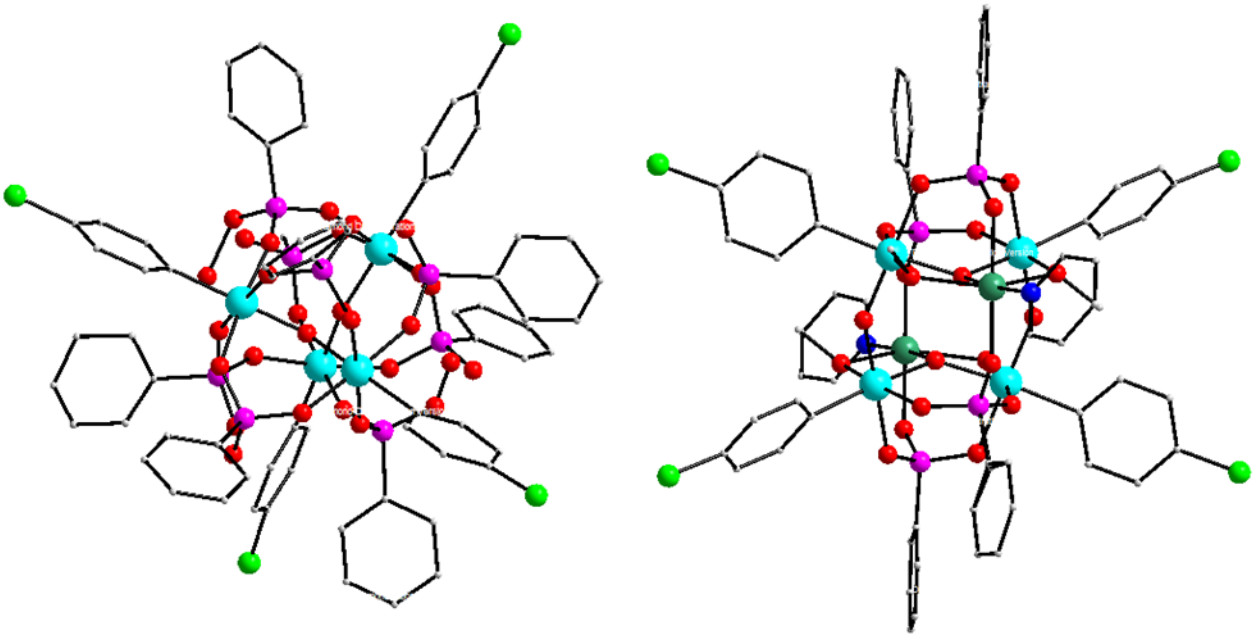

(a) **(b)**

Figure 5: Molecular structure ofa) pro-ligand $[(ArSb)_4O_2(O_3PPh)_4(HO_3PPh)_4]$ (**10**) and b) $[Co_2(ArSb)_4O_4(PhPO_3)_4(OCH_3)_4(py)_2]$ (**11**); Color code: Cyan: Sb, Grey: Co, Pink: P, Green: Cl, Blue: N, Red: O.

Similarly, anotherarylstibonic acid phosphonate pro-ligand $[(ArSb)_2O(t\text{-}BuPO_3H)_6]$ (**12**) (**Figure 6**) reacts with copper acetate under solvothermal conditions affords different types of organoantimony copper clusters. With pyridine base, it forms tetranuclear copper cage $[Cu_4O_2(ArSb)_2(t\text{-}BuPO_3)_2(CH_3CO_2)_2(OCH_3)_6]$ as a major product and trinuclear copper cage $[Cu_3O_4(ArSb)_2(t\text{-}BuPO_3)_4(py)_3]$ as a minor product.[44] In the presence of lithium methoxide as a

base it forms two different products like tetranuclear copper cage is major product and heterometallic cage is minor product $[Cu_5Li_4O_6(ArSb)_4(t\text{-}BuPO_3)_6(CH_3CO_2)_2(OCH_3)_4(CH_3OH)_4]$ (**13**) (**Figure 6**). With 2, 6-lutidine base in methanol, it forms octametallic cage $[Cu_8O_4(ArSb)_2(t\text{-}BuPO_3)_6(CH_3CO_2)_4(lutidine)_2]$.[44]

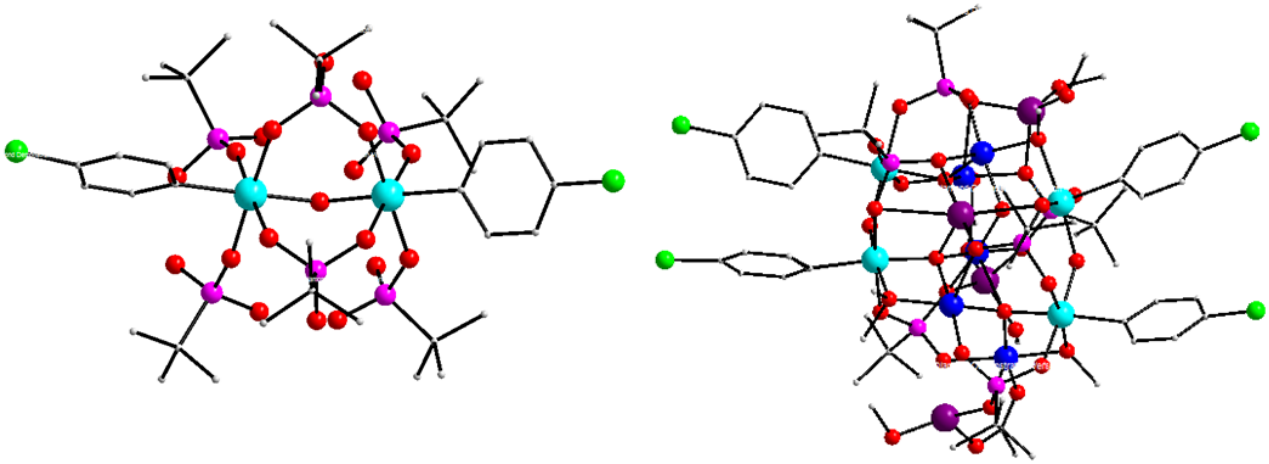

(a) **(b)**

Figure 6: Molecular structure of a) pro-ligand $[(ArSb)_2O(t\text{-}BuPO_3H)_6]$ (**12**) and b) $[Cu_5Li_4O_6(ArSb)_4(t\text{-}BuPO_3)_6(OAc)_2(OCH_3)_4(CH_3OH)_4]$ (**13**); Color code: Cyan: Sb, Blue: Cu, Green: Cl, Purple: Li, Pink: P, Red: O.

1.4.5 Reactions of arylstibonic acids with protic ligands:

Our group has been working on the synthesis and reactivity studies of organostibonic acid by using depolymerization reactions of arylstibonic acid with various protic ligands, like phosphonic acids, phenolic pyrazole, naphthyl phenolicpyrazole, 8-hydroxy quinoline, silane diol, silanetriol and phenyl seleninic acid. Structural characterization reveals the formation of multinuclear organoantimony oxo-hydroxo clusters resembling a cubane, butterfly, adamantane-type and triangle geometry. Condensation reactions of *p*-haloarylstibonic acid with phenolic pyrazolyl ligands with substitution at 5 position under reflux conditions yielded two organoantimony oxo-hydroxo clusters $[(RSb)_4O_5(OH)_2L_4]$ and $[(RSb)_4O_4L_4]$ (L=pyrazole ligand), here pyrazole ring nitrogen atoms either one or two were coordinated to antimony atoms. Reaction of phenyl or *t*-butyl substituted phenolic pyrazolyl with arylstibonic acid forms $[(p\text{-}ClC_6H_4Sb)_4O_5(OH)_2(HPhPzPh)_4]$ (**14**) (**Figure 7**) and without substitution forms [(*p*-

$ClC_6H_4Sb)_4(O)_4(PhPz)_4]$. Arylstibonic acids had the ability to self-condense to form hexa-decanuclearpolyoxostibonate Sb_{16} POM $[(p\text{-}ClC_6H_4Sb)_{16}O_{28}(OH)_8](3,5\text{-}DMPz)_6]$ (**15**) (**Figure 7**) in the presence of mild base 3,5 dimethyl pyrazole.[45]

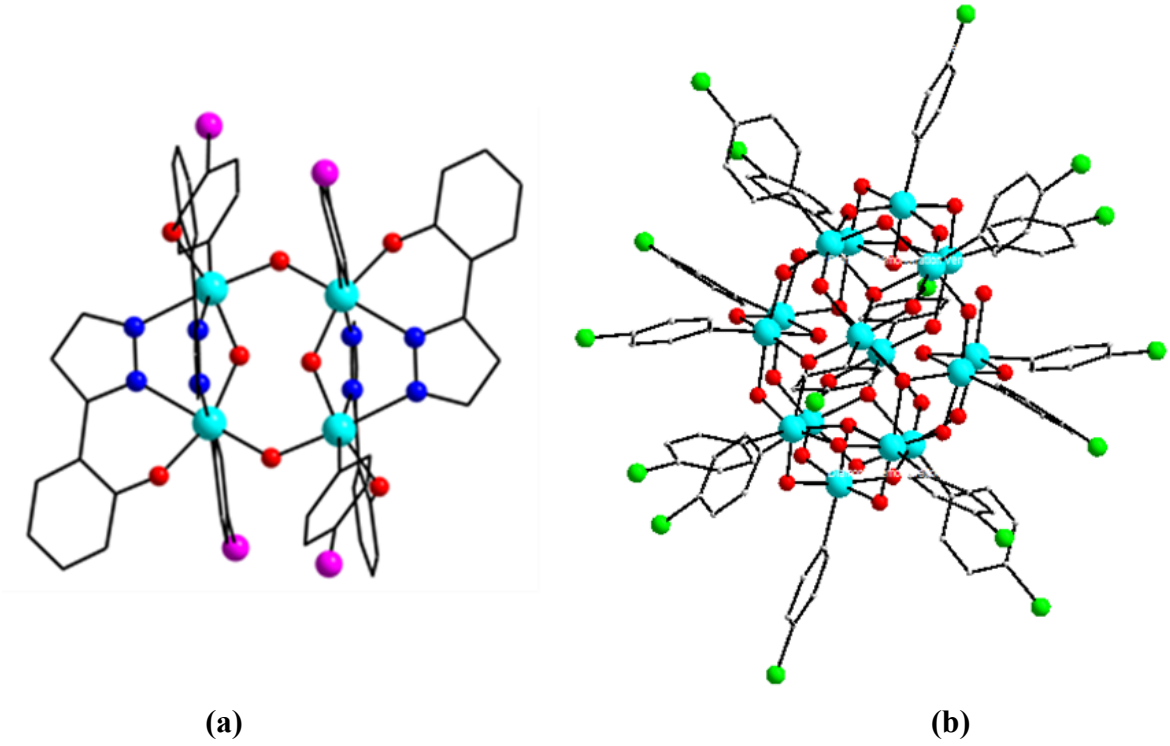

(a) **(b)**

Figure 7: Molecular structure of a) $[(p\text{-}ClC_6H_4Sb)_4O_5(OH)_2(HPhPzPh)_4]$ (**14**). b) Sb_{16} POM$[(p\text{-}ClC_6H_4Sb)_{16}O_{28}(OH)_8]$(**15**) Color code: Cyan: Sb, Blue: N, Green: Cl, Red: O.

1.4.6 Synthesis of Organoantimony(V) Oxido Cubane cluster:

Condensation reactions of arylstibonic acids with diphenyl silane diol in toluene at reflux condition results in the formation of tetranuclear organoantimony cubane clusters (**Scheme 4**) $[(p\text{-}Cl\text{-}C_6H_4Sb)_4(O)_4(Ph_2SiO_2)_4]$ (**16**) and $[(p\text{-}Br\text{-}C_6H_4Sb)_4(O)_4(Ph_2SiO_2)_4]$ (**17**).These two clusters are isostructural. The cluster's core consists of a rare Sb_4O_4 cubane framework (**Figure 8**). This is the first complex that contains $Sb^V\text{-}O\text{-}Si^{IV}$ framework.[46] Solution ^{29}Si NMR (in $CDCl_3$) of compounds **16&17** gives δ =-29.5 ppm signal; it shows that siloxides present in a unique environment in the crystal. Solution ^{29}Si NMR spectral values are correlates well with the observed solid-state structures.

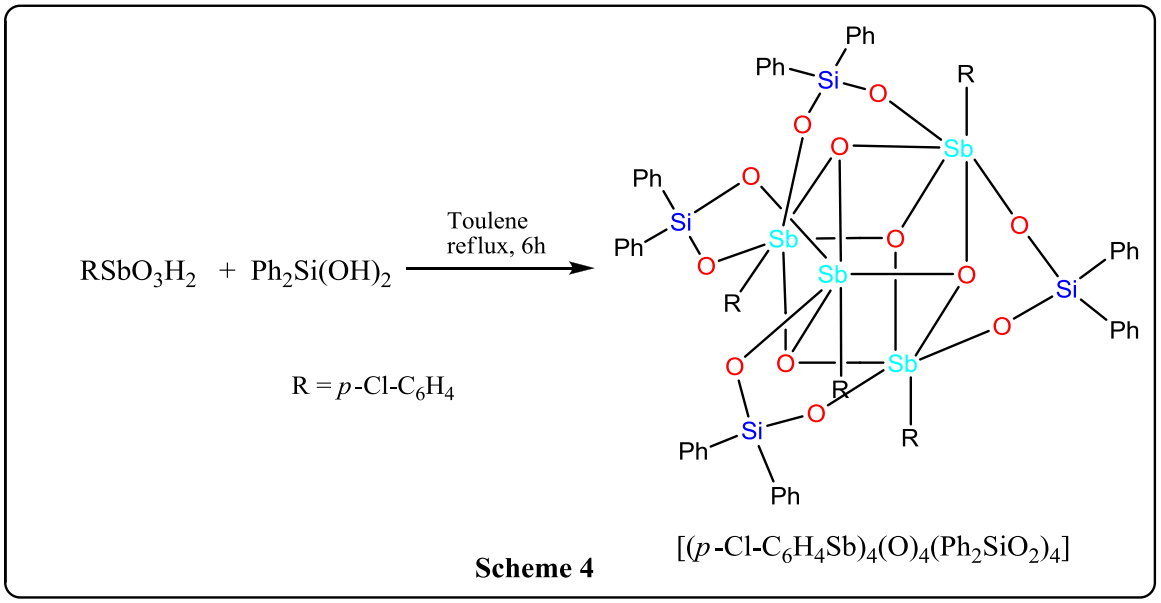

Scheme 4

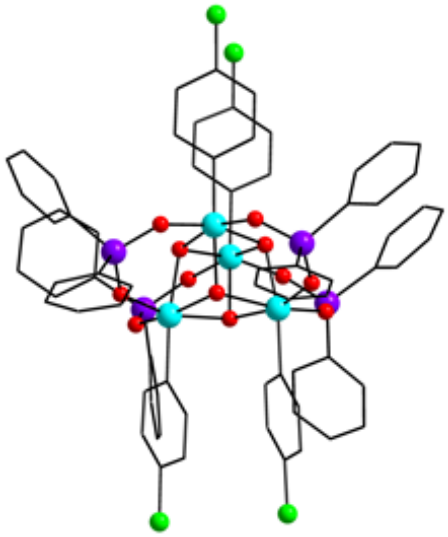

Figure 8: Molecular structure of $[(p\text{-Cl-}C_6H_4Sb)_4(O)_4(Ph_2SiO_2)_4]$ (**16**) Color code: Cyan: Sb, Blue: Si, Green: Cl, Purple: Li, Pink: P, Red: O.

1.4.7 Synthesis of Oxo-Centered Sb_3O triangle:

Reactions of arylstibonic acid with *t*-butylsilanetriol in toluene at reflux condition affords trinuclear organoantimony metal oxo centered cluster $\{[C_5H_5NH][(p\text{-Cl-}C_6H_4Sb)_3[(t\text{-}Bu)_4Si_4O_9][(t\text{-}Bu)_2Si_2O_5(\mu_3\text{-}O)(OH)]\}$ (**18**) (**Figure 9**). Interestingly, disolaxane and tetrasiloxane frameworks are *in situ* generated by silane triols' self-condensation by removing water molecules. This siloxane framework stabilized the oxo-centered Sb_3O triangle. Generally, oxo-centered metal triangles are very common in transition metals, whereas they are rare so far

as the main group metals are concerned. This is the first structurally characterized oxo-centered organoantimony (V) based triangle and stabilized by siloxane framework.[47] Solution ^{29}Si NMR (in $CDCl_3$) of above cluster gives δ =-22.0 ppm signal and ESI-MS studies of above compound show signals corresponding to the formula $[M+3H]^+$ and $[M+2H+NH4]^+$. Based on ESI-MS data, the above cluster maintains the structural integrity in the solution state also.

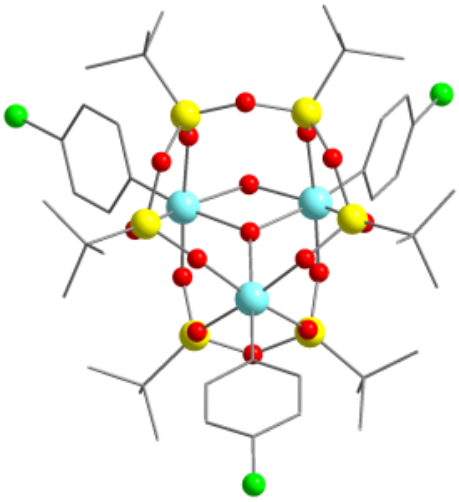

Figure 9: Molecular structure of {[(*p*-Cl-$C_6H_4Sb)_3$[(*t*-Bu)$_4Si_4O_9$][(*t*-Bu)$_2Si_2O_5$(μ_3-O)(OH)]} (**18**)

1.4.8 Synthesis of adamantane-type structures:

Reactions of arylstibonic acid with 8-hydroxy quinoline (8-HQ) or naphthyl phenolic pyrazole{2-[1H-pyrazol-5(3)-yl] naphthalene-1-ol}(H_2naPhPz) in toluene at reflux condition yielded adamantane-type tetranuclear organoantimony oxo clusters, [(*p*-$ClC_6H_4Sb)_4(O)_6(L)_4$] (**19**) (here L=8-hydroxy quinolone or naphthyl phenolic pyrazole) (**Scheme 5**). The solid-state structure contains an unprecedented Sb_4O_6 adamantane-type core stabilized by a ligand system and it structurally similar to the antimony mineral senarmonite Sb_2O_3 it is in dimeric form.[48] Main group metals concern like gallium, indium, aluminium and tin adamantane-type clusters are reported,[49] whereas with respect to antimony this is first report having adamantane-type Sb_4O_6 frameworks although Sb_4O_6 non-adamantane type clusters are known.[79b] Natural polyarsenic compound Arsenicin A was isolated from New Calodonian sponge *Echinochalina bargibanti* and interesting to note that its structure is similar to adamantane-type structure As_4O_6. Arsenicin A shows the important application as fungicidal and bacterial activities on human pathogenic strains and it also chemically synthesized by Wild *et al.*[50] Subsequently, Beckmann *et al* reported the second molecular organostibonic acid [$(ArSb)_4O_6(OH)_4$] (**20**) (**Figure 10**) by base

hydrolysis of $ArSbCl_4$ (Ar= 6-diphenylphospinoacenaphth-5-yl). It has an adamantane-type structure. Here one coordination site of the antimony atom was blocked by bulky ligand and it prevented extensive aggregation of organostibonic acid.[51]

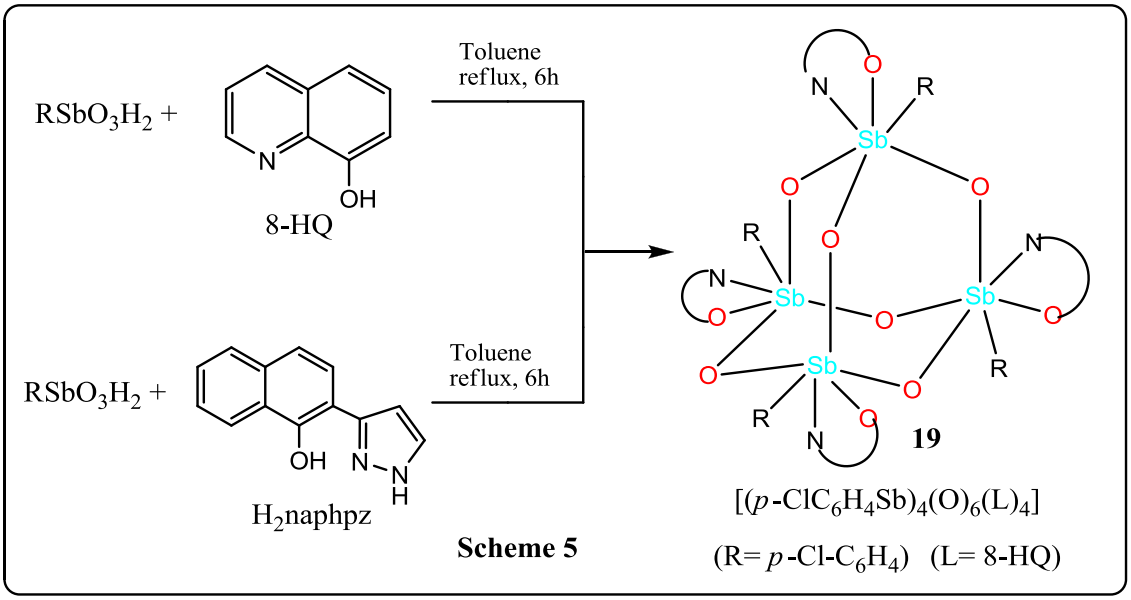

Scheme 5

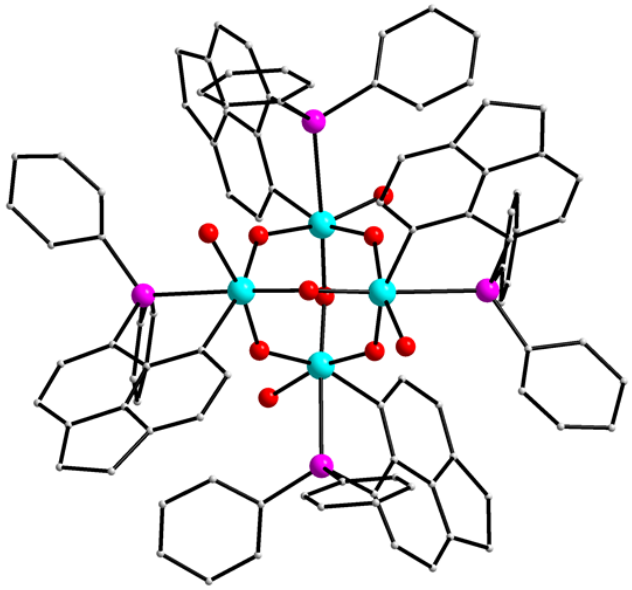

Figure 10: Molecular structure of adamantane-type tetranucleararylstibonic acid (**20**)

1.4.9 Synthesis of mixed valent Sb(V)/(III) polyoxostibonate:

The reaction of arylstibonic acid with diphenyltellurium oxide in toluene at reflux condition affords tetradecanuclear polyoxostibonate cluster (**21**) (**Figure 11**). Here Sb_{14} POM is chelated by diphenylditelluroxane moieties. It is a dianionic cluster and the charge of the cluster is balanced by two triphenyl tellurium cations. These cations crystalized along with Sb_{14} core. Interestingly, the complete dearylation of arylstibonic acid occurred in the presence of diphenyltellurium oxide. Solution ^{125}Te NMR ($CDCl_3$) gives two resonance signals at δ = 1162 & 787 ppm, correlates well with the two types of tellurium ions present. Here tetraorganoditelluroxane's framework behaves like ligand and stabilizes novel mixed valent Sb(V)/(III) Sb_{14} POM framework.[52]

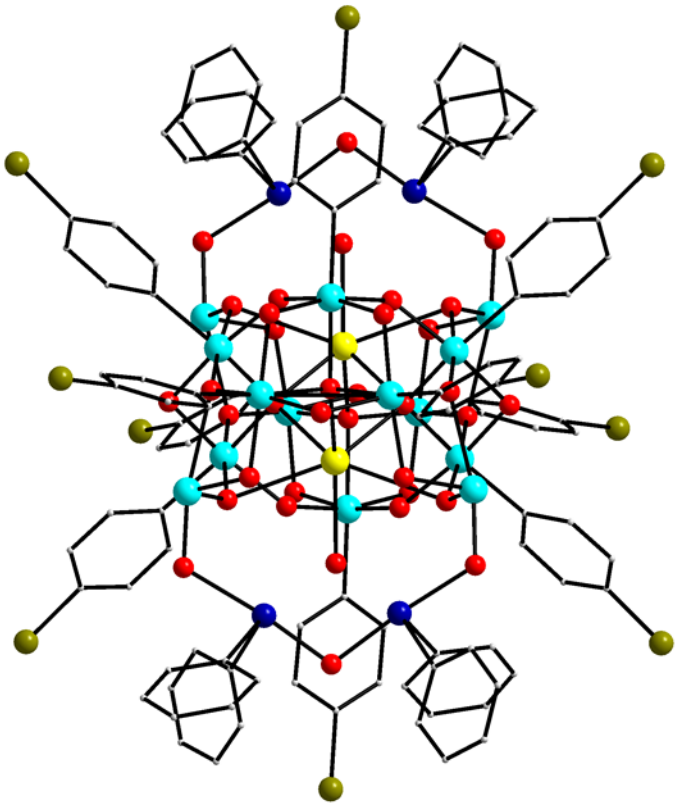

Figure 11: Molecular structure of tetradecanuclear polyoxostibonate Sb_{14} POM. (**21**)Color code: Cyan: Sb, Blue: Te, Grey: Br, Yellow: Na, Red: O.

1.5 Organoantimony(V) Compounds:

Organoantimony(V) compounds have been an area of interest not only owing to their biological and catalytic applications but also due to interesting structural variation they exhibit resulting in the isolation of novel rings and clusters. Organoantimony(V) compounds were also used for industrial applications, especially in the field of synthetic organic chemistry. Organoantimony compounds have been used as reagent or catalyst,[53] for example triphenylantimony oxide along with P_4S_{10} (Ph_3SbO/P_4S_{10}) catalyst system has been used for esterification reactions of various carboxylic acids with corresponding alcohols.[54] In the presence of tri-n-butylstibine, α-enones can be prepared by treating aldehydes with α-bromoketones. Trialkylstibines used as an effective reagent for double bond formation in between α-halogeno carboxylic esters and carbonyl compounds. Stiboniumylides or pentaorganylstiboranes are synthesized by treating quaternary stibonium salts with nucleophilic bases (RLi, LDA and potasium *t*-butoxide). The reaction of stibonium ylides with carbonyl compounds to produce epoxides or olefins.[55] Few organoantimony compounds have been used as substrates in palladium-catalyzed cross-coupling reactions.[56] In the presence of palladium catalysis organoantimony compounds (triphenylantimony dichloride, triphenylantimony diacetate) gave cross-coupling products with silyloxy alkenes[57] and organotin compounds.[58, 59]

1.5.1 Synthesis of organoantimony(V) halides:

Monoorganoantimony(V) tetrahalides are less stable as they easily undergo disproportion while on standing (**Scheme 6**).[60] Structural aspects of monoorganoantimony(V) tetra halides were not known properly.

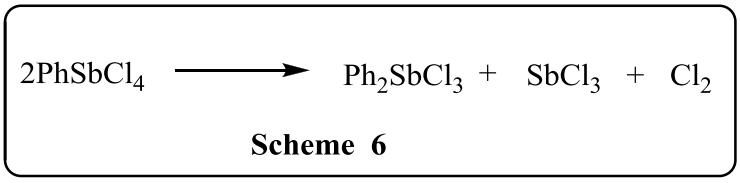

Scheme 6

Diorganoantimony(V) trihalides R_2SbX_3 can be synthesized by the reaction of $SbCl_5$ with an arylating agent such as tetraaryl lead or tetraaryl tin.[61] R_2SbX_3can also be synthesized by halogenation of corresponding diorganoantimony(III) halides R_2SbX with X_2 (X= Cl, Br) (Scheme 7).[62] There is a conflicting ideas regarding structural aspects of Ph_2SbCl_3. Some groups proposed trigonal bipyramid geometry[63] around the antimony atom and some other groups

reported the compound exists as a monohydrate with octahedral geometry.[64] Based on crystal structure analysis and ^{121}Sb Mössbauer spectroscopy can resolve the structure issue. In a solid state, anhydrous Ph_2SbCl_3 exists as a dimer (**Chart-1**) with chlorine bridges and trigonal bipyramid geometry was present around antimony atoms with three chlorine atoms occupy equatorial positions.[65]

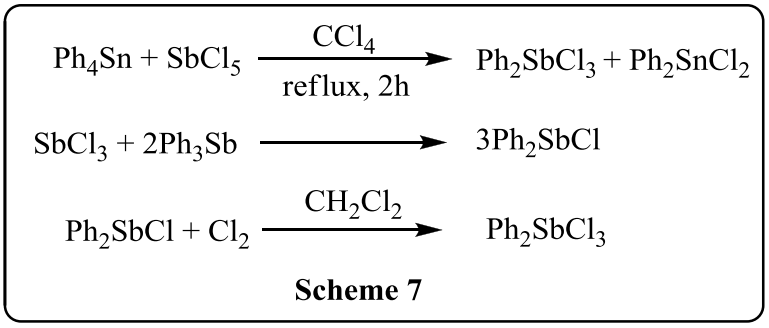

Scheme 7

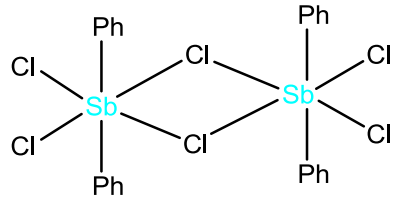

Structure of Ph_2SbCl_3

Chart-1

Triorganoantimony(V) dihalides R_3SbX_2 can be synthesized by treating SO_2Cl_2 with the corresponding triphenylantimony in dichloromethane (**Scheme 8**).[66] In the presence of various reducing agents, triorganoantimony(V) dihalides can be easily converted to corresponding antimony(III) derivatives. Similarly, triorganoantimony(V) dihalides when heated above their melting points in the inert atmosphere, can easily undergo elimination reactions. The solid state structure of Ph_3SbCl_2 revealed that the geometry around Sb is trigonal bipyramid with two chlorine atoms occupies axial positions.[67]

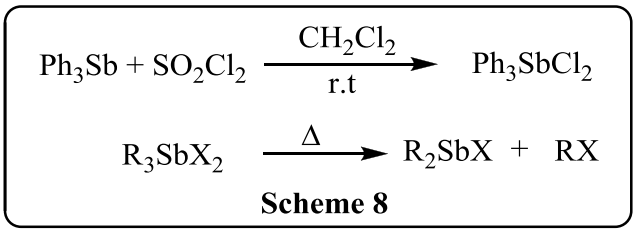

Scheme 8

1.5.2 Synthesis of organoantimony(V) Oxides:

Organoantimony(V) oxides can be prepared by the reaction of triphenylantimony with 30% H_2O_2 in ice-cold acetone. It gives an insoluble white fluffy solid material and it is characterized as polymeric triphenyl antimony oxide (**Scheme 9**).[68] Similarly, tris(2-methoxyphenyl)antimony oxide can be prepared by treating tris(2-methoxyphenyl)antimony dichloride with potassium *t*-butoxide in the presence of H_2O in dichloromethane at low temperature, interestingly it has a dimeric structure.[69]

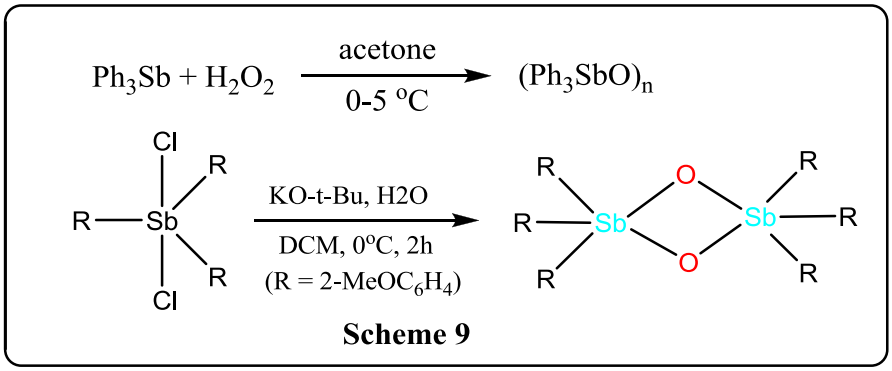

Scheme 9

1.6 Reactions oforganoantimony(V) compounds:

1.6.1 Reactions of Ph_3SbCl_2/Ph_2SbCl_3 with acetylacetone:

Reaction of monoorganoantimony(V) chloride with acetylacetone (Acac) at cooling conditions forms monoorganoantimony (acetylacetone) trichloride complex, the compound behaves as non-electrolyte in solution and it has monomeric structure. ^{1}H NMR spectra of this compound shows doublet and singlet for acetylacetone-Me protons and acetylacetone behaves like bidentate ligand. On the basis of ^{1}H NMR spectra, Okwara *et al* suggested a symmetric structure for $MeSb(acac)Cl_3$ and an asymmetric structure for $PhSb(acac)Cl_3$.[70] Similarly Ph_2SbCl_3 or Ph_3SbCl_2 reacts with acetylacetone resulting in the formation of complexes $Ph_2SbCl_2(Acac)$/ $Ph_3SbCl(Acac)$ respectively (**Scheme 10**).[71] Based on ^{1}H NMR and IR spectral studies, in $Ph_2SbCl_2(Acac)$ phenyl rings are in equatorial positions and chlorine atoms occupy axial positions, whereas in $Ph_3SbCl(Acac)$ chlorine atoms occupy equatorial positions. Compound $R_2SbCl_2(Acac)$ has three possible geometrical isomers as shown in **Chart-2**.

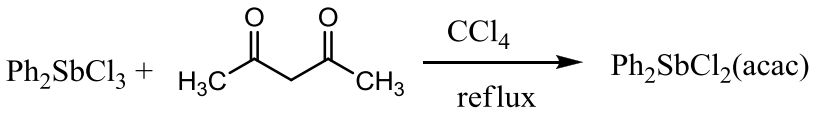

Scheme 10

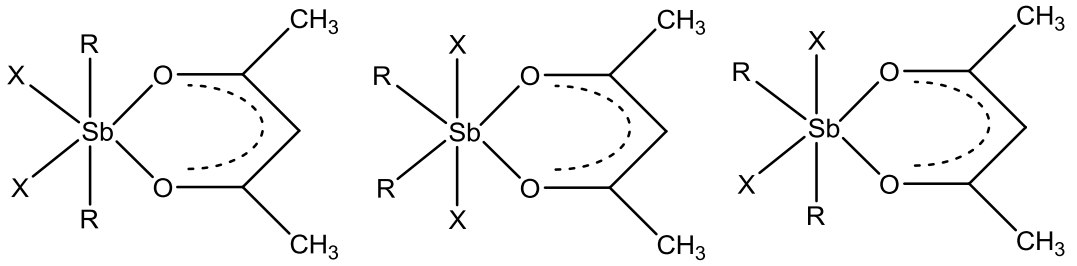

trans-diorgano *cis*-diorgano

Three geometrical isomers of $R_2SbCl_2(Acac)$

Chart-2

1.6.2 Reactions of Ph_3SbCl_2/$Ph_2SbCl_3$with Schiff base ligands:

Organoantimony(V) halides (R_2SbCl_3/R_3SbCl_2) reacted with various Schiff base ligand forms the compounds of the type $R_2SbCl(trid)$/$R_3Sb(trid)$ (R= Me or Ph; trid= tridentate Schiff base ligands with SNO or ONO donor atoms). Here various Schiff base ligands were used for example, 2-(o-hydroxyphenyl) benzothiazoline (H_2Sat), 2, 2'-(methylidynenitrilo) diphenyl (H2Sab), 4-(o-hydroxyphenyhmino)-2-pentanone (H_2Aah), 3-(o-hydroxyanilino) crotonophenone (H_2Bah) and 2-acetonyl-2-methylbenzothiazoline (H_2Aat). Based on X-ray diffraction studies and ^{121}Sb Mössbauer study of $Me_3Sb(Sab)$, it is suggested that the geometry around Sb atom was in the distorted octahedral and meridional arrangement of Schiff base ONO or SNO ligand around antimony atom (**Chart-3**).[72]

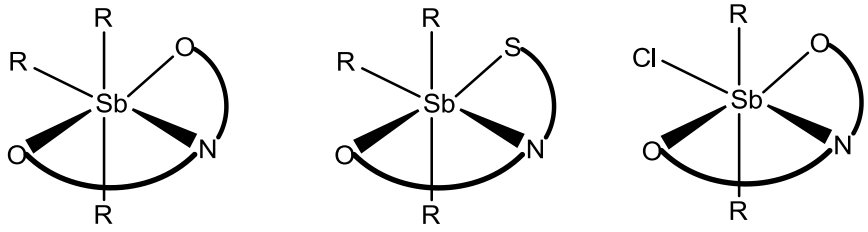

Octahedral and meridional arrangement of tridentate Schiff base ligand

Chart-3

1.6.3 Reactions of Ph_3SbCl_2/$Ph_2SbCl_3$with carboxylic acids:

Synthesis and structural characterization of organoantimony(V) carboxylates have gained significant attention due to their structural diversity and also they exhibit significant biological activities, especially their anti-tumor activities.[73] Sowerby*et al* reported organoantimony(V) oxalates by the reaction of triphenyl antimony dichloride with silver oxalate in toluene/methanol mixture solvent at a different temperature, resulting in the formation of $[SbPh_4][Ph_2Sb(ox)_2]$ and $[Ph_3Sb(OMe)]_2ox$ (here ox= oxalate) respectively.[74] Badshah *et al* investigated the reaction of triphenyl antimony dichloride with (m, p)-ferrocenyl benzoic acid in the presence of sodium methoxide base, it results in the formation of organoantimony(V) ferrocenyl benzoates$[(C_5H_5FeC_5H_4COO)Sb(p\text{-}CH_3C_6H_4)_3]$(**22**) (**Scheme 11**). The DNA interaction of this complex was investigated by U.V-Visible spectroscopy and cyclic voltammetry (CV). Interestingly this complex shows binding activity towards DNA. Based on X-ray diffraction studies, approximate trigonal bipyramid geometry around antimony has been proposed.[75]

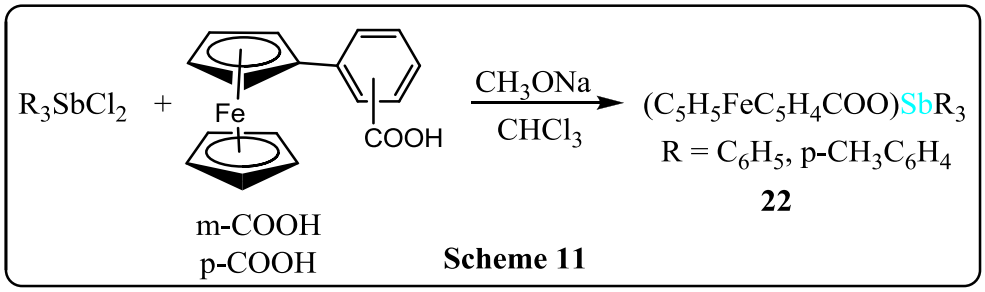

Scheme 11

Recently Han-Dong Yin *et al* successfully synthesized highly symmetrical 24-membered macrocyclic organoantimony(V) compounds $[Ph_3SbLa]$ (**23**) and $[Ph_3SbLb]$ (**24**) by the reaction of triphenyl antimony dichloride with Schiff base containing carboxylic acids (**Scheme 12**), where H_2La= 5-{[(2-carboxyphenyl)methylene]amino}-4-chloro benzoic acid and H_2Lb= 5-{[(2-carboxyphenyl)methylene]amino}-2-chloro benzoic acid. The modified Schiff base ligands possess two terminal carboxylic acid groups. Around antimony atoms trigonal bipyramid geometry was present with three phenyl rings occupying equatorial positions and two carboxylic acids occupy axial positions. In these complexes, secondary interactions (C-H….π, C-Cl….π, C-H….Cl) are responsible for the formation of a 1Dimentional infinite chain in $[Ph_3SbLa]$ and a 2Dimentional supramolecular networks structure in $[Ph_3SbLb]$.[76]

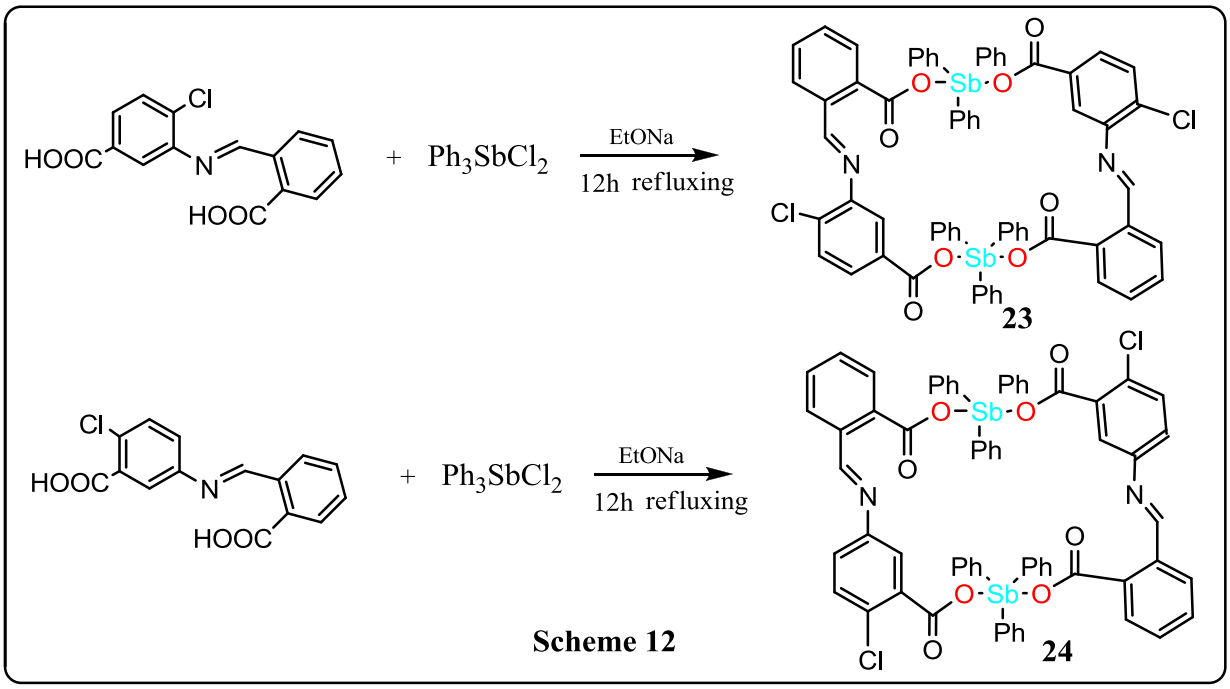

Scheme 12

The group reported the reaction of tetraphenyl antimony bromide with various carboxylic acids in the presence of sodium methoxide as a base in methanol medium, which results in the formation of novel dinuclear tetraorganantimony carboxylates(**25**) (**Scheme 13**). Interestingly CO_2 capture from atmosphere air forms a dinuclear complex and carbonate (HCO_3^-) bridge two antimony atoms. Two types of antimony atoms are present, the first type antimony was in five-coordinate trigonal bipyramid geometry and the second antimony was in six coordinate octahedral geometry.[77]

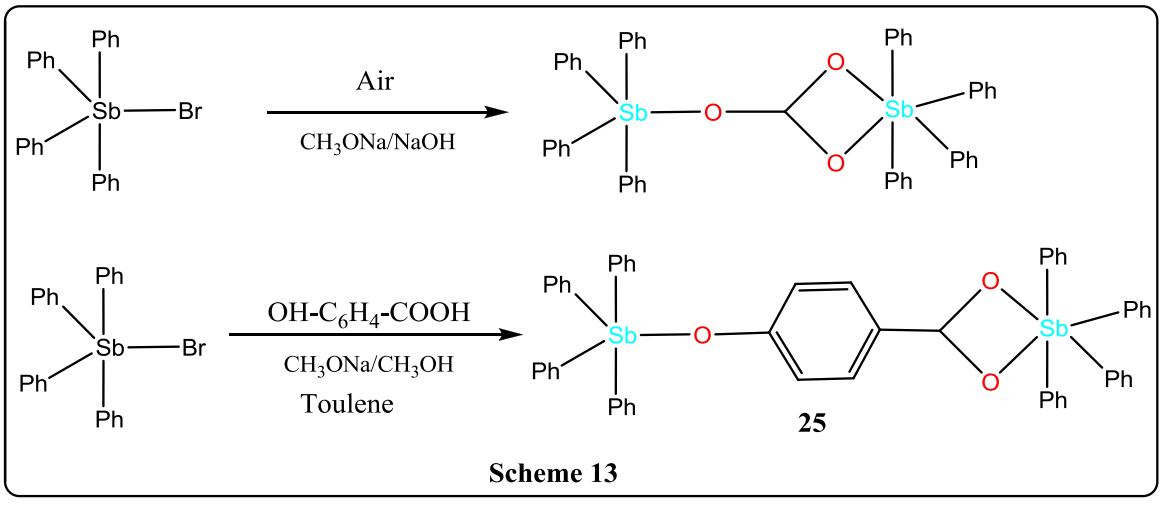

Scheme 13

Han-Dong Yin *et al* reported a novel cage-like tetranuclear organoantimony carboxylates by the reaction of triphenylantimony dichloride with various carboxylic acids like chiral (±)-mandelicacid, fluoromethylbenzoic acid and electron withdrawing groups containing aryl carboxylic acids in the presence of sodium ethoxide as a base (**Scheme 14**). The solid state structure of this compound reveals that four antimony centers in which each antimony is bounded with tridentate carboxylic group moiety and three phenyl rings; further, these four organoantimony centers are bridged together by oxo and hydroxo bridges to form cage-like tetranuclear organoantimony complex $[(Ph_2Sb)_4(\mu\text{-}O)_4(\mu\text{-}OH)_2(\mu\text{-}O_2CR)_2]$ (**26**) here R= 2-CHO-C_6H_4COOH, 4-CF_3-C_6H_4COOH. Here interestingly, the chelate ring which contains 16 atoms formation occurs during dicarboxylic ester interaction and the chelate ring resulting in boat conformation. The DNA binding properties have been investigated by fluorescence spectroscopy and found to be exhibit prominent cytotoxic activities *in vitro*studies.[78]

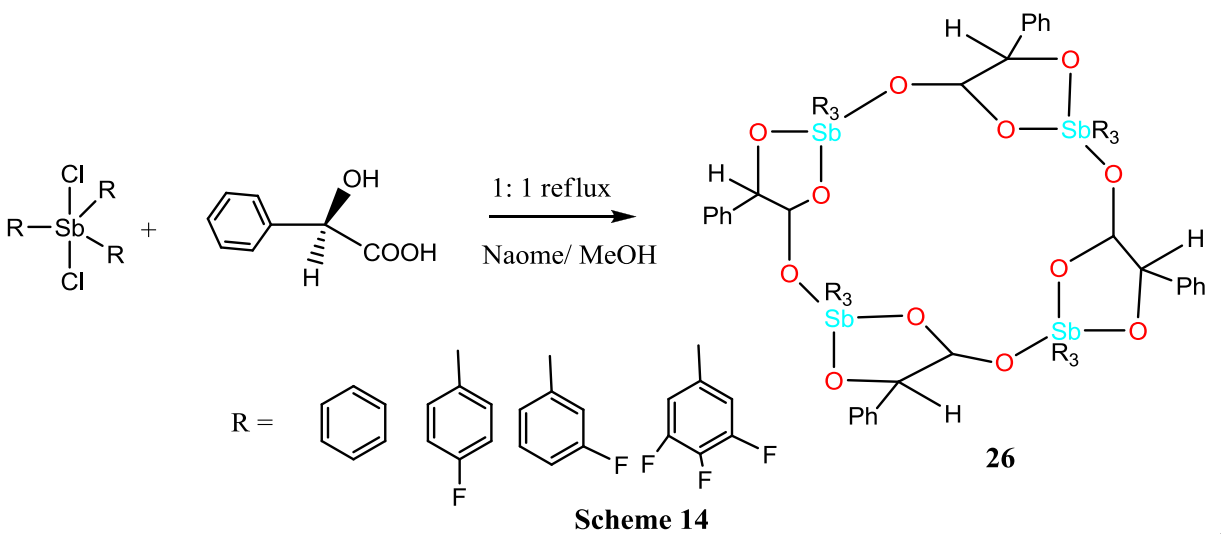

Scheme 14

1.6.4 Reactions of Ph_3SbCl_2/$Ph_2SbCl_3$with phosphinic acids:

Kumara swamy*et al* have successfully synthesized two oxo centered dinuclear and tetranuclear organoantimony(V) phosphinates $[Ph_2Sb(O_2PR_2)O]_2$ (R= cyclo-C_6H_{11} and cyclo-C_8H_{15}) and $[Ph_2Sb(O_2P(C_6H_{11})_2(O_2CMe)]_2O$ by the reactions of Ph_2SbCl_3 with three equivalence of silver acetate followed by one equivalence of dicyclohexylphosphinic acid or dicyclooctylphosphinic acid in dry toluene at reflux conditions (**Scheme 15**). Interestingly when dinuclear complex

$[Ph_2Sb(O_2P(C_6H_{11})_2(O_2CMe)]_2O$ (**27**)was treated with water/acetic acid mixture forms tetranuclear cage $\{Ph_8Sb_4O_4(OH)_2[(O_2P(C_6H_{11})_2]_2\}$ (**28**). Both di and tetranuclear organoantimony phosphinates had four-membered Sb_2O_2 rings with hexa coordinate antimony. Two Sb_2O_2 rings are further connected through oxo bridges results in Sb_4O_6 cage formation occurs in the tetranuclear cage. The group also reported reactions of diphenylantimonytrichloride with two equivalents of silver salts of phosphinates resulting in the formation of partially hydrolyzed product $\{SbPh_2Cl[O_2P(C_6H_{11})_2]\}_2O$ (**29**). Based on X-ray diffraction studies, it was found that the geometry around antimony is octahedral in which two phosphinates chelate Sb-O-Sb bridge on both sides.[79]

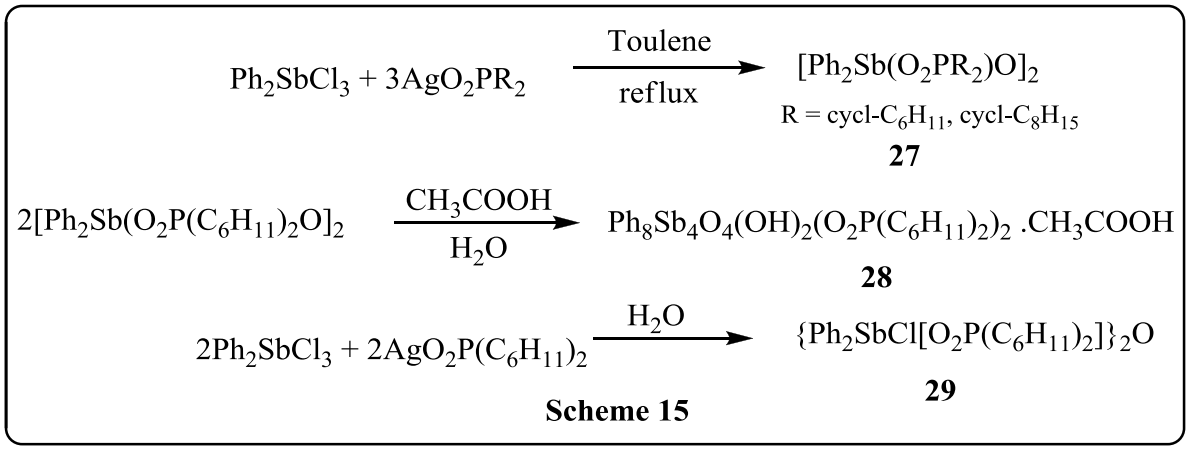

Scheme 15

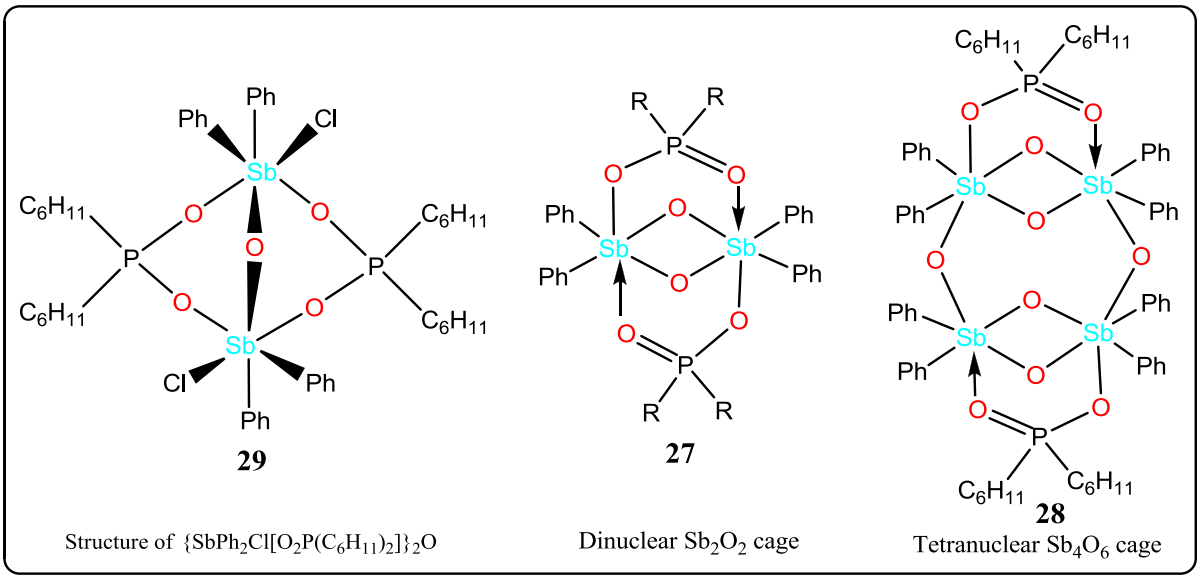

Chandrasekhar *et al* reported a novel nonanuclearorganostiboxane cage, here first a dinuclear organoantimony compound $[(Ph_3Sb)_2(\mu\text{-}O)(\mu\text{-}cycPO_2)_2]$ (**30**) was prepared by the reaction of Ph_2SbCl_3 with two equivalence of 1,1,2,3,3-pentamethyl trimethylenephosphinic acid (*cyc*PO_2H) in the presence of Et_3N base (**Scheme 16**). Interestingly further Sb-C bond cleavage followed by mild hydrolysis of this dimer in acetonitrile/water mixture (99:1) results in formation of a new organostiboxane cage. The molecular formula of this cage is $[(Ph_2Sb)_2(PhSb)_7(\mu\text{-}O)_{11}(\mu_3\text{-}O)_3(\mu\text{-}OH)_2(\mu\text{-}cycPO_2)_2(cycPO_2)_2(H_2O)_2]$ (**31**) (**Figure 12**). In Sb_9O_{16} core, two stibinic acid moieties are *in situ* generated and all antimony atoms are in a +5 oxidation state.[80]

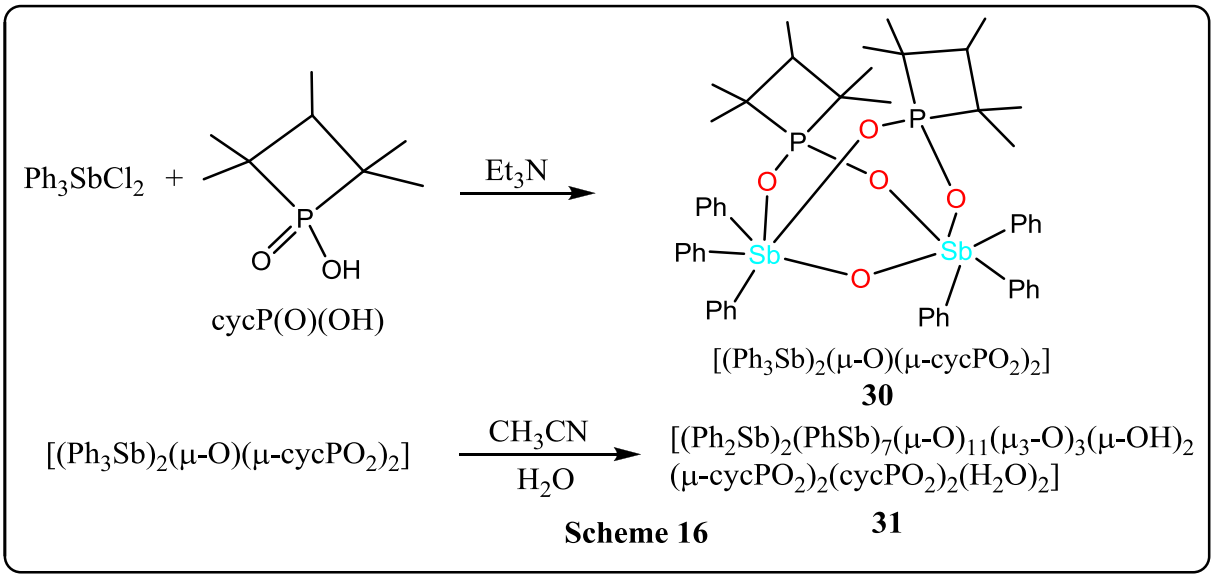

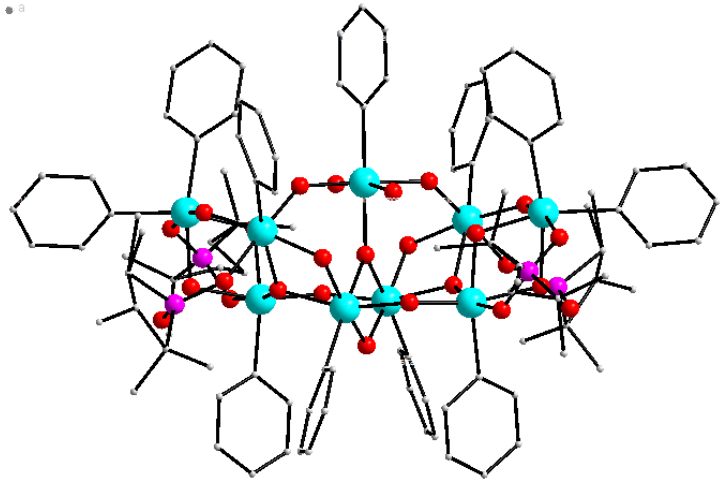

Figure 12: Molecular structure of organostiboxanecage(**31**).Color code: Cyan: Sb, Pink: P, Red: O.

Silvestru *et al* investigated the reactions of triorganoantimony dichloride with sodium salts of appropriate diorganophosphinic acid (e.g: diphenylphosphinic acid Ph_2PO_2H, diphenylmonothiophosphinic acid $Ph_2P(S)OH$, diphenyldithiophosphinic acid Ph_2PS_2H) led to the formation of monomeric bis(diorganophosphinato)triorganoantimony(V) complexes $R_3Sb(O_2PPh_2)$ (here R= Me or Ph), here two phosphinate ligands bound to central antimony in monodentate fashion. Around antimony, distorted trigonal bipyramid geometry was observed with two phosphinate oxygen atoms occupy axial positions and three methyl groups are occupying equatorial positions. They also reported metathesis reactions between diphenylantimonytrichloride and alkali salts of oxo- and thioimidodiphosphinic acids, $Na[(OPPh_2)(XPPh_2)N]$ (X= S, O) affords $Ph_2SbCl_2[(OPPh_2)(XPPh_2)N]$ (here X= O, S). Here imidodiphosphinato ligand bonds to central antimony through oxygen or sulfur atoms results in the formation of novel inorganic ring $SbO_2P_2N/SbOSP_2N$. Distorted octahedral geometry was present around the antimony.[81]

1.6.5 Reactions of $Ph_3SbCl_2/Ph_2SbCl_3$with phenolic pyrazole:

Our group has also investigated reactivity studies of various organoantimony(V) compounds with different protic ligands, for example, phenolic pyrazoles, naphthalicpyrazole,*t*-butylsilane triol and diol. Reactions of tri- and diorganoantimony halides (Ph_2SbCl_3, Ph_3SbCl_2) with phenolic pyrazoles (H_2PzPh, $H_2PhPzPh$) or naphthalicpyrazole (H_2NpPzH) in the presence of trimethylamine base yielded mono, di- and tetranuclear organoantimony oxo-hydroxo compounds $[(Ph_2Sb)_2(O)(PhPz)_2]$ (**32**), $[(Ph_2Sb)_2(O)(NpPz)_2]$ (**33**), $[(Ph_2Sb)_4(O)_4(OH)_2(HPhPzPh)_2]$ (**34**) respectively (**Scheme 17**). Based on single crystal XRD revealed that the presence of four-membered (Sb_2O_2), five-(Sb_2N_2O), Six- (Sb_2N_4) and eight-membered (Sb_4O_4) ring systems stabilized by phenolic pyrazole ligand system. A similar reaction of tri- and diorganoantimony halides (Ph_2SbCl_3, Ph_3SbCl_2) with N, O-donor ligands for example with 8-hydorxy quinolone (8-HQ) forms organoantimonyoxo bridged dimer $[(Ph_2Sb)_2(8\text{-}Hq)_2(O)_2]$,with 2-pyridine methanol(HPM) forms $[(Ph_3Sb)(PM)(Cl)]$, with triethanolamine (TEA) forms mononuclear organoantimony compound $[(Ph_2Sb)(TEA)]$, which crystalized in chiral space group.[82]

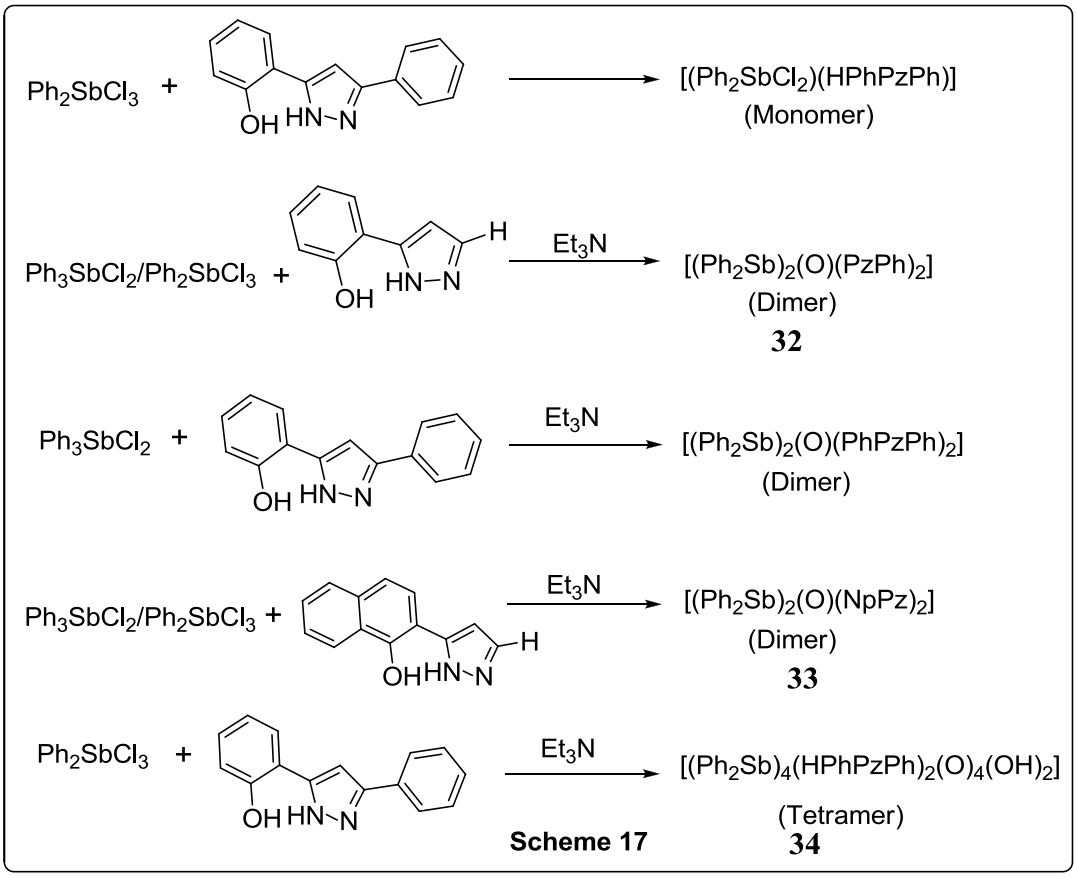

Scheme 17

1.6.6 Reactions of Ph_3SbCl_2/$Ph_2SbCl_3$with silanetriols and diols:

Reaction of diphenylantimonytrichloride with *t*-butyl or cyclohexylsilane triol and diphenyl silane diol in toluene at reflux conditions with Et_3N as a base affords hexanuclear organoantimony(V) oxo-hydroxo clusters, $[(Ph_2Sb)_4(PhSb)_2(RSiO_3)_2(O)_6(OH)_2]$ (**35**) (here R= *t*-butyl, cyclo-C_6H_{11}) and trinuclear antimony(V) and hexanuclear mixed valent antimony(III/V) oxo-hydroxo clusters $[(Ph_2Sb)(PhSb)_2(Ph_2SiO_2)_2(O)_3(OH)_2]$, (**36**) $[(Ph_2Sb)_4(Sb)_2(PhSiO_2)_2(O)_6(OH)_2]$, (**37**) respectively (**Scheme 18**). Interestingly this cluster assembly is built up of incomplete Sb_3O_4cubane sub units. Sb-C bond cleavage was also observed during the cluster formation. Here mixed valent antimony (III/V) cluster formation occurs from the reduction of organoantimony (V) starting material.[83]

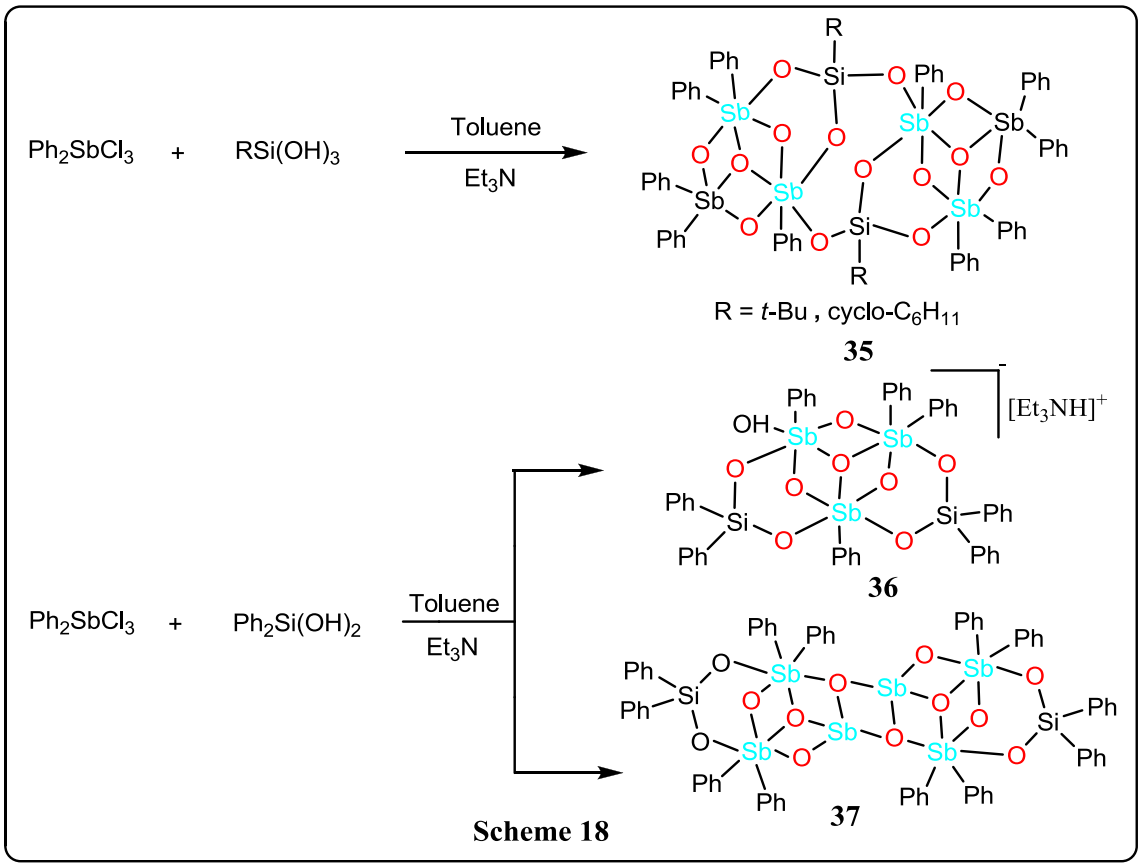

Scheme 18

1.6.7 Reactions of Ph_3SbCl_2/$Ph_2SbCl_3$with diorganotellurium oxides:

The reaction of diphenylantimonytrichloride with diphenyltellurium oxide in toluene solvent under reflux conditions results in the formation of Ph_2TeCl_2 as a major product and $[(PhSb)_4(O)_4(Ph_2ClSbO_2)_4]$ (**38**) as a minor product. Interestingly, the same reaction between diphenylantimony trichloride and dimesityltellurium oxide results in the formation of a lewis acid-base adduct $Ph_2SbCl_3.Mes_2TeO$ (Mes= mesityl) as the only product. Similar reaction of triphenylantimony dichloride with diphenyltellurium oxide/dimesityltellurium oxide affords Ph_3TeCl and $[(ClMes_2Te)_2O]$ respectively (**Scheme 19**).Here triphenylantimony dichloride/ diphenylantimony trichloride acts as a halogen transfer reagents. All the compounds were structurally characterized by single crystal XRD, IR, (^1H, ^{13}C and ^{125}Te) NMR spectroscopy. Here, diphenylantimony trichloride self-assembled in the presence of diphenyltellurium oxide to form a octanuclear organoantimony oxo cluster $[(PhSb)_4(O)_4(Ph_2ClSbO_2)_4]$, where four diphenylchlorostibinates formed the central Sb_4O_4 cubane core. In compound tetramesityl

ditelluroxane dichloride $[(ClMes_2Te)_2O]$ secondary C-H…Cl interactions are present and responsible for the formation of wave-like supramolecular structure.[84]

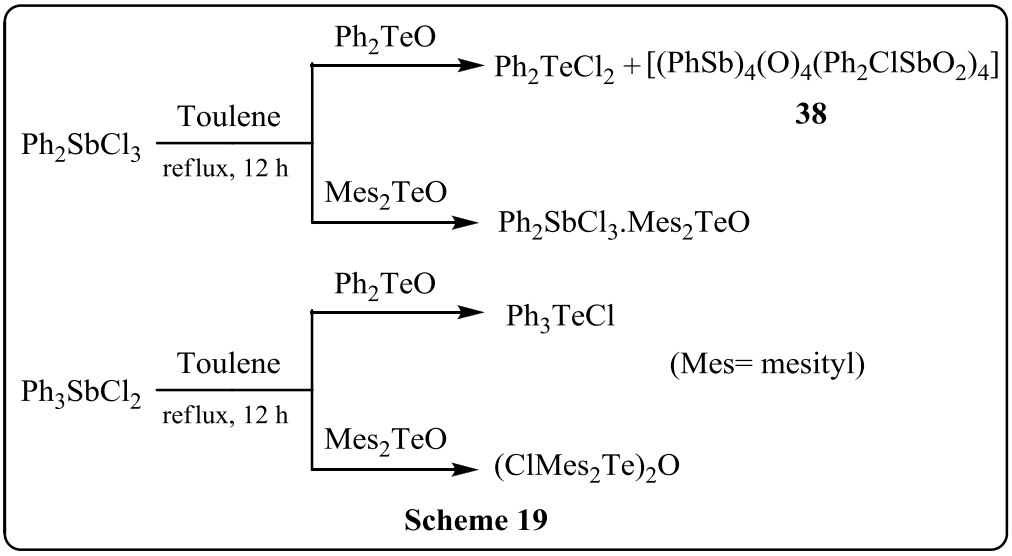

Scheme 19

1.6.8 Reaction of triarylantimony(V) oxide with phosphonic acids:

The reaction of polymeric triarylantimony oxide with phosphonic acids in the presence of dichloromethane solvent at room temperature affords organoantimony(V) complexes. With diphenylphosphinic acid and*t*-butylphosphonic acid it forms $[Ph_3Sb(Ph_2PO_2)_2]$ (**39**) and $[Ph_3Sb(t\text{-}BuPO_3H)_2]$ (**40**) respectively (**Scheme 20**). With phenylphosphinic acid, dinuclear organoantimony complex $[Ph_3Sb(HPhPO_2)_2]_2$ (**41**) is formed, this complex shows P-H three-bond coupling in solution ^{31}P NMR spectrum. With phenylseleninic acid, it forms different types of products depends on the crystallization solvent. If crystallized in dichloromethane solvent forms $[Ph_3Sb(PhSeO_2)_2]_2$ (**42**) and if crystalized in acetonitrile solvent, it forms $[(Ph_3Sb)_2(\mu\text{-}O)(\mu\text{-}PhSeO_2)_2]$ (**43**). Here interestingly, the compound $[Ph_3Sb(t\text{-}BuPO_3H)_2]$ undergoes further hydrolysis in toluene at reflux conditions in the presence of tetraethylammonium hydroxide as a base resulting in the formation of trinuclear organoantimony complex $\{(Ph_2Sb)_2(PhSb)(\mu_3\text{-}O)(\mu_2\text{-}O)_2(OH)_2(t\text{-}BuPO_3)_2[(C_2H_5)_4N]_2\}$, (**44**) in which *in situ* dearylation occur and also phenylstibinic acid $Ph_2Sb(O)(OH)$ and phenylstibonic acid $PhSbO_3H_2$ moieties are *in situ* generated during complex formation. All the compounds were structurally characterized by single crystal XRD, IR, (^1H, ^{13}C, ^{31}P and ^{77}Se) NMR spectroscopy.[85]

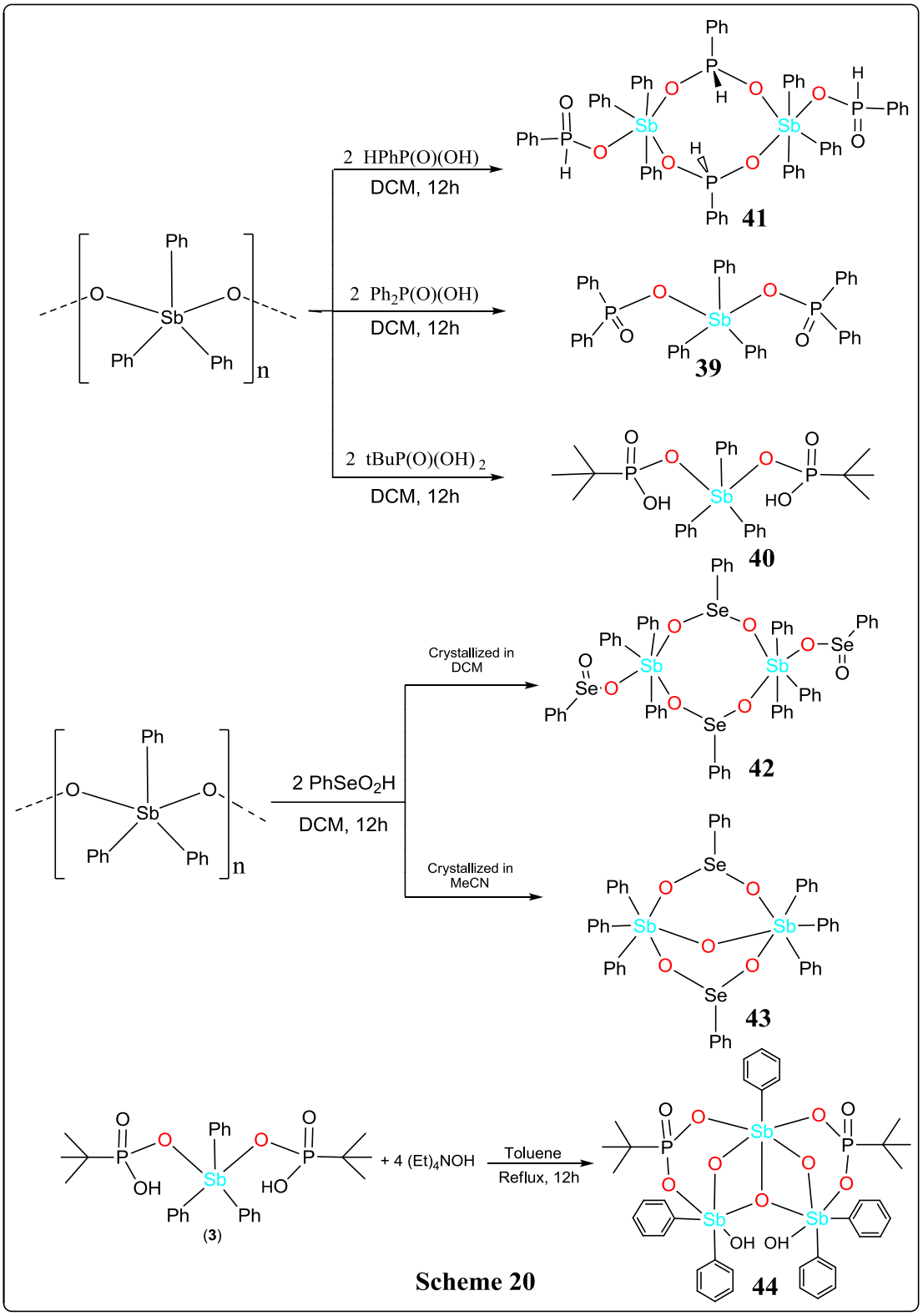
2 HPhP(O)(OH)
DCM, 12h
41
2 Ph2P(O)(OH)
DCM, 12h
39
2 tBuP(O)(OH)2
DCM, 12h
40
Crystallized in DCM
42
2 PhSeO2H
DCM, 12h
Crystallized in MeCN
43
(3)
+ 4 (Et)4NOH
Toluene
Reflux, 12h
44

Scheme 20

1.6.9 Reaction of triphenylantimony (V) oxide withdiphenyltellurium oxide:

The reaction of polymeric triphenylantimony oxide with diphenyltellurium oxide (1:2 molar ratios) in toluene at reflux conditions affords $\{(C_6H_5)_3Te\}_4\{[(C_6H_5)_2Sb^V]_4(Sb^{III})_4(O)_{12}(OH)_4\}$ (**45**) (**Scheme 21**) (**Figure 13**). The tetra anionic cluster core is stabilized with the help of weakly bounded four triphenyltellurium cations. Here two antimony tetramers are connected through μ_2-oxo bridges results in the formation of the Sb_8O_{16} core. Here interestingly mono dearylation occur and reduction of organoantimony(V) starting material happen, resulting in the formation of mixed valent organoantimony(III/V) clusters.[52]

$$(Ph_3SbO)_n + Ph_2TeO \xrightarrow[\text{reflux, 12h}]{\text{Toulene}} \{(C_6H_5)_3Te\}_4\{[(C_6H_5)_2Sb^V]_4(Sb^{III})_4(O)_{12}(OH)_4\}$$

45

Scheme 21

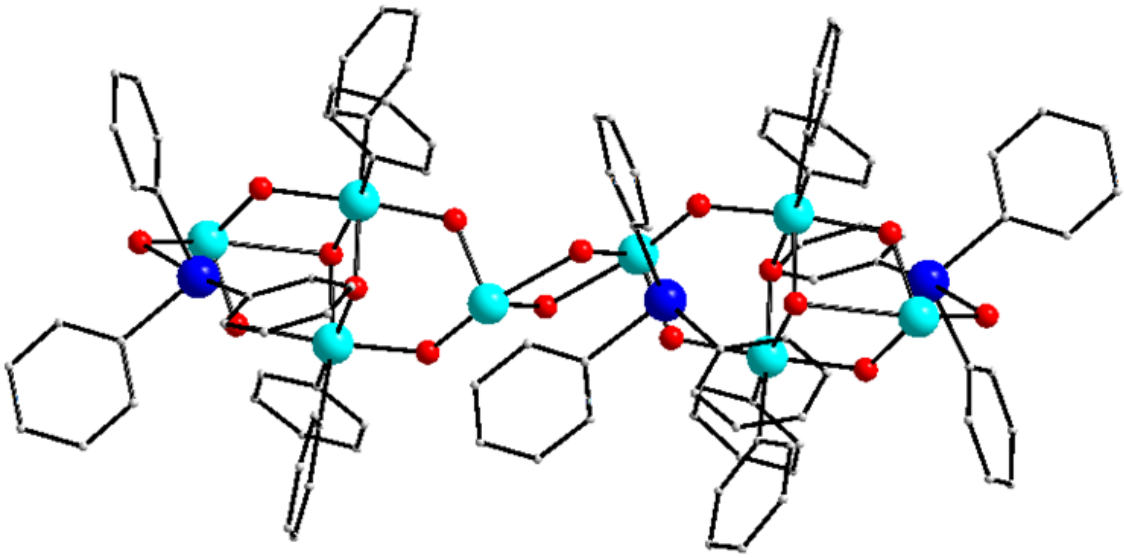

Figure 13: Molecular structure of $\{(C_6H_5)_3Te\}_4\{[(C_6H_5)_2Sb^V]_4(Sb^{III})_4(O)_{12}(OH)_4\}$ (**45**). Color code: Cyan: Sb, Blue: Te, Red: O.

1.6.10 Reactions of Ph_2SbCl_3 with silver acetate:

Sowerby *et al* reported the reaction of diphenylantimony trichloride with silver acetate in toluene, which affords oxygen-bridged compound $[Ph_2Sb(OAc)_2]_2O$ (**46**). In this compound around antimony, seven coordination numbers were present and the geometry around antimony is distorted pentagonal bipyramid. Further hydrolysis of diphenylantimony triacetate leads to the formation of the tetrameric complex $[Ph_8Sb_4O_6.(HOAc)_3]$ (**47**) (**Figure 14**). The structure consists of a non-adamantane type Sb_4O_6 basic structural unit. Two four-membered Sb_2O_2 rings are further connected through the μ_2-oxo bridge that forms the Sb_4O_6 cage.[86]

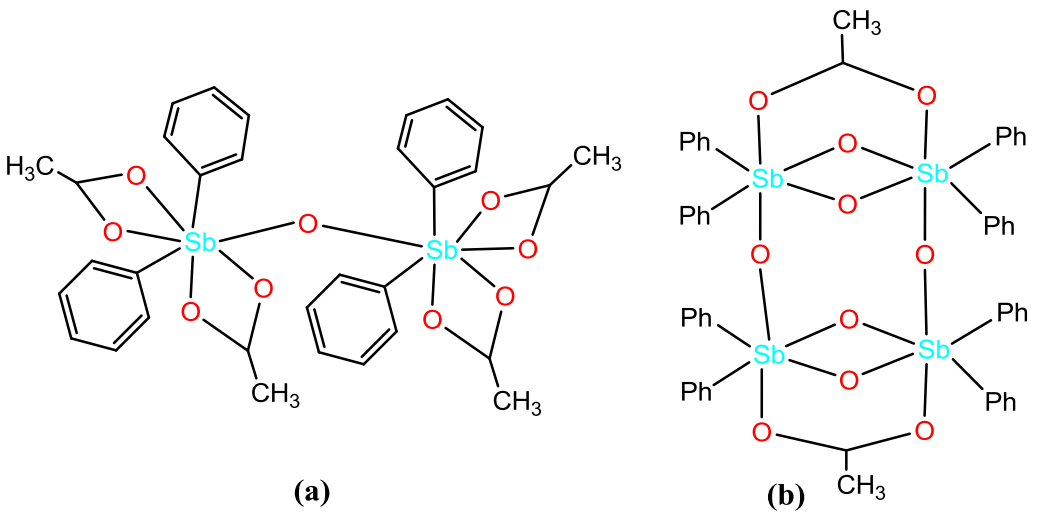

Figure 14: Structures of (a) $[Ph_2Sb(OAc)_2]_2O$ and (b) $[Ph_8Sb_4O_6.(HOAc)_3]$

1.7 Diorganoantimony based μ_4-peroxo complex:

Tetraorganodistibanes $(R_2Sb)_2$ (R= alkyl or aryl) are highly air-sensitive. Tetraaryldistibanes (aryl= Ph, *o*-Tol, *p*-Tol) are prepared by the reaction of R_2SbNa with $BrCH_2CH_2Br$ in liquid ammonia. Diorganoantimony based μ_4-peroxo complex was synthesized by treating tetra-*o*-tolyldistibines $R_2Sb\text{-}SbR_2$ with oxygen O_2(in the presence of air) and subsequent oxidation with H_2O_2 forms an intermediate compound $[(o\text{-Tol})_2Sb]_4O_6$ (**48**) (**Scheme 22**).The solution stability of this complex was identified by mass spectrometry. In solid state structure, all antimony atoms are present in corners of square planar arrangement.[87]

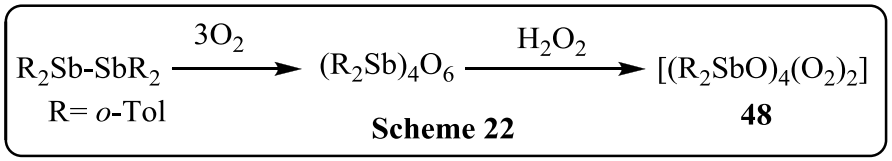

Scheme 22

1.8 Triply and Quadruply bridged organoantimony(V) compounds:

Sowerby *et al* synthesized several triply and quadruply bridged organoantimony(V) compounds by the reactions of $[(Ph_2SbBrO)_2]$ with $Na(O_2AsR_2)$ (R= Ph, Me). Quadruply bridged organoantimony(V) compound $[(Ph_2Sb)_2(\mu\text{-}O)_2(\mu\text{-}O_2AsMe_2)_2]$ (**49**) (**Figure 15**) were synthesized by treating $[(Ph_2SbBrO)_2]$ with 1 mole of $Na(O_2AsMe_2)$ in dichloromethane. The structure consists of a four-membered Sb_2O_2 ring chelated by arsenate ligands on both sides. Triply bridged organoantimony(V) compound $[(Ph_3Sb)_2(\mu\text{-}O)(\mu\text{-}O_2AsMe_2)_2]$(**50**) (**Figure 15**) was synthesized by treating $[(Ph_3SbBr)_2O])$ with 2 moles of $Na(O_2AsMe_2)$ in dichloromethane. All the compounds were structurally characterized by single crystal XRD, IR, ^1H, ^{13}C NMR spectroscopy and ESI-MS studies.[88]

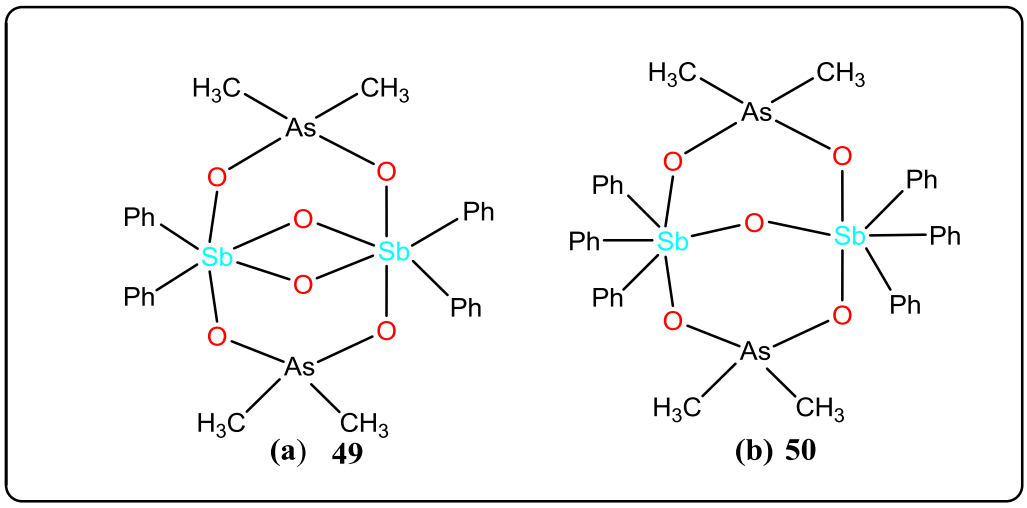

Figure 15: Structures of (a) Quadruply bridged compound and (b)Triply bridged compound

1.9 Hypervalency in Organoantimony (V) compounds:

In general, most of the organoantimony(V) complexes, antimony has a coordination number of five. In certain complexes, antimony shows six or seven coordination numbers. Even some times, it might reach eight due to the hypervalent nature of antimony. Bi- and tridentate ligands generally promote hypervalency, usually when the pendent arm's donor atoms coordinate through a dative bond to the antimony center. Reactions of diphenylantimony(V) trihalides (Ph_2SbCl_3), with silver salts of carboxylic acids, affords oxo- bridged carboxylates $[Ph_2Sb(O_2CPh)_2]_2O$ (**51**).Here antimony atoms are present in seven coordination numbers. Reaction of triphenylantimony(V) dihalides (Ph_3SbCl_2, Ph_3SbBr_2) with N-phenyl glycine or aryloxy acetic acids or triphenylgermanyl propionic acids results in the formation of seven coordinated organoantimony complexes (**Scheme 23**).[89]

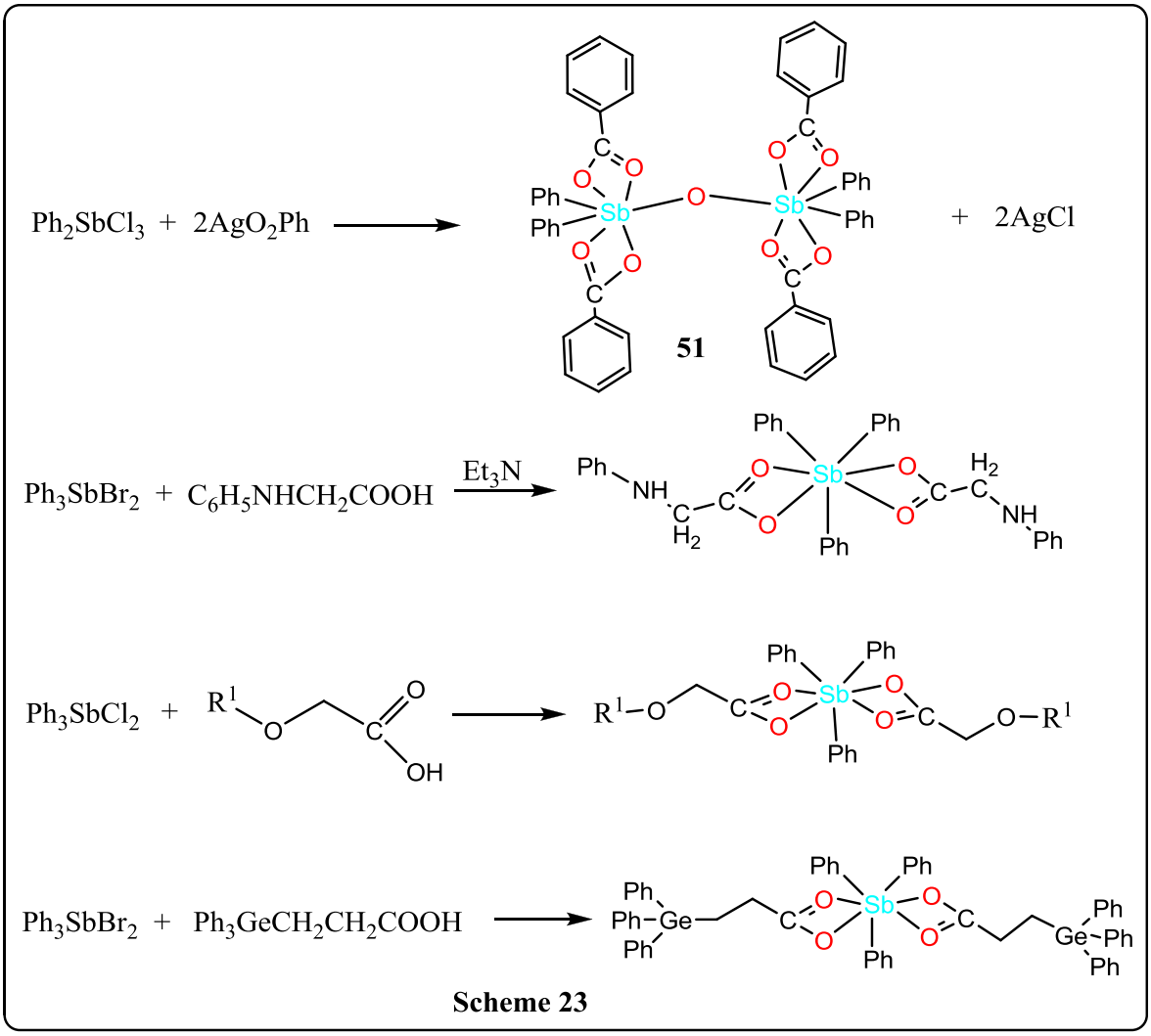

Scheme 23

1.9.1 Synthesis of hypervalent antimoniated Schiff base:

Sharma *et al* reported antimoniated Schiff bases by treating tris(*o*-formyl phenyl)stibine with (R)-4-dimethyl benzylamineor(R)-2-aminobutan-1-ol affords 1-[2-(bis{2-[(1-R-*p*-tolylethylimino)methyl]phenyl}stibanyl)benz-E-ilidene]-(1-R-*p*-tolylethyl)amine (**52**) and tris[(R)-2-benzyliden-2-yl-amino)butan-1-ol]stibine (**53**) respectively (**Scheme 24**). These two chiral antimoniated Schiff bases have been structurally characterized by ^{1}H, ^{13}C NMR spectroscopy, IR, single crystal XRD and mass spectrometry. In solid state structures, hypervalent interactions are present in between Sb and sp^2 N atoms. Interestingly in tris[(R)-2-benzyliden-2-yl-amino)butan-1-ol]stibine, around antimony atom eight coordination was possible due to intramolecular Sb-O interactions.[90]

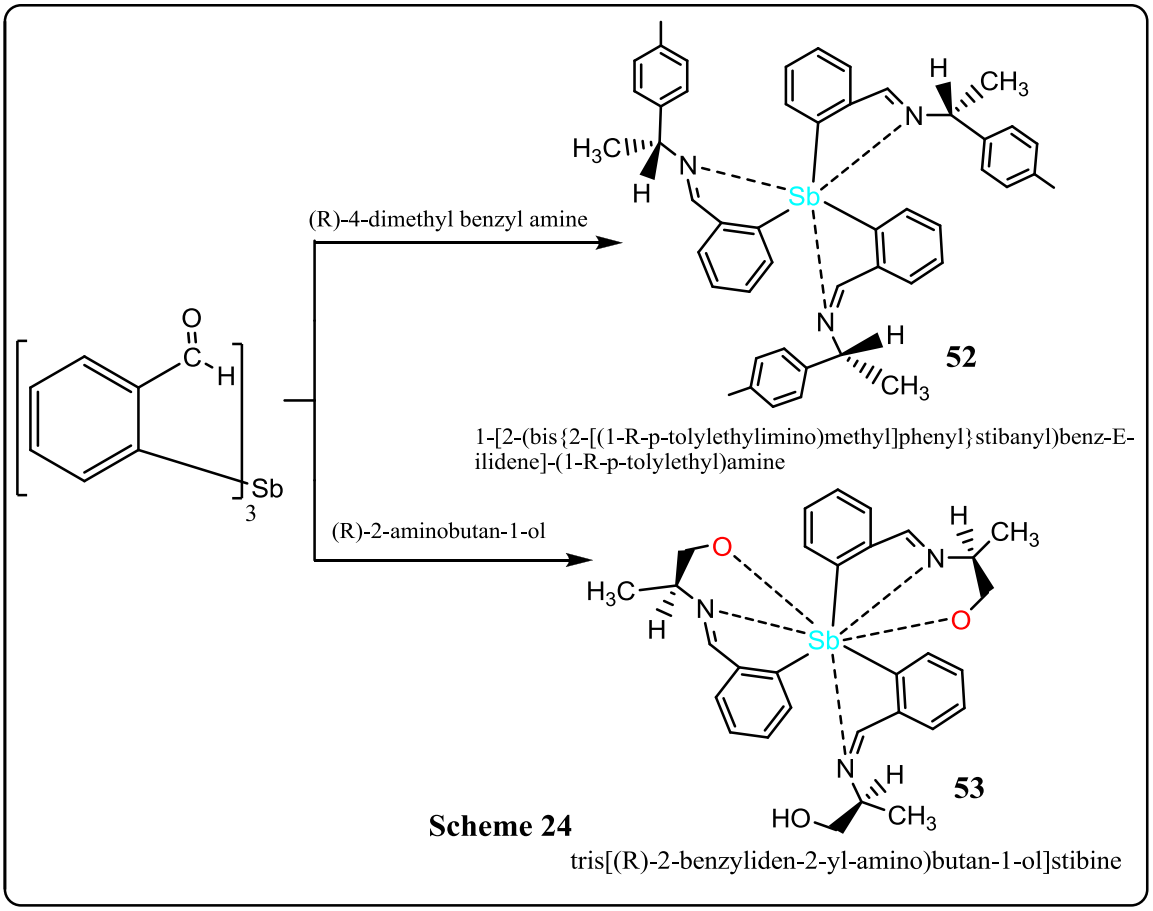

Scheme 24

1.10 Polyoxometalates (POMs):

Polyoxometalates (POMs) can be defined as a distinctive class of discrete anionic metal-oxygen clusters of early d-block elements in their higher oxidation states (e.g., W^{+6}, Mo^{+6}, V^{+5}). Berzelius synthesized the first POM in 1826 from the mixture of ammonium molybdate and phosphoric acid forms a yellow precipitate called ammonium 12-molybdophosphonate $(NH_4)_3[PMo_{12}O_{40}]$.[91] Few years later, heteropolymolybdate of Cr^{3+} and Fe^{3+} was reported by Struve.[92]In the early stage of the twentieth-century Keggin anion[93] $[PW_{12}O_{40}]$, Anderson-Evans isopolyanion $[Mo_7O_{24}]^{6-}$ and heteropolyanion[94]$[XMo_6O_{24}]^{n-}$, Lindquist anion[95] $[Mo_6O_{19}]^{2-}$and Wells-Dawson[96] $[P_2W_{18}O_{62}]^{6-}$ structures served as a platform for the discovery of new other compounds. In recent years, a number of researchers, for example, Pope and Muller have extensively investigated different polyoxoanions[97] and synthesized the largest POM, giant wheel-shaped polyoxomolybdate $\{Mo_{154}\}$, which is made up of 154 molybdenum atoms embedded in an oxygenatoms.[98]The coordination chemistry of POMs with transition metal cations was extensively studied for the last two decades. In contrast, exclusively only main group elements containing POMs are scarce, Although heteropolyoxometalates consist of main group elements reported in the literature.[99] Recently, Mehring *et al* reported that polynuclear giant bismuth (Bi_{38}) oxido clusters showed structural similarities with POMs.[100]POMs had an different structural topologies and various compositional versatility; they also show potential applications especially in the field of catalysis,[101] magnetism,[102] biochemistry[103] (electron transport inhibition), medicine[104] (anti-tumoral, antiviral and anti-HIV), electrochemistry,[105] photochromism[106], material science and nanotechnology.[107] Discrete polynuclear finite-sized metal oxo clusters and polyoxometalates are an important area of research; hence it is long believed that there finite-sized cluster assemblies/ POM could act as links between the molecular level components to extended metallic lattices. Studying properties of metal oxo-hydroxo clusters/ POMs could probably help in understanding the link between the properties exhibited by molecules at earlier stages of their associates to the stage wherein metallic networks are formed. Metal oxo-hydroxo clusters based on transition metal ions and lanthanides have been found to show various applications ranging from properties like SMMs to host for occlusion and transport of various gases.

The basic structural difference between metal oxo clusters and POM can be explained in the following manner. Metal clusters are finite compounds typically consisting of a large array of metal ions held together by ligand systems such as oxides, carboxylates, phosphinates, phosphonates and various well known Schiff base based systems. Usually metal oxo core is stabilized by ligand coordination present at the periphery of a cluster, which helps keep the metal oxo assembly together. The interaction between metal centers is determined by the varying manner of ligand coordination that binds the metal ion together. POM frameworks, on the other hand are usually assembled by varying pH of the solution wherein metal oxide-forming various cluster types as popularly known by some common structural form described as Keggin, Dawson wells and so on. At present, POMs functionalization with different organometallic moieties constitutes a fascinating area of interest and these substituted polyoxoanions can be used in crystal engineering.[108] Organotin functionalized polyoxoanions are used as an anti-tumor agents.[109]

1.10.1 Synthesis of first crystalline organostibonicmolybdate:

Sb (III) polyoxometalates (POMs) are well documented in the literature[110] due to their important applications in the field of biology, heterogenous oxidation catalysis. In contrast, the chemistry of organoantimony (V) functionalized POMs were quite rare. The first crystalline organoantimony (V) POM $[(Ph_2Sb)_2(\mu\text{-}O)_2(\mu\text{-}MoO_4)]^{2-}$ (**54**) (**Figure 16**) was reported by the Liu group in the year 1989.[111]Reaction of triphenylantimony di-iodide with tetra n-butylammoniummolybdate in dichloromethane solvent results in the formation of organostibonic molybdate, in which two MoO_4 tetrahedra units bridge to the Sb_2O_2 core. Here two octahedral Ph_2SbO_4 groups and two tetrahedral $MoO_4$are sharing four oxygen atoms alternatively. In the year 1994, Krebs *et al* synthesized isostructural tungsten analogue $(n\text{-}Bu_4N)_2[(Ph_2Sb)_2(\mu\text{-}O)_2(\mu\text{-}WO_4)]$ by treating Ph_2SbCl_3 with $(n\text{-}Bu_4N)[WO_4]$ in acetonitrile solvent.[112] Winpenny*et al* synthesized reverse Keggin ion $\{[Mn(PhSb)_{12}O_{28}][Mn_4(H_2O)]\}$, in which transition metal ions are encapsulated at the centerin the tetrahedral environment and twelve {PhSb} groups are present in addenda positions.[37] Nicholson *et al* also synthesized different polyoxostibonates $[M_2H_8(RSb)_{12}O_{30}]^{2-}$(M= Na, K) and $[LiH_3(p\text{-}MeC_6H_4Sb)_{12}O_{28}]^{4-}$ in the presence of the basic medium, detail study discussed in organostibonic acid reactivity part.[38]

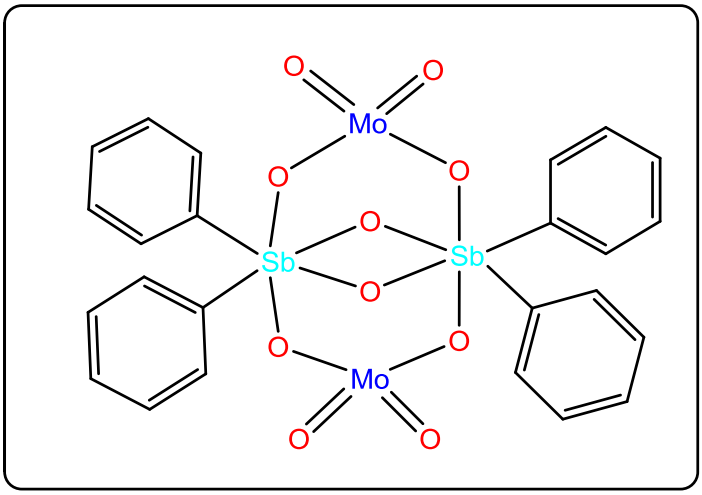

Figure 16: Structure of Organostibonicmolybdate $[(Ph_2Sb)_2(\mu\text{-}O)_2(\mu\text{-}MoO_4)]^{2-}$ (**54**).

1.10.2 Synthesis of Polyantimonate:

Antimonate easily undergoes polymerization in acidic solution, but the chemistry of polyantimonate still has not been investigated properly due to their poor solubility. Yagasaki *et al* reported the first inorganic polyantimonate by the reaction of antimonic acid $KSb(OH)_6$ with tetra n-butylammonium hydroxide solution affords $(n\text{-}Bu_4N)_4[Sb_8O_{12}(OH)_{20}]$. Molecular structure of this compound reveals four tetra n-butylammonium cations are stabilized the tetraanionic core $[Sb_8O_{12}(OH)_{20}]^{4-}$. The structure comprises four Sb_2O_{10} sub units and each Sb_2O_{10}moietiesarefurtherconnected by sharing the corners of the SbO_6octahedraand formation of the Sb_8O_{32} core occurs. The connection pattern of SbO_6octahedra in the $[Sb_8O_{12}(OH)_{20}]^{4-}$ was similar to the rutile structure. Further reaction of this polyantimonate $[Sb_8O_{12}(OH)_{20}]^{4-}$ with $(CH_3)(t\text{-}C_4H_9)SiOH$ silanol affords new polyantimonate $[Sb_4O_6(OH)_{10}]^{2-}$, it built around a Sb_4O_6 core. Another polyantimonate hexameric oxo-chloro-antimonate $[Sb_6O_{10}Cl_{14}]^{4-}$was synthesized by the phosphoraneiminato complex $(Ph_3PN)SbCl_2$ with chlorine, followed by partial hydrolysis in acetonitrile. The compound has tetraanionic core $[Sb_6O_{10}Cl_{14}]^{4-}$ and is stabilized by four Ph_3PNH^{2+}counter cations, in which central unit Sb_4O_6 skeleton is present.[113]

1.10.3 Synthesis of Lanthanide Antimony(III)Oxohalides:

Lanthanide antimony oxohalide nanocluster $[Pr_4Sb^{III}_{12}O_{18}Cl_{17}]^{5-}$ was synthesized by the hydrothermal reaction of praseodymium acetate $Pr(OAc)_3.H_2O$ with $SbCl_3$ in a mixture of water and 2-methyl pyridine. Single crystal XRD studies reveals that the compound consists of $[Pr_4Sb^{III}_{12}O_{18}Cl_{17}]^{5-}$ anionic cluster core; it is stabilized by five mono protonated 2-methylpyridine cations. The discrete cluster contains four deca coordinated Pr^{3+} ions, twelve Sb^{3+} ions in tetra coordinate trigonal bipyramid geometry, twelve μ_3-O ions, six μ_4-O ions, one μ_4-Cl ion, twelve terminal chloride ions and four additional chloride ions forming secondary bonds with Sb^{3+} cations only.[114]

X-Y Haung *et al* reported the first largest Sb(III) metal-based oxohalide cluster $[Ba_{13}Sb^{III}_{36}Cl_{34}O_{54}]^{8-}$. It is considered as the first example, consists of discrete alkaline earth metal ions and largest Sb metal based oxo chloride cluster. It was synthesized by the hydrothermal reaction of barium hydroxide, $SbCl_3$, water and 3-methyl pyridine results formation of barium-antimony-oxo-halide cluster $[Ba_{13}Sb^{III}_{36}Cl_{34}O_{54}]^{8-}$. The solid state structure consists of one centered eight coordinated Ba^{2+} ions, surrounded by twelve four coordinated Ba^{2+} ions and $\{Sb_{36}O_{54}\}$ moiety. Interestingly this cluster show high proton conductivity at room temperature as well as the high temperature at 70 ^oC.[115]

1.10.4 Synthesis of Sb(V), Sb(V/III) and Sb(III) functionalized POMs:

Synthesis and structural characterization of antimony containing polyoxomolybdates is an active research area due to molybdenum oxides containing antimony plays an important role in heterogeneous oxidation catalysis. Sasaki synthesized the first antimony containing polyoxomolybdate $[H_2Sb^{V}Mo_6O_{24}]$, it structure similar to well-known heptamolybdate.[116] J. Wang and coworkers reported novel mixed-valence antimony polyoxomolybdate $[Sb^{V}_4Sb^{III}_2Mo_{18}O_{73}(H_2O)_2]$. This polyoxoanion contains mixed-valence six antimony and 18 molybdenum atoms with oxygen networks, forming an unusual multilayer structure.[117] Novel antimony (V) substituted polyoxomolybdate $[Sb_4Mo_{12}(OH)_6O_{48}]$ has been synthesized by the reaction of heptamolybdate and antimony(V) oxide in an aqueous solution. The structure contains $Sb_4(OH)_6O_{14}$core,in which six oxygen atoms octahedrally coordinate to all antimony atoms. Based on bond valence calculations, all antimony atoms are in +5 oxidation state and all

the molybdenum are in +6 oxidation state. This POM was structurally characterized by single-crystal XRD, energy dispersive X-ray fluorescence analysis, Raman and IR spectroscopy.[118]

Recently U. Kortz's group reported various organoantimony functionalized POMs. Sandwich-type organoantimony (V) polyoxotungstophosphate $\{[PhSb^{V}(OH)_3[A\text{-}\alpha\text{-}PW_9O_{34}]\}^{9-}$ (**55**) (**Figure 17**)was obtained by the solvothermal reaction of diphenylantimony trichloride with $Na_9[A\text{-}\alpha\text{-}PW_9O_{34}]$ in a mixture of lithiumacetate buffer/methanol solution.[119] It has a dimeric, sandwich-type structure, in which three $\{PhSb^{V}(OH)\}$ octahedral fragments present in between two $\{PW_9\}$ Keggin units. Interestingly one phenyl ring is lost during the formation of this polyoxoanion.

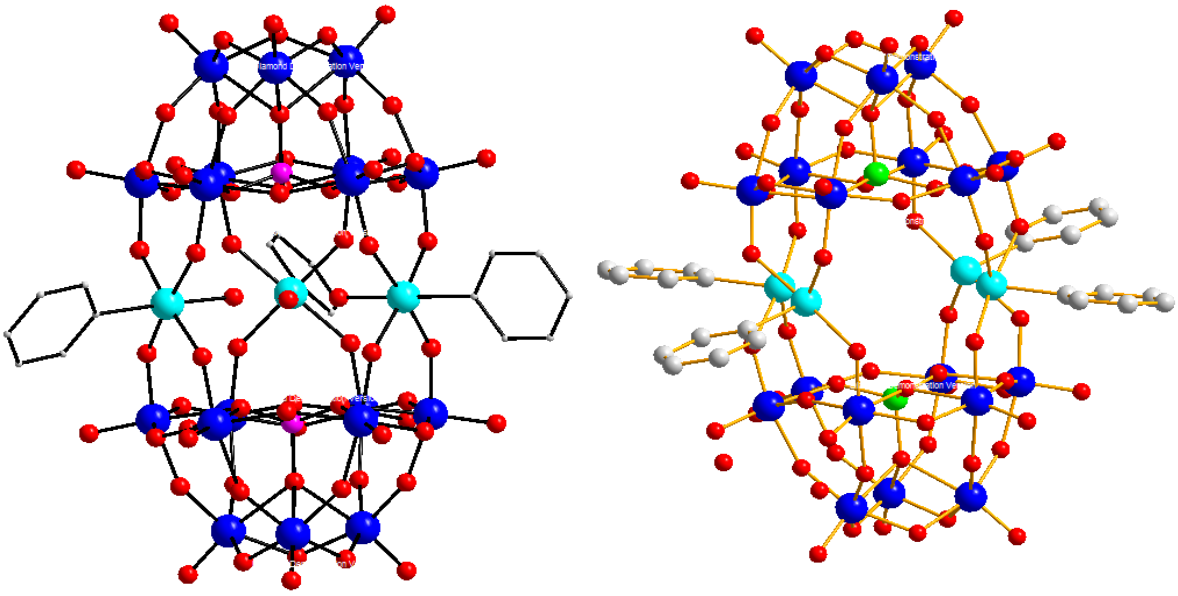

(a) **(b)**

Figure 17: Molecular structure of (a) $\{[PhSb^{V}(OH)_3[A\text{-}\alpha\text{-}PW_9O_{34}]\}^{9-}$ (**55**) and (b) $[(PhSb^{III})_4(A\text{-}\alpha\text{-}GeW_9O_{34})_2]^{12-}$ (**56**). Color code: Cyan: Sb, Blue: W, Pink: P, Green: Ge, Red: O.

The group also synthesized three discrete organoantimony(III) containing heteropolytungstates $[(PhSb^{III})_4(A\text{-}\alpha\text{-}GeW_9O_{34})_2]^{12-}$ (**56**), $[(PhSb^{III})_4(A\text{-}\alpha\text{-}PW_9O_{34})_2]^{10-}$, $\{[2\text{-}(Me_2NCH_2C_6H_4)Sb^{III}]_3(B\text{-}\alpha\text{-}AsW_9O_{33})]^{3-}$ and three sandwich-type phenylantimony(III) containing tungstoarsenates $[(PhSb^{III})(NaH_2O)As_2W_{19}O_{67}(H_2O)]^{11-}$, $[(PhSb^{III})_2As_2W_{19}O_{67}(H_2O)]^{10-}$, $[(PhSb^{III})_3(B\text{-}\alpha\text{-}AsW_9O_{33})_2]^{12-}$.

All the compounds were structurally characterized by heteronuclear (^{1}H, ^{13}C, ^{31}P and ^{183}W) NMR spectroscopy, IR, single crystal XRD and Thermogravimetric analysis (TGA). Solid state structure of these polyoxoanions suggest dimeric, sandwich-type structure, in which $\{PhSb^{(III)}\}$ fragments present in between two $\{A\text{-}\alpha\text{-}XW_9O_{34}\}$ (here X= Ge, P) Keggin units. Around antimony (III) atoms tetra coordination was present with sea saw geometry and lone pair of Sb(III) and phenyl groups are in equatorial positions. Based on biological studies of these POMs the gram-positive bacterium *Bacillus Subtills* has a slightly higher sensitivity towards these polyoxoanions as compared to the gram-negative organism *Escherichia Coli*, so based on the above observation, these polyoxoanions are may act as potent anti-microbial agents.[119]

1.11 Motivation and Aim of present work:

The first motivation of our work is to increase the solubility of arylstibonic acids. Arylstibonic acids are known since the last decade, but exact molecular structures are unknown due to their insolubility problems and they exist as white amorphous powders. To overcome insolubility problem of arylstibonic acids we introduced isopropyl, *t*-butyl, 2-butyl at para position of aniline resulting in the formation of soluble arylstibonic acids. Lipophilic arylstibonic acids have been synthesized and characterized.

Self-condensation reactions of arylstibonic acids with different protic ligands like phosphonic acids, phenylseleninic acid and silanetriol were carried out. Our aim is to synthesize the organoantimony clusters with other main group elements like phosphorus (P) and silicon (Si). Here arylstibonic acid phosphonate pro-ligands are also soluble in a common organic solvent, so we can further use this polydentate oxygen ligand to incorporate various metal ions.

An Arylstibonic acids partial condensation reaction with phosphonic acids affords organoantimony oxo-hydroxo clusters. These clusters act as pro-ligands and can coordinate with various transition metals under hydrothermal conditions in the presence of a base. Using a similar synthetic strategy, we plan to synthesize lanthanide metal clusters with mixed antimonate-phosphonate pro-ligand under hydrothermal conditions. The details of the experimental work carried out are given in chapter 2 to chapter 5.

1.12 References:

1. Wang and W. Chung, "*The Chemistry of Antimony*". 1919, London, 33.
2. U. S. Geological Survey, Mineral Commodity Summaries: Antimony (2016).
3. Grund, C. Sabina, K. Hanusch, H. J. Breuing and H. U. Wolf, "Antimony and Antimony Compounds" in Ullmann's Encyclopedia of Industrial Chemistry, Wiley-VCH, Weinheim (2016).
4. H. Ipser, H. Flandorfer, Ch. Luef, C. Schmetterer and U. Saeed, *J. Materials Sceince: Materials in Electronics.* 2007, **18**, 3-17.
5. Stellmann and M. Jeanne. Encyclopedia of Occupational Health and Safety: Chemical Industries and Occupations, 2000, 109
6. (a) K. Rajapure, C. Lokhande and C. Bhosle, *Thin Solid Films* 1997, **311**, 114; (b) I. Kim, *Mater. Lett.* 2000, **43**, 221; (c) B. Roy, B. R. Chakraborty, R. Bhattacharya and A. K. Dutta, *Solid State Commun.* 1978, **25**, 937; (d) O. Savadogo and K. C. Mandal, *Sol. Energy Mater. Sol. Cells* 1992, **26**, 117.
7. R. E. Krebs, *The History and Use of our Earth's Chemical Elements*, Greenwood Press, Westport, Conn, 2004, 219.
8. N. Ulrich, *Chem. Eng. News*, 2003, **81**, 126.
9. U. Brahmachari, *Br. Med. J.,* 1908, **1**, 1286–1288; (b) U. Brahmachari, *Br. Med. J.,* 1920, **2**, 324.
10. H. Schmidt, *J. Tropical Medicine and Hygiene* 1950, **53**, 95.
11. (a) J. V. Griensven, M. Balasegaram, F. Meheus, J. Alvar, L. Lynen and M. Boelaert, *Lancet Infect. Dis.*, 2010, **10**, 184–194; (b) A. Davis, Comparative Trials of Antimonial Drugs on urinary Schistosomiasis. Bull. W. H. O. 1968, **38**, 197.

12. (a) C. Silvestru, L. Silaghi-Dumitrescu, I. Haiduc, M. J. Begley, M. Nunn and D. B. Sowerby, *J. Chem. Soc., Dalton Trans.* 1986, 1031; (b) C. Silvestru, M. Curtui, I. Haiduc, M. J. Begley and D. B. Sowerby, *J. Organomet. Chem*. 1992, **49**, 426.

13. C. Silvestru, C. Socaciu, A. Baba and I. Haiduc, *Anticancer Res.* 1990, **10**, 803.

14. (a) R. Kant, A. K. Chandrashekar and K. S. Anil, *Phosphorus, Sulphur and Silicon* 2008, **183**, 1410; (b) R. Kant, K. Singhal, S. K. Shukla, A. K. Chandrashekar, A. K. Saxena, A. Rajan and P. Raj, *Phosphorus, Sulphur and Silicon* 2008, **183**, 2029.

15. K. Kohri, E. Yoshida, S. Yasuike, T. Fujie, C. Yamamoto and T. Kaji, *J. Toxicol. Sci.,* 2015, **40**, 321.

16. T. Fujie, M. Murakami, E. Yoshida, S. Yasuike, T. Kimura, Y. Fujiwara, C. Yamamoto and T. Kaji, *Int. J. Mol. Sci.,* 2016, **17**, 1381.

17. N. Fahmi, A. Kumari and R. V. Singh, *Int. J. Pharm. Sci.,and Research.* 2014, **5**, 5260.

18. (a) L. F. Piedra-Garza, M. H. Dickman, O. Moldovan, H. J. Breunig and U. Kortz, *Inorg. Chem*., 2009, **48**, 411.(b) M. Barsukova-Stuckart, L. F. Piedra-Garza, B. Gautam, G. Alfaro-Espinoza, N. V. Izarova, A. Banerjee, B. S. Bassil, M. S. Ullrich, H. J. Breunig, C. Silvestru and U. Kortz, *Inorg. Chem*., 2012, **51**, 12015; (c) P. Yang, B. S. Bassil, Z. Lin, A. Haider, G. Alfaro-Espinoza, M. S. Ullrich, C. Silvestru and U. Kortz, *Chem. Eur. J*. 2015, **21**, 15600.

19. (a) P. Yang, Z. Lin, B. S. Bassil, G. Alfaro-Espinoza, M. S. Ullrich, Ming-Xing Li, C. Silvestru and U. Kortz, *Inorg. Chem*., 2015, **21**, 15600. (b) P. Yang, Z. Lin, G. Alfaro-Espinoza, M. S. Ullrich, C. I. Rat, C. Silvestru and U. Kortz, *Inorg. Chem*., 2015, **21**, 15600.

20. (a) V. Rishi, W. J. Oha, S. L. Heyerdahl, J. Zhao, D. Scudiero, R. H. Shoemaker and C. Vinson, *Journal of Structural Biology,* 2010, **170**, 216–225; (b) S. L. Heyerdah, J. Rozenberg, L. Jamtgaard, V. Rishi, L.Varticovski, K. Akah, D. Scudiero, R. H. Shoemaker, T. S. Karpova, R. N. Day, J. G. McNally and C. Vinson*, European Journal*

of Cell Biology 2010, **89,** 564–573. (c) Y. Fujiwara, M. Mitani, S. Yasuike, J. Kurita and T. Kaji, *J. Health Sci*., 2005, **51**, 333.

21. (a) H. Kim, J. H. Cardellina, R. Akee, J. J. Champoux and J. T. Stivers, *Bioorganic Chemistry*, 2008, **36**,190–197; (b) L. A. Seiple, J. H. Cardellina, R. Akee and J. T. Stivers, *Mol Pharmacol.*, 2008, **73**, 669–677.

22. L. H. Mak, J. Knott, K. A. Scott, C. Scott, G. F. Whyte Yu Ye, D. Mann, O. Ces, J. Stivers and R. Woscholski, *Bioorg Med Chem*., 2012, **20**, 4371-4376.

23. J. Zhao, J. R. Stagno, L. Varticovski, E. Nimako, V. Rishi, K. McKinnon, R. Akee, R. H. Shoemaker, X. Ji and C. Vinson, *Molecular Pharmacology*, 2012, **82**, 814-823.

24. Q. Yang, A. G. Stephen, J. W. Adelsberger, P. E. Roberts, W. Zhu, M. J. Currens, Y. Feng, B. J. Crise, R. J. Gorelick, A. R. Rein, R. J. Fisher, R. H. Shoemaker and S. Sei, *Journal of virology*, 2005, **79**, 6122–6133.

25. J. McKelvie1, M. Richards, J. E Harmer, T. S Milne, P. L Roach and P. C. F. Oyston, *British Journal of Pharmacology,* 2013, **168** 172–188.

26. G. O. Doak, *J. Am. Chem. Soc*., 1940, 62, 167.

27. (a) H. Schmidt, *Justus* Liebigs *Ann. Chem.,* 1920, **421**, 174; (b) G. O. Doak, *J. Am. Chem. Soc.,* 1946, **68**, 1991.

28. G. O. Doak and H.G. Steinman, *J. Am. Chem. Soc.,* 1946, **68**, 1987.

29. M. Weiber and J. Waltz, *Z. Naturforsch. B: Chem. Sci.,* 1990, **45**, 1615.

30. (a) H. Schmidt, *Justus Liebigs Ann. Chem*., 1920, **421**, 174; (b) H. Schmidt, *Ber. Dtsh. Chem. Ges. B*., 1922, **55**, 697.

31. A. D. Macallum, *J. Soc. Chem. Ind.,* 1923, **42**, 468T.

32. L. H. Bowen and G. G. Long, *Inorg. Chem.,* 1978, **17**, 551.

33. (a) J. Beckmann, P. Finke, M. Hesse and B. Wettig, *Angew. Chem., Int. Ed*., 2008, **47**, 9982; (b) J. Brunig, E. Hupf, E. Lork, S. Mebs and J. Beckmann, *Dalton Trans*., 2015, **44**, 7105.

34. J. Beckmann, T. Heek and M. Takahashi, *Organometallics* 2007, **26**, 3633-3635.

35. M. Wieber, U. Simonis and D. Kraft, *Z. Naturforsch*. 1991, **B46**, 139.

36. J. Beckmann and M. Hesse, *Organometallics* 2009, **28**, 2345-2348.

37. V. Baskar, M. Shanmugam, M. Helliwell, S.J. Teat and R.E.P. Winpenny, *J. Am. Chem. Soc.,* 2007, **129**, 3042.

38. (a) C. J. Clark, B. K. Nicholson and C. E. Wright, *Chem. Commun*., 2009, 923; (b) B. K. Nicholson, C. J. Clark, C. E. Wright and T. Groutso, *Organometallics*, 2010, **29**, 6518.

39. B. K. Nicholson, C. J. Clark, C. E. Wright, S. G. Telfer and T. Groutso, *Organometallics*, 2011, **30**, 6612.

40. B. K. Nicholson, C. J. Clark, G. B. Jameson and S. G. Telfer, *Inorg. Chim. Acta*, 2013, **406**, 53.

41. B. K. Nicholson, C. J. Clark, S. G. Telfer and T. Groutso, *Dalton Trans*., 2012, **41**, 9964.

42. (a) S. Ali, V. Baskar, C. A. Muryn, and R. E. P. Winpenny, *Chem. Commun*., 2008, 6375; (b) S. Ali, C. A. Muryn, F. Tuna and R. E. P. Winpenny, *Dalton Trans*., 2010, **39**, 9588.

43. (a) E. K. Brechin, R. A. Coxall, A. Parkin, S. Parsons, P. A. Tasker and R. E. P. Winpenny, *Angew. Chem., Int. Ed*., 2001, **40**, 2700; (b) S. Maheswaran, G. Chastanet, S. J. Teat, T. Mallah, R. Sessoli, W. Wernsdorfer and R. E. P. Winpenny, *Angew. Chem., Int. Ed*., 2005, **44**, 5044; (c) M. Shanmugam, G. Chastanet, T. Mallah, R. Sessoli, S. J. Teat, G. A. Timco and R. E. P. Winpenny, *Chem.–Eur. J*., 2006, **12**, 8777; (d) M. Shanmugam, G. Chastanet, R. Sessoli, T. Mallah, W. Wernsdorfer and R. E. P. Winpenny, *J. Mater. Chem*., 2006, **16**, 2576; (e) H.-C. Yao, Y.-Z. Li, Y. Song, Y.-S. Ma, L.-M. Zheng and X.-Q. Xin, *Inorg. Chem*., 2006, **45**, 59; (f) Y.-S. Ma, Y. Song, Y.-Z. Li and L.-M. Zheng, *Inorg. Chem*., 2007, **46**, 5459; (g) M. Wang, C.-B. Ma, D.-Q. Yuan,

H.-S. Wang, C.-N. Chen and Q.-T. Liu, *Inorg. Chem*., 2008, **47**, 5580; (h) S. Konar and A. Clearfield, *Inorg. Chem*., 2008, **47**, 3489; (i) M. Wang, C. Ma, H. Wen and C. Chen, *Dalton Trans*., 2009, 994; (j) C. Dendrinou-Samara, C. A. Muryn, F. Tuna and R. E. P. Winpenny, *Eur. J. Inorg. Chem*., 2010, 3097.

44. S. Ali, C. A. Muryn, F. Tuna and R. E. P. Winpenny, *Dalton Trans.,* 2010, **39**, 124.

45. A. K. Jami and V. Baskar, *Organometallics*, 2010, **29**, 1137.

46. M. S. R. Prabhu, A. K. Jami and V. Baskar, *Organometallics*, 2009, **28**, 3953.

47. M. S. R. Prabhu, U. Ugandhar and V. Baskar, *Dalton Trans.,* 2016, **45**, 6963.

48. A. K. Jami and V. Baskar, *Dalton Trans.,* 2012, **41**, 12524.

49. (a) J. J. Vittal, *Polyhedron*, 1996, **15**, 1585; (b) W. Uhl, D. Kovert, S. Zemke and A. Hepp, *Organometallics*, 2011, **30**, 4736; (c) F. Bottomley, C. P. Magill and B. Zhao, *Organometallics*, 1991, **10**, 1946; (d) C. Schnitter, H. W. Roesky, T. Albers, H.-G. Schmidt, C. Röpken, E. Parisini and G. M. Sheldrick, *Chem.–Eur. J*., 1997, **3**, 1783; (e) K. Wraage, T. Pape, R. Hebrst-Irmer, M. Noltemeyer, H.-G. Schmidt and H. W. Roesky, *Eur. J. Inorg. Chem*., 1999, 869.

50. (a) D. Lu, A. D. Rae, G. Salem, M. L. Weir, A. C. Willis and S. B. Wild, *Organometallics* 2010, **29**, 32; (b) D. Lu, M. L. Coote, J. Ho, N. L. Kalih, C.-Y. Lin, G. Salem, M. L. Weir, A. C. Willis, S. B. Wild and P. J. Dilda, *Organometallics* 2012, **31**, 1808.

51. J. Brunig, E. Hupf, E. Lork, S. Mebs and J. Beckmann, *Dalton Trans*., 2015, **44**, 7105.

52. N. K. Srungavruksham and V. Baskar, *Dalton Trans*., 2015, **44**, 6358.

53. (a) Y. Z. Huang, Acc. *Chem. Res*. 1992, ***25***, 182. (b) W. I. Cross, S. M. Godfrey, C. A. McAuliffe, A. G. Mackie, R. G. Pritchard and N. C. Norman, (Ed.), *Chemistry of Arsenic, Antimony and Bismuth,* Ch. 5, Blackie Academic and Professional, London, 1998.

54. (a) R. Nomura, Y. Yamada and H. Matsuda, *Appl. Organomet. Chem*., 1989, **3**, 355. (b) R. Nomura, S. –I. Miyazaki, T. Nakano and H. Matsuda, *Appl. Organomet. Chem*., 1991, **5**, 513; (c) R. Nomura, Y. Yamada, T. Nakano and H. Matsuda, *J. Org. Chem*., 1991, **56,** 4076.

55. (a) Y. Z. Huang, C. Chen and Y. Shen, *J. Organomet. Chem*., 1989, **366**, 87;(b) Y. Z. Huang, Y. Shen and C. Chen, *Synth. Commun*., 1989, **83**; (c) Y. Z. Huang, *Acc. Chem. Res*., 1992, **25**, 182.

56. N. Kakusawa, Y. Tobiyasu, S. Yasuike, K. Yamaguchi, H. Seki and J. Kurita, *J. Organomet. Chem*., 2006, **691**, 2953.

57. (a) S-K. Kang, H-C. Ryu and Y-T. Hong, *J. Chem. Soc. Perkin Trans*. 2000, **1**, 3350; (b) S-K. Kang, H-C. Ryu and Y-T. Hong, *J. Chem. Soc. Perkin Trans*. 2000, **1**, 736.

58. S-K. Kang, H-C. Ryu and S-W Lee, *J. Organomet. Chem.* 2000, ***610*,** 38.

59. A. V. Gushchin, D. V. Moiseev and V. A. Dodonov, *Russ. Chem. Bull*. 2001, **50**, 1291.

60. (a) H. Schmidt, Liebigs. *Ann. Chem.* 1920, **421**, 174. (b) D. E. Worrall, *J. Am. Chem. Soc.* 1930, **52**, 2046.

61. I. Haiduc, C. Silvestru, K. J. Irgolic and K. A. French, *Inorg. Synth*., 1985, **23**, 194.

62. S. P. Bone and D. B. Sowerby, *J. Chem. Soc. Dalton Trans*., 1979, 715.

63. J. Bordner, G. O. Doak and J. R. Peters Jr, *J. Am. Chem. Soc*., 1974, **96**, 6763

64. T. N. Polynova and M. A. Porai-Koshits, *Zh. Strukt. Khim*., 1961, **2,** 477; (b) T. N. Polynova and M. A. Porai-Koshits, *Zh. Strukt. Khim*., 1966, **7,** 642.

65. S. E. Gukasyan, V. P. Gofkov, P. N. Zaikin and V. S. Sphinel, *Zh. Strukt. Khim*., 1973, **14**, 650.

66. A. F. M. M. Rahman, T. Murafuji, M. Ishibashi, Y. Miyoshi and Y. Sugihara, *J. Organomet. Chem*., 2005, **690**, 4280.

67. T. N. Polynova and M. A. Porai-Koshits, *J. Struct. Chem*., 1966, **5**, 691;

68. (a) J. Bordner, G. O. Doak and T. S. Everett, *J. Am. Chem. Soc*., 1986, **108**, 4206; (b) D. L. Venezky, C. W. Sink, B. A. Nevett and W. F. Fortescue, *J. Organomet. Chem*., 1972, **35**, 131; (c) W. E. McEwen, G. H. Briles and D. N. Schulz, *Phosphorus*, 1972, **2**, 147; (d) R. Rüther, F. Huber and H. Preut, *Z. Anorg. Allg. Chem*., 1986, **539**, 110

69. Y. Matano, H. Nomura, T. Hisanaga, H. Nakano, M. Shiro and H. Imahori, *Organometallics*, 2004, **23**, 5471.

70. (a) Y. Kawasaki and R. Okawara, *Bull. Chem. Soc. Japan* 1967, **40**, 428; (b) H. A. Meinema and J. G. Noltes, *J. Organometal. Chem*., 1969, **16**, 257; (c) H. A. Meinema, A. Mackor and J. G. Noltes, *J. Organometal. Chem*., 1972, **37**, 285; (d) N. Nishii, *Inorg. Nucl. Chem. Lett.* 1969, **5**, 529.

71. (a) H. A. Meinema and J. G. Noltes, *J. Organomet. Chem*., 1969, **16**, 257;(b) H. A. Meinema, A. Mackor and J. G. Noltes, *J. Organomet. Chem*., 1972, **37**, 285.

72. (a) F. D. Bianca, E. Rivarola, A. L. Spek, H. A. Meinema and J. G. Noltes, *J. Organomet. Chem*., 1973, **63**, 293; (b) H. A. Meinema, J. G. Noltes, F. D. Bianca, N. Bertazzi, E. Rivarola and R. Barbieri, *J. Organomet. Chem*., 1976, **107**, 249; (c) N. Bertazzi, F. D. Bianca, T. C. Gibb, N. N. Greenwood, H. A. Meinema and J. G. Noltes, *J. Chem. Soc. Dalton Trans*., 1977, 957.

73. A. Islam, J. G. D. Silva, F. M. Berbet, S. M. D. Silva, B. L. Rodrigues, H. Beraldo, M. N. Melo, F. Frézard and C. Demicheli, *Molecules*, 2014, **19**, 6009.

74. P. L. Millington and D. B. Sowerby, *J. Chem. Soc. Dalton Trans*., 1992, 1199.

75. F. Asghar, A. Badshah, A. Shah, M. Khawar Rauf, M. Irshad Ali, M. N. Tahir, E. Nosheen, Z-U. Rehman and R. J. Qureshi, *Organometal. Chem*., 2012, **717**, 8.

76. M. Hong, H. –D. Yin, W. –K. Li and X. –Y. You, *Inorg. Chem. Commun*., 2011, **14**, 1616.

77. Li. Quan, H. Yin, J. Cui, M. Hong, L. Cui, M. Yang and D. Wang, *J. Organometal. Chem*., 2009, **694**, 3683.

78. (a) H. –D. Yin, L. –Y. Wen, J. –C. Cui and W. –K. Li, *Polyhedron*, 2009, **28**, 2919; (b) J. Jiang, H. –D. Yin, F. Wang, Z. Han, F. Wang, S. Cheng and M. Hong, *Dalton Trans*., 2013, **42**, 8563; (c) L. Quan, H. –D. Yin, J. –C. Cui, M. Hong and D. Wang, *J. Organomet. Chem*., 2009, **694**, 3708; (d) H. –D. Yin, Q. Wu, M. Hong andW. Li, *Z. Anorg. Allg. Chem*., 2012, ***638*****,** 725.

79. (a) M. A. Said, K. C. K. Swamy, K. Babu, K. Aparna and M. Nethaji, *J. Chem. Soc., Dalton Trans*., 1995, 2151; (b) M. A. Said, K. C. K. Swamy, D. M. Poojary, A. Clearfield, M. Veith and V. Huch, *Inorg. Chem*., 1996, **35**, 3235.

80. V. Chandrasekhar and R. Thirumoorthi, *Organometallics*, 2009, **28,** 2637.

81. (a) C. Silvestru, A. Silvestru, I. Haiduc, D. B. Sowerby, K. H. Ebert and H. J. Bruenig, *Polyhedron*, 1997, **16**, 2643; (b) C. Silvestru and I. Haiduc, *Coord. Chem. Rev*., 1996, **147**, 117; (c) C. Silvestru, R. Rösler, I. Haiduc, R. A. Toscano and D. B. Sowerby, *J. Organomet. Chem*., 1996, **515,** 131.

82. (a) Pilli V. V. N Kishore, Junaid Ali, Gujju Narsimhulu and V. Baskar, *J. Chem. Sci.,* 2018*,* **130**, 100.

83. Pilli V V N Kishore and V. Baskar, *Inorg. Chem*., 2014, **53**, 6737.

84. N. K. Srungavruksham and V. Baskar, *Dalton Trans*., 2015, **44**, 6358.

85. N. K. Srungavruksham and V. Baskar, *Eur. J. Inorg. Chem., 2013*, 4345.

86. D. B. Sowerby, Michael J. Begley and P. L. Millington, *J. Chem. Soc. Chem. Commun.,* 1984, 896.

87. H. J. Breunig, T. Kruger and E. Lork, *J. Organomet. Chem.,* 2012, **648**, 209.

88. M. N. Gibbons and D. B. Sowerby, *J. Chem. Soc., Dalton Trans*., 1997, 2785.

89. (a) M. A. Said, K. C. Kumara Swamy, K. Babu, K. Aparna and M. J. Nethaji, *Chem. Soc. Dalton Trans.* 1995, 2151; (b) M. Dogamala, F. Huber and H. Preut, *Z. Anorg. Allg. Chem*. 1989, **571**, 130; (c) J. S. Li, G. Q. Huang, Y. T. Wei, C. H. Xiong, D. Q. Zhu and Q. L. Xie, *Appl Organomet Chem.,* 1998, **12**, 31; (d) Y. Q. Ma, J. S. Li, Z. N. Xuan and

R. C. Liu, *J .Organomet Chem.,* 2001, **620**, 235; (e) Y. Q. Ma, L. Yu and J. S. Li, *Heteroat.Chem*. 2002, **13,** 299.

90. P. Sharma, D. Perez, J. Vazquez, A. Toscano and R. Gutierrez, *Inorg. Chem. Commun*. 2007, **10**, 389.

91. Berzelius, *J. Pogg. Ann*., 1826, **6**, 369.

92. H. Struve, *J. Prakt. Chem.* 1854, **55**, 888.

93. (a) J. F. Keggin, *Nature* 1933, **131**, 968; (b) J. F. Keggin, *Nature* 1933, **132,** 351; (c) J. F. Keggin, *Proc. R. London Ser. A* 1936, **157**, 113.

94. H. T. Evans, *J. Am. Chem. Soc.* 1948, **70,** 1291.

95. I. Lindqvist, *Arkiv Kemi* 1950, **2**, 325.

96. B. Dawson, *Acta Crystallogr.* 1953, **6**, 113.

97. (a) M. T. Pope and A. Müller, *Angew. Chem. Int. Ed. Engl.* 1991, **30,** 34; *Angew. Chem*. 1991, **103**, 56;(b) L. C. W. Baker and D. C. Glick, *Chem. Rev.* 1998, **98**, 3;(c) G. M. Maksimov, *Russ. Chem. Rev.* 1995, **64**, 445; (d) M. T. Pope, *Heteropoly and Isopoly Oxometalates*; Springer-Verlag: Berlin, Germany, 1983.

98. A. Müller, E. Krickemeyer, J. Meyer, H. Bögge, F. Peters, W. Plass, E. Diemann, S. Dillinger, F. Nonnenbruch, M. Randerath and C. Menke, *Angew. Chem. Int. Ed. Engl.* 1995, **34,** 2122.

99. a) Y. Jeannin and J. Martin-Frère, *J. Am. Chem. Soc*., 1981, **103**, 1664; b) M. Bösing, I. Loose, H. Pohlmann and B. Krebs, *Chem. Eur. J*. 1997, **3**, 1232; c) P. Gouzerh and A. Proust, *Chem. Rev*. 1998, **98**, 77; d) A. M. Khenkin, L. J. W. Shimon and R. Neumann, *Eur. J. Inorg. Chem.* 2001, 789; e) U. Kortz, M. G. Savelieff, F. Y. A. Ghali, L. M. Khalil, S. A. Maalouf and D. I. Sinno, *Angew. Chem., Int. Ed*. 2002, **41**, 4070.

100. a) M. Mehring, D. Mansfeld, S. Paalasmaa and M. Schürmann, *Chem. Eur. J*. 2006, **12**, 1767; b) L. Miersch, M. Schlesinger, R. W. Troff, C. A. Schalley, T. Rüffer, H. Lang, D. Zahn and M. Mehring, *Chem. Eur. J*. 2011, **17**, 6985; c) L. Miersch, T. Rüffer,

D. Schaarschmidt, H. Lang, R. W. Troff, C. A. Schalley and M. Mehring, *Eur. J. Inorg. Chem.* 2013, 1427; d) M. Schlesinger, A. Pathak, S. Richter, D. Sattler, A. Seifert, T. Rüffer, P. C. Andrews, C. A. Schalley, H. Lang and M. Mehring, *Eur. J. Inorg. Chem.* 2014, 4218.

101. (a) F. Cavani and F. Trifiro, *Catal*. *Today* 1999, **51**, 561; b) S. Ellis and I. V. Kozhevnikov, *J. Mol*. *Catal*. 2002, **187**, 227; c) B. B. Bardin and R. J. Davis, *Appl*. *Catal*. 1999, **185**, 283; d) A. M. Khenkhin and R. Neumann, *J. Am*. *Chem*. *Soc*. 2001, **123**, 6437; e) H. Weiner and R. G. Finke, *J. Am*. *Chem*. *Soc*. 1999, **121**, 983.

102. (a) J. M. Clemente-Juan and E. Coronado *Coord. Chem. Re*v. 1999, **193**, 361. (b) P. Kogerler, B. Tsukerblat and A. Muller, A. *Dalton Trans.* 2010, **39,** 21.

103. (a) J. T. Rhule, C. L. Hill, D. A. Judd and R. F. Schinazi, *Chem*. *Rev*. 1998, **98**,327; b) R. Zheng and F. Schinazi, *Top*. *Biol*. *Inorg*. *Chem*. 1999, **2**, 117.

104. (a) T. Yamase, H. Fujita and K. Fukishima, *Inorg*. *Chim*. *Acta* 1988, **151**, 15; b) T. Yamase, Y. Tomita and H. Fujita, *Biomed*. *Pharm*. *Appl*. 1991, **13**, 187; c) Y. Tajima, *Biol*. *Pharm*. *Bull*. 2001, **24**, 1079; d) Y. Tajima, *Biomed*. *Res*. 2002, **23**, 115; e) Y. Tajima, *J. Inorg*. *Biochem*. 2003, **94**, 155.

105. B. Keita and L. Nadjo, Electrochemistry of Polyoxometalates. In *Encyclopedia of Electrochemistry*; A. J. Bard and M. Stratmann, Eds.; Wiley-VCH: New-York, 2006; Vol. 7, p 607.

106. T. He and J. Yao, *Prog. Mater. Sci.* 2006, **51**, 810.

107. (a) D. L. Long, E. Burkholder and L. Cronin, *Chem. Soc. Rev.*, 2007, **36**, 105; (b) C. L. Hill, *J. Molec. Catal. A: Chem.*, 2007, **262**(1-2); (c) D. L. Long, R. Tsunashima and L. Cronin, *Angew. Chem., Int. Ed.*, 2010, **49**, 1736; (d) A. Dolbecq, E. Dumas, C. R. Mayer and P. Mialane, *Chem. Rev.*, 2010, **110**, 6009.

108. P. Gómez-Romero, *Adv*. *Mater*. 2001, **13**, 163. (b) F. Ribot and C. Sánchez, *Comments Inorg*. *Chem*. 1999, **20**, 327.

109. Z. Dong, R. Tan, J. Cao, Y. Yang, C. Kong, J. Du, S. Zhu, Y. Zhang, J. Lu, B. Huang and S. Liu, *Eur. J. Med. Chem*. 2011, **46**, 2477−2484.

110. (a) J. Fisher, L. Ricard, R. Weiss, *J. Am. Chem. Soc.* 1976, **98**, 3050; (b) T. Yamase, H. Naruke, Y. Sasaki, *J. Chem. Soc., Dalton Trans.*1990, 1687; (c) Y. Ozawa, Y. Sasaki, *Chem. Lett.* 1987, 923; (d) M. Bösing, I. Loose, H. Pohlmann, B. Krebs, *Chem. Eur. J.* 1997, **3**, 1232; (e) I. Loose, E. Droste, M. Bösing, H. Pohlmann, M.H. Dickman, C. Rosu, M. T. Pope, B. Krebs, *Inorg. Chem.* 1999, **38**, 2688.

111. B. Liu, Y. Ku, M. Wang, B. Wang and P. Zheng, *J. Chem. Soc., Chem. Commun.*1989, 651.

112. B. Krebs, In: *Polyoxometalates: From Platonic Solids to Antiretroviral Activity*; M. T. Pope, A. Müller, Eds.; Kluwer: Dordrecht, The Netherlands, 1994.

113. H. Nakand, Y. Ozawa and A. Yagasaki, *J. Am.Chem. Soc*., 1995, **117**, 12007. (b) H. Nakand, Y. Ozawa and A. Yagasaki, *Inorg. Chem*., 2001, **40**, 2634.

114. B. Hu, M. L. Feng, J. R. Li, Q. P. Lin and X. Y. Huang, *Angew. Chem., Int. Ed*., 2011, **50**, 8110.

115. Z-F Wu, B. Hu, Z-H Fu, H. Wang, G. Xu, L-K.Gong, G-D. Zou, X. Y. Huang and J. Li, *Chem. Comm*., 2019, **55**,7442.

116. Y. Sasaki and A. Ogawa, *Some Recent Developments in the Chemistry of Chromium, Molybdenum and Tungsten*; J. R. Dilworth, M. F. Lappert, Eds.; Royal Society of Chemistry: London, 1982; p 59.

117. G. Xue, X. Liu, H. Xu, H. Hu, F. Fu and J. Wang, *Inorg. Chem*., 2008, **47**, 2011.

118. D. Drewes, G.Vollmer and B. Krebs, *Z. Anorg. Allg. Chem.* 2004, **630**, 2573.

119. a) L. F. Piedra-Garza, M. H. Dickman, O. Moldovan, H. J. Breunig and U. Kortz, *Inorg. Chem.* 2009, **48**, 411; b) M. Barsukova-Stuckart, L. F. Piedra-Garza, B. Gautam, G. Alfaro-Espinoza, N. V. Izarova, A. Banerjee, B. S. Bassil, M. S. Ullrich, H. J. Breunig, C. Silvestru and U. Kortz, *Inorg. Chem*., 2012, **51**, 12015; c) P. Yang, B. S. Bassil, Z. Lin, A. Haider, G. Alfaro-Espinoza, M. S. Ullrich, C. Silvestru and U. Kortz, *Chem. Eur. J.* 2015, **21**, 15600; d) P. Yang, Z. Lin, B. S. Bassil, G. Alfaro-Espinoza, M. S. Ullrich, Ming-Xing Li, C. Silvestru and U. Kortz, *Inorg. Chem*., 2016, **55**, 3718; e) P. Yang, Z. Lin, G. Alfaro-Espinoza, M. S. Ullrich, C. I. Rat, C. Silvestru and U. Kortz, *Inorg. Chem*., 2016, **55**, 251.

Monoorganoantimony (V) Phosphonates and PhosphoSelininates

Chapter 2

Abstract: Molecular oxo-hydroxo clusters based on monoorganoantimony(V) motifs have been assembled by the reactions of arylstibonic acids with protic ligands like *t*-butylphosphonic acid, phenylphosphonic acid, phenylseleninic acid and *t*-butylsilane triol. Interestingly reaction of arylstibonic acid with *t*-butylsilanetriol has led to the isolation of organoantimony(V) based molecular triangle stabilized by siloxane frameworks. Single crystal X-ray structural elucidation revealed the formation of [(*p*-iPr-$C_6H_4Sb)_4(OH)_4$(*t*-$BuPO_3)_6$](**2.1**), [(*p*-*t*-Bu-$C_6H_4Sb)_4(O)_2(PhPO_3)_4(PhPO_3H)_4$](**2.2**), [(*p*-iPr-$C_6H_4Sb)_4(O)_4(PhSeO_2)_2$(*t*-$BuPO_3)_4$(*t*-$BuPO_3H_2)_2$](**2.3**), [(*p*-Me-$C_6H_4Sb)_4(O)_4(PhSeO_2)_2$(*t*-$BuPO_3)_4$(*t*-$BuPO_3H_2)_2$](**2.4**), [(*p*-*t*-Bu-$C_6H_4Sb)_2(O)(PhSeO_2)_2$(*t*-$BuPO_3H)_4$] (**2.5**) and [(*p*-iPr-$C_6H_4Sb)_3${(*t*-$BuSiO_2)_4$(*t*-$BuSiO_2OH)_2$}(μ_3-O)(μ-$OH)_2$] (**2.6**) respectively. ESI-MS studies revealed that the clusters maintain their structural integrity in the solution also. Solution NMR studies (^{1}H, ^{31}P, ^{77}Se and ^{29}Si) show spectral patterns which correlates well with the observed solid state structures of **2.1-2.6**.

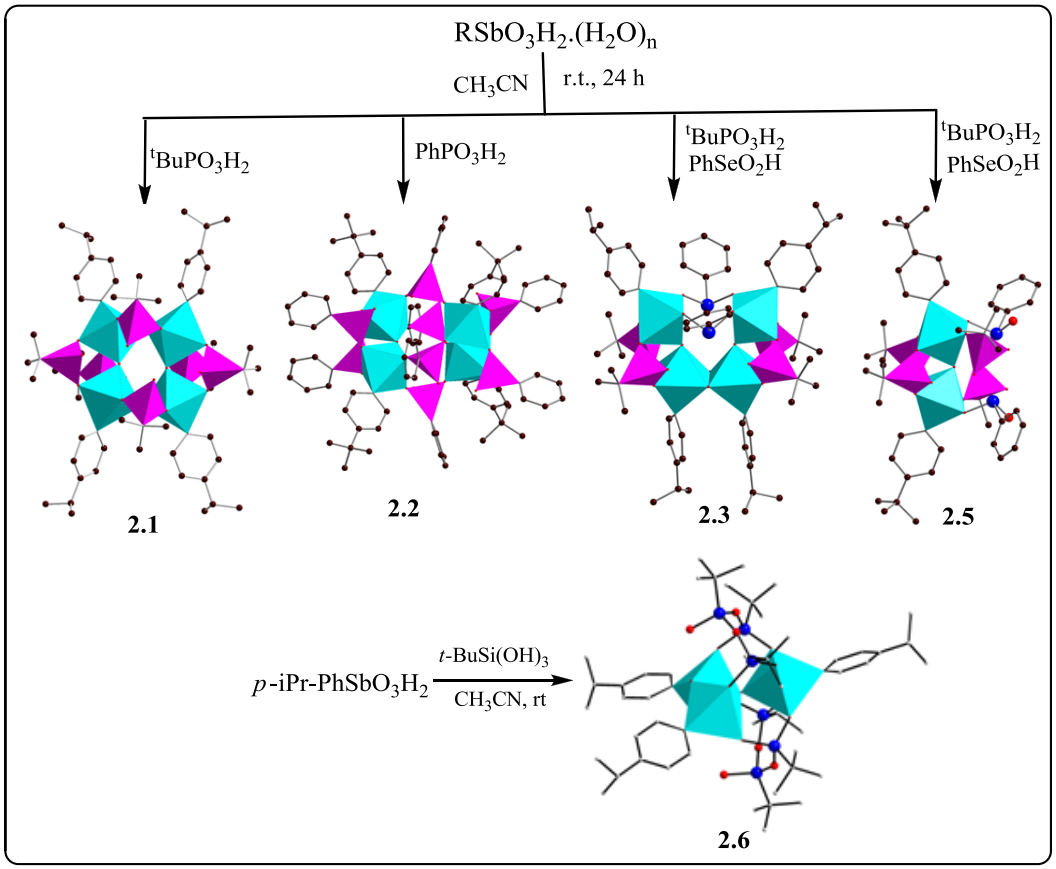

2.1 Introduction

The ability of organostibonate-phosphonate cluster to act as pro-ligand for assembling cobalt based molecular clusters has been reported in 2007.[1] Though stibonates and phosphonates can independently act as ligands towards metal ions, the pro-ligand cluster method provides a single source precursor combining the coordinating ability of stibonates and phosphonates motifs, that can serve as a novel ligand platform which could be employed for stabilizing new types of polynuclear metal based oxo hydroxo systems. Synthesis and structural characterization of organoantimony (V) based molecules and clusters have gained attention and is currently an area of active research.[2] Beckmann *et al* reported the synthesis and structural characterization of organostibonic acids stabilized by bulky organic substituents on the antimony atom.[3] Apart from X-ray structure determination, mass spectrometry has also been used to understand the basic structural motifs involved in the assembly of organostibonate based polyoxometallates (POMs) systems.[4] The biological activity exhibited by organostibonic acids needs a special mention.[5] Recent reports have also suggested the potential application of organostibonic acids as antimicrobial agents.[6]

In this manuscript, synthesis of new organostibonates / phosphonates based molecular clusters and a three component system (Sb/P/Se) involving reactions of organostibonates with phosphonic acid and seleninic acid are discussed. Reaction of *p*-chlorophenylstibonic acid with *t*-butylphosphonic acid led to the isolation of the dinuclear organoantimony (V) oxo cluster as reported by Winpenny *et al*.[7] In the present study, use of *p*-isopropyl and *p*-tertiary butyl substituents on phenylstibonic acid have been used as starting materials. Importantly these organostibonic acids are soluble in common organic solvents, unlike the literature reported example wherein the *p*-halophenylstibonic acids are insoluble white powders.[4] The intention of this study is twofold, 1) to investigate the change in reactivity of organostibonic acids with the change in organic substituents on the Sb atom and 2) to analyze the solubility difference of the organostibonic acids would affect the reactivity part on reaction with various protic ligand systems. Synthesis and structural characterization of discrete main group based molecular oxo-hydroxo clusters containing antimony, phosphorus and selenium atoms are reported in this manuscript. ESI-MS studies reveal that the integrity of solid state structures is retained in solution as well.

2.2 Experimental Section

2.2.1 General Information:

Arylstibonic acids[8] (aryl= *p*-isopropylphenyl, *p*-*t*-butylphenyl and *p*-methylphenyl), *t*-butylphosphonic acid[9] and *t*-butylsilane triol[10] were synthesized according to literature reports. Phenylseleninic acid, phenylphosphonic acid, solvents and common reagents were purchased from commercial sources. All the compounds used were dried under a high vacuum for half an hour before subjected to spectroscopic and elemental analysis.

2.2.2 Instrumentation:

Infrared spectra were recorded with a JASCO-5300 FT-IR spectrometer as KBr pellets. The solution ^{1}H, ^{13}C, ^{31}P, ^{77}Se and ^{29}Si NMR spectra were recorded with a Bruker AVANCEIII 400 instrument. Elemental analysis was performed with a Flash EA Series 1112 CHNS analyzer. ESI-MS spectra were recorded using Bruker Maxis HRMS (ESI-TOF analyzer) equipment. Single-crystal X-ray data collection for compounds **2.1–2.6** was carried out at 100(2) K with a Bruker Smart Apex CCD area detector system [λ (Mo-Kα) = 0.71073 Å] with a graphite monochromator. The data were reduced using SAINTPLUS. The structures were solved using SHELXS-97[11] and refined using the program SHELXL-2014/7.[12, 13] All non-hydrogen atoms were refined anisotropically. In **2.2** the disorder associated with phenyl rings were constrained using EADP, ISOR, DELU, SIMU instructions in SHELXL-2014/7. The compound **2.3** have residual electron density owing to solvent of crystallization (acetonitrile) which could not be properly fixed. In, **2.4** disordered solvent accessible voids are present in the asymmetric unit. These solvent contributions were removed by using the SQUEEZE[14] command in PLATON[15]. The total electron count 64 (belongs to three disordered acetonitrile solvent molecules) with a void volume of 343 $Å^3$ (8%) per unit cell in **2.4** was removed by SQUEEZE.

2.2.3 Synthetic procedure for compounds 2.1-2.6:

The general synthetic methodology adopted is as follows: The appropriate reagents (Organostibonic acid/Phosphonic acid/Seleninic acid/*t*-butylsilanetriol) were taken in 1:2 (or) 1:1:1 mole ratios and stirred in acetonitrile (15mL) for 24 h at room temperature resulting in the formation of a white cloudy solution. The solution was filtered and on slow evaporation of

acetonitrile, crystals were isolated. Colorless block crystals suitable for single crystal X-ray studies were grown from acetonitrile filtrate in one week time. Molar ratios and weights of the reactants used are as follows.

Compound **2.1:** *p*-Isopropylphenylstibonic acid (0.100g, 0.343 mmol) and *t*-butylphosphonic acid (0.095g, 0.687 mmol). Yield: 0.136 g (86% based on *p*-isopropylphenylstibonic acid). Decp temp: 275-276 ^{o}C. Anal, Calcd (%) for $C_{60}H_{102}O_{22}P_6Sb_4$ (1848.32): C 38.99, H 5.56. Found: C 39.12, H 5.41. ^{1}H NMR (400 MHz, $CDCl_3$, ppm) δ: 7.78 (d, 8H), 7.21(d, 8H), 3.00-2.90 (m, 4H), 1.25(d, 24H), 1.21(d, 18H), 1.14(d, 18H), 0.86(d, 18H).^{13}C NMR (100 MHz, $CDCl_3$) δ: 150.47, 133.09, 125.94, 34.06, 32.42, 30.96, 25.26, 23.93 ppm. ^{31}P{^{1}H} NMR (162 MHz, $CDCl_3$) δ: 34.47, 32.09, 24.99 ppm. IR (cm-1, KBr pellet): 3402(wide), 2964(s), 2909(m), 2876(s), 1479(s), 1397(s), 1364(w), 1252(m), 1074(m), 986(m), 816(s), 652(s), 553(s).

Compound **2.2**: *p*-t-Butylphenylstibonic acid (0.100g, 0.327 mmol) and phenylphosphonic acid (0.103 g, 0.655 mmol). Yield: 0.148 g (79% based on *p*-t-butylphenylstibonic acid). Decp temp: 267-268 ^{o}C. Anal, Calcd (%) for $C_{88}H_{96}O_{26}P_8Sb_4$ (2304.51): C 45.86, H 4.20. Found: C 45.62, H 4.38. ^{1}H NMR (400 MHz, $CDCl_3$, ppm) δ: 7.90-7.75 (m, 16H), 7.65 (d, 8H), 7.53-7.40(m, 16H), 7.35(d, 8H), 7.15(d, 8H), 1.20(s, 36H). ^{13}C NMR (100 MHz, $CDCl_3$,) δ: 153.44, 144.68, 132.45, 129.51, 127.67, 126.25, 125.44, 34.69, 31.08 ppm. ^{31}P{^{1}H} NMR (162 MHz, $CDCl_3$) δ: 12.09, 0.85 ppm. IR (cm-1, KBr pellet): 3063(wide), 2959(s), 2866(m), 1436(s), 1397(s), 1140(m), 1090(s), 1014(s), 981(s), 822(m), 756(s), 718(m), 690(s), 542(s).

Compound **2.3**: *p*-Isopropylphenylstibonic acid (0.100g, 0.343 mmol), *t*-butylphosphonic acid (0.048g, 0.343 mmol), and phenylseleninic acid (0.065g, 0.343 mmol). Yield: 0.124 g (65% based on *p*-isopropylphenylstibonic acid). Decp temp: 280-281 ^{o}C. Anal, Calcd (%) for $C_{72}H_{114}O_{26}P_6Se_2Sb_4$ (2226.46): C 38.84, H 5.16. Found: C 38.76, H 5.21. ^{1}H NMR (400 MHz, $CDCl_3$) δ: 8.02-7.80(m, 10H), 7.56(d, 8H), 7.45(d, 8H), 3.35-3.60(m, 4H), 1.36 (d, 24H), 1.19 (d, 18H), 1.03(d, 36H). ^{13}C NMR (100 MHz, $CDCl_3$) δ: 151.28, 149.20, 146.78, 141.69, 133.12, 128.62, 116.35, 34.07, 30.92, 24.92, 23.73 ppm. ^{31}P{^{1}H} NMR (162 MHz, $CDCl_3$) δ: 34.97, 30.32 ppm. ^{77}Se{^{1}H} NMR (76.3 MHz, $CDCl_3$) δ: 1079.14 ppm. IR (cm-1, KBr pellet): 3408(wide), 3035(m), 2958(s), 2926(m), 2904(m), 2871(s), 1669(s), 1489(s), 1397(s), 1364(s), 1240(m), 1118(s), 1030(m), 1008(m), 822(s), 767(s), 734(s), 668(s), 542(s).

Compound **2.4**: *p*-Methylphenylstibonic acid (0.091g, 0.343 mmol), *t*-butylphosphonic acid (0.048g, 0.343 mmol), and phenylseleninic acid (0.065g, 0.343 mmol). Yield: 0.122 g (68% based on *p*-methylphenylstibonic acid). Decp temp: 278-279 ºC. Anal, Calcd (%) for $C_{64}H_{98}O_{26}P_6Se_2Sb_4$ (2114.25): C 36.36, H 4.67. Found: C 36.28, H 4.63. ^{1}H NMR (400 MHz, $CDCl_3$) δ: 7.72-7.58(m, 10H), 7.18(d, 8H), 6.80(d, 8H), 2.25(s, 12H), 1.25 (d, 18H), 1.12(d, 36H). ^{13}C NMR (100 MHz, $CDCl_3$) δ: 143.61, 141.24, 138.72, 132.23, 129.30, 128.65, 127.95, 31.59, 30.98, 29.73, 24.88, 21.49 ppm. ^{31}P{^{1}H} NMR (162 MHz, $CDCl_3$) δ: 35.01, 30.42 ppm. ^{77}Se{^{1}H} NMR (76.3 MHz, $CDCl_3$) δ: 1081.00 ppm. IR (cm-1, KBr pellet): 3430(wide), 3050(m), 2963(s), 2926(m), 2854(m), 1635(s), 1479(s), 1443(m), 1396(s), 1256(m), 1096(s), 799(s), 749(s), 663(s), 559(s).

Compound **2.5**: *p-t*-Butylphenylstibonic acid (0.105g, 0.343 mmol), *t*-butylphosphonic acid (0.048g, 0.343 mmol), and phenylseleninic acid (0.065g, 0.343 mmol). Yield: 0.135 g (54% based on *p*-t-butylphenylstibonic acid). Decp temp: 269-270 ^{o}C. Anal, Calcd (%) for $C_{48}H_{76}O_{17}P_4Se_2Sb_2$ (1450.44): C 39.75, H 5.28. Found: C 39.68, H 5.23. ^{1}H NMR (400 MHz, $CDCl_3$) δ: 8.06-8.04(m, 10H), 7.79(d, 4H), 7.56(d, 4H), 1.36(s, 18H), 1.21(d, 18H), 1.05(d, 18H). ^{13}C NMR (100 MHz, $CDCl_3$) δ: 153.44, 143.61, 132.51, 129.24, 127.65, 125.48, 34.87, 32.66, 31.26, 25.32 ppm. . ^{31}P{^{1}H} NMR (162 MHz, $CDCl_3$) δ: 32.41, 29.43 ppm. ^{77}Se{^{1}H} NMR (76.3 MHz, $CDCl_3$) δ: 1065.02 ppm. IR (cm-1, KBr pellet): 3413(br), 3061(m), 2965(s), 2904(w), 2869(m), 1589(m), 1479(s), 1443(m), 1395(s), 1364(s), 1267(m), 1061(m), 1008(s), 822(s), 744(s), 686(s), 665(m), 550(s).

Compound **2.6**: *p*-Isopropylphenylstibonic acid (0.100 g, 0.343 mmol) and *t*-butylsilanetriol (0.093 g, 0.687 mmol). Yield: 0.094 g (18.20% based on weight of *p*-Isopropylphenylstibonic acid. Decp. temp: 290-293 ºC. Anal. Calcd. (%) for compound $C_{51}H_{87}O_{17}Si_6Sb_3$: C, 40.67; H, 5.82. Found: C, 40.75; H, 5.73. ^{1}H NMR (400 MHz, $CDCl_3$): δ 7.63-8.13 ppm (m, 12 H), 3.5 ppm (m, 3 H), 1.21 ppm (d, 18 H), 0.96 ppm (s, 54 H). ^{13}C NMR (100 MHz, $CDCl_3$): δ 134.73, 127.48, 49.27, 48.84, 34.09, 26.91, 26.83, 23.58. ^{29}Si{^{1}H} NMR in $CDCl_3$; δ -22.07 ppm. IR (cm-1, KBr Pellet): 2948 (m), 2931 (w), 2854 (m), 1654 (m), 1479 (s), 1397 (m), 1358 (s), 1052 (w), 948 (m), 821 (s).

2.3 Results and Discussions

Compound **2.1** was synthesized by the reaction of *p*-isopropylphenylstibonic acid with *t*-butylphosphonic acid in acetonitrile (Scheme 2.1). Single crystals suitable for X-ray diffraction were grown from acetonitrile filtrate. Solution NMR of **2.1** was performed in $CDCl_3$ solvent. ^1H NMR of **2.1** shows two distinct doublets (at 7.8 and 7.2 ppm) corresponding to the two sets of aromatic protons of the isopropylphenyl group attached to antimony and in the alkyl region, three closely spaced doublets (at 1.2, 1.1 and 0.8 ppm) are present, corresponding to the presence of three sets of *t*-butyl group protons attached to phosphorus. Solution $^{31}P\{^1H\}$ NMR of **2.1** shows three resonance peaks at δ = 34.5, 32.0 and 25.0 ppm which indicates the presence of three different phosphorus environments in **2.1**. Reaction of *p*-chlorophenylstibonic acid with *t*-butylphosphonic acid leading to isolation of dinuclear organoantimony (V) oxo cluster was reported by Winpenny *et al*.[7] A change in R group on arylstibonic acid from *p*-chlorophenylstibonic acid to *p*-isopropylphenylstibonic acid results in the isolation of novel tetranuclear organoantimony (V) oxo cluster.

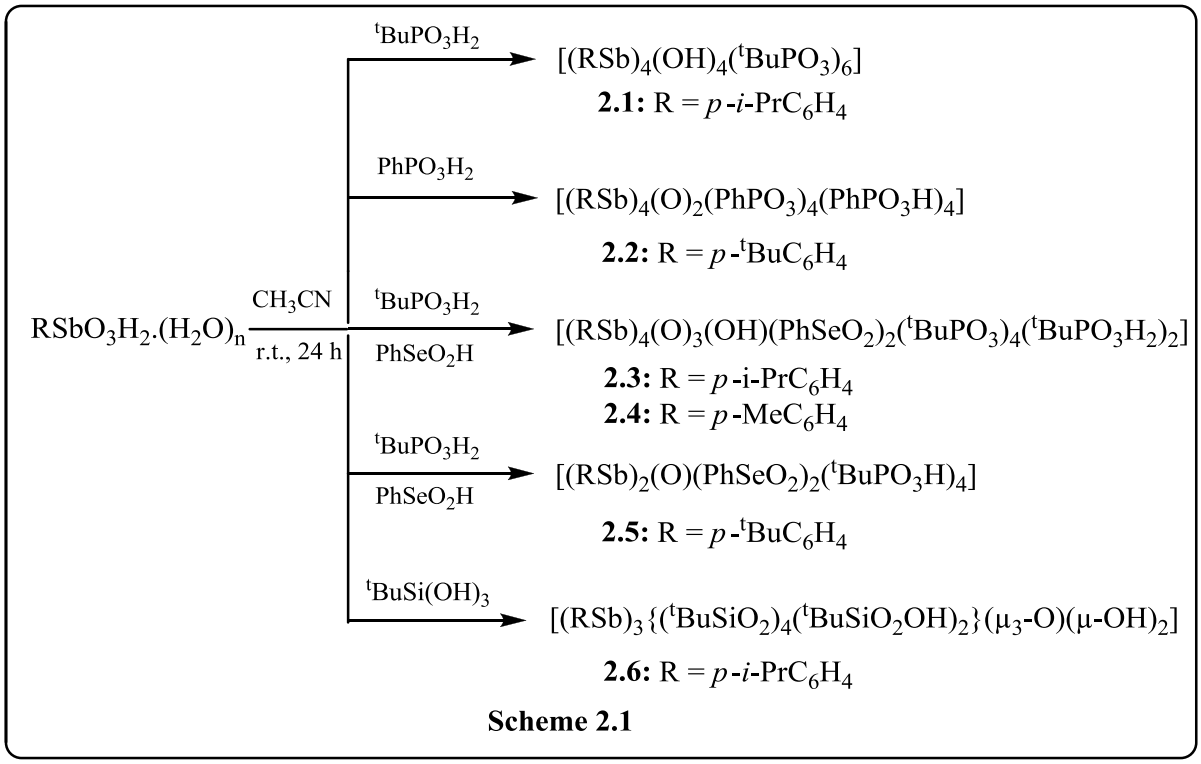

Scheme 2.1

Compound **2.1** crystallizes in triclinic space group P-1. Selected bond lengths (Å) and bond angles (°) of **2.1** are given in the table 2.2. The molecular structure of **2.1** (**Figure 2.1**) reveals the formation of a puckered eight-membered Sb_4O_4 core held together by six phosphonate ligands. The structure can be described as follows; each Sb is present in an octahedral geometry with the O_5SbC coordination. Of the six phosphonates found in the structure, four phosphonates (two pairs) bridge Sb-O-Sb motifs, while the other two phosphonates link the two Sb-O-Sb units along with the hydroxo group resulting in the formation of a tetra nuclear cluster. The phosphonate coordination mode based on Harris notation is 2.110. As mentioned earlier, the solution ^{31}P NMR shows the appearance of three discrete signals corresponding to the three types of phosphonates present in the cluster. ESI-MS data suggests that the structural integrity is maintained in solution also [M+H moiety, m/z =1849.1473]. The Sb-O bond lengths involving in the μ_2-hydroxide fall in the range 1.915(14) to 1.942(14) Å. In **2.1**, the P-O bond distances falls in the range of 1.502(17) to 1.561(17) Å. These P-O distances are found to be similar and comparable with the values reported in an organooxotin phosphonate cage [1.516(2) to 1.556(3)Å][16] and the corresponding distances in gallium phosphonate cages [1.504(2) to 1.555(2)][17] whereas the P-O distances are found to be slightly longer than those found in a borophosphonate cages [1.490(6) to 1.506(5) Å].[18] The Sb-O bond lengths involving phosphonates are in the range of 2.008(15) to 2.098(15) Å which is similar to the Sn-O bond lengths involving phosphonates in an organooxotin phosphonate cage [2.065(2) to 2.095(2)Å][16] whereas the bond lengths are slightly longer than in gallium phosphonate cages [1.908(2) to 1.946(2)Å].[17] The corresponding distances were also longer than those found in a borophosphonate cages [1.452(10) to 1.493(10)Å] reported.[18] The Sb-O-Sb bond angles falls in the range 132.8(8) to 140.1(8)^o.

Compound **2.2** was synthesized by the reaction of *p*-t-butylphenylstibonic acid with phenylphosphonic acid in acetonitrile (**Scheme 2.1**). Solution ^{1}H NMR of **2.2** shows two regions of aromatic protons. First region shows two multiplets (at 7.9 and 7.5 ppm) and one doublet (at 7.6 ppm) corresponding to the protons of the phenyl group attached to phosphorus is present. Second region shows two distinct doublets (at 7.3 and 7.1 ppm) corresponding to two sets of aromatic protons of the *p*-*t*-butyl phenyl group attached to the Sb atom. In the alkyl region a singlet (at 1.2 ppm) corresponding to the *t*-butyl group protons attached to phenyl ring are observed. Solution ^{31}P NMR of **2.2** shows two resonance peaks at δ = 12.0 and 0.8 ppm

indicating the presence of two different phosphonates present in **2.2**. Compound **2.2** crystallizes in tetragonal space group I-4 with ¼ of the molecule present in the asymmetric unit. Selected bond lengths (Å) and bond angles (°) of **2.1** are given in the table 2.2. Solid state structure of **2.2** is similar to earlier reports, where *p*-chlorophenylstibonic acid is used as a starting precursor.[1] When the R group on the arylstibonic acid was changed to *p*-t-butylphenyl stibonate and phosphorus bound organic group has been changed to phenyl, the reaction between the organostibonate and phosphonic acid led to the isolation of structure that is quite different from compound **2.1**. Molecular structure of **2.2** (**Figure 2.1**) reveals the formation of a tetra nuclear organoantimony (V) oxo cluster made up of two Sb-O-Sb frameworks. Two pairs of phosphonate bridge the two Sb-O-Sb units. The two Sb-O-Sb motifs are approximately at right angle to each other. Of the eight phosphonates present, four are in dianionic form while the other four are monoanioinic. Each phosphonate chelate to antimony in 2.110 coordination mode. ESI-MS data reveals the presence of $\{M-[(RSb)_2O(PhPO_3)_2]\}$ +3H (m/z =1469.0205) as a major peak. The spatial arrangement around each antimony atom is in an octahedral geometry with the O_5SbC coordination. The Sb-O bond length involving in the μ_2-oxide is 1.918(5) Å. In **2.2**, the P-O bond distances falls in the range of 1.504(10) to 1.558(8)Å similar to those found in an organooxotin phosphonate cage[16] and gallium phosphonate cages[17] whereas the corresponding distances were slightly longer than those found in a borophosphonate cages.[18] The Sb-O bond lengths involving phosphonates falls in the range of 1.982(9) to 2.036(8)Å, similar to those found in Sn-O bond lengths involving phosphonates in an organooxotin phosphonate cage[16] and slightly longer than the gallium phosphonate cages[17] whereas the corresponding distances were relatively longer than those found in a borophosphonate cages.[18] The Sb-O-Sb bond angle is 136.3(7)^o.

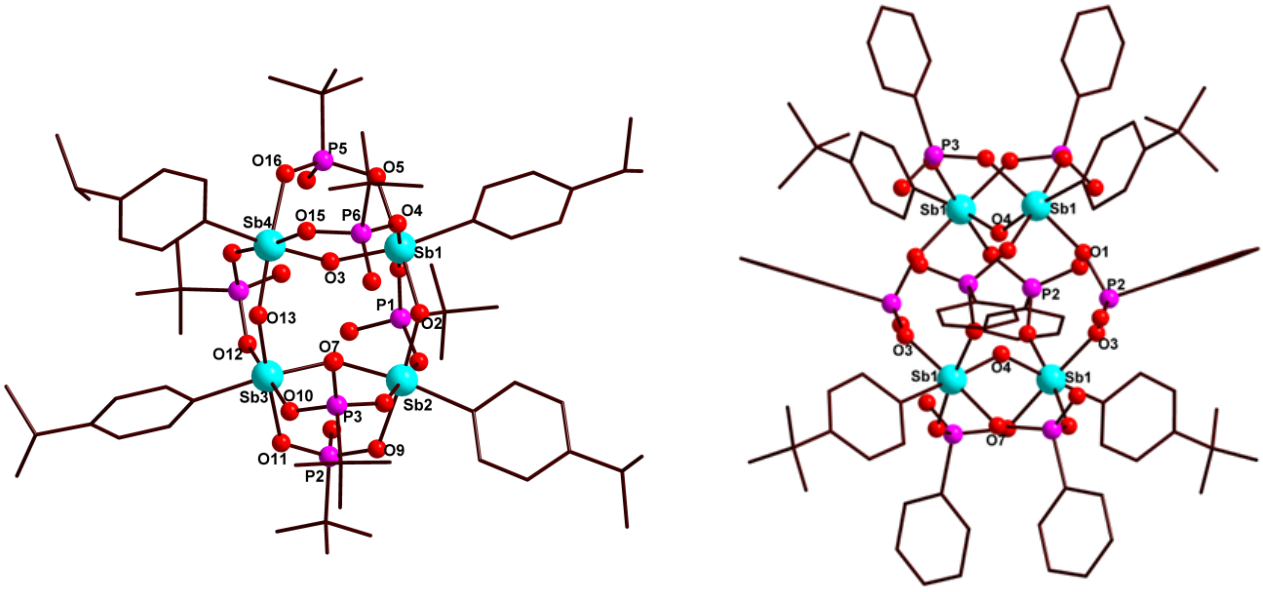

Figure 2.1: (Left) Molecular structure of **2.1**. (Right) Molecular structure of **2.2**. H atoms and solvent molecule are omitted. Color Code: Cyan: Sb, Pink: P, Red: O.

Compounds **2.3-2.5** were synthesized by the reaction of organostibonic acid with phosphonic acid and seleninic acid in acetonitrile (**Scheme 2.1**). The idea was to observe the reactivity of organostibonic acid in the presence of phosphonic acid and seleninic acid. Solution NMR studies for compounds **2.3-2.5** was performed in $CDCl_3$ solvent. Solution $^{31}P\{^1H\}$ NMR of **2.3** shows two resonance peaks at δ = 35.0 and 30.3 ppm while $^{77}Se\{^1H\}$ NMR shows a single resonance at δ = 1079.1 ppm, which indicates presence of two different phosphorus environments and a unique selenium environment in **2.3**. Similarly, solution $^{31}P\{^1H\}$ NMR of **2.4** also shows two resonance peaks at δ = 35.0 and 30.4 ppm and $^{77}Se\{^1H\}$ NMR shows a single resonance at δ = 1081.0 ppm. Solution $^{31}P\{^1H\}$ NMR of **2.5** also shows two resonance peaks at δ = 32.4, 29.4 ppm and $^{77}Se\{^1H\}$ NMR shows a signal at δ = 1065.0 ppm. Compound **2.3** crystallizes in the orthorhombic space group Pbca and **2.4** crystallize in triclinic space group P-1. Since compounds **2.3** and **2.4** are isostructural, the structure of **2.3** is considered for discussion (**Figure 2.2**). Selected bond lengths (Å) and bond angles (°) of **2.3-2.4** are given in the table 2.3–2.4. The molecular structure of **2.3** reveals the formation of tetranuclear organoantimony (V) oxo cluster whose structure is described as follows. Each Sb is present in an octahedral geometry with the

O_5SbC coordination. The cluster core has four Sb centers, in which two sets of Sb atoms are found in the cluster. The first set of Sb atoms, Sb_1 and Sb_2, are connected between themselves through two μ_2- oxo bridges. The second set of two Sb atoms, Sb_3 and Sb_4, are connected through two phenylseleninic acid O-Se-O bridges. The two different set of Sb atoms are further connected by the two oxo bridges. Four phosphonates bridge to Sb-O-Sb edge in 2.110 coordination mode. The two phenylseleninic acids form a symmetrical bridge between two antimony atoms in a bent on fashion. Interestingly the solid state structure of **2.3** has two uncoordinated *t*-butylphosphonic acids which crystallize along with the core. These two phosphonic acids sacrifice their bonding to phenylseleninic acid and are free from coordination to Sb and stabilize the cluster core by hydrogen bonding. Out of four μ_2-oxo bridges present, three are considered as oxide bridges and one considered as hydroxyl, this would account for the charge balance and hydrogen bonding present in **2.3**. As mentioned earlier the solution ^{31}P NMR shows the appearance of two discrete signals corresponding to the two types of phosphonates: one phosphonate group bridges the Sb atoms and other is a free phosphonate. The Sb-O bond lengths involving in the μ_2-oxide fall in the range of 1.911(5) to 2.025(5) Å. In **2.3**, the P-O bond distances falls in the range of 1.499(6) to 1.567(5) Å similar to those found in an organooxotin phosphonate cage[16] and gallium phosphonate cages[17] and slightly longer than those found in a borophosphonate cages.[18] The Sb-O bond lengths involving phosphonates falls in the range of 2.005(5) to 2.040(5)Å similar to those found in Sn-O bond lengths involving phosphonates in an organooxotin phosphonate cage[16] and slightly longer than gallium phosphonate[17] whereas the corresponding distances were longer than those found in a borophosphonate cages.[18] The Se-O bond distances falls in the range of 1.725(5) to 1.740(5) Å similar to those found in Mn_7 seleninate cluster [1.703(2) to 1.741(3) Å][19] whereas the corresponding distances were slightly longer than those found in an organotin selininate ester [1.682(5) to 1.696(5)Å][20] and the recently reported selenotelluroxane macrocycle [1.678(4) to 1.690(2) Å].[21] The Sb-O bond lengths involving phenylseleninates fall in the range of 2.024(5) to 2.033(5) Å, these distances are comparable with reported Mn_7 seleninate cluster [1.944(6) to 2.002(6) Å][19], organotin selininate ester 2.225(5)Å[20] and selenotelluroxane macrocycle [2.329(4) to 2.361(4) Å].[21] Bond angles of Sb-O-Sb, Sb-O-Se and O-Se-O fall in the range of 102.3(2) to 139.7(3)^o, 122.7(3) to 124.3(3)^o and 99.7(2) to 100.9(2)^o respectively. Bond angles of C-Sb-O fall in the range of 174.7(2) to 179.3(3)^o clearly indicating that the geometry around each Sb center is regular

octahedral (180°). Compounds **2.3** and **2.4**, ESI-MS data shows M-(2 *t*-$BuPO_3H_2$) (m/z = 1950.9436, 1838.8250 respectively) as a major peak, suggesting structural integrity in solution as well.

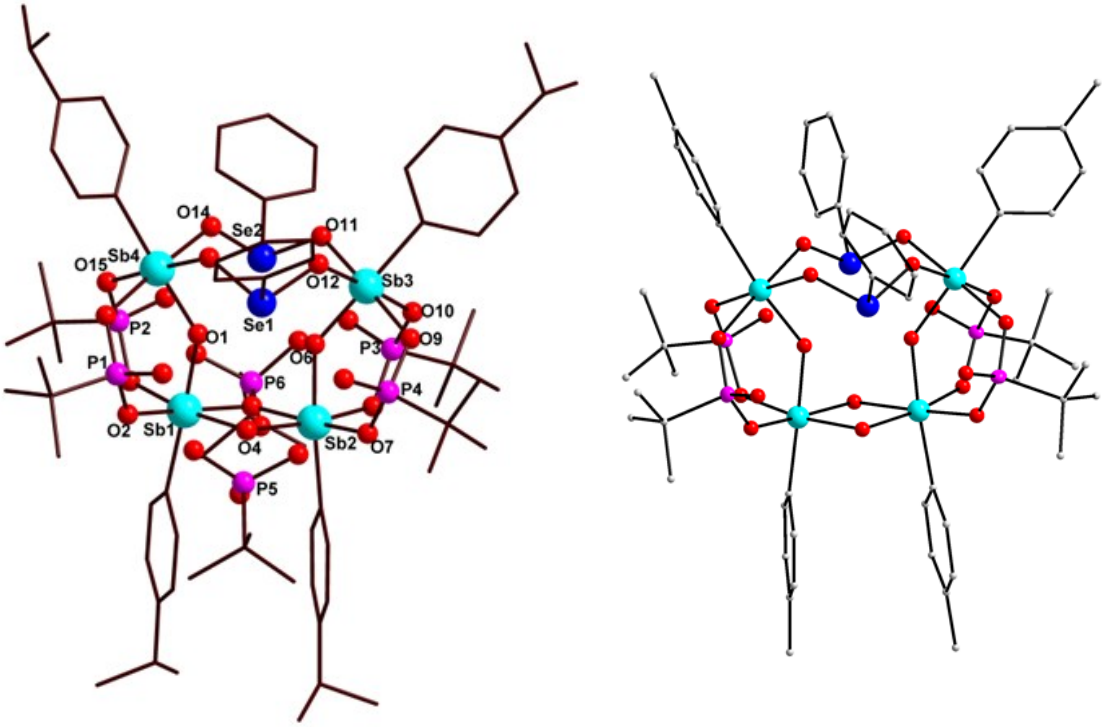

Figure 2.2: (Left) Molecular structure of **2.3.** (Right) Molecular structure of **2.4**. H atoms and solvent molecules are omitted. Color Code: Cyan: Sb, Blue: Se, Pink: P, Red: O, Brown: C

In **2.4** Sb-O bond lengths involving in the μ_2-oxide fall in the range of 1.900(3) to 2.033(3) Å. The Se-O bond distances falls in the range of 1.717(3) to 1.732(3) Å similar to those found in Mn_7 seleninate cluster [1.703(2) to 1.741(3) Å][19] whereas the corresponding distances were slightly longer than those found in an organotin selininate ester [1.682(5) to 1.696(5) Å][20] and the recently reported selenotelluroxane macrocycle [1.678(4) to 1.690(2) Å].[21] Bond angles of Sb-O-Sb, Sb-O-Se and O-Se-O fall in the range of 101.03(14) to 138.13(18)°, 122.8(17) to 128.61(18)° and 98.64(15) to 101.67(15)° respectively. O_5SbC coordination present around antimony atom and geometry around each Sb center is regular octahedral.

Compound **2.5** crystallizes in monoclinic $P2_1/c$ space group. Selected bond lengths (Å) and bond angles (°) of **2.5** are given in the table 2.5. The solid state structure of **2.5** (**Figure 2.3**) reveals the formation of a dinuclear organoantimony (V) oxo cluster. The molecular structure of **2.5** is

described as follows; two arylstibonates bridged by a μ_2-oxide form Sb-O-Sb edge, and this edge is further chelated by two phosphonic acids in 2.110 coordination mode. Each Sb atom is further connected with one protonated phosphonate and one phenylseleninic acid. As mentioned earlier the solution ^{31}P NMR shows the appearance of two discrete signals corresponding to the two types of phosphonates: one phosphonate group forms a symmetrical bridge between two Sb atoms and other phosphonate form terminal bond with Sb in 1.100 coordination mode. Phenylseleninic acid is bound to Sb in a monodentate fashion. For the charge neutrality of cluster all *t*-butyl phosphonates are considered as protonated phosphonates. The Sb-O bond lengths involving in the μ_2-oxide are 1.929(8) and 1.957(7) Å. In **2.5**, the P-O bond distances fall in the range of 1.488(9) to 1.558(8)Å similar to those found in an organooxotin phosphonate cage[16], gallium phosphonate cages[17] and slightly longer than those found in a borophosphonate cages.[18] The Se-O bond distances fall in the range of 1.707(8) to 1.735(8)Å similar to those found in Mn_7 seleninate cluster[19], slightly longer than those found in organotin selininate ester[20] and selenotelluroxane macrocycle.[21] The Sb-O bond lengths involving phenylseleninates fall in the range of 2.023(8) to 2.038(8)Å, these distances are comparable with reported Mn_7 seleninate cluster[19], organotin selininate ester[20] and selenotelluroxane macrocycle.[21] Bond angles of Sb-O-Sb, Sb-O-Se and O-Se-O fall in the range of 134.7(4)^o, 123.0(4) to 124.0(4)^o and 101.5(4) to 103.9(4)^o respectively. ESI-MS data of **2.5** shows M+H (m/z = 1451.0415) as a major peak.

Compound **2.6** was synthesized by the reaction of organostibonic acid with *t*-butylsilanetriol in acetonitrile (**Scheme 2.1**). Selected bond lengths (Å) and bond angles (°) of **2.6** are given in the table 2.5. Crystals of **2.6** were grown by slow evaporation from acetonitrile. The ^{29}Si{^{1}H} solution NMR spectra of **2.6** in $CDCl_3$ show the appearance of single resonance signal at -22.07 ppm. Structural elucidation of **2.6** (**Figure 2.3**) led to the isolation of μ_3-oxo centered triangle but with a variation in the siloxane ligand system present. In this case, three molecules of *t*-silane triols self-condense to yield a tetra coordinate ligand which binds to the Sb atoms of the triangle from both sides, hence a more symmetric siloxane bridging present in compound **2.6** and also in the molecular structure of **2.6** two μ-oxo groups are bridging two Sb atoms. The Sb-O bond distances, Sb-O-Sb and Sb-O-Si bond angles in **2.6** falls in the range of 1.9149(18) to 2.1316 (18) Å, 92.16(7) to 132.66(8)° and 133.23(11) to 141.45(11)° respectively. ESI-MS of **2.6** shows signals corresponding to formula $[M+H]^+$ (m/z = 1509.2145) confirming that the structural stability of **2.6** is maintained in solution also. Interestingly, *t*-butylsilane triols self-

condense *in situ* leading to the formation of two motifs of trisiladioxane leading to the stabilization of the first structurally characterized oxo-centered organoantimony(V) based triangular assembly. Though oxo-centered metal triangles are very common in transition metal chemistry,[22] they are a rarity as far as main group metals are concerned.[23]

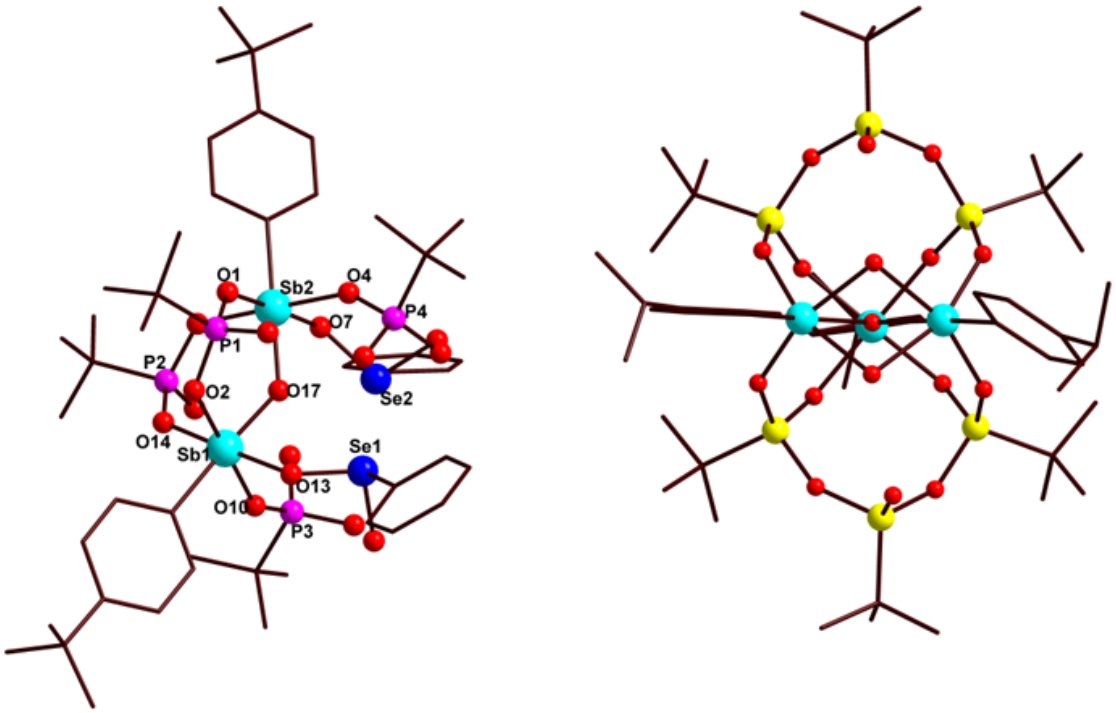

Figure 2.3 (Left) Molecular structure of **2.5. (**Right) Molecular structure of **2.6.** H atoms and solvent molecules are omitted. Color Code: Cyan: Sb, Blue: Se, Yellow: Si, Pink: P, Red: O.

2.4 Conclusion

Tetra- and dinuclear organoantimony oxo-hydroxo clusters stabilized by phosphonate and a combination of phosphonate/selininate ligation are reported. ESI-MS data reveals that the structural integrity is maintained in solution as well. ^{31}P, ^{77}Se and ^{29}Si solution NMR values observed are in accordance to the expected values based on the solid state structure observed and its solution stability. *t*-Butyl silanetriols self-condense *in situ* leading to the stabilization of the first structurally characterized oxo-centered organoantimony(V) based triangular assembly. It may thus be noted that clusters **2.1-2.6** are potentially new main group elements based pro-ligand systems. Their coordination behavior towards transition metals and lanthanides are currently being investigated.

Table 2.1: Crystal data for compounds **2.1-2.6**

	2.1	**2.2**	**2.3**
Formula	$C_{62}H_{101}NO_{22}P_6Sb_4$	$C_{88}H_{92}O_{26}P_8Sb_4$	$C_{78}H_{123}N_3O_{26}P_6Sb_4Se_2$
F.wt g/mol^{-1}	1885.25	2300.37	2349.53
T, K	100(2)	100(2)	100(2)
Crystal system	Triclinic	Tetragonal	Orthorhombic
Space group	P-1	I-4	Pbca
Crystal size mm^3	0.25 x 0.23 x 0.20	0.20 x 0.15 x 0.13	0.21 x 0.20 x 0.18
a, Å	13.7494(11)	13.1600(14)	24.238(2)
b, Å	17.0061(14)	13.1600(14)	27.209(2)
c, Å	19.0775(16)	26.614(4)	30.177(2)
α, deg	74.8200(10)	90	90
β, deg	83.9290(10)	90	90
γ, deg	70.7270(10)	90	90
V, Å^3	4062.9(6)	4609.1(12)	19901(3)
Z	2	2	8
D_{calcd} Mg/m^3	1.541	1.658	1.568
μ, mm^{-1}	1.499	1.374	1.971
F(000)	1900	2304	9456
Theta range, deg	1.307 to 26.384	1.530to 26.404	1.312 to 26.059
Index ranges	-17<=h<=17 -21<=k<=21 -23<=l<=23	-16<=h<=16 -16<=k<=16 -33<=l<=33	-29<=h<=29 -33<=k<=33 -37<=l<=37
Total reflns	43677	24759	200512
Ind. reflns / R(int)	16508/0.0218	4738/0.0307	19642/0.0883
Completeness to θ_{max}, %	99.6	100.0	100.0
GooF(F^2)	1.052	1.076	1.098
R1(F)[I>2σ(I)]	0.0244	0.0595	0.0569
$wR_2(F^2)$ (all data)	0.0642	0.1604	0.1700
Largest diff peak/hole, e.Å^{-3}	0.951/-0.507	2.936/-0.550	3.038/-0.963

	2.4	2.5	2.6
Formula	$C_{66}H_{101}NO_{26}P_6Sb_4Se_2$	$C_{50}H_{77}NO_{17}P_4Sb_2Se_2$	$C_{51}H_{87}O_{17}Si_6Sb_3$
F.wt g/mol^{-1}	2155.21	1489.43	1508.01
T, K	100(2)	100(2)	100(2)
Crystal system	Triclinic	Monoclinic	0.71073
Space group	P-1	$P2_1/c$	Triclinic
Crystal size mm^3	0.26 x 0.25 x 0.20	0.12 x 0.10 x 0.09	P -1
a, Å	13.9433(12)	17.124(3)	15.0752(12)
b, Å	15.4586(13)	16.730(3)	16.0739(13)
c, Å	21.2655(18)	22.614(4)	16.9080(14)
α, deg	82.2130(10)	90	100.488(1)
β, deg	83.783(2)	107.967(4)	91.038(1)
γ, deg	71.5500(10)	90	91.518(1)
V, Å3	4297.5(6)	6162.6(18)	4026.14(10)
Z	2	4	2
D_{calcd} Mg/m3	1.666	1.605	1.244
μ, mm-1	2.273	2.226	1.138
F(000)	2148	3000	1536
Theta range, deg	1.397 to 26.375	1.250 to 26.412	1.23 to 25.04
Index ranges	-17<=h<=17 -19<=k<=19 -26<=l<=26	-21<=h<=21 -20<=k<=20 -28<=l<=28	-17 ≤ h ≤ 17 -19 ≤ k ≤ 19 -20 ≤ l ≤ 20
Total reflns	46258	64916	38923
Ind. reflns / R(int)	17457/0.0435	12629/0.1884	14152/0.0264
Completeness to θ_{max}, %	99.7	99.7	99.8
GooF(F^2)	1.036	1.107	1.083
R1(F)[I>2σ(I)]	0.0414	0.0911	0.0294
$wR_2(F^2)$ (all data)	0.1096	0.2173	0.0807
Largest diff peak/hole, e.Å-3	3.696/-0.898	2.924/-1.123	1.418/ -0.799

Table 2.2: Selected bond lengths (Å) and bond angles (º) in **2.1 – 2.2**

2.1				**2.2**	
Sb(1)-O(3)	1.9196(14)	P(2)-O(9)	1.5345(16)	Sb(1)-O(1)	1.982(9)
Sb(1)-O(2)	1.9389(15)	P(2)-O(20)	1.5610(17)	Sb(1)-O(4)	1.918(5)
Sb(1)-O(4)	2.0134(15)	P(3)-O(19)	1.5021(17)	Sb(1)-O(8)#1	2.014(8)
Sb(1)-O(1)	2.0615(15)	P(3)-O(8)	1.5480(16)	Sb(1)-O(3)#2	2.016(7)
Sb(1)-O(5)	2.0884(15)	P(3)-O(10)	1.5545(16)	Sb(1)-O(7)	2.036(8)
Sb(2)-O(7)	1.9218(14)	P(4)-O(22)	1.5350(16)	O(3)-Sb(1)#3	2.017(7)
Sb(2)-O(2)	1.9350(15)	P(4)-O(12)	1.5365(16)	O(8)-Sb(1)#1	2.015(8)
Sb(2)-O(8)	2.0123(15)	P(4)-O(14)	1.5395(16)	P(2)-O(2)	1.506(10)
Sb(2)-O(6)	2.0508(15)	P(5)-O(5)	1.5325(16)	P(2)-O(1)	1.512(10
Sb(2)-O(9)	2.0984(15)	P(5)-O(16)	1.5406(16)	P(2)-O(3)	1.525(8)
Sb(3)-O(7)	1.9228(14)	P(5)-O(17)	1.5604(17)	P(3)-O(6)	1.504(10)
Sb(3)-O(13)	1.9389(15)	P(6)-O(18)	1.5108(17)	P(3)-O(7)	1.549(8)
Sb(3)-O(10)	2.0080(15)	P(6)-O(4)	1.5447(16)	P(3)-O(8)	1.558(8)
Sb(3)-O(12)	2.0597(15)	P(6)-O(15)	1.5483(16)	Sb(1)#1-O(4)-Sb(1)	136.3(7)
Sb(3)-O(11)	2.0898(15)			O(4)-Sb(1)-O(1)	82.7(4)
Sb(4)- O(3)	1.9148(14)	Sb(3)-O(13)-	132.81(8)	O(4)-Sb(1)-O(8)#1	91.5(3)
Sb(4)-O(14)	2.0343(15)	Sb(2)-O(7)-Sb(3)	139.86(8)	O(1)-Sb(1)-O(8)#1	173.4(3)
Sb(4)-O(13)	1.9417(14)	Sb(4)-O(3)-Sb(1)	140.10(8)	O(4)-Sb(1)-O(3)#2	90.4(3)
Sb(4)-O(15)	2.0199(15)	Sb(2)-O(2)-Sb(1)	133.32(8)	O(1)-Sb(1)-O(3)#2	93.9(4)
Sb(4)-O(16)	2.0775(15)			O(8)#1-Sb(1)-O(3)#2	89.4(3)
P(1)-O(1)	1.5363(16)			O(4)-Sb(1)-O(7)	90.2(3)
P(1)-O(6)	1.5371(16)			O(1)-Sb(1)-O(7)	88.7(4)
P(1)-O(23)	1.5400(16)			O(8)#1-Sb(1)-O(7)	88.1(4)
P(2)-O(11)	1.5302(16)			O(3)#2-Sb(1)-O(7)	177.5(4)

Symmetry transformations used to generate equivalent atoms:

#1 -x+1,-y,z #2 y+1/2,-x+1/2,-z+1/2 #3 -y+1/2,x-1/2,-z+1/2

Table 2.3: Selected bond lengths (Å) and bond angles (°) in **2.3**

2.3					
Sb(1)-O(1)	1.937(5)	P(1)-O(17)	1.499(6)	Se(2)-O(14)-Sb(4)	123.7(3)
Sb(1)-O(2)	2.014(5)	P(1)-O(16)	1.543(5)	Se(1)-O(13)-Sb(4)	124.3(3)
Sb(1)-O(5)	2.017(5)	P(1)-O(2)	1.550(5)	O(14)-Se(2)-O(11)	100.9(2)
Sb(1)-O(3)	2.017(5)	P(2)-O(20)	1.518(5)	O(13)-Se(1)-O(12)	99.7(2)
Sb(1)-O(4)	2.022(5)	P(2)-O(15)	1.551(5)	O(1)-Sb(4)-C(52)	177.9(3)
Sb(2)-O(6)	1.939(4)	P(2)-O(3)	1.555(5)	O(1)-Sb(1)-C(25)	177.5(2
Sb(2)-O(5)	2.005(5)	P(3)-O(19)	1.499(6)	O(6)-Sb(2)-C(20)	174.7(2)
Sb(2)-O(8)	2.010(5)	P(3)-O(10)	1.552(5)	O(6)-Sb(3)-C(43)	179.3(3)
Sb(2)-O(4)	2.025(5)	P(3)-O(8)	1.567(5)		
Sb(2)-O(7)	2.040(5)	P(4)-O(18)	1.510(5)		
Sb(3)-O(6)	1.911(5)	P(4)-O(7)	1.554(5)		
Sb(3)-O(9)	2.017(5)	P(4)-O(9)	1.557(5)		
Sb(3)-O(10)	2.024(5)	P(5)-O(21)	1.513(6)		
Sb(3)-O(11)	2.027(5)	P(5)-O(23)	1.537(6)		
Sb(3)-O(12)	2.033(5)	P(5)-O(22)	1.538(6)		
Sb(4)-O(1)	1.915(5)	P(6)-O(24)	1.509(6)		
Sb(4)-O(15)	2.019(5)	P(6)-O(25)	1.520(6)		
Sb(4)-O(16)	2.019(5)	P(6)-O(26)	1.524(6)		
Sb(4)-O(13)	2.025(5)	Sb(1)-O(4)-Sb(2)	102.3(2)		
Sb(4)-O(14)	2.032(5)	Sb(2)-O(5)-Sb(1)	103.2(2)		
Se(1)-O(13)	1.725(5)	Sb(4)-O(1)-Sb(1)	139.7(3)		
Se(1)-O(12)	1.735(5)	Sb(3)-O(6)-Sb(2)	139.3(3)		
Se(2)-O(14)	1.726(5)	Se(2)-O(11)-	123.4(3)		
Se(2)-O(11)	1.740(5)	Se(1)-O(12)-	122.7(3)		

Table 2.4: Selected bond lengths (Å) and bond angles (º) in **2.4**

2.4					
Sb(1)-O(1)	1.900(3)	P(1)-O(20)	1.499(4)	Sb(2)-O(9)-Sb(3)	101.03(14)
Sb(1)-O(2)	2.009(3)	P(1)-O(7)	1.551(3)	Sb(2)-O(8)-Sb(3)	103.15(14)
Sb(1)-O(3)	2.023(3)	P(1)-O(3)	1.557(4)	Sb(1)-O(1)-Sb(2)	137.97(18)
Sb(1)-O(4)	2.028(3)	P(2)-O(19)	1.499(4)	Sb(4)-O(10)-Sb(3)	138.13(18)
Sb(1)-O(5)	2.041(3)	P(2)-O(6)	1.556(3)	Se(2)-O(16)-Sb(4)	122.80(17)
Sb(2)-O(1)	1.936(3)	P(2)-O(2)	1.561(3)	Se(1)-O(5)-Sb(1)	128.61(18)
Sb(2)-O(8)	2.000(3)	P(3)-O(12)	1.497(4)	Se(1)-O(15)-Sb(4)	125.25(17)
Sb(2)-O(7)	2.008(3)	P(3)-O(14)	1.546(3)	Se(2)-O(4)-Sb(1)	127.07(18)
Sb(2)-O(9)	2.031(3)	P(3)-O(13)	1.552(3)	O(5)-Se(1)-O(15)	101.67(16)
Sb(2)-O(6)	2.032(3)	P(4)-O(17)	1.500(4)	O(4)-Se(2)-O(16)	98.64(15)
Sb(3)-O(10)	1.946(3)	P(4)-O(18)	1.556(3)		
Sb(3)-O(8)	2.004(3)	P(4)-O(11)	1.553(3)		
Sb(3)-O(11)	2.012(3)	P(5)-O(23)	1.525(4)		
Sb(3)-O(13)	2.021(3)	P(5)-O(21)	1.531(4)		
Sb(3)-O(9)	2.033(3)	P(5)-O(22)	1.544(4)		
Sb(4)-O(10)	1.922(3)	P(6)-O(26)	1.501(4)		
Sb(4)-O(14)	2.010(3)	P(6)-O(25)	1.541(4)		
Sb(4)-O(18)	2.018(3)	P(6)-O(24)	1.549(4)		
Sb(4)-O(16)	2.022(3)				
Sb(4)-O(15)	2.045(3)				
Se(1)-O(5)	1.717(3)				
Se(1)-O(15)	1.723(3)				
Se(2)-O(4)	1.732(3)				
Se(2)-O(16)	1.732(3)				

Table 2.5: Selected bond lengths (Å) and bond angles (º) in **2.5 - 2.6**

2.5		**2.6**			
Sb(1)-O(17)	1.929(8)	Sb(1)-O(4)	1.9149(18)	Si(4)-O(15)	1.632(2)
Sb(1)-O(14)	1.997(8)	Sb(1)-O(5)	1.9224(18)	Si(4)-O(10)	1.641(2)
Sb(1)-O(10)	2.014(8)	Sb(1)-O(3)	2.0792(17)	Si(5)-O(16)	1.607(2)
Sb(1)-O(2)	2.034(8)	Sb(1)-O(2)	2.1046(18)	Si(5)-O(15)	1.618(2)
Sb(1)-O(13)	2.038(8)	Sb(1)-O(1)	2.1080(17)	Si(5)-O(17)	1.646(2)
Sb(2)-O(17)	1.957(7)	Sb(2)-O(9)	1.9627(18)	Si(6)-O(7)	1.6100(19)
Sb(2)-O(1)	1.998(8)	Sb(2)-O(8)	1.9689(18)	Si(6)-O(16)	1.6294(19)
Sb(2)-O(4)	2.005(8)	Sb(2)-O(6)	1.9697(18)	Si(6)-O(4)	1.6395(18)
Sb(2)-O(15)	2.007(8)	Sb(2)-O(7)	1.9712(18)	Si(1)-O(9)-Sb(2)	141.00(11)
Sb(2)-O(7)	2.023(8)	Sb(2)-O(3)	2.0958(17)	Si(6)-O(7)-Sb(2)	139.01(11)
Se(1)-O(13)	1.707(8)	Sb(3)-O(11)	1.9191(18)	Si(4)-O(6)-Sb(2)	138.71(11)
Se(1)-O(12)	1.732(8)	Sb(3)-O(10)	1.9228(18)	Sb(1)-O(2)-Sb(3)	92.96(7)
Se(2)-O(8)	1.730(8)	Sb(3)-O(3)	2.0444(17)	Si(6)-O(4)-Sb(1)	134.10(11)
Se(2)-O(7)	1.735(8)	Sb(3)-O(2)	2.1068(18)	Sb(1)-O(1)-Sb(3)	92.16(7)
P(1)-O(3)	1.503(9)	Sb(3)-O(1)	2.1316(18)	Si(4)-O(10)-Sb(3)	135.22(11)
P(1)-O(2)	1.550(9)	Si(1)-O(9)	1.6078(19)	Si(5)-O(16)-Si(6)	150.51(13)
P(1)-O(1)	1.551(8)	Si(1)-O(14)	1.630(2)	Sb(3)-O(3)-Sb(1)	95.56(7)
P(2)-O(16)	1.488(9)	Si(1)-O(5)	1.6368(19)	Sb(3)-O(3)-Sb(2)	131.77(8)
Sb(1)-O(17)-Sb(2)	134.7(4)	Si(2)-O(12)	1.610(2)	Sb(1)-O(3)-Sb(2)	132.66(8)
Se(1)-O(13)-Sb(1)	123.0(4)	Si(2)-O(14)	1.614(2)	Si(1)-O(5)-Sb(1)	133.23(11)
Se(2)-O(7)-Sb(2)	124.0(4)	Si(2)-O(13)	1.643(2)	Si(3)-O(8)-Sb(2)	141.45(11)
O(13)-Se(1)-O(12)	101.5(4)	Si(3)-O(8)	1.602(2)	Si(5)-O(15)-Si(4)	142.78(13)
O(8)-Se(2)-O(7)	103.9(4)	Si(3)-O(12)	1.619(2)	Si(3)-O(11)-Sb(3)	135.29(11)
Sb(1)-O(17)-Sb(2)	134.7(4)	Si(3)-O(11)	1.642(2)	Si(2)-O(14)-Si(1)	145.47(14)
		Si(4)-O(6)	1.6080(19)	Si(2)-O(12)-Si(3)	145.16(14)

2.5 Analytical and Spectroscopic Data

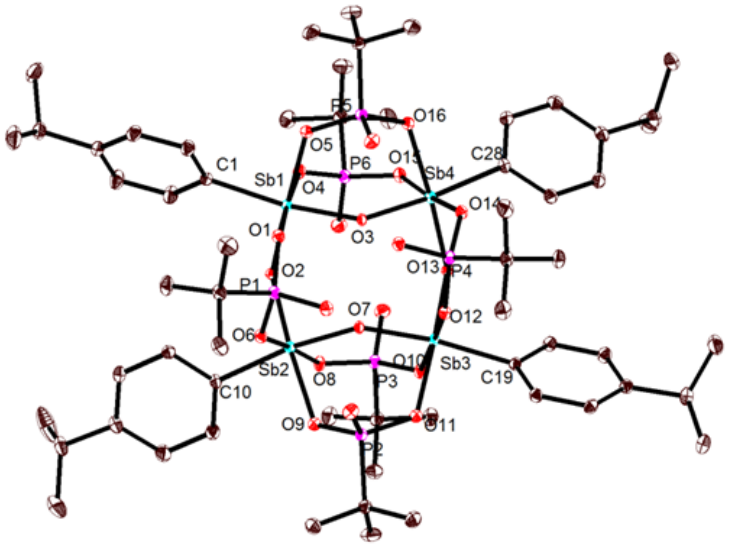

Figure S1. ORTEP view of **2.1** with thermal ellipsoids shown at 30% probability.

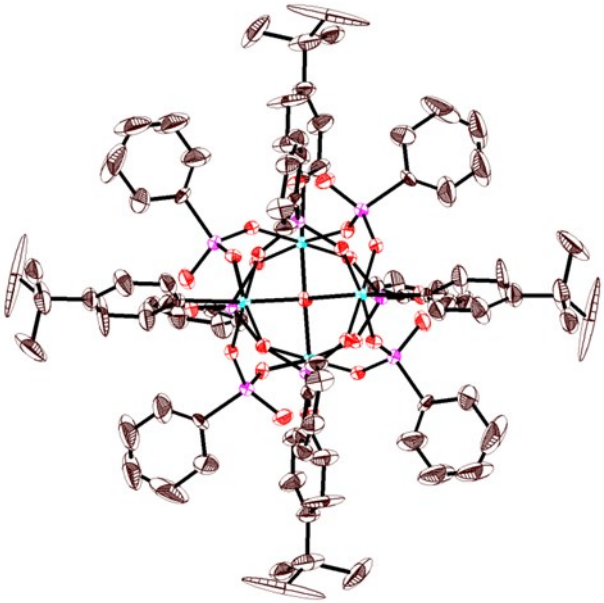

Figure S2. ORTEP view of **2.2** with thermal ellipsoids shown at 30% probability.

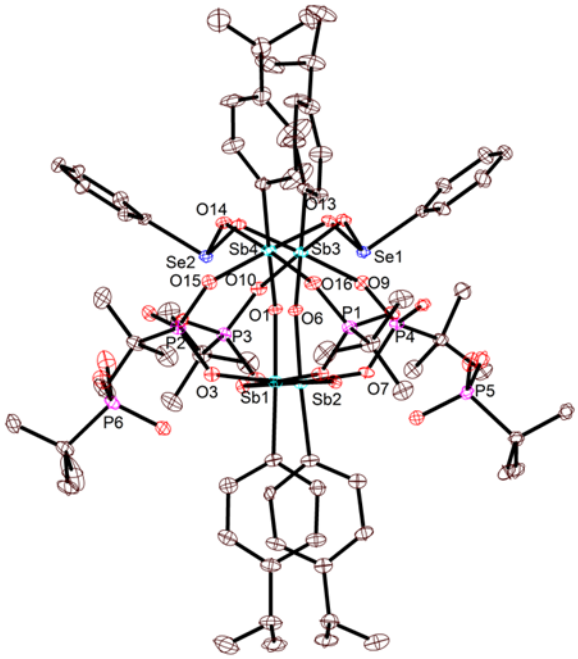

Figure S3. ORTEP view of **2.3** with thermal ellipsoids shown at 30% probability.

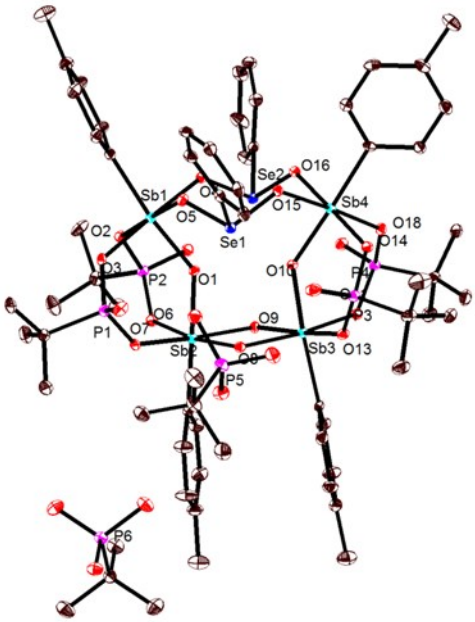

Figure S4. ORTEP view of **2.4** with thermal ellipsoids shown at 30% probability.

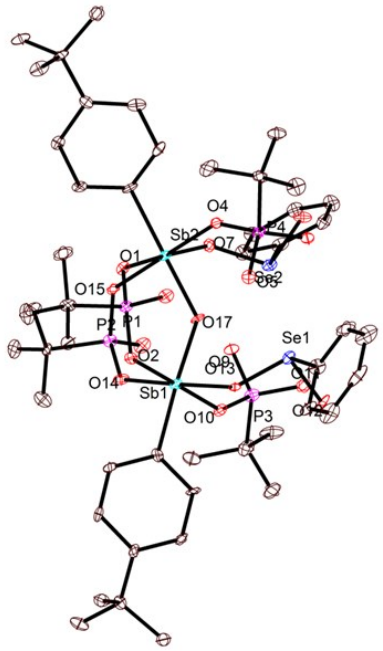

Figure S5. ORTEP view of **2.5** with thermal ellipsoids shown at 30% probability.

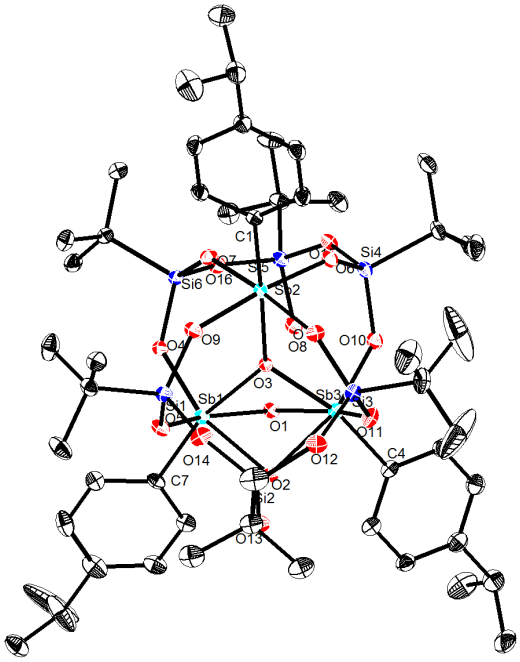

Figure S6. ORTEP view of **2.6** with thermal ellipsoids shown at 30% probability.

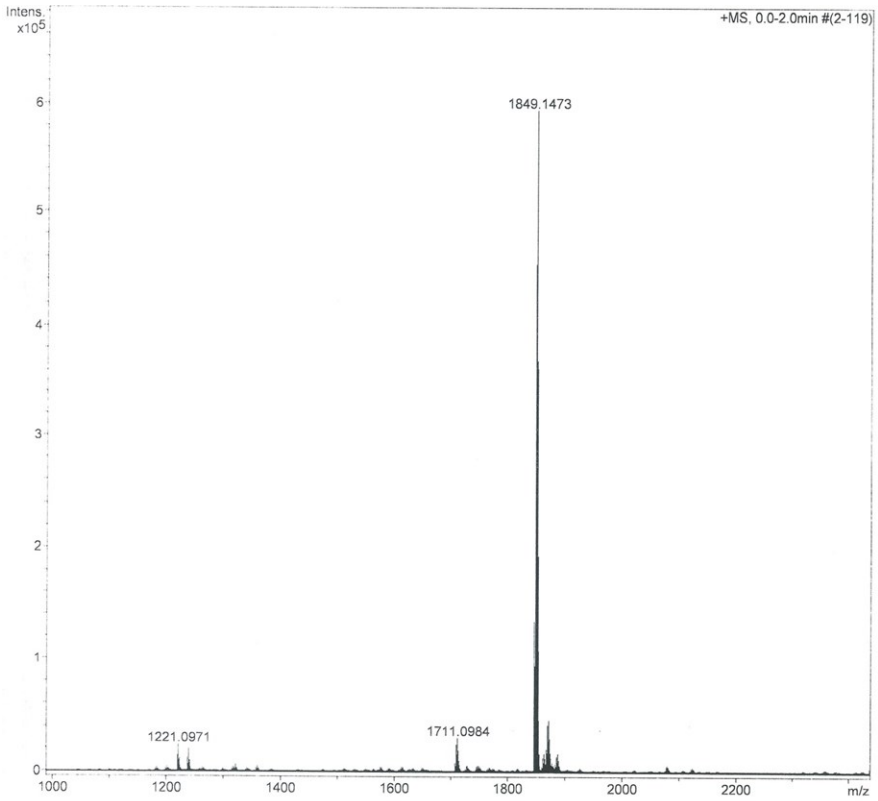

Figure S7. ESI-MS of compound **2.1** in $CHCl_3$-CH_3CN.

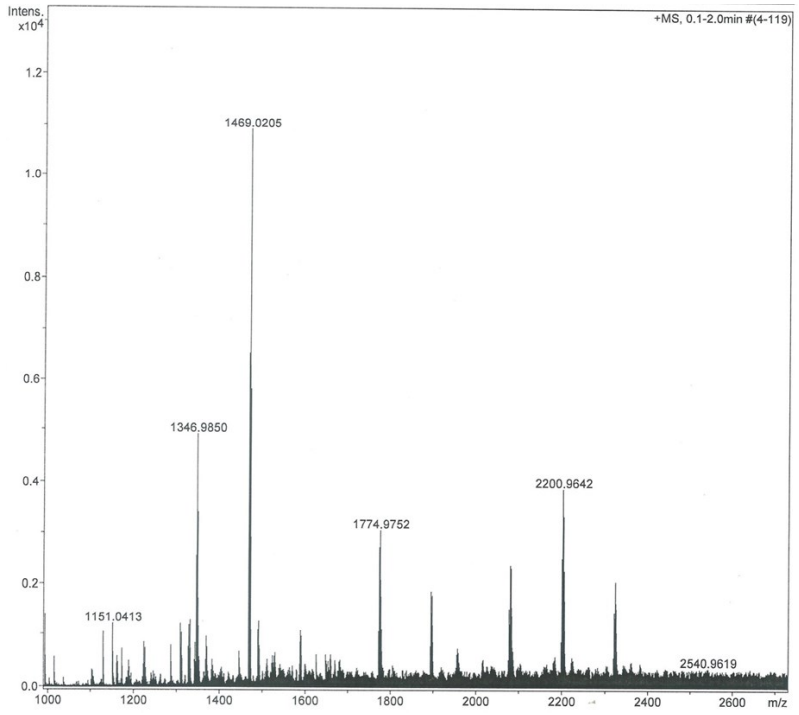

Figure S8. ESI-MS of compound **2.2** in $CHCl_3$-CH_3CN.

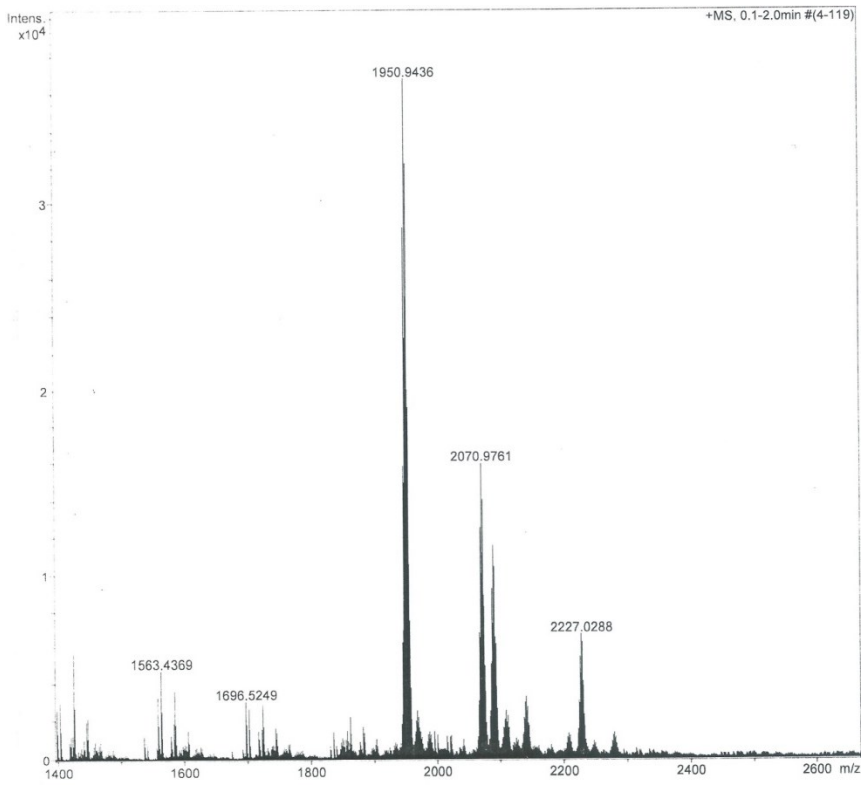

Figure S9. ESI-MS of compound **2.3** in $CHCl_3$-CH_3CN.

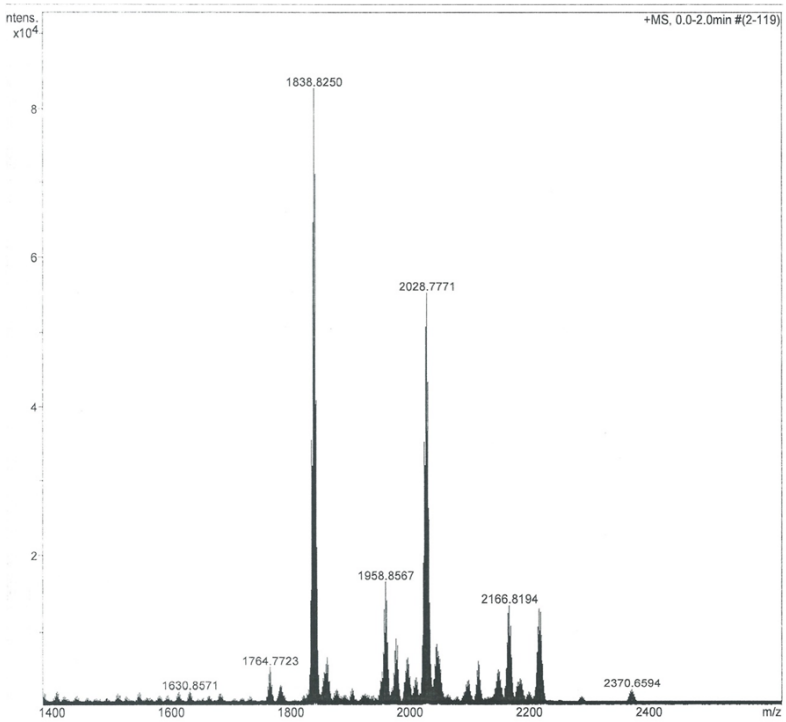

Figure S10. ESI-MS of compound **2.4** in $CHCl_3$-CH_3CN.

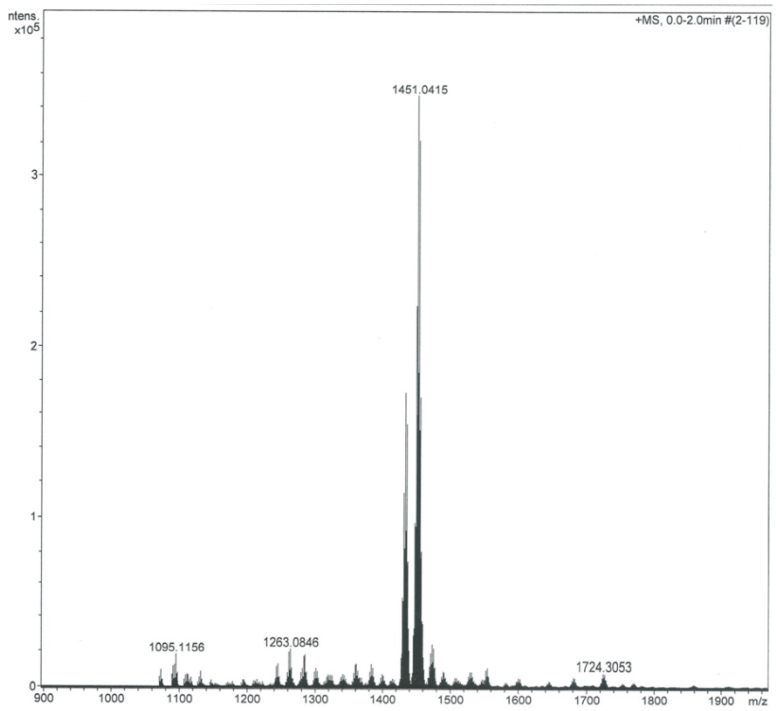

Figure S11. ESI-MS of compound **2.5** in $CHCl_3$-CH_3CN.

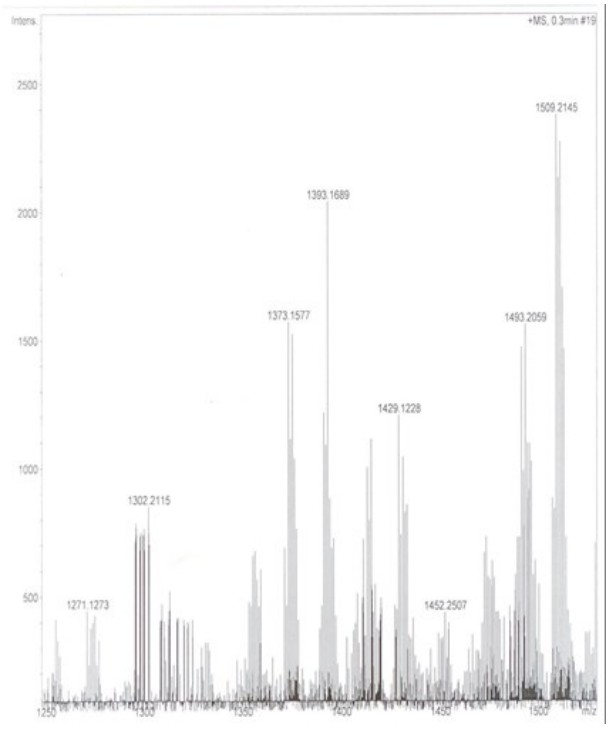

Figure S12. ESI-MS of compound **2.6** in $CHCl_3$-CH_3CN.

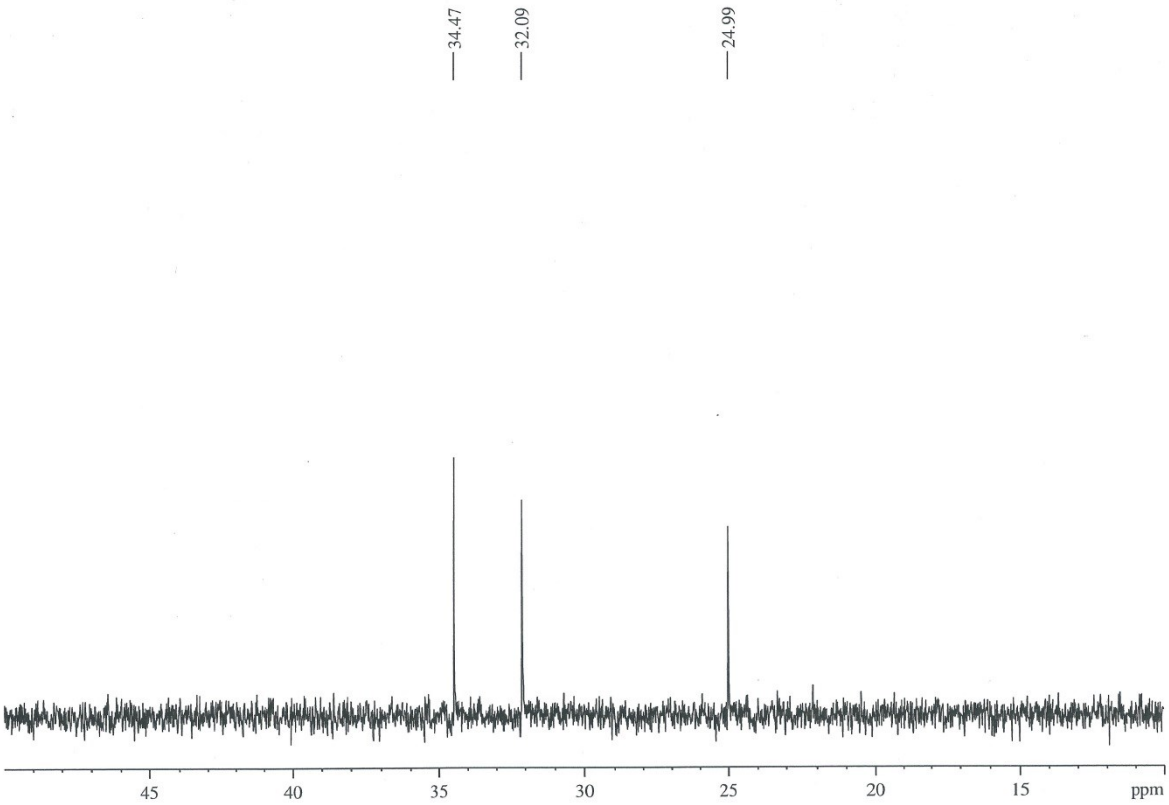

Figure S13. Solution ^{31}P NMR spectrum of **2.1** in $CDCl_3$ solvent.

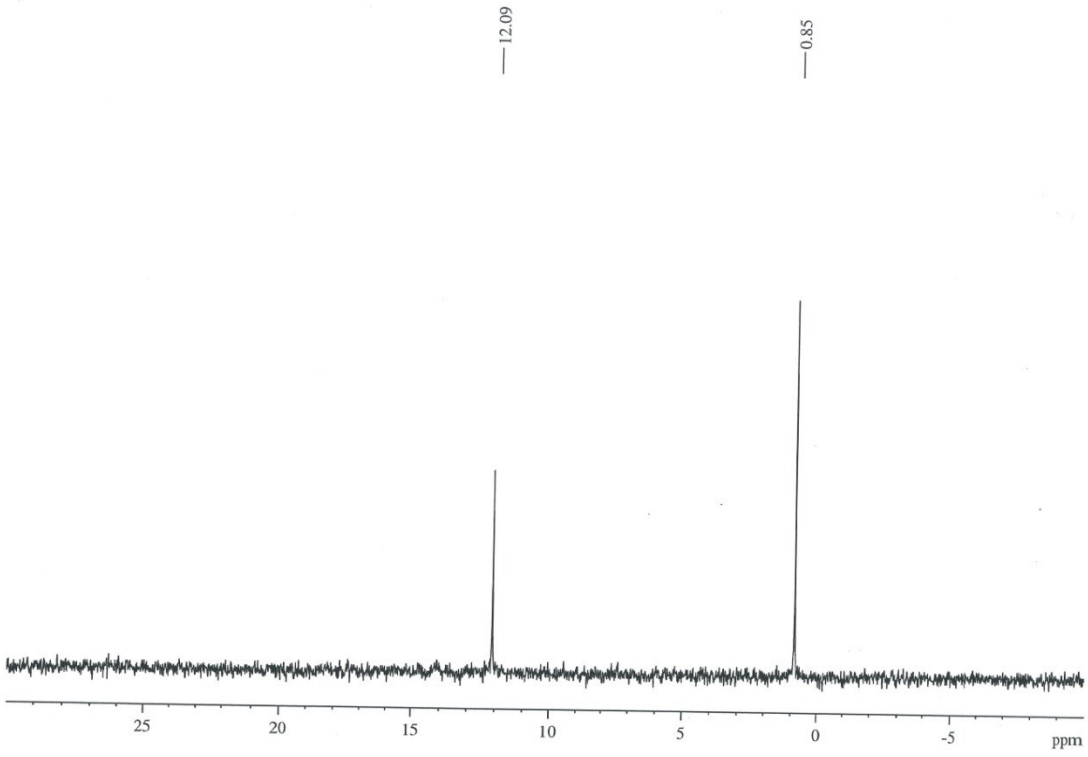

Figure S14. Solution ^{31}P NMR spectrum of **2.2** in $CDCl_3$ solvent

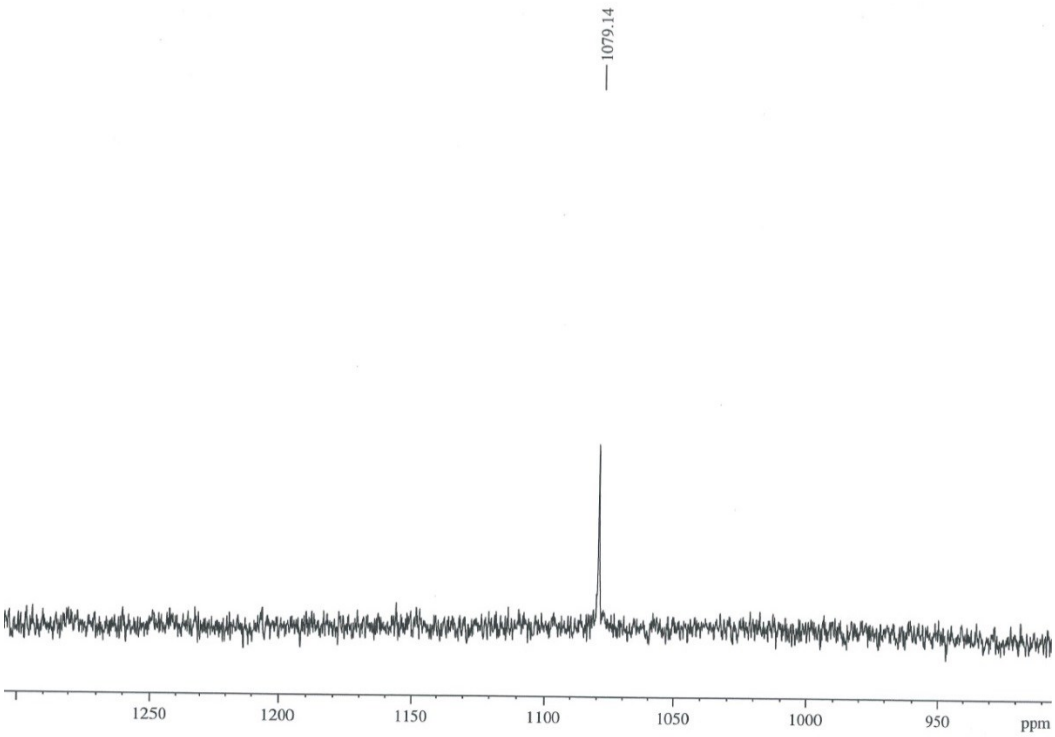

Figure S15. Solution ^{77}Se NMR spectrum of **2.3** in $CDCl_3$ solvent.

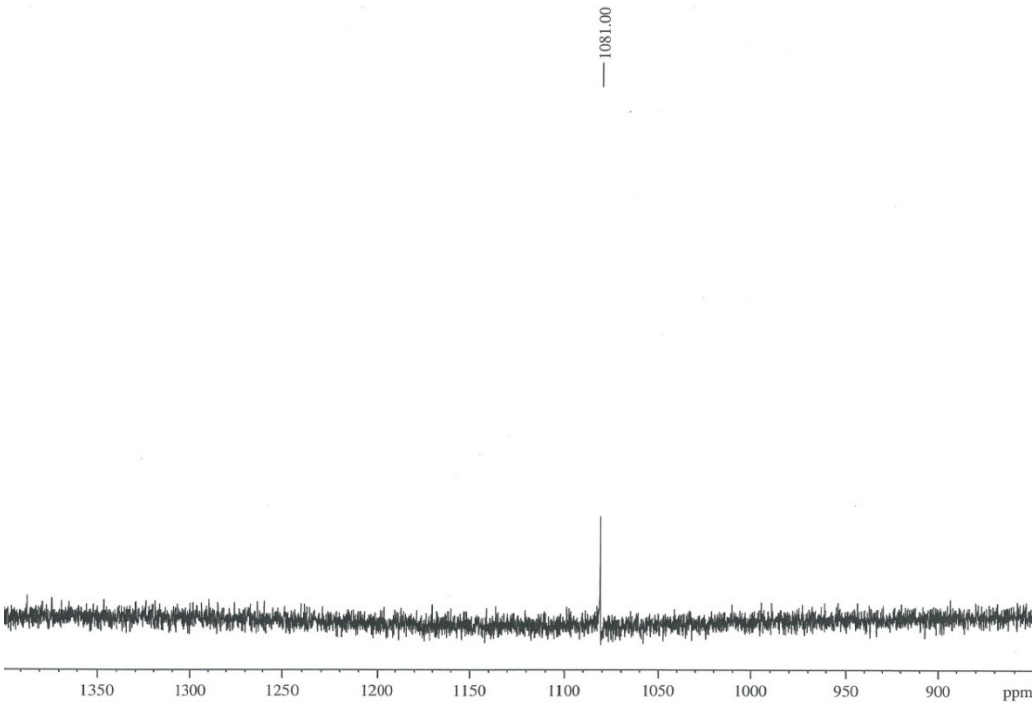

Figure S16. Solution ^{77}Se NMR spectrum of **2.4** in $CDCl_3$ solvent.

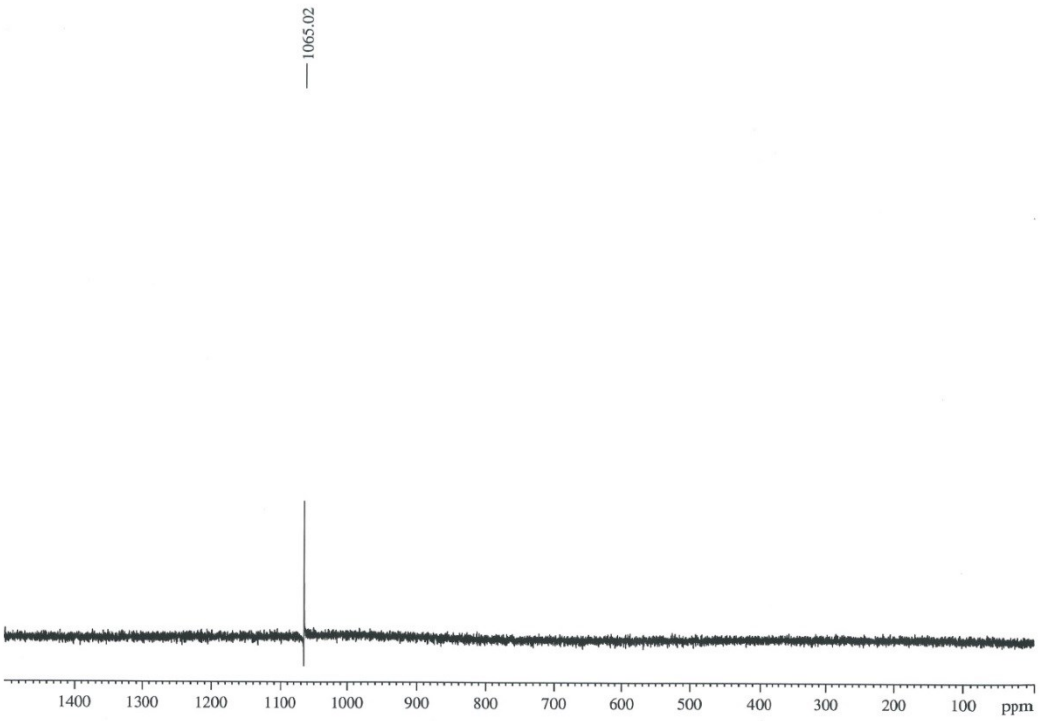

Figure S17. Solution ^{77}Se NMR spectrum of **2.5** in $CDCl_3$ solvent.

2.6 References

1. (a) S. Ali, V. Baskar, C. A. Muryn, and R. E. P. Winpenny, *Chem. Commun*., 2008, 6375; (b) S. Ali, C. A. Muryn, F. Tuna and R. E. P. Winpenny, *Dalton Trans*., 2010, **39**, 9588.
2. (a) V. Baskar, M. Shanmugam, M. Helliwell, S. J. Teat and R. E. P. Winpenny, *J. Am. Chem. Soc*., 2007, **129**, 3042; (b) M. S. R. Prabhu, A. K. Jami and V. Baskar, *Organometallics*, 2009, **28**, 3953; (c) A. K. Jami, M. S. R. Prabhu and V. Baskar, *Organometallics*, 2010, **29**, 1137; (d) A. K. Jami and V. Baskar, *Dalton Trans*., 2012, **41**, 12524; (e) N. K. Srungavruksham and V. Baskar, *Dalton Trans*., 2015, **44**, 6358; (f) J. Beckmann and M. Hesse, *Organometallics*, 2009, **28**, 2345; (g) J. Beckmann, T. Heck and M. Takahashi, *Organometallics*, 2007, **26**, 3633; (h) V. Chandrasekhar and R. Thirumoorthi, *Organometallics*, 2009, **28**, 2637; (i) L. F. Piedra-Garza, M. H. Diekman, O. Moldovan, H. J. Breunig and U. Kortz, *Inorg. Chem*., 2009, **48**, 411. (j) M. A. Said, K. C. Kumara Swamy, D. M. Poojary, A. Clearfield, M. Vieth and V. Huch, *Inorg. Chem*., 1996, **35**, 3235; (k) M. A. Said, K. C. Kumara Swamy, K. Babu, K. Aparna and M. Nethaji, *J. Chem. Soc., Dalton Trans.,* 1995, 2151;
3. J. Beckmann, P. Finke, M. Hesse and B. Wettig, *Angew. Chem., Int. Ed*., 2008, **47**, 9982; (b) J. Brunig, E. Hupf, E. Lork, S. Mebs and J. Beckmann, *Dalton Trans*., 2015, **44**, 7105.
4. (a) C. J. Clark, B. K. Nicholson and C. E. Wright, *Chem. Commun*., 2009, 923; (b) B. K. Nicholson, C. J. Clark, C. E. Wright and T. Groutso, *Organometallics*, 2010, **29**, 6518; (c) B. K. Nicholson, C. J. Clark, C. E. Wright, S. G. Telfer and T. Groutso, *Organometallics*, 2011, **30**, 6612; (d) B. K. Nicholson, C. J. Clark, S. G. Telfer and T. Groutso, *Dalton Trans*., 2012, **41**, 9964; (e) B. K. Nicholson, C. J. Clark, G. B. Jameson and S. G. Telfer, *Inorg. Chim. Acta*, 2013, **406**, 53.
5. (a) Y. Fujiwara, M. Mitani, S. Yasuike, J. Kurita and T. Kaji, *J. Health Sci*., 2005, **51**, 333; (b) V. Rishi, W. J. Oh, S. L. Heyerdahl, J. Zhao, D. Scudiero, R. H. Shoemaker and C. Vinson, *J. Struct. Biol*., 2010, **170**, 216; (c) S. L. Heyerdahl, J. Rozenberg, L. Jamtgaard, V. Rishi, L. Varticovski, K. Akash, D. Scudiero, R. H. Shoemaker, T. S. Karpova, R. N. Day, J. D. McNally and C. Vinson, *Eur. J. Cell Biol*., 2010, **89**, 564.

6. J. C. McKelvie, M. I. Richards, J. E. Harmer, T. S. Milne, P. L. Roach and P. C. Oyston, *Br. J. Pharmacol*., 2013, **168**, 172.
7. S. Ali, C. A. Muryn, F. Tuna and R. E. P. Winpenny, *Dalton Trans*., 2010, **39**, 124.
8. (a) H. Schmidt, *Liebigs Ann. Chem*., 1920, **421**, 174; (b) G. O. Doak and H. G. Steinman, *J. Am. Chem. Soc*., 1946, **68**, 1987; (c) G. O. Doak, *J. Am. Chem. Soc*., 1946, **68**, 1991.
9. (a) R. Rüther, F. Huber and H. Preut, *Z. Anorg. Allg. Chem*., 1986, **539**, 110; (b) P. C. Croft and G. M. Kosolapoff, *J. Am. Chem. Soc*., 1953, **75**, 3379.
10. N. Winkhofer, H.W. Roesky, M. Noltemeyer and W.T. Robinson, *Angew. Chem. Int. Ed*. 1992, **31**, 599.
11. G. M. Sheldrick, SHELXS-97, Program for Crystal Structure Solution, University of Göttingen, Göttingen, Germany, 1997.
12. G. M. Sheldrick, *Acta Crystallogr., Sec. A: Fundam. Crystallogr.,* 2008, **64**, 112.
13. G. M. Sheldrick, *Acta Crystallogr., Sect. C: Cryst. Struct. Commun.,* 2015, **71,** 3.
14. P. Van Der Sluis and A. L. Spek, BYPASS: an effective method for the refinement of crystal structures containing disordered solvent regions. *Acta Crystallogr., Sec. A*, 1990, **46**, 194.
15. 13. (a) A. L. Spek, Single-crystal structure validation with the program *PLATON. J. Appl. Cryst*., 2003, **36**, 7; (b) A. L. Spek, Structure validation in chemical crystallography. *Acta Crystallogr., Sec. D*, 2009, **65**, 148.
16. V. Chandrasekhar, V. Baskar, A. Steiner and S. Zacchini, *Organometallics*, 2002, **21**, 4528.
17. (a) M. G. Walawalkar, R. Murgavel, A. Voigt, H. W. Roesky and H. G. Schmidt, *J. Am. Chem. Soc*., 1997, **119**, 4656; (b) M. G. Walawalkar, R. Murgavel, H. W. Roesky, I. Uson and R. Kraetzner, *Inorg. Chem*., 1998, **37**, 473.
18. (a) M. G. Walawalkar, R. Murgavel, H. W. Roesky and H. G. Schmidt, *Organometallics*, 1997, **16**, 516; (b) M. G. Walawalkar, R. Murgavel, H. W. Roesky and H. G. Schmidt, *Inorg. Chem*., 1997, **36**, 4202.
19. N. E. Chakov, W. Wernsdorfer, K. A. Abboud and G. Christou, *Inorg. Chem*., 2004, **43**, 5919.
20. V. Chandrasekhar, M. G. Muralidhara, K. R. J. Thomas and E. R. T. Tiekink, *Inorg. Chem*., 1992, **31**, 4707.

21. N. K. Srungavruksham and V. Baskar, *Eur. J. Inorg. Chem*., 2012, 136.

22. (a) P. Christian, G. Rajaraman, A. Harrison, M. Helliwel, J. J. W. Mcdouall, J. Raftery and R. E. P. Winpenny, *Dalton Trans*., 2004, 2550. (b) R. X, Yao, Y. L. Qin, F. Ji, Y. F. Zhao and X. M. Zhang, *Dalton Trans*., 2013, **42**, 6611; (c) R. Biswas, Y. Ida, M. L. Baker, S. Biswas, P. Kar, H. Nojiri, T. Ishida and A. Ghosh, *Chem. Eur. J,* 2013, **19**, 3943; (d) M. Rancan, A. Dolmella, R. Seraglia, S. Orlandia, S. Quici and L. Armelao, *Chem. Comm*., 2012, **48**, 3115; (e) K. Wang, D. Feng, T.-F. Liu, J. Su, S. Yuan, Y.-P. Chen, M. Bosch, X. Zon and H. C. Zhou, *J. Am. Chem. Soc,* 2014, **136**, 13983.

23. (a) C. Ma, J. Zhang, F. Li and R. Zhang, *Eur. J. Inorg. Chem*, 2004, 2775; (b) Q. Gao, X. Wang, M. T. Conato, T. Makarenko and A. J. Jacobson, *Cryst. Growth. Des*, 2011, **11**, 4638.

Base Induced Assembly of Hexa-, Undeca- and Tetradecanuclear Polyoxostibonates

Chapter 3

Abstract: Isolation and structural characterization of novel organoantimony (V) based polyoxometalates are reported. $(RSb)_4(OH)_4(t\text{-}BuPO_3)_6$ and $(RSb)_2(O)(t\text{-}BuPO_3H)_6$ independently in the presence of pyridine as a base under solvothermal conditions which affords hexanuclear organoantimonate clusters $[(RSb)_6(\mu_3\text{-}O)_2(\mu_2\text{-}O)_6(t\text{-}BuPO_3)_4]$, [where R = *p*-iPr-$C_6H_4$ (**3.1**) and *p*-Cl-C_6H_4 (**3.2**)]. Further, the reaction of organostibonic acids with diorganophosphinic acid (diclyclohexyl, diphenyl phosphinic acid) in the presence of a tetraethyl ammonium hydroxide affords colorless products which on structural characterization reveals the formation of undecanuclear and tetradecanuclear polyoxostibonates stabilized by phosphinates binding in the peripheral part of the POMs $Na_5(p\text{-}MeC_6H_4Sb)_{11}(O)_{28}\{(C_6H_{11})_2PO_2\}_2$ (**3.3**) and $Na_2(p\text{-}iPr\text{-}C_6H_4Sb)_{14}(O)_{28}(Ph_2PO_2)_8$ (**3.4**).

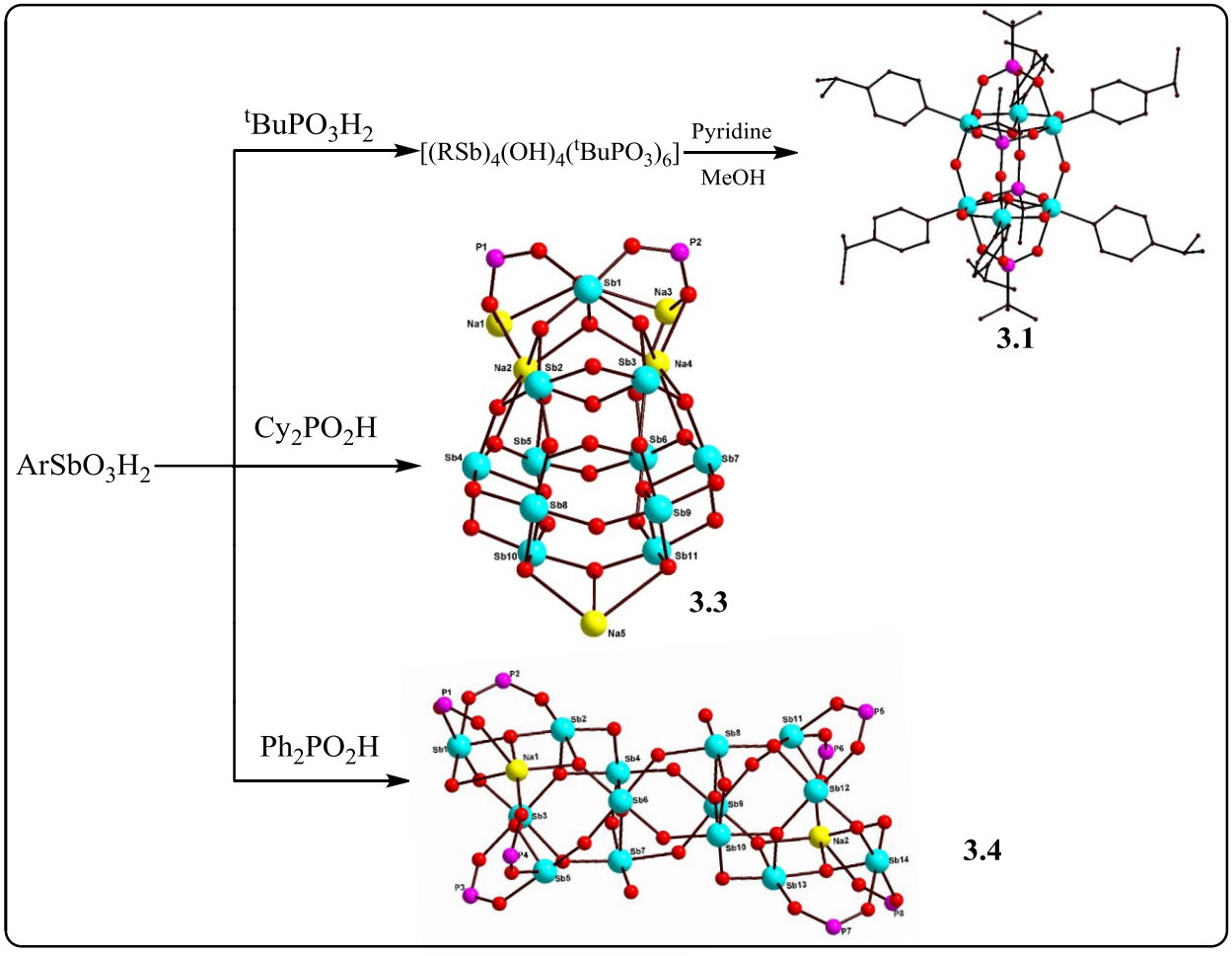

3.1 Introduction

Phosphonic and phosphinic acids have been used as versatile ligands for synthesizing multinuclear clusters based on main group metals,[1] transition metals[2] and lanthanides.[3] Some of the molecular clusters have been found to exhibit interesting magnetic properties like showing SMM behavior at lower temperatures.[4] Poly-phosphates have been used as ligands for synthesizing large number of interesting supramolecular frameworks.[5] Our group has been involved in investigating the chemistry of higher analogues of phosphonic acids namely organostibonic acids and reaction of organostibonic acids with various protic ligands has led to stabilization of interesting discrete molecular clusters displaying varied geometries like cube,[6] triangle,[7] adamantane,[8] tetrameric butterfly cores,[9] dodeca and hexadeca nuclear organoantimony based POM frameworks.[10, 11] Herein, $(RSb)_4(OH)_4(t\text{-}BuPO_3)_6$ and $(RSb)_2(O)(t\text{-}BuPO_3H)_6$ have been used as starting materials which independently in the presence of pyridine as base under solvothermal conditions affords hexanuclear organoantimonate clusters $[(RSb)_6(\mu_3\text{-}O)_2(\mu_2\text{-}O)_6(t\text{-}BuPO_3)_4]$, [where R = *p*-iPr-$C_6H_4$ (**3.1**) and *p*-Cl-C_6H_4 (**3.2**)] which has been characterized by single crystal X-ray diffraction studies. Interestingly, irrespective of the pre-formed clusters used with varying nuclearity of antimonates-phosphonates as starting materials, self-association in the presence of pyridine results in the isolation of isostructural hexanuclear organoantimonate clusters. Organostibonic acids have tendency to self-condense in the presence of base forms dodeca$\{Sb_{12}\}$ and hexadecanuclear $\{Sb_{16}\}$organoantimony based POM frameworks. We further extended our study by reacting individually organostibonic acids with phosphinic acids in the presence of a stronger base like tetraethyl ammonium hydroxide. Remarkably two novel undeca$\{Sb_{11}\}$ and tetradecanuclear $\{Sb_{14}\}$organoantimony molecular aggregates which can be visualized as a hybrid of metal-oxo cluster and POMs have been assembled in the presence of phosphinate ligands. $[Na_5(p\text{-}MeC_6H_4Sb)_{11}(O)_{28}\{(C_6H_{11})_2PO_2\}_2]$ (**3.3**) and $[Na_2(p\text{-}iPr\text{-}C_6H_4Sb)_{14}(O)_{28}(Ph_2PO_2)_8]$ (**3.4**) have been isolated and structurally characterized. The details of the study are reported herein.

3.2 Experimental Section

3.2.1 General Information:

Arylstibonic acids[12] (aryl= *p*-isopropylphenyl, *p*-chlorophenyl and *p*-methylphenyl), *t*-butylphosphonic acid[13] and dicyclohexylphosphinic acid[14] were synthesized according to literature reports. Diphenylphosphinic acid, solvents and common reagents were purchased from commercial sources. Mixed antimonate-phosphonate pro ligands $[(p\text{-iPr-}C_6H_4Sb)_4(OH)_4(t\text{-}BuPO_3)_6]$ and $[(p\text{-Cl-}C_6H_4Sb)_2(O)(t\text{-}BuPO_3H)_6]$ were synthesized by condensation reactions of organostibonic acid with *t*-butylphosphonic acid.[9, 15] All the compounds used were dried under a high vacuum for half an hour before subjected to spectroscopic and elemental analysis.

3.2.2 Instrumentation:

Infrared spectra were recorded with a JASCO-5300 FT-IR spectrometer as KBr pellets. The solid state ^{31}P NMR spectra were recorded with a Bruker AVANCEIII 400 instrument. Elemental analysis was performed with a Flash EA Series 1112 CHNS analyzer. Single crystal X-ray data collection for compounds **3.1-3.4** were carried out at 100(2) K with a Bruker Smart Apex CCD area detector system [λ (Mo-Kα) = 0.71073 Å] with a graphite monochromator. The data were reduced using SAINTPLUS. The structures were solved using SHELXS-97 and refined using the program SHELXL-2014/7[16]. All non-hydrogen atoms were refined anisotropically. Several attempts were made to obtain better quality data for compound **3.4**; however, due to poor crystal quality the data quality could not be enhanced. In compound **3.4** the disorder associated with phenyl rings and terminal methyl groups were constrained using EADP, DELU, FLAT, DFIX instructions in SHELXL-2014/7. In compounds **3.3** and **3.4** disordered acetonitrile solvent accessible voids are present in the asymmetric units which are not modeled. These solvent contributions were removed by using the SQUEEZE[17] command in PLATON[18]. The total electron count removed by SQUEEZE corresponded to 188 with a void volume of 1554.2 Å3 (20.7%) per unit cell in **3.3** and 135 with a void volume of 1411.8 $Å^3$ (22.7%) per unit cell in **3.4**.

3.2.3 Synthetic procedures:

3.2.3a Synthetic procedure for compounds 3.1-3.2:

The corresponding mixed antimonate-phosphonate pro-ligand was dissolved in methanol (15 mL) to which dropwise addition of pyridine formed a clear solution. It was stirred for 15 minutes and then transferred into a Teflon digestion bomb. The bomb was sealed properly and the mixture heated to 100^{o}C for 12 h and then cooled slowly for 48 h. Colorless crystals were obtained at the base of the Teflon bomb. Molar ratios and weights of the reactants used are as follows.

Compound 3.1: Pro-ligand [(*p*-iPr-$C_6H_4Sb)_4(OH)_4$(*t*-$BuPO_3)_6$] (0.1 g, 0.05 mmol) and pyridine (0.04 mL). Yield 0.036g (32% based on pro ligand). Decp temp: 275-276 ^{0}C. Anal. Calcd (%) for $C_{70}H_{102}O_{20}P_4Sb_6$ (2118.00): C, 39.70; H, 4.85. found: C, 39.62; H, 4.76. ^{31}P {^{1}H} NMR δ: 38.30, 12.26 ppm. IR (cm-1, KBr pellet): 3440(wide), 2961(s), 2928(m), 2870(m), 1631(m), 1592(w), 1480(s), 1458(s), 1402(s), 1364(s), 1082(s), 1013(s), 979(m), 821(s), 732(m), 680(m), 634(s), 594(m), 539(s).

Compound 3.2: Pro-ligand [(*p*-Cl-$C_6H_4Sb)_2$(O)(*t*-$BuPO_3H)_6$] (0.1 g, 0.076 mmol) and pyridine (0.04 mL). Yield 0.042g (40% based on pro ligand). Decp temp: 269-270 ^{o}C. Anal. Calcd (%) for $C_{52}H_{60}O_{20}Cl_6P_4Sb_6$ (2072.19): C, 30.14; H, 2.92. found: C, 30.26; H, 2.85. ^{31}P{^{1}H} NMR δ: 37.84, 13.43 ppm. IR (cm-1, KBr pellet): 3417(wide), 2963(s), 2905(w), 2864(w), 1598(m), 1493(s), 1445(s), 1394(m), 1262(s), 1179(m), 1086(w), 1033(s), 989(m), 802(s), 758(m), 744(s), 701(s), 563(s).

3.2.3b Synthetic procedure for compounds 3.3-3.4:

Organostibonic acid and corresponding phosphinic acid were taken in 1:2 molar ratios in acetonitrile (15 mL) and simultaneously tetraethylammonium hydroxide was added dropwise to the reaction mixture and stirring was continued for 24 h at room temperature. The resulting colorless solution was filtered and the filtrate was allowed to crystallize by slow evaporation at room temperature. Colorless single crystals suitable for X-ray diffraction studies were grown

from acetonitrile filtrate in a week time. Molar ratios and weights of the reactants used are as follows.

Compound 3.3: *p*-methylphenylstibonic acid (0.092, 0.343 mmol), dicyclohexyl phosphinic acid (0.158g, 0.686 mmol) and tetraethyl ammonium hydroxide (0.2 ml, 1.37 mmol). Yield: 0.036g (34% based on *p*-methylphenylstibonic acid). Decp temp: 279-280 ^{0}C. Anal, Calcd (%) for $C_{109}H_{141}NO_{32}Na_5P_2Sb_{11}$ (3493.52): C, 37.47; H, 4.07; N, 0.40. Found: C, 37.56; H, 4.13; N, 0.48. ^{1}H NMR (100 MHz, $CDCl_3$-CD_3OD, ppm) δ: 7.94-7.78 (m, 22H), 7.16-6.98 (m, 22H), 2.34-1.20 (br m, 44H), 0.83 (s, 33H), ^{13}C NMR (100 MHz, $CDCl_3$-CD_3OD) δ: 134.21, 133.87, 133.40, 128.49, 128.42, 128.09, 52.06, 37.15, 36.42, 29.56, 26.86, 26.76, 26.36, 25.74, 25.71, 21.11, 21.01 ppm. ^{31}P{^{1}H} NMR (162 MHz, $CDCl_3$-CD_3OD) δ: 40.24 ppm. IR (cm-1, KBr pellet): 3407 (wide), 2923(s), 2851(m), 1741(w), 1637(m), 1593(w), 1493(w), 1450(s), 1393(s), 1261(s), 1185(w), 1171(w), 1137(m), 1073(s), 1020(m), 803(s), 717(m), 580(m), 489(s).

Compound 3.4: *p*-isopropylphenylstibonic acid (0.100, 0.343 mmol), diphenylphosphinic acid (0.150g, 0.686 mmol) and tetraethyl ammonium hydroxide (0.2 ml, 1.37 mmol). Yield: 0.040g (29% based on *p*-isopropylphenylstibonic acid). Decp temp: 286-287 ^{0}C. Anal, Calcd (%) for $C_{222}H_{234}O_{44}P_8Na_2Sb_{14}$ (5604.61): C, 47.57; H, 4.21. Found: C, 48.13; H, 4.16. ^{1}H NMR (400 MHz, $CDCl_3$, ppm) δ: 7.77-7.72 (m, 80H), 7.45-7.35 (m, 56H), 3.29-3.27 (m, 14H), 1.27(d, 28H), 1.19 (d, 28H), 0.90(d, 28H). ^{13}C NMR (100 MHz, $CDCl_3$) δ: 134.20, 132.82, 131.56, 131.53, 131.31, 131.20, 128.30, 128.17, 52.64, 35.67, 34.23, 29.70 ppm. ^{31}P{^{1}H} NMR (162 MHz, $CDCl_3$) δ: 30.90 ppm. IR (cm-1, KBr pellet): 3417(wide), 3058(m), 2960(s), 2925(m), 1650(m), 1439(s), 1402(s), 1204(m), 1036(m), 1012(s), 991(m), 822(s), 748(s), 722(m), 692(s), 583(s).

3.3 Results and discussions

Compounds **3.1** and **3.2** were synthesized by reacting $(RSb)_4(OH)_4(t\text{-}BuPO_3)_6$ and $(RSb)_2(O)(t\text{-}BuPO_3H)_6$ independently in the presence of pyridine under solvothermal conditions. Single crystal X-ray characterization reveals the formation of hexanuclear organoantimonate clusters $[(RSb)_6(\mu_3\text{-}O)_2(\mu_2\text{-}O)_6(t\text{-}BuPO_3)_4]$, [where R = *p*-iPr-$C_6H_4$ (**3.1**) and *p*-Cl-C_6H_4 (**3.2**)] (**Scheme-3.1**). Single crystals of **3.1** and **3.2** suitable for X-ray diffraction studies were obtained directly at cthe base of the Teflon bomb. The solubility of the isolated crystals of **3.1** and **3.2** were poor in

common organic solvents. Hence solid state NMR was used for characterizing the phosphorous atom environment. Solid state ^{31}P $\{^{1}H\}$ NMR of **3.1** shows two resonance peaks at δ= 38.3 and 12.2 ppm which indicates the presence of two different phosphorus environments. Similarly Solid state ^{31}P $\{^{1}H\}$ NMR of **3.2** shows two resonance peaks at δ= 37.8 and 13.4 ppm. Compound **3.1** crystallizes in monoclinic space group P21/c with two half of the molecules present in asymmetric unit. Compound **3.2** crystal

lizes with orthorhombic space group Pbcn. Crystallographic data and bond metric parameters of **3.1** and **3.2** are given in the table 3.1-3.2. Since the molecular structures of compounds **3.1** and **3.2** are similar, **3.1** (**Figure 3.1**) is considered for structural discussions.

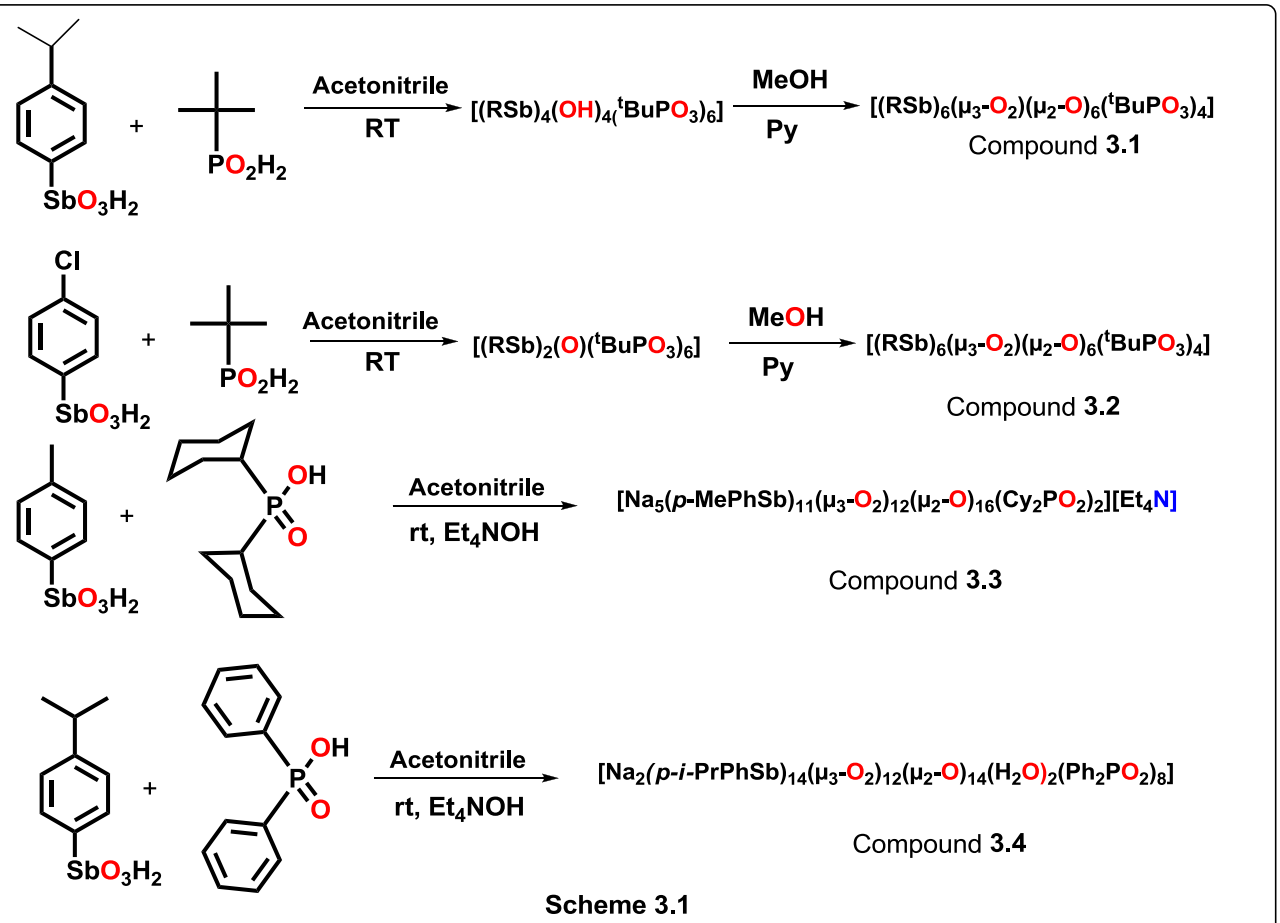

Scheme 3.1

The solid state structure of **3.1** reveals the formation of hexanuclear organoantimony (v) oxo cluster $[(p\text{-iPr-}C_6H_4Sb)_6(\mu_3\text{-}O)_2(\mu_2\text{-}O)_6(t\text{-}BuPO_3)_4]$. It contains a puckered eight-membered Sb_4O_4 core held together by four phosphonates ligands. Interestingly, the molecular structure can

also be visualized as being built up of two *in situ* generated Sb_3O triangles. The Sb atoms in the triangular units are linked together by a μ_3-oxo bridge and further the two μ_2-oxide bridges link each Sb atoms in the triangle to the neighboring Sb atom. The Sb_3O triangles are connected to each other through two bridged phosphonates, two μ_2-oxide bridges and each Sb_3O triangles periphery is further coordinated by a phosphonate ligand. There are four phosphonates in **3.1**, each bound to three Sb centers in 3.111 coordination modes [based on Harris notation]. The Sb atoms present in octahedral geometry with the O_5SbC coordination mode. The Sb-O bond lengths involving μ_3-oxo, μ_2-oxo bridges and phosphonates falls in the range of 2.008(4) to 2.117(3) Å, 1.915(3) to 1.987(4) Å and 2.018(4) to 2.088(3) Å respectively. The Sb-μ_3O-Sb and Sb-μ_2O-Sb bond angles are in the range of 99.16(15) to 143.39(19)° and 106.34(16) to 147.2(2)° respectively. Bond angles of C-Sb-O fall in the range of 171.33(7) to 179.37(17)^0, which clearly indicates the geometry around each Sb center is a regular octahedron.

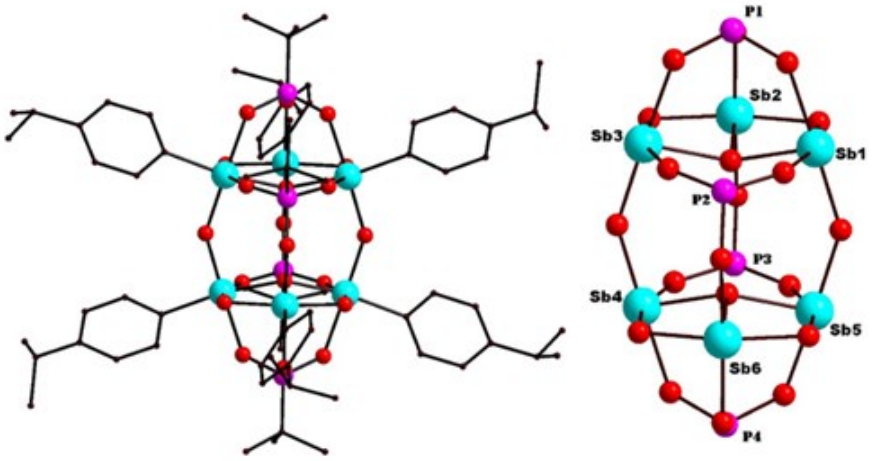

Figure 3.1: Molecular and Core structure of **3.1**. Color code: Cyan: Sb, Pink: P, Red: O, Grey: C. Hydrogen's are omitted for clarity.

Interestingly, a different pro-ligand, [(*p*-Cl-$C_6H_4Sb)_2$(O)(*t*-$BuPO_3H)_6$] used as a starting material, in presence of pyridine under solvothermal conditions also led to the isolation of a hexanuclear cluster **3.2** (**Figure 3.2**), which is similar to **3.1**. It should be noted that in the case of starting precursor used in the first case where the structure of the cluster was a tetra nuclear cluster with antimonate:phosphonate ratio being 4:6 and in the second one, the dimer where the antimonate:phosphonate ratio was 2:6 does not vary the structure of the end product obtained.

The reason could probably be due to the more stable hexanuclear cluster obtained. Moreover the hexanuclear cluster itself can be visualized as built up of two triangular motifs held together by phosphonate ligands. Recently such triangular motifs containing organoantimony clusters have been synthesized and structurally characterized from our group wherein the assembled triangles are stabilized by *in situ* generated siloxane bridges.[7] In compound **3.2** Sb-O bond lengths involving μ_3-oxo, μ_2-oxo bridges and phosphonates falls in the range of 2.013(2) to 2.115(2) Å, 1.961(2) to 1.980(2) Å and 2.017(2) to 2.078(2) Å respectively. The Sb-μ_3O-Sb and Sb-μ_2O-Sb bond angles are in the range of 99.44(10) to 142.72(13)° and 106.13(11) to 145.36(14)° respectively. O_5SbC coordination present around the antimony and the geometry around each Sb center is a regular octahedron.

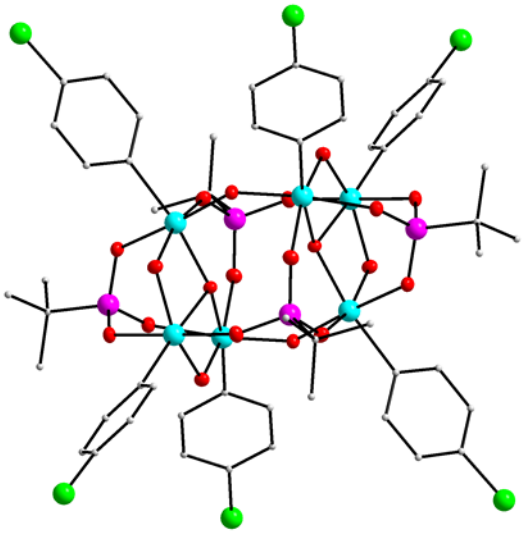

Figure 3.2: Molecular structure of **3.2.** Color code: Cyan: Sb, Pink: P, Red: O, Green: Cl. Hydrogen's are omitted for clarity.

Compound **3.3** have been synthesized by condensation reactions of organostibonic acid with diclyclohexyl phosphinic acid in the presence of tetraethylammonium hydroxide as a base in acetonitrile solvent (**Scheme 3.1**). Colorless single crystals of **3.3** were grown from acetonitrile solution. Solution $^{31}P\{^1H\}$ NMR studies of **3.3** were performed in $CDCl_3$-CD_3OD mixture. Solution ^{31}P NMR of **3.3** shows single resonance peak at δ = 40.24 ppm, it indicates presence of a unique phosphorus environment present in the cluster. Compound **3.3** crystallizes in triclinic space group P-1. Crystallographic data and bond metric parameters of **3.3** are given in the table 3.2 & 3.4. Molecular structure of **3.3** reveals the formation of undecanuclear organoantimony

(V) oxo cluster (**Figure 3.3**). The charge of the cage is balanced by the presence of one tetraethylammonium cation, which crystallizes along with core. The cluster core has two triads (Sb_3O_4) and two diads (Sb_2O_2). Each triad consists of Sb_3O_4 unit which can be described as a cube with a vertex missing (**Figure 3.4**). The three Sb metal atoms are connected to each other by μ_2-oxo groups, and further a μ_3-oxo group bridges all three Sb atoms forming Sb_3O_4 core. These two Sb_3O_4 cores are connected through two μ_2-oxo bridges. In each diad Sb atoms are connected to Sb_3O_4 core through two μ_2-oxo bridges. In the diad two Sb atoms are connected between themselves through two μ_2-oxo bridges. One of the diad is connected to 11^{th} Sb atom through two μ_3-oxo bridges. The 11^{th} Sb atom occupies apex position of the cage and it is completely different from the other ten Sb atoms. All Sb centers exhibit oxidation state of +5 and are six coordinate with regular octahedral geometry. Of the ten Sb atoms present in **3.3** and which forms part of triads and diads, the coordination sphere of each metal atom is O_5SbC satisfied by five oxygen atoms from framework and one from phenyl ring carbon attached to antimony. The 11^{th} Sb atom is differently coordinated as of the six coordination present, two are from oxygen atoms of bridged phosphinates, and three are from μ_3-oxo bridges and one from phenyl ring carbon attached to antimony. Of the 32 framework oxygen atoms present, 11 are doubly bridged to two Sb atoms (Sb-O distance fall in the range 1.946(4) to 2.121(4) Å), one Oxygen doubly bridge present between two Na atoms (an average Na-O distance is 2.776(10) Å), 16 are μ_3-bridged Oxo groups (Sb-O distance falls in the range 1.932(4) to 2.132(4) Å). Four acetonitrile solvent molecules crystallizes along with cage, in which two acetonitrile molecules chelate to sodium ions with average Na-N distance is 2.889(10) Å. Two phosphinic acid moieties symmetrically chelate to 11^{th} Sb atom and four encapsulated sodium ions in 3.21 coordination modes. Within every phosphinate present, one μ_2-oxo group chelate to 11^{th} Sb atom and other μ_3-oxo group chelates to two sodium ions. In total five sodium ions are encapsulated in Sb_{11} cage. Out of five sodium ions, four are present in the one half of the cage and remaining one is in the bottom half of the cage. Na_1 is seven coordinate and Na_2 is six coordinate while the remaining three sodium ions are three coordinate with triangular geometry, Na-O bond lengths falls in the range of 2.314(7) to 2.996(4) Å. These sodium ions presumably come from leaching of glassware when kept for crystallization. Crystallization in Teflon vessels were tried which failed to yield crystals good enough for structure solution. The presence of sodium ions in the cage indicates the strong affinity of arylstibonic acids towards sodium ions and it also plays a crucial

role in crystallization of **3.3** There has been earlier reports from our laboratory and others where similar incorporation of sodium ions have been noticed.[11(e)]

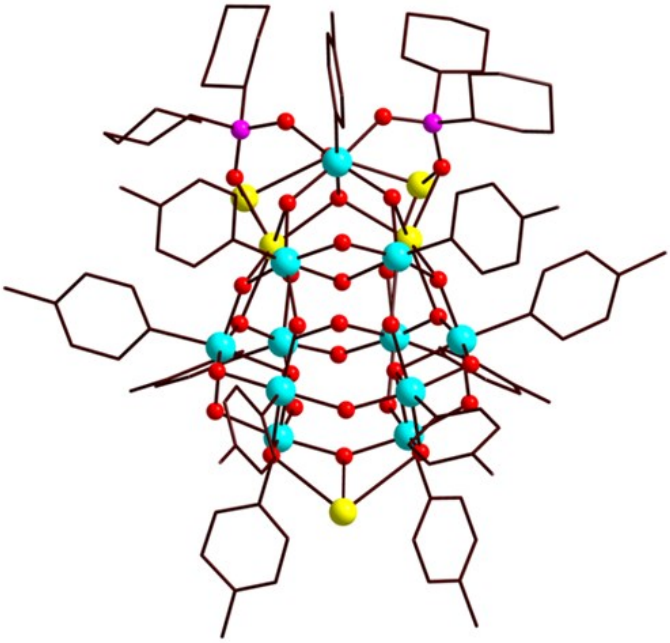

Figure 3.3: Solid state structure of **3.3**; Color code: Cyan: Sb, Yellow: Na, Pink: P, Red: O, Grey: C. Hydrogens, tetraethyl ammonium cation and solvate molecules omitted for clarity.

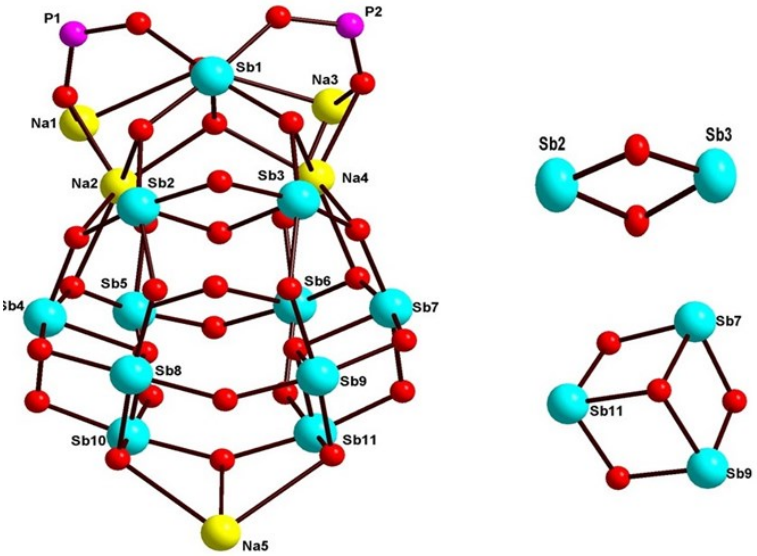

Figure 3.4: (left) Core structures of **3.3** and (right) Sub units of **3.3** diad (Sb_2O_2) and triad (Sb_3O_4): Color code: Cyan: Sb, Yellow: Na, Pink: P, Red: O, Grey: C

Compound **3.4** have been synthesized by condensation reactions of organostibonic acid with diphenyl phosphinic acid in the presence of tetraethylammonium hydroxide as a base in acetonitrile solvent (**Scheme 3.1**). Colorless single crystals of **3.4** were grown from acetonitrile solution. Solution $^{31}P\{^{1}H\}$ NMR studies of **3.4** were performed in $CDCl_3$ respectively. Solution $^{31}P\{^{1}H\}$ NMR of **3.4** shows single resonance peak at δ = 30.91 ppm, indicates presence of unique phosphorus environment. Interestingly, change in R group attached to phosphorus will be influence the self-assembly of arystibonic acids and forms different nuclearities. While dicyclohexyl group forms $\{Sb_{11}\}$ cage and diphenyl group forms $\{Sb_{14}\}$ cage. Compound **3.4** crystallizes in a triclinic space group P-1 with half of the molecule present in the asymmetric unit. Crystallographic data and bond metric parameters of **3.4** are given in the table 3.2 & 3.5. Solid state structure of **3.4** reveals the formation of tetradecanuclear organoantimony (V) based polyoxometalates $\{Sb_{14}\}$ (**Figure 3.5**).

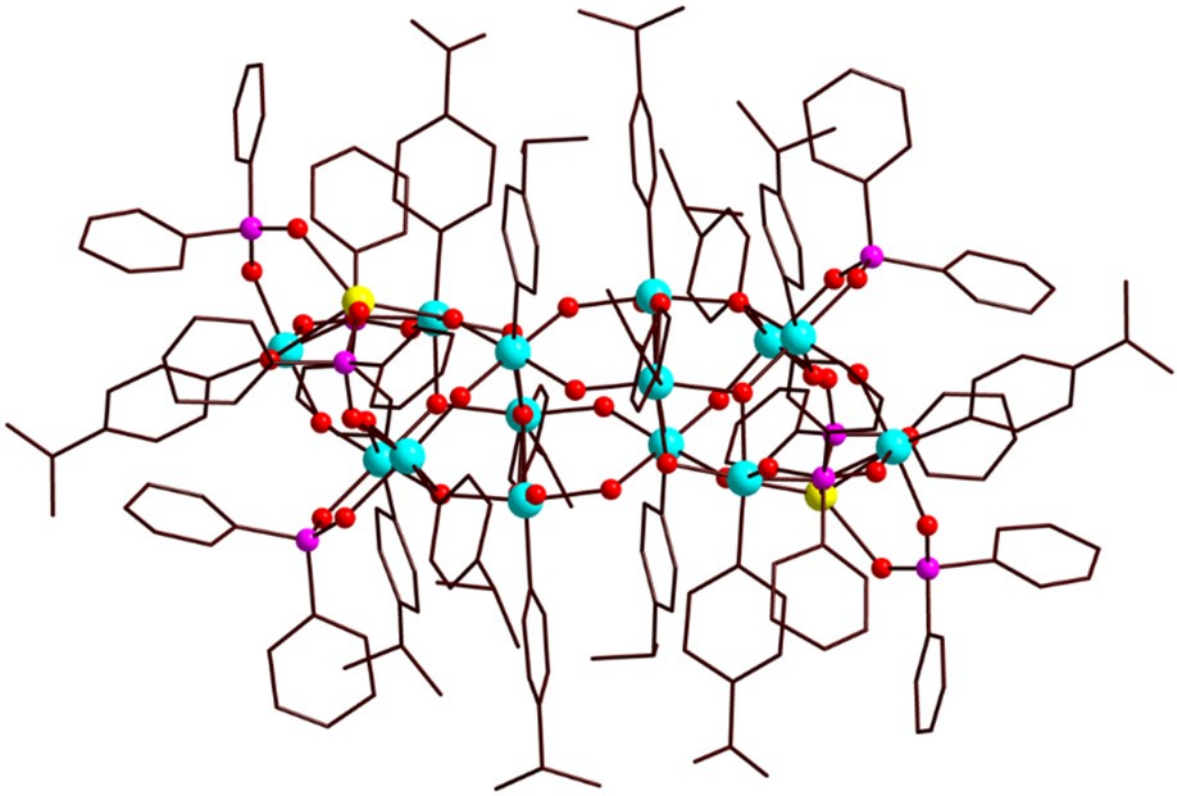

Figure 3.5: Molecular structure of **3.4**. Color code; Cyan: Sb, Yellow: Na, Pink: P, Red: O.

POM **3.4** contains fourteen arylstibonic acids self-condensed and linked by twelve triply-bridged, fourteen doubly-bridged and two terminal oxygens forming an extended ladder-shaped structure. Both edges of the ladder were capped by diphenylphosphinic acid moiety and further encapsulation of sodium ions in Sb_{14} core results in complete cage formation occurs. The $\{Sb_{14}\}$ cage contains two symmetrically equivalent heptameric units connected through four μ_2-oxo bridges. Each heptameric unit contains Sb_7O_{10} core stabilized by three μ_3-oxo and six μ_2-oxo bridge. Further, this core is connected to encapsulated sodium ions through two μ_3-oxo and a μ_2-oxo bridges. Each heptameric unit's edge is ligated by diphenylphosphinic acid moiety in a bidentate fashion. In each heptameric core one free oxygen is present and it is considered as neutral water molecule (H_2O). Each Sb is in +5 oxidation state and all are six coordinate with regular octahedral geometry. Out of six coordination present five are satisfied by framework oxygen atoms and one by phenyl ring carbon attached to antimony. The Sb-O bond lengths fall in the range of 1.909(6) to 2.130(7) Å. There are two sodium ions encapsulated in Sb_{14} cage from glassware leaching. The sodium ions are present in six coordinate with distorted octahedral geometry. Of the six coordination's present around Na+ ion, two from oxygen atoms of bridged phosphinate and four are from Sb attached framework oxygen atoms. The Na-O bond lengths falls in the range of 2.223(11) to 2.914(8) Å. Out of eight phosphinates present in the cage, four phosphinates chelate Sb-O-Sb edges, remaining four phosphinates chelate Sb-O-Na edges in 2.11 coordination fashion. Subtle differences in the electronic and steric substituents on the Sb / P atoms seems to be playing a very important role in deciding whether a discrete metal oxo cluster / POM type-frameworks are formed.

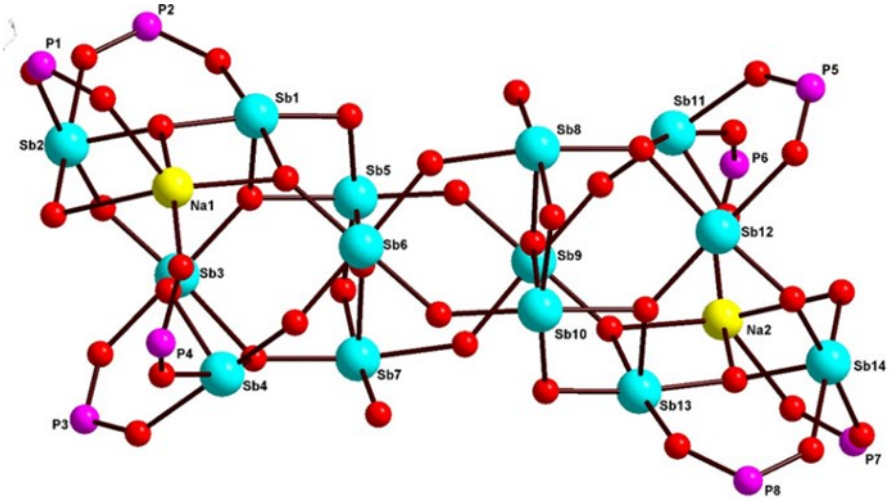

Figure 3.6: Core structures of **3.4**. Color code Cyan: Sb, Yellow: Na, Pink: P, Red: O, Grey: C

3.4 Conclusion

Base assisted self-assembly of arylstibonic acids in the presence of phosphinates as ligands have been shown to be useful for assembling novel POM frameworks. The work reported here contains essentially two parts. The first part is where pre-formed antimonate-phosphonate clusters are used as starting precursors which in the presence of pyridine under solvothermal conditions led to the formation of novel hexanuclear orgnoantimonate-phosphonate clusters. Irrespective of the pre-formed clusters used with varying nuclearity of antimonates-phosphonates as starting materials, self-association in the presence of base results in the isolation of isostructural molecular clusters. In the second part, organostibonic acids self-condensation in the presence of tetraethylammonium hydroxide and phoshinates as coordinating ligands has led to the isolation and structural characterization of undeca- and tetradecanuclear organoantimony based molecular aggregates which can be visualized as hybrids of metal-oxo cluster and POMs. Fine-tuning the electronic and steric substituent on organostibonic acids and varying bases opens up possibilities for assembling novel POMs based on organoantimony frameworks.

Table 3.1: Crystallographic tables of compounds **3.1-3.2**

	3.1	**3.2**
Formula	$C_{142}H_{212}O_{42}P_8Sb_{12}$	$C_{54}H_{60}Cl_6O_{22}P_4Sb_6$
F.wt g/mol^{-1}	4299.86	2128.10
T, K	100(2)	100(2)
Crystal system	Monoclinic	Orthorhombic
Space group	P 21/c	P b c n
Crystal size mm^3	0.230 x 0.200 x 0.190	0.210 x 0.160 x 0.120
a, Å	25.76(2)	16.397(2)
b, Å	17.056(10)	20.252(3)
c, Å	18.448(10)	21.265(3)
α, deg	90	90
β, deg	94.656(8)	90
γ, deg	90	90
V, Å^3	8080(9)	7061.6(17)
Z	2	4
D_{calcd} Mg/m^3	1.767	2.002
μ, mm^{-1}	2.125	2.651
F(000)	4264	4112
Theta range, deg	1.433 to 26.587	1.598 to 26.395
Index ranges	-32<=h<=32 -21<=k<=21 -22<=l<=23	-20<=h<=20 -25<=k<=25 -26<=l<=26
Total reflns	83682	72084
Ind. reflns / R(int)	16718 / 0.0980	7250 /0.0443
Completeness to θ_{max}, %	100.0	100.0
GooF(F^2)	1.023	1.141
R1(F)[I>2σ(I)]	0.0482	0.0314
$wR_2(F^2)$ (all data)	0.1238	0.0755
Largest diff peak/hole, e.Å^{-3}	1.487 /-0.962	1.382 /-0.875

Table 3.2: Crystallographic tables of compounds **3.3-3.4**

	3.3	**3.4**
Formula	$C_{115}H_{150}O_{32}N_4Na_5P_2Sb_{11}$	$C_{222}H_{234}O_{44}Na_2P_8Sb_{14}$
F.wt g/mol^{-1}	3616.53	5604.32
T, K	100(2)	100(2)
Crystal system	Triclinic	Triclinic
Space group	P-1	P-1
Crystal size mm^3	0.23 x 0.21 x 0.18	0.15 x 0.12 x 0.08
a, Å	18.2330(18)	19.418(4)
b, Å	18.3845(19)	19.443(4)
c, Å	23.323(2)	19.515(4)
α, deg	93.955(2)	95.014(4)
β, deg	100.037(2)	110.439(3)
γ, deg	101.722(2)	112.073(3)
V, Å^3	7493.5(13)	6192(2)
Z	2	1
D_{calcd} Mg/m^3	1.603	1.503
μ, mm^{-1}	2.049	1.620
F(000)	3540	2774
Theta range, deg	1.14 to 26.44	1.151 to 26.516
Index ranges	-22<=h<=22 -22<=k<=23 -29<=l<=29	-24<=h<=24 -24<=k<=24 -24<=l<=24
Total reflns	80528	65853
Ind. reflns / R(int)	30493/0.0419	25372 /0.0734
Completeness to θ_{max}, %	98.9	99.6
GooF(F^2)	1.028	0.897
R1(F)[I>2σ(I)]	0.0505	0.0745
w$R_2(F^2)$ (all data)	0.1323	0.2052
Largest diff peak/hole, e.Å^{-3}	2.343/-1.316	2.689/ -1.352

Table 3.3: Selected bond lengths (Å) and bond angles (º) in **3.1-3.2**

3.1				**3.2**	
Sb(1)-O(5)	1.945(4)	Sb(5)-O(14)	2.008(4)	Sb(1)-O(8)	1.922(2)
Sb(1)-O(9)	1.964(3)	Sb(5)-O(13)	2.034(4)	Sb(1)-O(6)	1.976(2)
Sb(1)-O(6)	2.018(4)	Sb(5)-O(16)	2.088(3)	Sb(1)-O(3)	2.027(2)
Sb(1)-O(2)	2.066(3)	Sb(6)-O(17)	1.952(4)	Sb(1)-O(4)	2.036(2)
Sb(1)-O(4)	2.117(3)	Sb(6)-O(19)	1.956(3)	Sb(1)-O(7)	2.078(2)
Sb(2)-O(10)	1.918(3)	Sb(6)-O(11)	2.025(4)	Sb(2)-O(8)#1	1.917(2)
Sb(2)-O(9)	1.987(4)	Sb(6)-O(18)	2.064(4)	Sb(2)-O(5)	1.980(2)
Sb(2)-O(4)	2.024(3)	Sb(6)-O(14)	2.109(4)	Sb(2)-O(4)	2.013(2)
Sb(2)-O(8)	2.040(4)	Sb(1)-O(5)-Sb(3)	106.81(16)	Sb(2)-O(1)	2.040(2)
Sb(2)-O(3)	2.069(4)	Sb(3)-O(4)-Sb(2)	143.27(18)	Sb(2)-O(10)	2.086(2)
Sb(3)-O(10)#1	1.920(3)	Sb(3)-O(4)-Sb(1)	99.16(15)	Sb(3)-O(5)	1.961(2)
Sb(3)-O(5)	1.979(3)	Sb(2)-O(4)-Sb(1)	99.72(14)	Sb(3)-O(6)	1.963(2)
Sb(3)-O(4)	2.021(3)	Sb(1)-O(9)-Sb(2)	106.50(17)	Sb(3)-O(2)#1	2.017(2)
Sb(3)-O(7)	2.029(3)	Sb(5)-O(14)-Sb(4)	143.39(19)	Sb(3)-O(9)	2.072(2)
Sb(3)-O(1)	2.086(3)	Sb(5)-O(14)-Sb(6)	99.50(15)	Sb(3)-O(4)	2.115(2)
Sb(4)-O(21)#2	1.924(4)	Sb(4)-O(14)-Sb(6)	99.29(14)	Sb(3)-O(6)-Sb(1)	107.03(11)
Sb(4)-O(19)	1.979(4)	Sb(6)-O(17)-Sb(5)	106.34(16)	Sb(3)-O(5)-Sb(2)	106.13(11)
Sb(4)-O(14)	2.026(3)	Sb(2)-O(10)-Sb(3)#1	145.4(2)	Sb(2)-O(4)-Sb(1)	142.72(13)
Sb(4)-O(12)#2	2.038(4)	Sb(5)-O(21)-Sb(4)#2	147.5(2)	Sb(2)-O(4)-Sb(3)	99.47(10)
Sb(4)-O(15)	2.078(4)	Sb(6)-O(19)-Sb(4)	106.42(16)	Sb(1)-O(4)-Sb(3)	99.44(10)
Sb(5)-O(21)	1.915(3)			Sb(2)#1-O(8)-Sb(1)	145.36(14)
Sb(5)-O(17)	1.974(4)				

Compound 3.1 Symmetry transformations used to generate equivalent atoms:

#1 -x,-y+1,-z+1 #2 -x+1,-y+1,-z+1

Compound 3.2 Symmetry transformations used to generate equivalent atoms:

#1 -x+1,-y,-z+1

Table 3.4: Selected bond lengths (Å) and bond angles (º) in **3.3**

Sb(1)-O(4)	1.949(4)	Sb(6)-O(16)	2.000(4)	Sb(11)-O(13)	2.149(4)
Sb(1)-O(3)	1.963(4)	Sb(6)-O(13)	2.089(4)	O(30)-Na(2)	2.341(5)
Sb(1)-O(5)	1.964(4)	Sb(6)-O(17)	2.100(4)	O(30)-Na(4)	2.739(7)
Sb(1)-O(2)	2.065(4)	Sb(7)-O(18)	1.945(5)	O(23)-Na(2)	2.594(5)
Sb(1)-O(1)	2.078(4)	Sb(7)-O(21)	1.963(5)	O(23)-Na(4)	2.742(7)
Sb(2)-O(6)	2.133(4)	Sb(7)-O(26)	1.991(4)	O(12)-Na(5)	2.940(8)
Sb(2)-O(8)	1.949(4)	Sb(7)-O(22)	2.063(4)	O(27)-Na(1)	2.490(5)
Sb(2)-O(4)	1.963(4)	Sb(7)-O(19)	2.104(4)	O(28)-Na(1)	2.964(5)
Sb(2)-O(9)	1.989(4)	Sb(8)-O(11)	1.965(4)	O(29)-Na(1)	2.332(6)
Sb(2)-O(7)	2.021(4)	Sb(8)-O(25)	1.974(4)	O(29)-Na(3)#1	2.680(8)
Sb(3)-O(11)	1.933(4)	Sb(8)-O(21)	1.983(4)	O(11)-Na(2)	2.409(5)
Sb(3)-O(5)	1.951(4)	Sb(8)-O(20)	1.989(4)	O(6)-Na(1)	2.998(5)
Sb(3)-O(9)	1.959(4)	Sb(8)-O(19)	2.128(4)	O(17)-Na(5)	2.710(8)
Sb(3)-O(6)	2.107(4)	Sb(9)-O(25)	1.938(4)	O(26)-Na(5)	2.928(9)
Sb(3)-O(10)	2.124(4)	Sb(9)-O(24)	1.969(4)	O(25)-Na(2)	2.397(5)
Sb(4)-O(12)	1.948(5)	Sb(9)-O(23)	1.970(4)	O(4)-Na(1)	2.622(5)
Sb(4)-O(14)	1.956(5)	Sb(9)-O(22)	2.083(4)	O(32)-Na(1)	2.447(5)
Sb(4)-O(7)	1.980(4)	Sb(9)-O(28)	2.120(4)	Sb(5)-O(19)-Sb(7)	97.70(17)
Sb(4)-O(17)	2.090(5)	Sb(10)-O(32)	1.940(4)	Sb(5)-O(19)-Sb(8)	96.31(17)
Sb(4)-O(13)	2.098(4)	Sb(10)-O(24)	1.976(4)	Sb(7)-O(19)-Sb(8)	96.37(17)
Sb(5)-O(12)	1.938(5)	Sb(10)-O(27)	1.991(4)	Sb(5)-O(12)-Sb(4)	143.7(2)
Sb(5)-O(20)	1.954(5)	Sb(10)-O(16)	2.021(4)	Sb(6)-O(13)-Sb(4)	103.29(17)
Sb(5)-O(26)	2.010(4)	Sb(10)-O(28)	2.114(4)	Sb(6)-O(13)-Sb(11)	95.38(17)
Sb(5)-O(10)	2.073(4)	Sb(11)-O(8)	1.966(4)	Sb(4)-O(13)-Sb(11)	95.23(17)
Sb(5)-O(19)	2.099(4)	Sb(11)-O(32)	1.971(4)	Sb(10)-O(28)-Sb(9)	97.52(17)
Sb(6)-O(18)	1.943(5)	Sb(11)-O(15)	1.972(5)	Sb(3)-O(11)-Sb(8)	139.1(2)
Sb(6)-O(15)	1.957(5)	Sb(11)-O(14)	1.978(4)	Sb(3)-O(6)-Sb(2)	97.30(16)

Table 3.5: Selected bond lengths (Å) and bond angles (º) in **3.4**

Sb(1)-O(13)	1.932(6)	Sb(6)-O(4)	1.934(7)	Sb(5)-O(15)-Sb(4)	97.5(2)
Sb(1)-O(14)	1.933(6)	Sb(6)-O(8)	1.954(7)	Sb(5)-O(11)-Sb(3)	142.4(4)
Sb(1)-O(15)	2.057(6)	Sb(6)-O(9)	1.957(7)	Sb(3)-O(9)-Sb(6)	134.4(4)
Sb(1)-O(19)	2.073(6)	Sb(6)-O(7)	2.059(6)	Sb(3)-O(9)-Na(1)	123.5(4)
Sb(1)-O(10)	2.084(5)	Sb(6)-O(6)	2.113(8)	Sb(6)-O(9)-Na(1)	98.3(3)
Sb(2)-O(18)	1.929(6)	Sb(7)-O(4)	1.934(6)	Sb(1)-O(19)-Sb(3)#1	136.7(3)
Sb(2)-O(13)	1.942(6)	Sb(7)-O(22)	1.962(8)	Sb(4)-O(12)-Sb(5)	111.2(3)
Sb(2)-O(8)	1.979(6)	Sb(7)-O(3)	1.970(7)	Sb(4)-O(12)-Na(1)	127.9(3)
Sb(2)-O(10)	2.101(6)	Sb(7)-O(20)	2.049(7)	Sb(5)-O(12)-Na(1)	108.9(3)
Sb(2)-O(7)	2.130(7)	Sb(7)-O(5)	2.103(9)	Sb(1)-O(13)-Sb(2)	108.4(3)
Sb(3)-O(9)	1.952(6)	O(9)-Na(1)	2.468(9)	Sb(6)-O(4)-Sb(7)	141.8(5)
Sb(3)-O(11)	1.954(6)	O(12)-Na(1)	2.914(8)	Sb(6)-O(4)-Na(1)	103.6(3)
Sb(3)-O(18)#1	1.982(6)	O(4)-Na(1)	2.336(10)	Sb(7)-O(4)-Na(1)	107.7(4)
Sb(3)-O(10)	2.053(6)	O(22)-Na(1)	2.669(9)	Sb(6)-O(8)-Sb(2)	108.2(3)
Sb(3)-O(19)#1	2.125(6)	O(17)-Na(1)	2.223(11)	Sb(4)-O(3)-Sb(7)	130.9(4)
Sb(4)-O(3)	1.923(6)	O(21)-Na(1)	2.329(10)	Sb(7)-O(22)-Na(1)	95.3(3)
Sb(4)-O(12)	1.947(7)	Sb(3)-O(10)-Sb(1)	129.5(3)		
Sb(4)-O(7)	2.033(6)	Sb(3)-O(10)-Sb(2)	132.9(3)		
Sb(4)-O(2)	2.113(6)	Sb(1)-O(10)-Sb(2)	97.2(2)		
Sb(4)-O(15)	2.207(6)	Sb(2)-O(18)-Sb(3)#1	135.6(3)		
Sb(5)-O(11)	1.909(6)	Sb(4)-O(7)-Sb(6)	128.3(3)		
Sb(5)-O(12)	1.971(7)	Sb(4)-O(7)-Sb(2)	129.2(3)		
Sb(5)-O(16)	2.028(8)	Sb(6)-O(7)-Sb(2)	99.0(2)		
Sb(5)-O(15)	2.093(7)	Sb(1)-O(15)-Sb(5)	120.4(3)		
Sb(5)-O(1)	2.108(6)	Sb(1)-O(15)-Sb(4)	126.0(3)		

Symmetry transformations used to generate equivalent atoms:

#1 -x+1,-y+1,-z+1

3.5 Analytical and Spectroscopic Data

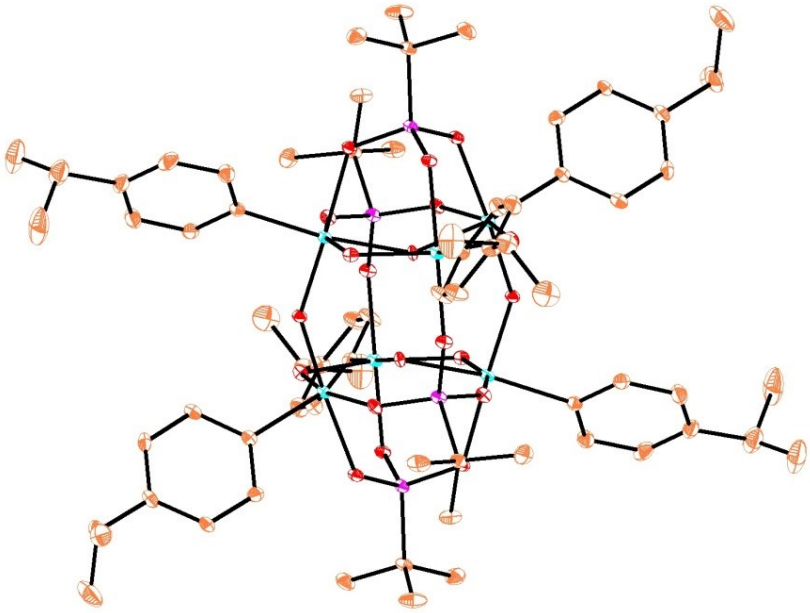

Figure S1: ORTEP view of **3.1** with thermal ellipsoids shown at 30% probability.

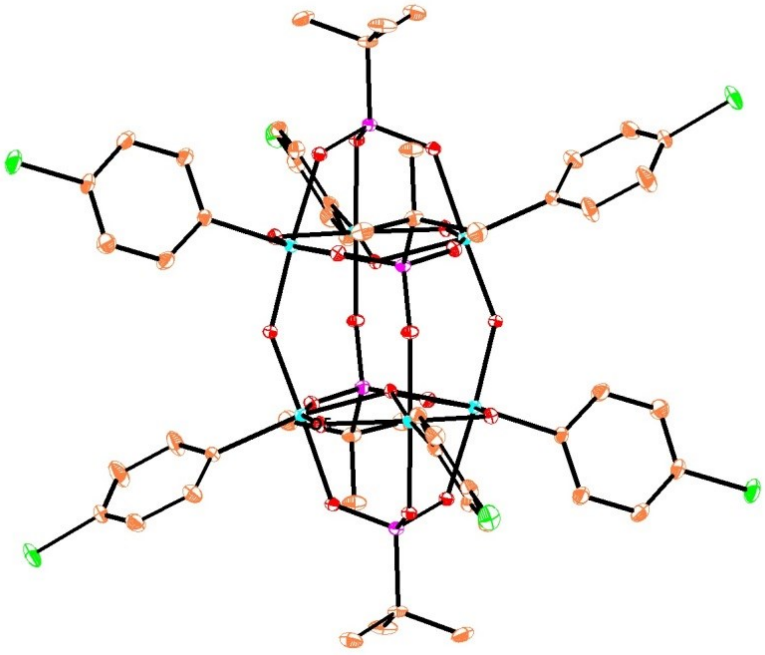

Figure S2: ORTEP view of **3.2** with thermal ellipsoids shown at 30% probability.

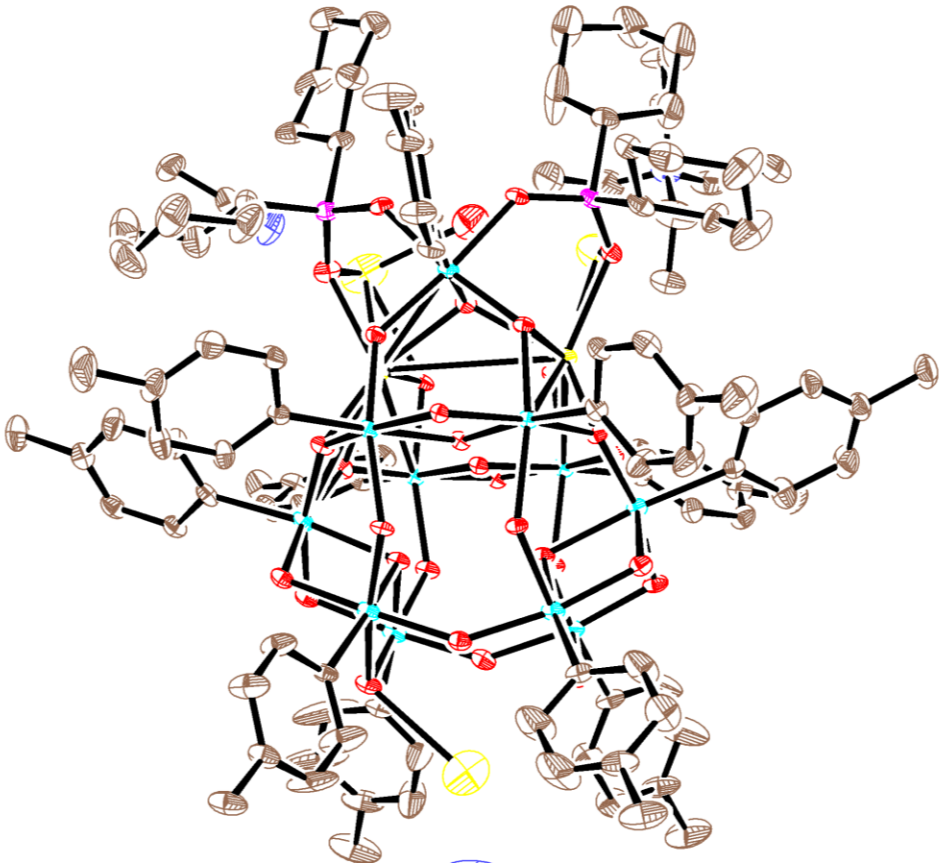

Figure S3: ORTEP view of **3.3** with thermal ellipsoids shown at 30% probability.

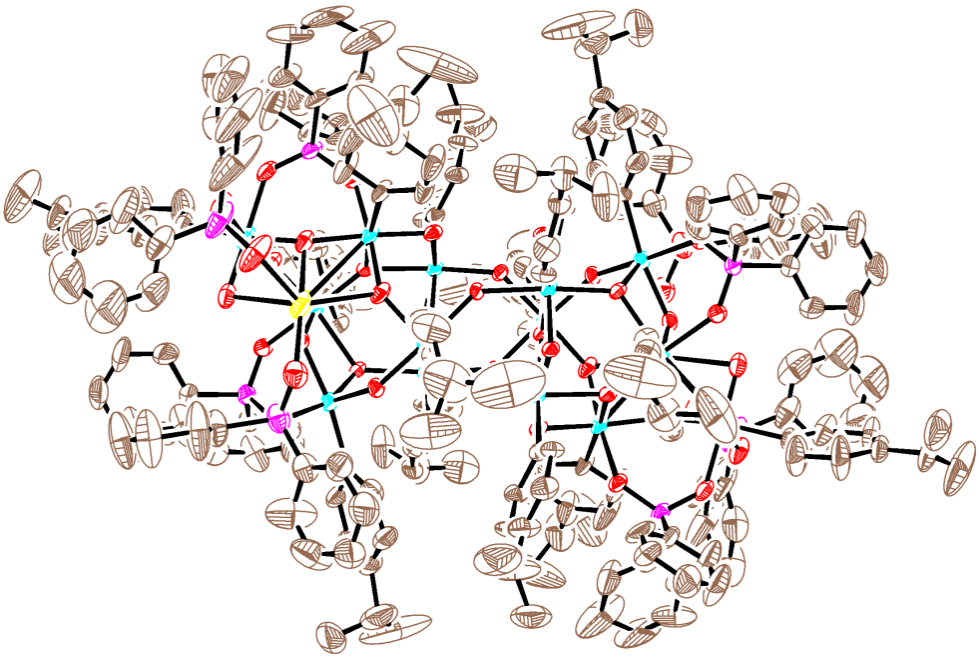

Figure S4: ORTEP view of **3.4** with thermal ellipsoids shown at 30% probability.

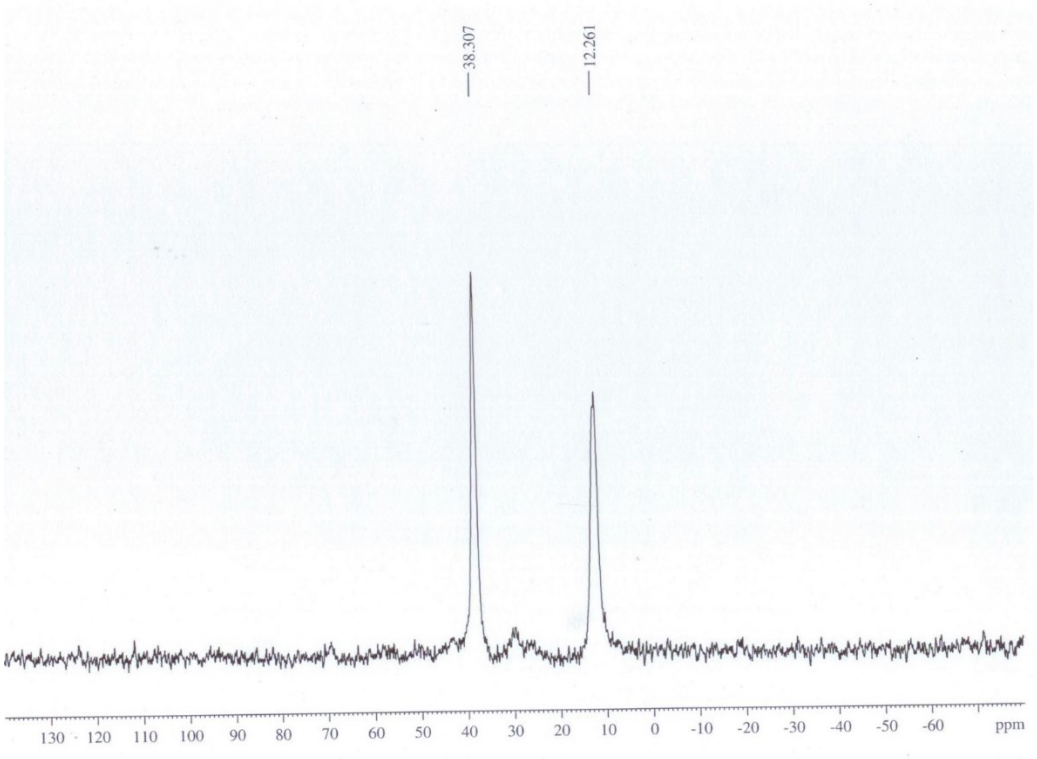

Figure S5: Solid state ^{31}P $\{^{1}H\}$ NMR of **3.1**

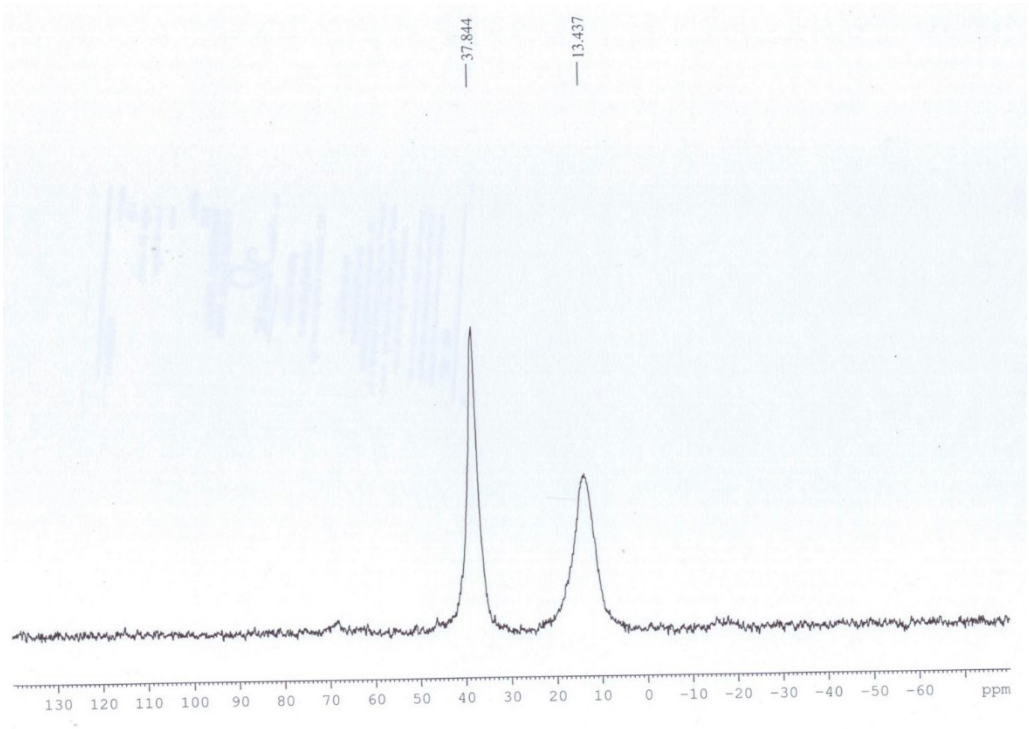

Figure S6: Solid state ^{31}P $\{^{1}H\}$ NMR of **3.2**

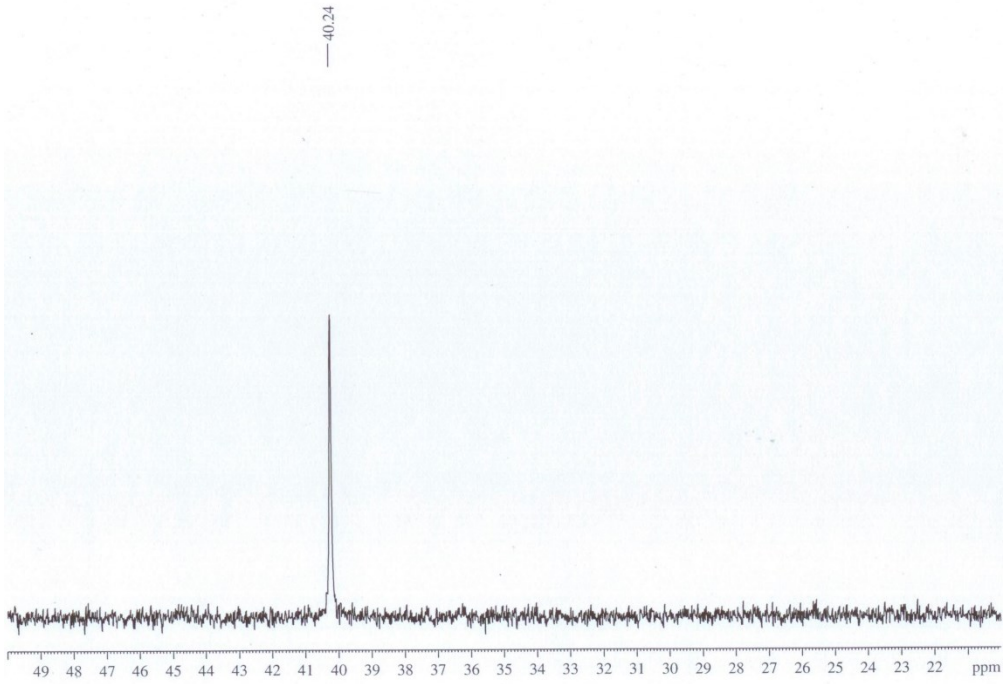

Figure.S7: Solution ^{31}P NMR ($CDCl_3$-CD_3OD) of **3.3**

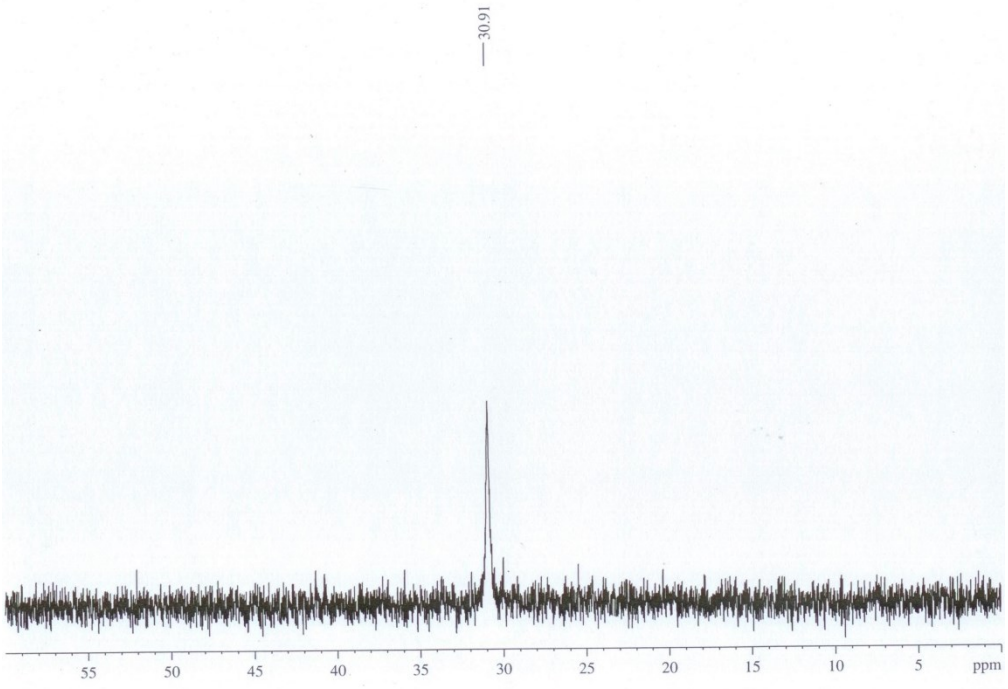

Figure.S8: Solution ^{31}P NMR ($CDCl_3$-CD_3OD) of **3.4**

3.6 References

1. (a) M. G. Walawalkar, H. W. Roesky, R. Murugavel, *Acc. Chem. Res.* 1999, **32**, 117. (b) R. Murugavel, S. Shanmugan, *Chem. Commun.,* 2007, 1257−1259; (c) V. Chandrasekhar, K. Gopal, *Appl. Organomet.Chem.,* 2005, **19**, 429; (d) R. Murugavel, S. Shanmugan, *Dalton Trans*., 2008, 5358; (e) G. Anantharaman, V. Chandrasekhar, M. G. Walawalkar, H. W. Roesky, D. Vidovic, J. Magull, M. Notlemeyer, *Dalton Trans.,* 2004, 1271; (f) G. Anantharaman, M. Walawalkar, R. Murugavel, B. Gabor, R. Herbst-Irmer, M. Baldus, B. Angerstein, H. W. Roesky, *Angew. Chem., Int. Ed.,* 2003, **42**, 4482; (g) Y. Yang, H. G. Schmidt, M. Noltemeyer, J. Pinkas and H. W. Roesky, *J. Chem. Soc., Dalton Trans.,* 1996, 3609; (h) M. G. Walawalkar, R. Murugavel, H. W. Roesky and H. G. Schmidt, *Organometallics*, 1997, **16**, 516; (i) M. G. Walawalkar, R. Murugavel and H. W. Roesky, *Inorg.Chem.,* 1998, **37**, 473; (j) Y. Yang, J. Pinkas, M. Noltemeyer and H. W. Roesky, *Inorg. Chem.,* 1998, **37**, 473; (k) Y. Yang, J. Pinkas, M. Schafer and H. W. Roesky, *Angew. Chem., Int. Ed.,* 1998, **37**, 2650; (l) K. Diemert, U. Englert, W. Kuchen and F. Sandt, *Angew. Chem.,* 1997, **109**, 251; (m) K. Diemert, U. Englert, W. Kuchen and F. Sandt, *Angew. Chem., Int. Ed.,* 1997, **36**, 241; (n) V. Chandrasekhar, K. Gopal, *Appl. Organomet. Chem*., 2005, **19**, 429.
2. (a) V. Chandrasekhar, S. Kingsley, *Angew. Chem., Int. Ed*. 2000, **39**, 2320; (b) V. Chandrasekhar, S. Kingsley, A. Vij, K.C. Lam, A. L. Rheingold, *Inorg. Chem*., 2000, **39**, 3238; (C) R. Clarke, K. Latham, C. Rix, M. Hobday, J. White, *CrystEngComm,* 2004, **6**, 42; (d) V. Chandrasekhar, V. Baskar, J. Vittal, *J. Am. Chem. Soc.* 2003, **125**, 2392; (e) E. I. Tolis, M. Helliwell, S. Langley, J. Raftery and R. E.P. Winpenny, *Angew. Chem., Int. Ed*., 2003, **42**, 3804; (f) S. Konar, N. Bhuvanesh and A. Clearfield*, J. Am. Chem. Soc*., 2006, **128**, 9604; (g) Y. S. Ma, Y. Song, Y.-Z. Li andL.-M. Zheng, *Inorg. Chem.,* 2007, **46**, 5459; (h) H. C. Yao, Y.-Z. Li,Y. Song, Y. S. Ma, L.-M. Zheng and X. Q. Xin, *Inorg. Chem*., 2006, **45**, 59; (i) M. Wang, C. B. Ma, D. Q. Yuan, M. Q. Hu,C. N. Chen and Q. T. Liu, *New J. Chem*., 2007, **31**, 2103; (j) M. Braumüller, M. Schulz, M. Staniszewska, D. Sorsche M. Wunderlin, J. Popp, J. Guthmuller, B. Dietzek and S. Rau*, Dalton Trans*., 2016, **45**, 9216; (k) Y. -Y. Zhu, M. -L. Wang, M. –X. Ma, Z.-G. Sun, C.-Q. Jiao, C. Ma and H.-Y. Li, *New J. Chem*. , 2016, **40**, 578; (l) T.-H. Yang, Z.-S. Cai, F.-

N.Shi, L. –M. Zheng, *Dalton Trans*., 2015, **44**, 19256; (m) Y. M. Klein, M. Willgert, A. Prescimone, E. C. Constable, C. E. Housecroft, *Dalton Trans*., 2016, **45**,4659; (n) P. Gerbier, C. Guérin, B. Henner .J. R. Unal, *J. Mater. Chem*., 1999, **9**, 2559; (o) E. M.-Jon, B. Kurzak, W. S. -Dobrowolska, P. Kafarski ,B. Lejczak, *Dalton Trans.,* 1996, 3455; (p) L. F. Piedra-Garza, M. H. Diekman, O. Moldovan, H. J. Breunig and U. Kortz, *Inorg. Chem.,* 2009, **48**, 411; (q) J. A. Sheikh, A. Adhikary, H. S. Jena, S. Biswas, and S. Konar, *Inorg. Chem.* 2014, **53**, 1606; (r). S. Speed, R. Vicente, D. Aravena, E. Ruiz, O. Roubeau, S. J. Teat, M. Salah El Fallah, *Inorg. Chem.* 2012, **51**, 6842; (s) R. Gillet, A. Roux, J. Brandel, S. H. Markai, F. Camerel, O. Jeannin, A. M. Nonat, L. J.Charbonnière, *Inorg. Chem*. 2017, **56**, 11738; (t) Y. Yu. Enakieva, M. V. Volostnykh, S. E. Nefedov, G. A. Kirakosyan, Y. G. Gorbunova, A. Yu. Tsivadze, A. G. Bessmertnykh-Lemeune, C. Stern, and R. Guilard, *Inorg. Chem*. 2017, **56**, 3055; (u) V. Luca, J. J. Tejada, D. Vega, G. Arrachart, and C. Rey, *Inorg. Chem.* 2016, **55**, 7928; (v) M. B. García, G. K. Angeli, K. E. Papathanasiou, I. R. Salcedo, P. O. Pastor, E. R. Losilla, D. C.-Lazarte, G. B. Hix, A. Cabeza, and K. D. Demadis, *Inorg. Chem*. 2016, **55**, 7414; (w) J. C. Amicangelo and W. R. Leenstra*, J. Am. Chem. Soc*., 1998, **24**, 120.

3. (a) M. Wang, D. Q. Yuan, C. B. Ma, M. J. Yuan, M. Q. Hu, N. Li, H. Chen, C. N. Chen, Q. T. Liua, *Dalton Trans*. 2010, **39**,7276; (b) J. G. Mao*, Coord. Chem. Rev*. 2007, **251**, 1493; (c)) Z.-Y. Du, H.-B. Xu, J.–G. Mao*, Inorg. Chem*. 2006, **45**, 9780; (d). S. Comby, R. Scopelliti, D. Imbert, L. Charbonniere, R. Ziessel, J. G. C. Bunzli, *Inorg. Chem*. 2006, **45**, 3158; (e) R. Ferreira, P. Pires, B. Castro, R. A. Sa´ Ferreira, L. D. Carlos, U. Pischel. *New J. chem*, 2004, **28**, 1506; (f) K. H. Zangana, E. M. Pineda and R. E. P. Winpenny *Dalton Trans*., 2014, **43**, 17101; (g) Z. M. Zhang, K. H. Zangana, A. K. Kostopoulos ,M. L. Tong and R. E. P. Winpenny *Dalton Trans*., 2016, **45**, 9041; (h) E. M. Pineda, F. Tuna, Y.-Z. Zheng, S. J. Teat, R. E. P. Winpenny, J. Schnack, and E. J. L. McInnes*, Inorg. Chem*. 2014, **53**, 3032.
4. (a) D. N. Woodruff, R. E. P. Winpenny and R. A. Layfield, *Chem. Rev*., 2013, **113**, 5110; (b) S. M. Neville, G. J. Halder, K. W. Chapman, M. B. Duriska, B. Moubaraki, K. S. Murray and C. J. Kepert, *J. Am. Chem. Soc*., 2009, **131**, 12106; (c) L. Ungur, S. K. Langley, T. N. Hooper, B. Moubaraki, E. K. Brechin, K. S. Murray and L. F. Chibotaru, *J. Am. Chem. Soc*., 2012, **134**, 18554; (d) J. J. Le Roy, L. Ungur, L. Korobkov, L. F.

Chibotaru and M. Murugesu*, J. Am. Chem. Soc*., 2014, **136**, 8003; (e) N. F. Chilton, D. Collison, E. J. L. McInnes, R. E. P. Winpenny and A. Soncini, *Nat. Commun*., 2013, **4**, 2551; (f) V. Chandrasekhar, A. Dey, S. Das, M. Rouzières and R. Clérac, *Inorg. Chem*., 2013, **52**, 2588; (g) J. Goura, J. P. S. Walsh, F. Tuna and V. Chandrasekhar*, Inorg. Chem*., 2014, **53**, 3385; (h) A. Baniodeh, V. Mereacre, N. Magnani, Y. Lan, J. A. Wolny, V. Schünemann, C. E. Anson and A. K. Powell, *Chem. Commun*., 2013, **49**, 9666; (i) A. Baniodeh, N. Magnani, S. Bräse, C. E. Anson and A. K. Powell, *Dalton Trans*., 2015, **44**, 6343; (j) B. Hussain, D. Savard, T. J. Burchell, W. Wernsdorfer and M. Murugesu, *Chem. Commun*., 2009, 1100; (k) R. J. Blagg, L. Ungur, F. Tuna, J. Speak, P. Comar, D. Collison, W. Wernsdorfer, E. J. L. McInnes, L. F. Chibotaru and R. E. P. Winpenny, *Nat. Chem*., 2013, **5**, 673; (l) C. A. P. Goodwin, F. Ortu, D. Reta, N. F. Chilton and D. P. Mills, *Nature*, 2017, **548**, 439; (m) F.-S. Guo, B. M. Day, Y.-C. Chen, M.-L. Tong, A. Mansikkamaeki and R. A. Layfield*, Angew. Chem., Int. Ed*., 2017, **56**, 11445; (n) L. Ungur, S.-Y. Lin, J. Tang and L. F. Chibotaru, *Chem. Soc. Rev*., 2014, **43**, 6894 and references therein. (o) C. Das, S. Vaidya, T. Gupta, J. M. Frost, M. Righi, E. K. Brechin, M. Affronte, G. Rajaraman and M. Shanmugam, *Chem. – Eur. J.,* 2015, **44**, 15639; (p) K. R. Vignesh, A. Soncini, S. K. Langley, W. Wernsdorfer, K. S. Murray and G. Rajaraman*, Nat. Commun*., 2017, **8**, 1023.

5. (a) J. M. Taylor, R. K. Mah, I. L. Moudrakovski, C. Ratcliffe, R. Vaidhyanathan, G. K. H. Shimizu, *J. Am. Chem. Soc*. 2010, **132**,14055; (b) J. M. Aylor, A.H. Mahmoudkhani, G. K. H Shimizu, *Angew. Chem., Int. Ed*. 2007, **46**, 795; (c) S. S. Iremonger, J. Liang, R. Vaidhyanathan, I. Martens, G. Shimizu, T. D. Daff, M. Z. Aghaji, S. Yeganegi, T. K. Woo, *J. Am. Chem. Soc*., 2011, **133**, 20048; (d) K. J. Gagnon, H. P. Perry, and A. Clearfield, *Chem. Rev*. 2012, **112**, 1034; (d) A. Dolbecq, E. Dumas, C. R. Mayer, and P. Mialane*, Chemical Reviews*, 2010, **10**, 6011; (e) R. Murugavel, A. Choudhury, M. G. Walawalkar, R. Pothiraja, and C. N. R. Rao, *Chemical Reviews,* 2008, **108**, 3551; (f) S. Zheng, J. Zhang, X. X. Li, W. Fang, and G. Yang*, J. Am. Chem. Soc*., 2010, **132**, 15102; (g) M. T. Wharmby, J. P. S. Mowat, S. P. Thompson, and P. A. Wright*, J. Am. Chem. Soc.* 2011, **133**, 1266.
6. M. S. R. Prabhu, A. K. Jami and V. Baskar, *Organometallics*, 2009, **28**, 3953.
7. M. S. R. Prabhu, U. Ugandhar and V. Baskar, *Dalton Trans.,* 2016, **45**, 6963.

8. A. K. Jami and V. Baskar, *Dalton Trans.,* 2012, **41**, 12524.
9. U. Ugandhar and V. Baskar, *Dalton Trans.,* 2016, **45**, 6269.
10. A. K. Jami, M. S. R. Prabhu and V. Baskar, *Organometallics*, 2010, **29**, 1137.
11. (a) C. J. Clark, B. K. Nicholson and C. E. Wright, *Chem. Commun.,* 2009, 923; (b) B. K. Nicholson, C. J. Clark, C. E. Wright and T. Groutso, *Organometallics*, 2010, **29**, 6518; (c) B. K. Nicholson, C. J. Clark, C. E. Wright, S. G. Telfer and T. Groutso, *Organometallics*, 2011, **30**, 6612; (d) B. K. Nicholson, C. J. Clark, G. B. Jameson and S. G. Telfer, *Inorg. Chim. Acta*, 2013, **406**, 53. (e) N. K. Srungavruksham and V. Baskar, *Dalton Trans.,* 2015, **44**, 6358.
12. 12.(a) H. Schmidt*, Liebigs Ann. Chem*., 1920, **421**, 174; (b) G. O. Doak and H. G. Steinman, *J. Am. Chem. Soc*., 1946, **68,** 1987; (c) G. O. Doak, *J. Am. Chem. Soc.,* 1946, **68**, 1991.
13. (a) R. Rüther, F. Huber and H. Preut, *Z. Anorg. Allg. Chem.,* 1986, **539**, 110; (b) P. C. Croft and G. M. Kosolapoff, *J. Am. Chem. Soc.,* 1953, **75**, 3379.
14. (a) A. R. Shles, F. F. Rust and W. E. Vaughan, J. Amer. Chem. Soc., 1952, 74, 3282; (b) R. H. Williams and L. A. Hamilton, J. Amer. Chem. Soc., 1955, 77, 3411.
15. (a) S. Ali, V. Baskar, C. A. Muryn, and R. E. P. Winpenny, *Chem. Commun*., 2008, 6375; (b) S. Ali, C. A. Muryn, F. Tuna and R. E. P. Winpenny, *Dalton Trans*., 2010, **39**, 9588.
16. (a) SAINT Software Reference manuals, Version 6.45, Bruker Analytical X-ray Systems, Inc., Madison, WI, 2003; (b) G. M. Sheldrick, SHELXS-97, Program for Crystal Structure Solution, University of Göttingen, Göttingen, Germany, 1997; (c) G. M. Sheldrick, *Acta Crystallogr., Sect. A: Found. Adv*., 2015, **71**, 3; (d) G. M. Sheldrick, *Acta Crystallogr, Sect. C: Struct. Chem.,* 2015, **71**, 3.
17. P. Van Der Sluis and A. L. Spek, BYPASS: an effective method for the refinement of crystal structures containing disordered solvent regions. *Acta Crystallogr, Sec. A; Fundam. Crystallogr*., 1990, **46**, 194.
18. (a) A. L. Spek, Single-crystal structure validation with the program PLATON. *J. Appl. Crystallogr.,* 2003, **36**, 7; (b) A. L. Spek, Structure validation in chemical crystallography. *Acta Crystallogr. Sec. D; Biol. Crystallogr.,* 2009, **65**, 148.

Transition metal stibonate-phosphonate clusters: Isolation of M_2Sb_4 (M= Mn, Co, Ni & Cu) Clusters.

Chapter 4

Abstract: Arylstibonic acid phosphonate pro-ligand, [(*p*-iPr-$C_6H_4Sb)_4(OH)_4$(*t*-$BuPO_3)_6$] was synthesized by condensation reaction of *p*-isopropylphenylstibonic acid ($ArSbO_3H_2$) with *t*-butylphosphonic acid. It contains four antimony centers, forms a puckered eight-member Sb_4O_4 core held together by six *t*-butyl phosphonates. The synthesis and structural characterization of arylstibonic acid-transition metal-based molecular phosphonate clusters are reported. The reaction of transition metal acetate with antimonate-phosphonate pro-ligand [(*p*-iPr-$C_6H_4Sb)_4(OH)_4$(*t*-$BuPO_3)_6$] under solvothermal conditions with pyridine as a base produced novel arylstibonic acid-transition metal-based phosphonate clusters (compounds **4.1-4.4**). Single crystal structural elucidation revealed the formation of [M_2((*p*-iPr-$C_6H_4Sb)_4(\mu_3$-$O)_2(\mu_2$-$O)_2(\mu_2$-$OCH_3)_4$(*t*-$BuPO_3)_4(Py)_2.2CH_3OH$] {M= Mn(**4.1**), Co(**4.2**), Ni(**4.3**) and Cu(**4.4**)}.

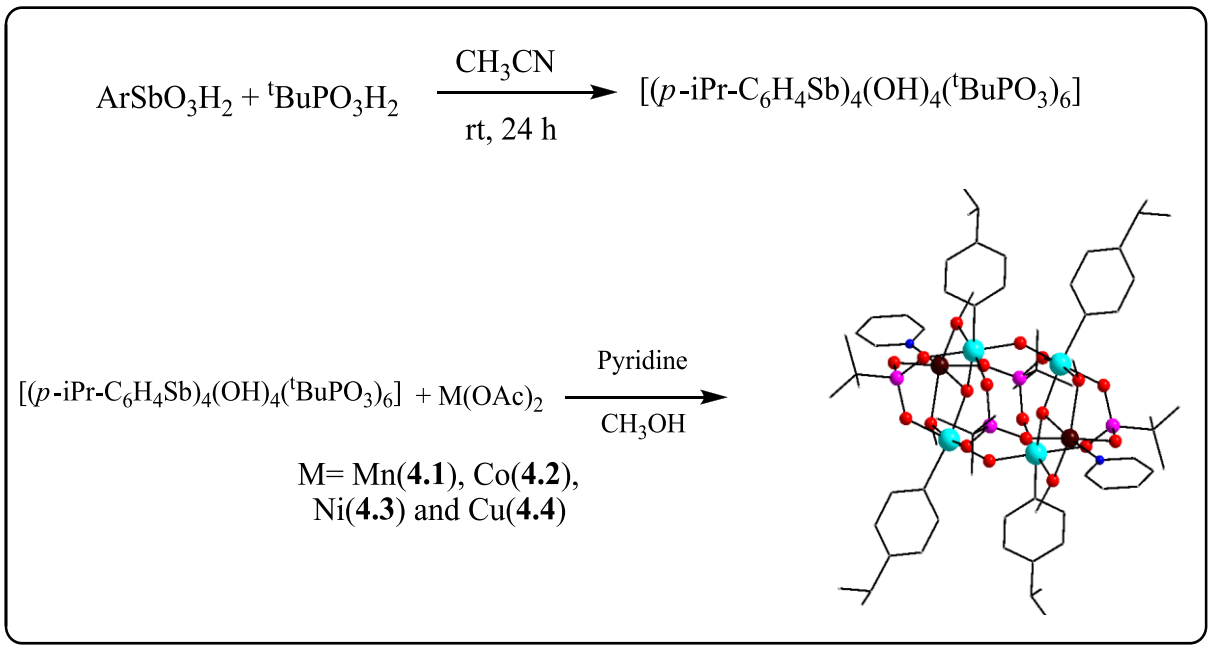

4.1 Introduction

The phosphonate-based molecular assemblies encompassing metal ions are inducing a great deal of interest in recent years.[1] Transition metal phosphonates synthesis and structural characterization is an active area of research in the last decades due to their potential applications in magnetism,[2] biology,[2] cation exchange,[3] sorption,[4] sensors,[5] catalysis,[6] catalyst supports, and non-linear optics.[7] However, the multidentate coordinating ability of phosphonate ligands, can lead to formation of insoluble metal complexes. To overcome this problem, co-ligands or bulky organic groups or preformed metal carboxylate cage as metal precursors can be used in addition to phosphonic acids.[8] The co-ligand can occupy a certain number of coordination sites on the metal ion; thus, phosphonate ligands accessible coordination sites are decreased and forms soluble products, which can be easily characterized by using single crystal X-ray diffraction. By adopting this methodology, a large number of manganese,[9] iron,[10] cobalt,[11] nickel,[12] copper[13], and vanadium[14] phosphonate molecular cages have been reported. Some of the transition metal molecular clusters have been found to exhibit interesting properties like showing SMM behavior at low temperatures.[9] Last decade onwards, chemists have been attracted to synthesize novel organoantimony oxo clusters due to their potential applications in the field of biology and catalysis, especially arylstibonic acids have been used as anti-cancer agents and anti-microbial agents.[15] Although the synthesis of arylstibonic acid is known; still, the exact molecular structure and reactivity is a matter of considerable debate. It may be due to the reason that arylstibonic acids are generally amorphous, non-crystalline white powders and possess cross-linked polymeric structures in solid-state.[16] Depolymerisation reactions of arylstibonic acids with different protic ligands like phosphonic acids, phenylseleninic acid, phenolic pyrazoles, 8-hydroxy quinolone, silane diol, and triol have been investigated. It has been found that such systems led to metal oxo clusters displaying interesting structural diversity.[17] The synthesis of reverse Keggin ions by R. Winpenny is another noteworthy example of the structural heterogeneity reflected by organostibonic acid.[18] Beckmann *et al*. reported first well-defined molecular arylstibonic acid by introducing sterically hindered bulky R groups on antimony atom, which prevent higher aggregation and in solid-state it crystallize as a dimer, similarly a second molecular arylstibonic acid have been reported and it consist adamantane core type structure.[19] Besides, arylstibonic acids have been found to undergo self-condensation in the presence of a

base; thus, Sb_{12}, Sb_{14}, and Sb_{16} polyoxostibonates have been isolated. ESI-MS has proved to be a very useful technique to understand the basic building block of arylstibonic acid aggregates in a solution state.[20] Recently, our group has been reported the synthesis and structurally characterized series of organostibonic acid phosphonate clusters.[17e] Owing to the fact that stibonic acid self-condenses in the presence of base, and mixed antimony-phosphonate clusters acting as potential pro-ligand, it was predicted the stibonic-phosphonate framework open up a gateway to study the behavior of those clusters towards base. Winpenny *et al* reported the ability of the organostibonate-phosphonate cluster to act as pro-ligand for assembling cobalt and copper-based molecular clusters.[21] Though stibonates and phosphonates can independently act as ligands towards metal ions, the pro-ligand cluster method provides a single source precursor method combining the coordinating ability of stibonates and phosphonates motifs can serve as a novel ligand platform which could be employed for stabilizing new types of polynuclear metal-based oxo-hydroxo systems. Herein, we report four novel transition metal-phosphonate clusters by employing organostibonate-phosphonate pro-ligand system $[M_2((p\text{-iPr-}C_6H_4Sb)_4(\mu_3\text{-}O)_2(\mu_2\text{-}O)_2(\mu_2\text{-}OCH_3)_4(t\text{-}BuPO_3)_4(Py)_2.2CH_3OH]$ {M= Mn(**4.1**), Co(**4.2**), Ni(**4.3**) and Cu(**4.4**)}.

4.2 Experimental section

4.2.1 General Information:

p-Isopropylphenylstibonic acid[16] and *t*-butylphosphonic acid[22] were synthesized according to literature reports. Solvents and common reagents were purchased from commercial sources. Mixed antimonate-phosphonate pro ligand $[(p\text{-iPr-}C_6H_4Sb)_4(OH)_4(t\text{-}BuPO_3)_6]$ was synthesized by condensation reactions of organostibonic acid with *t*-butylphosphonic acid.[17e] All the compounds used were dried under a high vacuum for half an hour before subjected to spectroscopic and elemental analysis.

4.2.2 Instrumentation:

Infrared spectra were recorded with a JASCO-5300 FT-IR spectrometer as KBr pellets. Elemental analysis was performed with a Flash EA Series 1112 CHNS analyzer. Single crystal X-ray data collection for compounds **4.1-4.4** was carried out at 100(2) K with a Bruker Smart Apex CCD area detector system [λ (Mo-Kα) = 0.71073 Å] with a graphite monochromator. The data were reduced using SAINTPLUS. The structures were solved using SHELXS-97[23] and

refined using the program SHELXL-2014/7[24, 25]. All non-hydrogen atoms were refined anisotropically.

4.2.3 Synthetic procedure for compounds 4.1-4.4:

Mixed antimonate-phosphonate pro ligand and metal acetate were dissolved in methanol (15 mL) and simultaneous dropwise addition of pyridine forms clear solution, stirred for one hour then transferred into Teflon digestion bomb. The bomb was sealed properly, and the mixture was heated at 100 °C for 12 h and then cooled slowly to room temperature for 48 h. X-ray quality single crystals were obtained at the bomb's base and walls upon slow cooling of methanol solution. The isolated crystals were powdered and subjected to high vacuum for half an hour before being characterized by standard spectroscopic and analytical techniques. The molar ratios of the corresponding reagents used are as follows.

Compound **4.1**: Pro-ligand (0.05 g, 0.027 mmol) and manganese acetate tetrahydrate (0.025 g, 0.1 mmol) pyridine (0.02 mL). Colorless single crystals formed upon slow cooling (48 h) of methanol solution. Yield: 0.019g (36 % based on Pro-ligand). Anal, Calcd (%) for $C_{66}H_{102}O_{20}N_2P_4Mn_2Sb_4$ (1964.32): C, 40.36; H, 5.23; N, 1.43. Found: C, 40.21; H, 5.18; N, 1.51. IR (cm-1, KBr pellet): 3417(wide), 2965(s), 2871(m), 1646(m), 1481(s), 1461(m), 1400(s), 1112(s), 1045(m), 980(m), 832(s), 662(s), 516(m).

Compound **4.2**: Pro-ligand (0.05 g, 0.027 mmol) and cobalt acetate tetrahydrate (0.026g, 0.1 mmol) pyridine (0.02 mL). Pink colored single crystals formed upon slow cooling (48 h) of methanol solution. Yield: 0.015g (28 % based on Pro-ligand). Anal, Calcd (%) for $C_{66}H_{102}O_{20}N_2P_4Co_2Sb_4$ (1972.32): C, 40.19; H, 5.21; N, 1.42. Found: C, 40.27; H, 5.18; N, 1.36. IR (cm-1, KBr pellet): 3433(wide), 2964(s), 2925(m), 2867(m), 1602(s), 1479(m), 1447(s), 1390(m), 1140(s), 1101(s), 1038(s), 977(m), 950(m), 833(m), 701(s), 659(s), 542(m).

Compound **4.3**: Pro-ligand (0.05 g, 0.027 mmol) and nickel acetate tetrahydrate (0.027g, 0.1 mmol) pyridine (0.02 mL). Light green colored single crystals formed upon slow cooling (48 h) of methanol solution. Yield: 0.021g (39 % based on compound 1). Anal, Calcd (%) for $C_{66}H_{102}O_{20}N_2P_4Ni_2Sb_4$ (1971.84): C, 40.20; H, 5.21; N, 1.42. Found: C, 40.31; H, 5.19; N, 1.36. IR (cm-1, KBr pellet): 3439(wide), 2962(s), 2927(m), 2868(m), 1605(s), 1479(m), 1448(m), 1402(m), 1150(m), 1041(s), 1011(s), 959(s), 821(s), 791(m), 699(m), 658(s), 542(s).

Compound **4.4**: Pro-ligand (0.05 g, 0.027 mmol) and copper acetate monohydrate (0.022 g, 0.1 mmol) pyridine (0.02 mL). Blue colored single crystals formed upon slow cooling (48 h) of methanol solution. Yield: 0.018g (33 % based on compound 1). Anal, Calcd (%) for $C_{66}H_{102}O_{20}N_2P_4Cu_2Sb_4$ (1981.54): C, 40.00; H, 5.19; N, 1.41. Found: C, 40.12; H, 5.23; N, 1.49. IR (cm-1, KBr pellet): 3418(wide), 2961(s), 2925(m), 2867(m), 1744(m), 1608(m), 1480(s), 1393(s), 1263(m), 1149(s), 1106(m), 1046(s), 1013(s), 967(s), 822(s), 696(m), 674(s), 551(s).

4.3 Results and discussions

Compounds **4.1-4.4** were synthesized by the reaction of antimonate-phosphonate pro-ligand [(*p*-iPr-$C_6H_4Sb)_4(OH)_4$(*t*-$BuPO_3)_6$] with transition metal acetate hydrate [M= Mn(**4.1**), Co(**4.2**), Ni(**4.3**) and Cu(**4.4**)] in methanol under solvothermal conditions, using pyridine as a base (**Scheme 4.1**). Single crystals of **4.1-4.4** for X-ray diffraction studies formed directly upon the methanol solution's slow cooling. Compound **4.1-4.3** crystallizes in monoclinic space group C2/c, and compound **4.4** crystallizes in triclinic space group P-1. The overall molecular structures of compounds **4.1-4.4** are similar, and all compounds are present as a neutral form in the crystal structure. The structure of **4.1** (**Figure 4.1**) is considered for structural discussions. Crystallographic data and bond metric parameters of **4.1** are given in the table 4.1 & 4.2. The solid-state structure of **4.1** reveals the formation of extranuclear organoantimony (v) oxo cluster [Mn_2((*p*-iPr-$C_6H_4Sb)_4(\mu_3$-$O)_2(\mu_2$-$O)_2(\mu_2$-$OCH_3)_4$(*t*-$BuPO_3)_4(Py)_2.2CH_3OH$]. The molecular structure of **4.1** (**Figure 4.1**) reveals the formation of a puckered eight-membered Sb_4O_4 core held together by four phosphonates and two Mn metal atoms. Interestingly *in situ* generated Sb_2Mn triangle present, here two arylstibonic acids self-condensed through one μ_3-oxo bridge and further connected to Mn metal atoms via μ_2-methoxy bridges. Four phosphonates are found in the structure, each phosphonate bound to two Sb centers and one Mn metal atom in 3.111 coordination mode based on Harris notation. Each Sb center is present in regular octahedral geometry with the O_5SbC coordination mode. The two Mn atoms are present in the cluster; around each Mn center is in an octahedral geometry. Of the six coordination present, two oxygens from phosphonates, one μ_3-oxo bridge, two μ_2-methoxy bridges, and the last coordination site are fulfilled by pyridine. Two pyridine molecules crystallize along with the core, and they also satisfy the sixth coordination site of Mn atoms. The Mn-O bond distances involving μ_3-oxo, μ_2-methoxy group, and phosphonates falls in the range of 2.264(2) Å, 2.199(2)

to 2.204(2) Å, and 2.069(3) to 2.181(3) Å, respectively. The Mn-N bond distance is 2.219(3) Å. The Sb-O bond lengths involving μ_3-hydroxo, μ_2-methoxy bridges, and phosphonates falls in the range of 1.961(2) to 1.962(2) Å, 1.926 (2) to 2.024(2) Å and 2.010(2) to 2.055(2) Å, respectively. The Sb-O-Sb bond angles are 138.76(13)° and 145.94(13)°.

$$[(p\text{-iPr-}C_6H_4Sb)_4(OH)_4(^tBuPO_3)_6] + M(OAc)_2 \xrightarrow[CH_3OH]{\text{Pyridine}} [M_2((p\text{-iPr-}C_6H_4Sb)_4(\mu_3\text{-}O)_2(\mu_2\text{-}O)_2(\mu_2\text{-}OCH_3)_4(^tBuPO_3)_4(Py)_2]$$

M= Mn(**4.1**), Co(**4.2**), Ni(**4.3**) and Cu(**4.4**)

Scheme 4.1

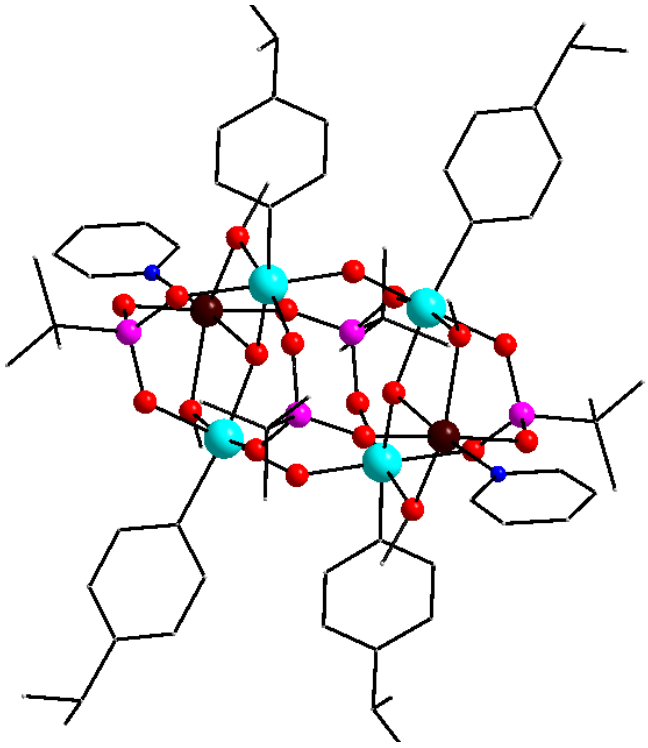

Figure 4.1: Solid-state structure of **4.1**. Color code Cyan: Sb, Grey: Mn, Pink: P, Red: O.

Single crystal X-ray studies of **4.2** reveal the formation of hexanuclear organoantimony (v) oxo cluster $[Co_2((p\text{-}iPr\text{-}C_6H_4Sb)_4(\mu_3\text{-}O)_2(\mu_2\text{-}O)_2(\mu_2\text{-}OCH_3)_4(t\text{-}BuPO_3)_4(Py)_2.2CH_3OH]$. . Compound **4.2** crystallizes in monoclinic space group C2/c. Crystallographic data and bond metric parameters of **4.2** are given in the table 4.1 & 4.2. The molecular structure of **4.2** (**Figure 4.2**) was isostructural to **4.1**. The Co-O bond distances involving μ_3-oxo, μ_2-methoxy group, and phosphonates falls in the range of 2.145(4) Å, 2.122(4) to 2.128(4) Å and 2.008(4) to 2.087(4) Å, respectively. The Co-N bond distance is 2.120(5) Å. The Sb-O bond lengths involving μ_3-hydroxo, μ_2-methoxy bridges, and phosphonates falls in the range of 1.959(3) to 1.966(3) Å, 1.919(4) to 2.031(4) Å, and 2.008(4) to 2.059(3) Å respectively. The Sb-O-Sb bond angles are 139.0(2)° and 145.9(2)°.

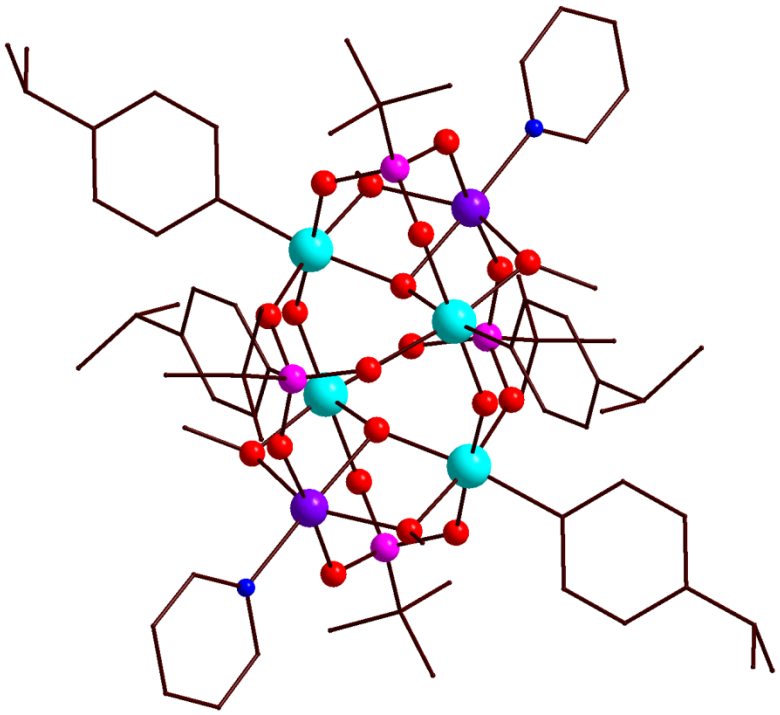

Figure 4.2: Solid-state structure of **4.2**. Color code: Cyan: Sb, Purple: Co, Pink: P, Red: O.

Single crystal X-ray studies of **4.3** reveal the formation of hexanuclear organoantimony (v) oxo cluster $[Ni_2((p\text{-}iPr\text{-}C_6H_4Sb)_4(\mu_3\text{-}O)_2(\mu_2\text{-}O)_2(\mu_2\text{-}OCH_3)_4(t\text{-}BuPO_3)_4(Py)_2.2CH_3OH]$. Compound **4.3** crystallizes in monoclinic space group C2/c. Crystallographic data and bond metric parameters of **4.3** are given in the table 4.1 & 4.3. The molecular structure of **4.3** (**Figure 4.3**) was isostructural to **4.1.** The Ni-O bond distances involving μ_3-oxo, μ_2-methoxy group, and phosphonates falls in the range of 2.076(3) Å, 2.090(3) to 2.101(3) Å, and 2.003(3) to 2.076(3) Å, respectively. The Ni-N bond distance is 2.069(3) Å. The Sb-O bond lengths involving μ_3-hydroxo, μ_2-methoxy bridges, and phosphonates falls in the range of 1.972(2) to 1.974(2) Å, 1.920(2) to 2.039(3) Å and 2.003(2) to 2.053(2) Å, respectively. The Sb-O-Sb bond angles are 138.57(13)° and 146.83(13)°.

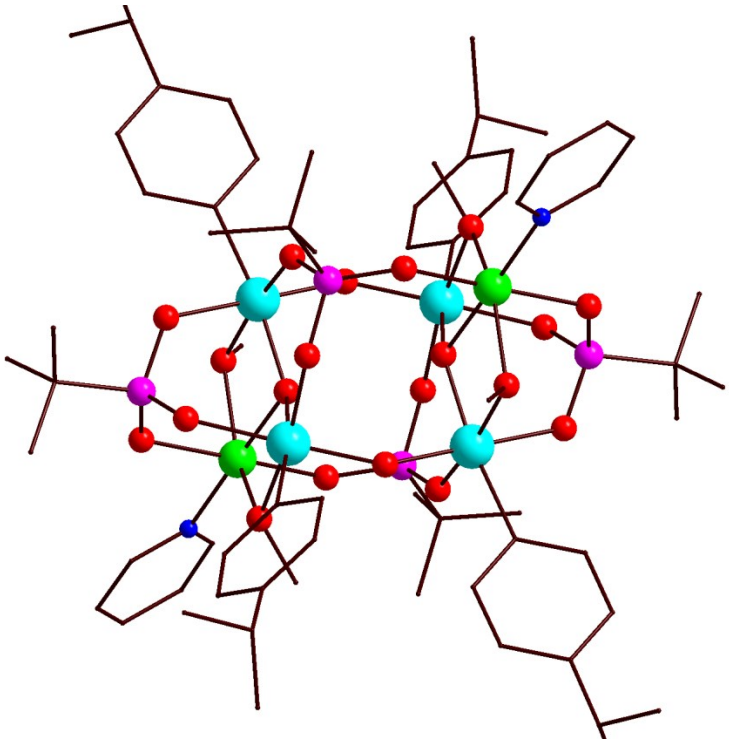

Figure 4.3: Solid state structure of **4.3**. Color code Cyan: Sb, Green: Ni, Pink: P, Red: O.

Single crystal X- ray studies of **4.4 reveals** the formation of hexanuclear organoantimony (v) oxo cluster $[Cu_2((p\text{-iPr-}C_6H_4Sb)_4(\mu_3\text{-}O)_2(\mu_2\text{-}O)_2(\mu_2\text{-}OCH_3)_4(t\text{-BuPO}_3)_4(Py)_2.2CH_3OH]$. Compound **4.4** crystallizes in triclinic space group P-1. Crystallographic data and bond metric parameters of **4.4** are given in the table 4.1 & 4.3. The molecular structure of **4.4** (**Figure 4.4**) was isostructural to **4.1**. The Cu-O bond distances involving μ_3-oxo, μ_2-methoxy group and phosphonates falls in the range of 2.076(2) Å, 2.326(2) to 2.348(2) Å and 1.941(2) to 1.985(2) Å respectively. The Cu-N bond distance is 2.004(3) Å. The Sb-O bond lengths involving μ_3-hydroxo, μ_2-methoxy bridges and phosphonates falls in the range of 2.0074(19) to 2.013(2) Å, 1.915(2) to 2.015(2) Å and 2.011(2) to 2.046 (2) Å respectively. The Sb-O-Sb bond angles are 136.37(10)° and 145.45(12)°.

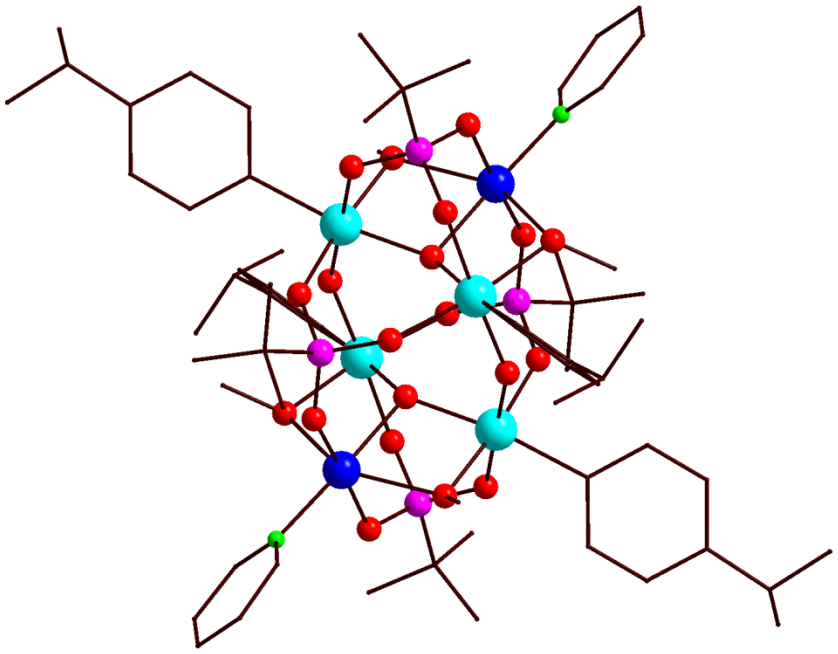

Figure 4.4: Solid-state structure of **4.4**. Color code: Cyan: Sb, Blue: Cu, Pink: P, Red: O.

Interestingly, however, arylstibonic acid-phosphonic acid pro ligand reacts with different transition metals but molecular structure of end product will be same in each case. It indicates hexanuclear M_2Sb_4 core is more stable. In all structures, each transition metal atom was coordinated by a pyridine ligand.

Simultaneously we also investigate independent three-component reactions of arylstibonic acids, copper acetate hydrate, and *t*-butylphosphonic acid in the presence of tetraethylammonium hydroxide results in the formation of novel high nuclearity heterometallic $\{Sb_{12}Cu_{11}\}$ cluster and sodium ions are trapped inside the heterometallic cage. Unfortunately, the quality of crystal data was very poor, so it's very difficult to analyze this compound's exact molecular structure.

4.4 Conclusion:

Herein, we have been successfully synthesized antimony-transition metals (M_2Sb_4) clusters. M_2Sb_4 clusters can be prepared by arylstibonic acid phosphonate pro-ligand under solvothermal conditions by using pyridine as a base. Interestingly the molecular structures are isostructural to our recent report Ti_4Sb_2 molecular oxo cluster.

Table 4.1: Crystallographic tables of compound **4.1-4.4**

	4.1	**4.2**	**4.3**
Formula	$C_{68}H_{110}Mn_2N_2O_{22}P_4Sb_4$	$C_{68}H_{102}Co_2N_2O_{22}P_4Sb_4$	$C_{68}H_{110}N_2Ni_2O_{22}P_4Sb_4$
F.wt g/mol^{-1}	2028.33	2028.25	2035.87
T, K	100(2)	100(2)	100(2)
Crystal system	Monoclinic	Monoclinic	Monoclinic
Space group	C 2/c	C 2/c	C 2/c
Crystal size mm^3	0.160 x 0.140 x 0.130	0.230 x 0.170 x 0.130	0.160 x 0.140 x 0.120
a, Å	25.252(3)	25.233(8)	25.249(3)
b, Å	20.379(3)	20.100(8)	20.009(3)
c, Å	16.0757(18)	16.085(6)	16.163(2)
α, deg	90	90	90
β, deg	91.123(2)	91.279(10)	91.427(2)
γ, deg	90	90	90
V, Å3	8271.1(16)	8156(5)	8163.4(18)
Z	4	4	4
D_{calcd} Mg/m^3	1.629	1.652	1.657
μ, mm^{-1}	1.730	1.851	1.904
F(000)	4088	4072	4112
Theta range, deg	1.284 to 26.419	1.295 to 26.864	1.299 to 26.388
Index ranges	-31<=h<=31 -25<=k<=25 -20<=l<=20	-31<=h<=31 -25<=k<=25 -20<=l<=20	-31<=h<=31 -24<=k<=24 -20<=l<=20
Total reflns	43796	43123	43188
Ind. reflns / R(int)	8474/0.0437	8521/0.0959	8336/0.0512
Completeness to θ_{max}, %	99.9	100	100
GooF(F^2)	1.117	1.028	1.078
R_1/wR_2 [I>2σ(I)]	0.0361	0.0509	0.0366
R_1/wR_2 [all data]	0.0848	0.1174	0.0873
Largest diff peak/hole, e.Å^{-3}	1.164 /0.594	1.281/ -1.503	1.139/ -0.656

	4.4
Formula	$C_{68}H_{110}Cu_2N_2O_{22}P_4Sb_4$
F.wt g/mol^{-1}	2045.53
T, K	100(2)
Crystal system	Triclinic
Space group	P-1
Crystal size mm^3	0.230 × 0.180 × 0.160
a, Å	12.8207(14)
b, Å	13.3637(15)
c, Å	13.7013(15)
α, deg	99.588(2)
β, deg	93.106(2)
γ, deg	114.547(2)
V, Å^3	2085.5(4)
Z	1
D_{calcd} Mg/m^3	1.629
μ, mm^{-1}	1.922
F(000)	1030
Theta range, deg	3.044 to 52.866
Index ranges	$-15 \leq h \leq 16$ $-16 \leq k \leq 16$ $-17 \leq l \leq 16$
Total reflns	16745
Ind. reflns / R(int)	8416/0.0245
Completeness to θ_{max}, %	100
GooF(F^2)	1.023
R1/wR2 [I>2σ(I)]	0.0313/0.0739
R1/wR2 [all data]	0.0354/0.0762
Largest diff peak/hole, e.Å^{-3}	0.84/-0.52

Table 4.2: Selected bond lengths (Å) and bond angles (º) in **4.1-4.2**

4.1		**4.2**	
Sb(1)-O(1)	1.961(2)	Sb(1)-O(1)	1.966(3)
Sb(1)-O(2)	2.053(2)	Sb(1)-O(2)	1.920(4)
Sb(1)-O(3)	2.024(2)	Sb(1)-O(3)	2.031(4)
Sb(1)-O(4)	1.926(2)	Sb(1)-O(4)	2.016(4)
Sb(1)-O(5)	2.017(2)	Sb(1)-O(5)	2.051(4)
Sb(2)-O(4)#1	1.928(2)	Sb(2)-O(2)#1	1.919(4)
Sb(2)-O(1)	1.962(2)	Sb(2)-O(1)	1.959(3)
Sb(2)-O(6)	2.010(2)	Sb(2)-O(8)	2.008(4)
Sb(2)-O(7)	2.055(2)	Sb(2)-O(9)	2.014(4)
Sb(2)-O(8)	2.014(2)	Sb(2)-O(7)	2.059(3)
Mn(1)-O(1)	2.264(2)	Co(1)-O(1)	2.145(4)
Mn(1)-O(9)#1	2.069(3)	Co(1)-O(3)	2.122(4)
Mn(1)-O(11)	2.181(3)	Co(1)-O(9)	2.128(4)
Mn(1)-O(8)	2.199(2)	Co(1)-O(11)#1	2.008(4)
Mn(1)-O(3)	2.204(2)	Co(1)-O(6)	2.087(4)
Mn(1)-N(1)	2.219(3)	Co(1)-N(1)	2.120(5)
Sb(1)-O(3)-Mn(1)	103.45(10)	Sb(1)-O(3)-Co(1)	101.45(16)
Sb(1)-O(1)-Sb(2)	138.76(13)	Sb(2)-O(9)-Co(1)	101.98(15)
Sb(1)-O(1)-Mn(1)	103.39(10)	Sb(2)-O(1)-Sb(1)	139.0(2)
Sb(2)-O(1)-Mn(1)	103.31(10)	Sb(2)-O(1)-Co(1)	103.25(16)
Sb(2)-O(8)-Mn(1)	103.89(10)	Sb(1)-O(1)-Co(1)	102.81(15)
Sb(1)-O(4)-Sb(2)#1	145.94(13)	Sb(2)#1-O(2)-Sb(1)	145.9(2)

Table 4.3: Selected bond lengths (Å) and bond angles (º) in **4.3-4.4**

4.3		4.4	
Sb(1)-O(1)	1.972(2)	Sb(1)-O(1)	2.0074(19)
Sb(1)-O(2)	2.050(2)	Sb(1)-O(2)	2.046(2)
Sb(1)-O(3)	2.039(3)	Sb(1)-O(3)	2.016(2)
Sb(1)-O(4)	2.010(2)	Sb(1)-O(4)	2.015(2)
Sb(1)-O(5)	1.920(2)	Sb(1)-O(6) #1	1.915(2)
Sb(2)-O(1)	1.974(2)	Sb(2)-O(1)	2.013(2)
Sb(2)-O(5)#1	1.926(2)	Sb(2)-O(5)	1.998(2)
Sb(2)-O(8)	2.003(2)	Sb(2)-O(8)	2.011(2)
Sb(2)-O(7)	2.025(3)	Sb(2)-O(7)	2.043(2)
Sb(2)-O(6)	2.053(2)	Sb(2)-O(6)	1.926(2)
Ni(3)-O(1)	2.076(3)	Cu(3)-O(1)	2.076(2)
Ni(3)-O(9)	2.003(3)	Cu(3)-O(9) #1	1.941(2)
Ni(3)-O(3)	2.090(3)	Cu(3)-O(4)	2.348(2)
Ni(3)-O(7)	2.101(3)	Cu(3)-O(5)	2.326(2)
Ni(3)-O(10)	2.076(3)	Cu(3)-O(10)	1.985(2)
Ni(3)-N(1)	2.069(3)	Cu(3)-N(1)	2.004(3)
Sb(1)-O(1)-Sb(2)	138.57(13)	Sb(1)-O(1)-Sb(2)	136.37(10)
Sb(1)-O(1)-Ni(3)	103.00(10)	Sb(1)-O(1)-Cu(3)	105.13(9)
Sb(2)-O(1)-Ni(3)	103.27(10)	Sb(2)-O(1)-Cu(3)	105.06(8)
Sb(1)-O(5)-Sb(2)#1	146.83(13)	Sb(1) #1-O(6)-Sb(2)	145.45(12)
Sb(1)-O(3)-Ni(3)	100.24(11)	Sb(1)-O(4)-Cu(3)	95.70(8)
Sb(2)-O(7)-Ni(3)	100.63(10)	Sb(2)-O(5)-Cu(3)	96.98(8)

4.5 Analytical and Spectroscopic Data

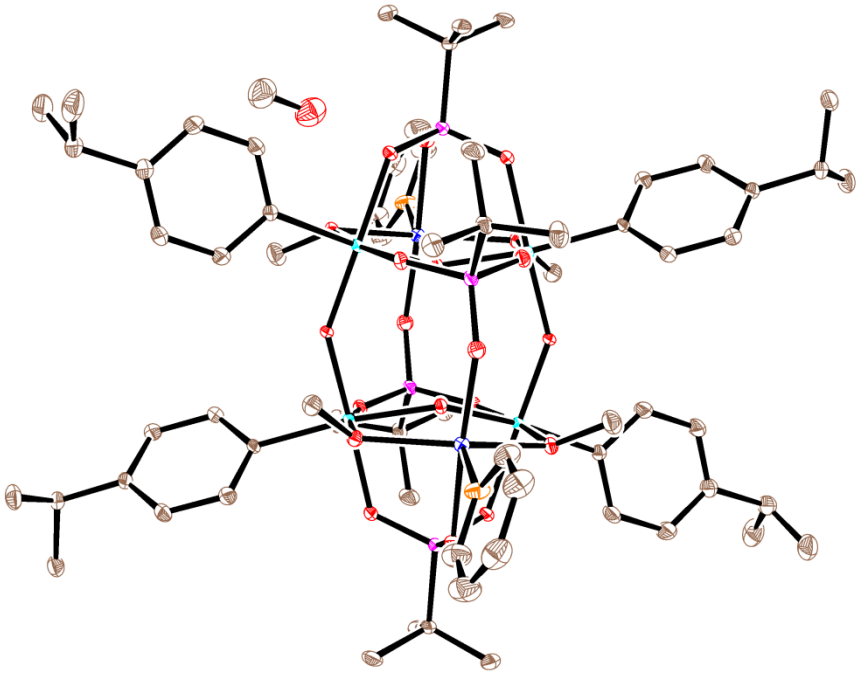

Figure S1: ORTEP view of **4.1** with thermal ellipsoids shown at 30% probability.

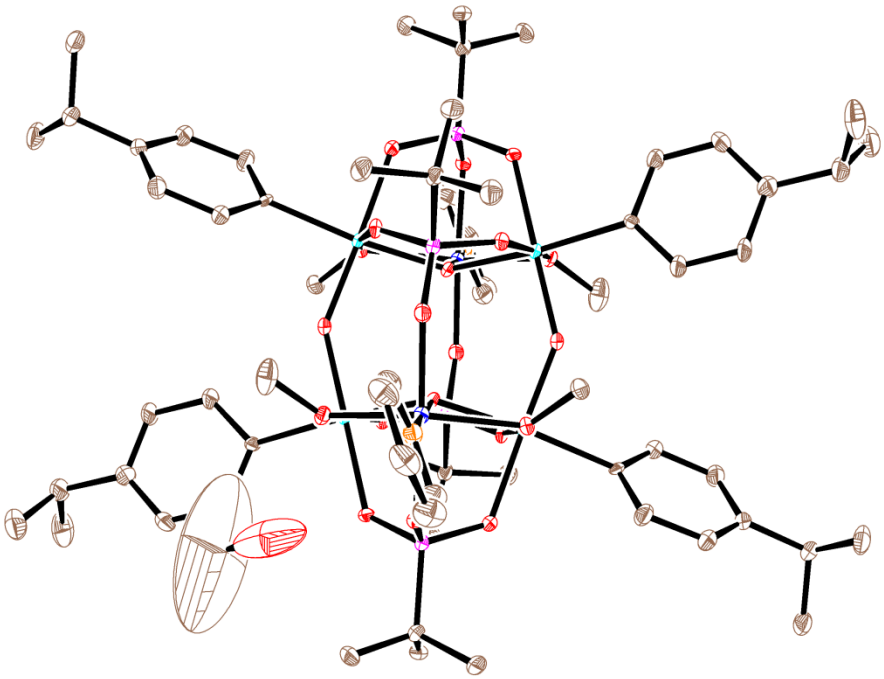

Figure S2: ORTEP view of **4.2** with thermal ellipsoids shown at 30% probability.

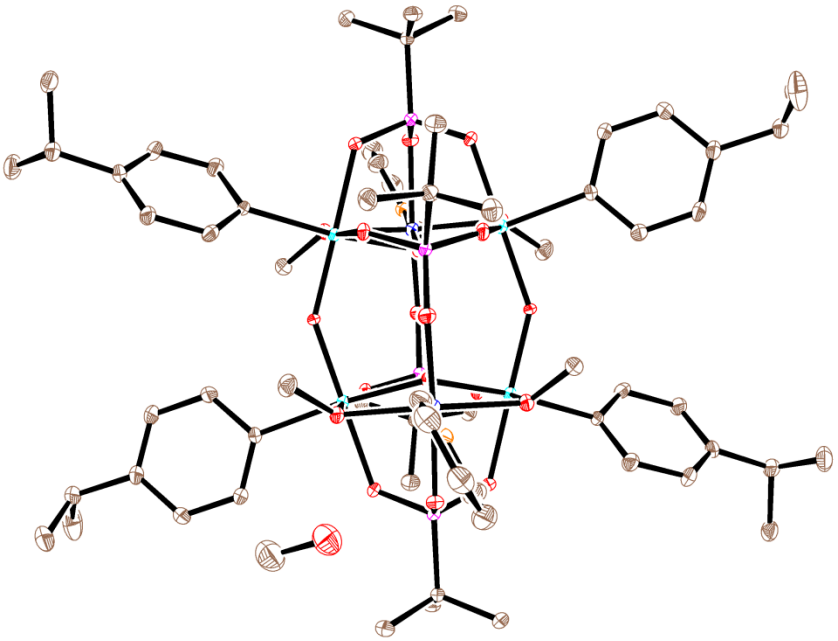

Figure S3: ORTEP view of **4.3** with thermal ellipsoids shown at 30% probability**.**

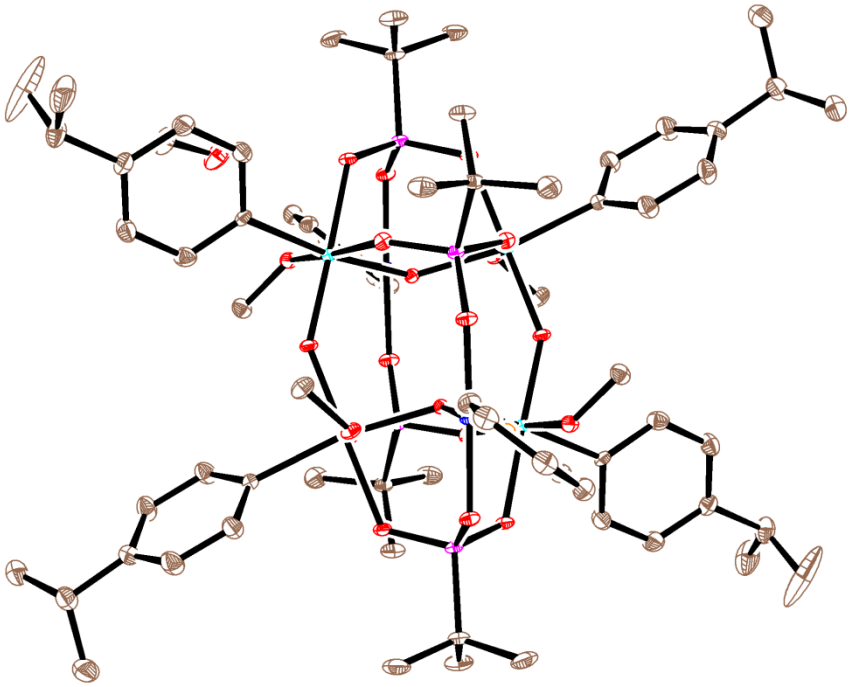

Figure S4: ORTEP view of **4.4** with thermal ellipsoids shown at 30% probability.

4.6 References

1) (*a*) P. DeBurgomaster, A. Aldous, H. Liu, C. J. O'Connor and J. Zubieta, *Cryst. Growth Des.*, 2010, **10**, 2209; (*b*) A. Clearfield, *Prog. Inorg. Chem.*, 1998, **47**, 371; (*c*)N.G.Armatas,W.Ouellette,K.Whitenack, J. Pelcher, H. Liu, E. Romaine, C. J. O'Connor and J. Zubieta, *Inorg. Chem.*, 2009, **48**, 8897; (*d*) P. DeBurgomaster, W. Ouellette, H. Liu, C. J. O'Connor and J. Zubieta, *Cryst. Eng. Comm.*, 2010, **12**, 446; (e) V. Chandrasekhar, S. Kingsley, *Angew. Chem., Int. Ed*. 2000, **39**, 2320; (f) V. Chandrasekhar, S. Kingsley, A. Vij, K. C. Lam, A. L. Rheingold, *Inorg. Chem*., 2000, **39**, 3238; (g) V. Chandrasekhar, V. Baskar, J. Vittal, *J. Am. Chem. Soc.* 2003, **125**, 2392; (h) E. I. Tolis, M. Helliwell, S. Langley, J. Raftery and R. E.P. Winpenny, *Angew. Chem., Int. Ed*., 2003, **42**, 3804; (i) S. Konar, N. Bhuvanesh and A. Clearfield*, J. Am. Chem. Soc*., 2006, **128**, 9604.
2. (a) B. L.Vallee and D. S. Auld, *Acc. Chem. Res.* 1993, **26**, 543; (b) B. L. Vallee and D. S. Auld, *Biochemistry* 1993, **32**, 6493; (c) E. Hough, L. K. Hansen, B. Birknes, K. Jynge, S. Hansen, A. Hordvik, C. Little, E. Dodson and Z. Derwnda, *Nature* 1989, **338**, 357; (d) H. Vahrenkamp, *Acc. Chem. Res*. 1999, **32**, 589.
3. (*a*) A. Clearfield, *Inorganic Ion Exchange Materials*, CRC Press, Boca Raton, FL, 1982; (*b*) J. D. Wang, A. Clearfield and G.-Z. Peng, *Mater. Chem. Phys.*, 1993, **35**, 208; (*c*) B. Zhang and A. Clearfield, *J. Am. Chem. Soc.*, 1997, **119**, 2751.
4. (a) F. Fredoueil, D. Massiot, P. Janvier, F. Gingl, M. B. Doeuff, M. Evian, A. Clearfield and B. Bujoli, *Inorg. Chem*., 1999, **38**, 1831; (b) K. Maeda, Y. Kiyozumi and F. Mizukami, *J. Phys. Chem. B*, 1997, **101**, 4402; (c) Q. Yue, J. Yang, G.-H. Li, G.-D. Li and J.-S. Chen, *Inorg. Chem*., 2006, **45**, 4431.
5. (a) S. B. Ungashe, W. L. Wilson, H. E. Katz, G. R. Scheller and T. M. Putvinski, *J. Am. Chem. Soc*., 1992, **114**, 8717; (b) M. J. Sanchez- Moreno, A. Fernandez-Botello, R. B. Gomez-Coca, R. Griesser, J. Ochocki, A. Kotynski, J. Niclos-Gutierrez, V. Moreno and H. Sigel, *Inorg. Chem*., 2004, **43**, 1311; (c) Z.-Y. Du, H.-B. Xu and J.-G. Mao, *Inorg. Chem*., 2006, **45**, 6424.
6. (a) B. Z. Wan, R. G. Anthony, G. Z. Peng and A. Clearfield, *J. Catal*., 1986, **101**, 19; (b) D. Deniaud, B. Schollorn, J. Mansury, J. Rouxel, P. Battion and B. Bujoli, *Chem. Mater*.,

1995, **7**, 995; (c) A. Hu, H. Ngo and W. Lin, *J. Am. Chem. Soc*., 2003, **125**, 11490; (d) A. Hu, G. T. Yee and W. Lin, *J. Am. Chem. Soc*., 2005, **127**, 12486.

7. (a) A. Cabeza, M. A. G. Aranda, S. Bruque, D. M. Poojary, A. Clearfield and J. Sanz, *Inorg. Chem.*, 1998, **37**, 4168; (b) D. M. Poojary and A. Clearfield, *Inorg. Chem*., 1998, **37**, 249; (c) P. Ayyappan, O. R. Evans, Y. Cui, K. A. Wheeler and W. Lin, *Inorg. Chem*., 2002, **41**, 4978.
8. V. Chandrasekhar and S. Kingsley, *Angew. Chem., Int. Ed*., 2000, **39**, 2320.
9. (a) E. K. Brechin, R. A. Coxall, A. Parkin, S. Parsons, P. A. Tasker and R. E. P. Winpenny, *Angew. Chem., Int. Ed*., 2001, **40**, 2700; (b) S. Maheswaran, G. Chastanet, S. J. Teat, T. Mallah, R. Sessoli, W. Wernsdorfer and R. E. P. Winpenny, *Angew. Chem., Int. Ed*., 2005, **44**, 5044; (c) M. Shanmugam, G. Chastanet, T. Mallah, R. Sessoli, S. J. Teat, G. A. Timco and R. E. P. Winpenny, *Chem.–Eur. J*., 2006, **12**, 8777; (d) M. Shanmugam, G. Chastanet, R. Sessoli, T. Mallah, W. Wernsdorfer and R. E. P. Winpenny, *J. Mater. Chem*., 2006, **16**, 2576; (e) H.-C. Yao, Y.-Z. Li, Y. Song, Y.-S. Ma, L.-M. Zheng and X.-Q. Xin, *Inorg. Chem*., 2006, **45**, 59; (f) S. Konar and A. Clearfield, *Inorg. Chem*., 2008, **47**, 3489; (g) M. Wang, C. Ma, H. Wen and C. Chen, *Dalton Trans*., 2009, 994; (h) C. Dendrinou-Samara, C. A. Muryn, F. Tuna and R. E. P. Winpenny, *Eur. J. Inorg. Chem*., 2010, 3097.
10. (a) E. I. Tolis, M. Helliwell, S. Langley, J. Raftery and R. E. P. Winpenny, *Angew. Chem., Int. Ed*., 2003, **42**, 3804; (b) S. Konar, N. Bhuvanesh and A. Clearfield, *J. Am. Chem. Soc*., 2006, **128**, 9604; (c) H.-C. Yao, J.-J. Wang, Y.-S. Ma, O. Waldmann, W.-X. Du, Y. Song, Y.-Z. Li, L.-M. Zheng, S. Decurtins and X.-Q. Xin, *Chem. Commun*., 2006, 1745; (d) S. Khanra, S. Konar, A. Clearfield, M. Helliwell, E. J. L. McInnes, E. Tolis, F. Tuna and R. E. P. Winpenny, *Inorg. Chem*., 2009, **48**, 5338; (e) E. I. Tolis, L. P. Engelhardt, P. V. Mason, G. Rajaraman, K. Kindo, M. Luban, A. Matsuo, H. Nojiri, J. Raftery, C. Schröder, G. A. Timco, F. Tuna, W. Wernsdorfer and R. E. P. Winpenny, *Chem.–Eur. J*., 2006, **12**, 8961; (f) S. Khanra, M. Helliwell, F. Tuna, E. J. L. McInnes and R. E. P. Winpenny, *Dalton Trans*., 2009, 6166; (g) S. Konar and A. Clearfield, *Inorg. Chem*., 2008, **47**, 5573; (h) R. Murugavel, N. Gogoi and R. Clérac, *Inorg. Chem*., 2009, **48**, 646; (i) K. Gopal, F. Tuna and R. E. P. Winpenny, *Dalton Trans*., 2011, **40**, 12044.

11. S. K. Langley, M. Helliwell, S. J. Teat and R. E. P. Winpenny, *Dalton Trans*., 2012, **41**, 12807. (a) S. Langley, M. Helliwell, J. Raftery, E. I. Tolis and R. E. P. Winpenny, *Chem. Commun*., 2004, 142; (b) S. Langley, M. Helliwell, R. Sessoli, P. Rosa, W. Wernsdorfer and R. E. P. Winpenny, *Chem. Commun*., 2005, 5029; (c) S. Langley, M. Helliwell, R. Sessoli, S. J. Teat and R. E. P. Winpenny, *Inorg. Chem*., 2008, **47**, 497; (d) S. Langley, M. Helliwell, R. Sessoli, S. J. Teat and R. E. P. Winpenny, *Dalton Trans*., 2009, 3102.
12. (a) Y.-Z. Zheng, M. Evangelisti and R. E. P. Winpenny, *Angew. Chem., Int. E*d., 2011, 50, 3692; (b) Y. Zheng, M. Evangelisti, F. Tuna and R. E. P. Winpenny, *J. Am. Chem. Soc*., 2012, **134**, 1057; (c) Y. Zheng, E. Moreno Pineda, M. Helliwell and R. E. P. Winpenny, *Chem.–Eur. J*., 2012, **18**, 4161.
13. (*a*) V. Chandrasekhar, S. Kingsley, A. Vij, K. C. Lam and A. L. Rheingold, *Inorg. Chem*, 2000, **39**, 3238; (*b*) V. Chandrasekhar, L. Nagarajan, K. Gopal, V. Baskar and P. K¨ogerler, *Dalton Trans.*, 2005, 3143; (*c*) V. Chandrasekhar, P. Sasikumar, R. Boomishankar and G. Anantharaman, *Inorg. Chem.*, 2006, **45**, 3344; (*d*) V. Chandrasekhar, L. Nagarajan, R. Cl´erac, S. Ghosh and S. Verma, *Inorg. Chem.*, 2008, **47**, 1067; (*e*) V. Chandrasekhar, L. Nagarajan, R. Cl´erac, S. Ghosh, T. Senapati and S. Verma, *Inorg. Chem.*, 2008, **47**, 5347; (*f*) V. Chandrasekhar, R. Azhakar, T. Senapati, P. Thilagar, S. Ghosh, S. Verma, R. Boomishankar, A. Steiner and P. K¨ogerler, *Dalton Trans.*, 2008, 1150; (*g*) V. Chandrasekhar, T. Senapati and E. C. Sañudo, *Inorg. Chem.*, 2008, **47**, 9553; (*h*) V. Chandrasekhar, T. Senapati, E. C. Sañudo and R. Cl´erac, *Inorg. Chem.*, 2009, **48**, 6192.
14. (a) V. Chandrasekhar, A. Dey, T. Senapati and E. C. Sañudo, *Dalton Trans*., 2012, **41**, 799; (b) S. Khanra, M. Kloth, H. Mansaray, C. A. Muryn, F. Tuna, E. C. Sañudo, M. Helliwell, E. J. L. McInnes and R. E. P. Winpenny, *Angew. Chem., Int. Ed*., 2007, **46**, 5568; (c) J. Salta, Q. Chen, Y.-D. Chang and J. Zubieta, *Angew. Chem., Int. Ed. Engl*., 1994, **33**, 757; (d) Y.-D. Chang, J. Salta and J. Zubieta, *Angew. Chem., Int. Ed. Engl*., 1994, **33**, 3.
15. (a) Y. Fujiwara, M. Mitani, S. Yasuike, J. Kurita and T. Kaji, *J. Health Sci*., 2005, **51**, 333; (b) V. Rishi, W. J. Oh, S. L. Heyerdahl, J. Zhao, D. Scudiero, R. H. Shoemaker and C. Vinson, *J. Struct. Biol*., 2010, **170**, 216; (c) S. L. Heyerdahl, J. Rozenberg, L.

Jamtgaard, V. Rishi, L. Varticovski, K. Akash, D. Scudiero, R. H. Shoemaker, T. S. Karpova, R. N. Day, J. D. McNally and C. Vinson, *Eur. J. Cell Biol*., 2010, **89**, 564.

16. (a) H. Schmidt*, Liebigs Ann. Chem*., 1920, **421**, 174; (b) G. O. Doak and H. G. Steinman, *J. Am. Chem. Soc*., 1946, **68,** 1987; (c) G. O. Doak, *J. Am. Chem. Soc.,* 1946, **68**, 1991.
17. (a) M. S. R. Prabhu, A. K. Jami and V. Baskar, *Organometallics*, 2009, **28**, 3953; (b) A. K. Jami, M. S. R. Prabhu and V. Baskar, *Organometallics*, 2010, **29**, 1137; (c) A. K. Jami and V. Baskar, *Dalton Trans*., 2012, **41**, 12524; (d) N. K. Srungavruksham and V. Baskar, *Dalton Trans*., 2015, **44**, 6358; (e) U. Ugandhar and V. Baskar, *Dalton Trans.,* 2016, **45**, 6269; (f) M. S. R. Prabhu, U. Ugandhar and V. Baskar, *Dalton Trans*., 2016, **45**, 6963.
18. V. Baskar, M. Shanmugam, M. Helliwell, S. J. Teat and R. E. P. Winpenny, *J. Am. Chem. Soc*., 2007, **129**, 3042.
19. (a) J. Beckmann, P. Finke, M. Hesse and B. Wettig, *Angew. Chem., Int. Ed*., 2008, **47**, 9982; (b) J. Brunig, E. Hupf, E. Lork, S. Mebs and J. Beckmann, *Dalton Trans*., 2015, **44**, 7105.
20. (a) C. J. Clark, B. K. Nicholson and C. E. Wright, *Chem. Commun*., 2009, 923; (b) B. K. Nicholson, C. J. Clark, C. E. Wright and T. Groutso, *Organometallics*, 2010, **29**, 6518; (c) B. K. Nicholson, C. J. Clark, C. E. Wright, S. G. Telfer and T. Groutso, *Organometallics*, 2011, **30**, 6612; (d) B. K. Nicholson, C. J. Clark, S. G. Telfer and T. Groutso, *Dalton Trans*., 2012, **41**, 9964; (e) B. K. Nicholson, C. J. Clark, G. B. Jameson and S. G. Telfer, *Inorg. Chim. Acta*, 2013, **406**, 53.
21. a) S. Ali, V. Baskar, C. A. Muryn, and R. E. P. Winpenny, *Chem. Commun*., 2008, 6375; (b) S. Ali, C. A. Muryn, F. Tuna and R. E. P. Winpenny, *Dalton Trans*., 2010, **39**, 9588: (c) S. Ali, C. A. Muryn, F. Tuna and R. E. P. Winpenny, *Dalton Trans*., 2010, **39**, 124.
22. (a) R. Rüther, F. Huber and H. Preut, *Z. Anorg. Allg. Chem*., 1986, **539**, 110; (b) P. C. Croft and G. M. Kosolapoff, *J. Am. Chem. Soc*., 1953, **75**, 3379.
23. G. M. Sheldrick, SHELXS-97, Program for Crystal Structure Solution, University of Göttingen, Göttingen, Germany, 1997.
24. G. M. Sheldrick, *Acta Crystallogr., Sec. A: Fundam. Crystallogr.*, 2008, **64**, 112.
25. G. M. Sheldrick, *Acta Crystallogr., Sect. C: Cryst. Struct. Commun*., 2015, **71**, 3.

Stibonate-Phosphonate Cluster Stabilizing Lanthanide ions (Ln = Pr, Gd & Dy)

Chapter 5

Abstract: Arylstibonic acid phosphonate pro-ligand, [(*p*-iPr-$C_6H_4Sb)_4(OH)_4$(*t*-$BuPO_3)_6$] was synthesized by condensation reaction of *p*-isopropylphenylstibonic acid ($ArSbO_3H_2$) with *t*-butylphosphonic acid. It contains four antimony centers, forms a puckered eight-member Sb_4O_4 core held together by six *t*-butyl phosphonates. The reaction of hydrated lanthanide acetate salt with antimonate-phosphonate pro-ligand [(*p*-iPr-$C_6H_4Sb)_4(OH)_4$(*t*-$BuPO_3)_6$] under solvothermal conditions in methanol, in the presence of pyridine as a base yielded two families of novel arylstibonic acid-lanthanide based metal phosphonate clusters. Single crystal structural elucidation revealed the formation of [$Pr_4(ArSb)_4(\mu_4\text{-}O)_2(\mu_2\text{-}OH)_2(\mu_2\text{-}OCH_3)_8(OCH_3)_4$(*t*-$BuPO_3H)_6$(*t*-$BuPO_3)_4$] (**5.1**), [$Gd_4(ArSb)_4(\mu_4\text{-}O)_2(\mu_2\text{-}OH)_2(\mu_2\text{-}OCH_3)_8(OCH_3)_4$(*t*-$BuPO_3H)_6$(*t*-$BuPO_3)_4$] (**5.2**) and [$Dy_{12}(ArSb)_{12}(\mu_3\text{-}OH)_6(\mu_2\text{-}OCH_3)_{12}(OCH_3)_{12}$(*t*-$BuPO_3H)_6$(*t*-$BuPO_3)_{18}${(*t*-$Bu)_2P_2O_5$}$_6$] (**5.3**). The clusters **5.1** and **5.2** are 1D coordination polymers whose repeating unit possesses a tetramer motif. While two lanthanide ions in a tetramer are in eight-coordinate with triangular dodecahedron geometry, the other two antimony centers are in hexa-coordinate with octahedral geometry. In contrast to **5.1** and **5.2**, interestingly **5.3** possesses novel twenty-four membered ring-type architecture, consist of six Dy(III) centers which are in eight-coordinate and present in square-antiprism geometry. While the other six Dy(III) centers which are in hexa-coordinate with octahedral geometry. Twelve antimony (V) centers are in hexa-coordinate with octahedral geometry. Interestingly rare di *t*-butylphosphonate {(*t*-$Bu)_2P_2O_5$} ligand system is generated *in situ* by self-condensation of two *t*-butylphosphonic acids which help in stabilizing the Dy_{12} cluster. Preliminary magnetic moment studies (Dc and Ac) have been performed and the results are explained in detail.

5.1 Introduction:

The design, synthesis and structural characterization of high-nuclearity heterometallic {3d-4f} clusters have been an area of focus due to their fascinating structures and potential applications in various fields such as magnetism,[1] luminescence,[2] electronics,[3] material science,[4] and nanotechnology.[5] To date, a great variety of nano-sized 3d-4f clusters of various nuclearities with fascinating structure types such as wheel-shaped $\{Dy_{10}Co_2\}$,[6] prism-type $\{La_{60}Ni_{76}\}$,[7] dumbbell-shaped,[8] nesting doll-like $\{Gd_{54}Ni_{54}\}$,[9] drum-like $\{Ln_8Cd_{24}\}$,[10] bowl-like $\{Ln_{42}Co_{10}\}$,[11] ring-like $\{Ln_{24}Cu_{36}\}$[12] and grid-like $\{Ln_8Co_8\}$[13] have been reported. Recently 3d-4f phosphonates especially where 4f ion is isotropic Gd (III) ion; reported as potential molecular magnetic refrigerants.[14] Reports on homo metallic 4f phosphonates are limited due to the reason that lanthanide phosphonate complexes generally have poor solubility and poor crystallinity in water and organic solvents and this can make them difficult to characterize. Mallouk *et al* reported first lanthanide phosphonates $[Ln(PhPO_3)(PhPO_3H)]$ (here Ln = La, Ce) and a series of lanthanide alkylphosphonates in the year of 1990.[15] Recently, Winpenny *et al* also have been synthesizing lanthanide phosphonate molecular cages and mixed 3d-4f phosphonate cages with interesting physical properties.[16] Lanthanide metal phosphonates and main group metal phosphonates have been studied independently for a number of years, but to the best of our knowledge, main group metal phosphonates are used as pro-ligands for assembling lanthanide metal atoms have not been reported. For the first time, we are reporting organostibonic acid-phosphonate based pro-ligand, which can be used for assembling lanthanide metal atoms under hydrothermal conditions in the presence of a base. In recent years considerable attention has been directed towards the synthesis and structural characterization of organoantimony (V) oxo clusters due to their potential applications in the field of biology and catalysis. Recent biological studies shows that arylstibonic acids are used as potential anticancer agents and antimicrobial agents.[17] Beckmann *et al* reported well-defined molecular stibonic acids by introducing sterically hindered bulky R groups on the antimony atom.[18] In the presence of base arylstibonic acid self-condenses leading to isolation of novel Sb_{12}, Sb_{14} and Sb_{16} polyoxostibonate type frameworks, wherein ESI-MS has been found to be a very useful technique to understand basic building block of arylstibonic acid aggregates in solution.[19] Although arylstibonic acids possess cross-linked polymeric structures in solid state, we have a long-standing interest in using arylstibonic acid as a ligand for the synthesis of polynuclear molecular clusters. Recently our group reported depolymerization

reactions of arylstibonic acids with protic ligands such as phosphonic acids, phenylseleninic acid, phenolic pyrazole, 8-hydroxy quinolone, silane diol and triol resulting in the isolation of tetra and trinuclear organoantimony oxo cluster.[20] Very recently, mixed valent Sb_{14}(III/V) POMs have been reported, which is stabilized by telluroxane ligands and counter triphenyltellurium cations.[21] Arylstibonic acids have been used as a ligand, like phosphonic acid and arsenic acid to bind with transition metals to form a reverse Keggin type structure.[22] However, arylstibonic acids and phosphonic acids can independently act as ligands towards metal ions, mixing of both ligands results partial condensation, giving polydentate oxygen donor ligands. The pro-ligand cluster method provides a single-source precursor for the combining the coordination ability of stibonates and phosphonates motifs that can serve as a novel ligand platform which could be employed for stabilizing new types of polynuclear metal based oxo hydroxo systems. The use of pro-ligand for assembling transition metals is a milestone in arylstibonic acid chemistry[23] as this concept can be used to investigate reactivity studies of arylstibonic acid with lanthanide metals by employing solvothermal conditions. For this purpose, we choose easily crystallizable and soluble *p*-isopropylphenylstibonic acid rather than insoluble *p*-halostibonic acids. In this study we understand that the solubility of arylstibonic acids has been influenced by organic substituents appended on Sb atom. They also plays important role in the end-product formation. Herein, the synthesis, magnetic properties and structural characterization of two types of arylstibonic acid-lanthanide based metal phosphonate clusters are reported. Single crystal X-ray diffraction studies reveals that formation of $[Pr_4(ArSb)_4(\mu_4\text{-}O)_2(\mu_2\text{-}OH)_2(\mu_2\text{-}OCH_3)_8(OCH_3)_4(t\text{-}BuPO_3H)_6(t\text{-}BuPO_3)_4]$ (**5.1**), $[Gd_4(ArSb)_4(\mu_4\text{-}O)_2(\mu_2\text{-}OH)_2(\mu_2\text{-}OCH_3)_8(OCH_3)_4(t\text{-}BuPO_3H)_6(t\text{-}BuPO_3)_4]$ (**5.2**) and $[Dy_{12}(ArSb)_{12}(\mu_3\text{-}OH)_6(\mu_2\text{-}OCH_3)_{12}(OCH_3)_{12}(t\text{-}BuPO_3H)_6(t\text{-}BuPO_3)_{18}\{(t\text{-}Bu)_2P_2O_5\}_6]$ (**5.3**). Detailed synthesis and structural characterization of compounds **5.1** to **5.3** are given in this chapter.

5.2 Experimental Section

5.2.1 General Information:

Arylstibonic acids[24] (aryl= *p*-isopropylphenyl) and *t*-butylphosphonic acid[25] were synthesized according to literature reports. Solvents, lanthanide metal acetate salts and common reagents were purchased from commercial sources. Mixed antimonate-phosphonate pro ligand [(*p*-iPr-$C_6H_4Sb)_4(OH)_4$(*t*-$BuPO_3)_6$] was synthesized by the condensation reaction of organostibonic acid with *t*-butylphosphonic acid.[20d]

5.2.2 Instrumentation:

Infrared spectra were recorded with a JASCO-5300 FT-IR spectrometer as KBr pellets. Elemental analysis was performed with a Flash EA Series 1112 CHNS analyzer. Single crystal X-ray data collection for compounds **5.1** to **5.2** was carried out at 100(2) K with a Bruker Smart Apex CCD area detector system [λ (Mo-Kα) = 0.71073 Å] with a graphite monochromator. Single crystal X-ray data collection for compound **5.3** was carried out at 100(2) K with a Bruker Axs Smart APEX II Single Crystal Diffractometer with Oxford Cryosystems 700 cooler plus. The data were reduced using SAINTPLUS. The structures were solved using SHELXS-97[26] and refined using the program SHELXL-2014/7.[27] All non-hydrogen atoms were refined anisotropically.

5.2.3 General synthetic procedures for compounds 5.1- 5.3:

The general synthetic methodology adopted is as follows, mixed antimonate-phosphonate pro ligand and lanthanide metal acetate hydrate were dissolved in methanol (15 mL) and simultaneous dropwise addition of pyridine forms clear solution, stirred for 1 h then transferred into Teflon digestion bomb. The bomb was sealed properly and the mixture heated to 100 ^oC for 12 h and then cooled slowly. X-ray quality single crystals were obtained at the base of the bomb. The isolated crystals were powdered and subjected to high vacuum for half an hour before being characterized by standard spectroscopic and analytical techniques. The molar ratios of the corresponding reagents used are as follows.

Compound **5.1**: Pro-ligand (0.05 g, 0.027 mmol) and praseodymium acetate (0.042 g, 0.1 mmol) pyridine (0.02 mL). Green block shaped single crystals formed upon slow cooling (48 h) of methanol solution. Yield: 0.017g (20 % based on Pro-ligand). Anal, Calcd (%) for

C80H152O40P8Pr4Sb4 (3052.49): C, 31.48; H, 5.02. Found: C, 31.72; H, 4.58. IR (cm-1, KBr pellet): 3413(wide), 2960(s), 1630(m), 1552(s), 1479(m), 1384(s), 1104(s), 1039(s), 1011(m), 671(s), 507(s).

Compound **5.2**: Pro-ligand (0.05 g, 0.027 mmol) and gadalonium acetate (0.044 g, 0.1 mmol) pyridine (0.02 mL). Colorless single crystals formed upon slow cooling (48 h) of methanol solution. Yield: 0.014g (16 % based on Pro-ligand). Anal, Calcd (%) for C80H152O40P8Gd4Sb4 (3117.86): C, 30.82; H, 4.91. Found: C, 30.85; H, 4.61. IR (cm-1, KBr pellet): 3397(wide), 2963(s), 2926(m), 1627(m), 1556(s), 1480(m), 1459(s), 1111(m), 1045(s), 832(m), 679(s), 508(m).

Compound **5.3**: Pro-ligand (0.05 g, 0.027 mmol) and dysprosium acetate (0.045 g, 0.1 mmol) pyridine (0.02 mL). Colorless single crystals formed upon slow cooling (48 h or 72 h) of methanol solution. Yield: 0.010g (12% based on Pro-ligand). Anal, Calcd (%) for C276H528O134P36Dy12Sb12 (10517.22): C, 31.52; H, 5.06. Found: C, 31.49; H, 5.15. IR (cm-1, KBr pellet): 3416(wide), 2962(s), 2870(m), 1633(m), 1557(m), 1458(s), 1384(s), 1117(m), 1046(s), 663(s), 544(m).

5.3 Results and Discussions

Compounds **5.1-5.3** were synthesized by the reaction of antimonate-phosphonate pro-ligand [(*p*-iPr-$C_6H_4Sb)_4(OH)_4$(*t*-$BuPO_3)_6$] with lanthanide(III) metal acetate hydrate [Ln= Pr(**5.1**), Gd(**5.2**) and Dy(**5.3**)] in methanol under solvothermal conditions, using pyridine as a base (Scheme 1). Single crystals of **5.1-5.3** for X-ray diffraction studies appeared directly upon slow cooling of the methanol solution. Compound **5.1** crystallizes in tetragonal chiral space group P41212. Crystallographic data and bond metric parameters of **5.1** are given in the table 5.4 & 5.5. Since the overall molecular structures of **5.1** and **5.2** are very similar. The structure of **5.1** (**Figure 5.1**) is considered for structural discussions. The molecular structure of **5.1** can be visualized as 1D coordination polymers whose repeating unit possess tetramer motif {Pr_2Sb_2} (**Figure 5.3**). The asymmetric unit of **5.1** (**Figure 5.1**) contains repeating tetramer units {Pr_2Sb_2} bridged with two *t*-butylphosphonic acid moieties. The tetramer unit core (**Figure 5.2**) displays boat-shaped geometry. In tetramer unit, two arylstibonic acid moieties self-condensed through one μ_4-oxido, one μ_2-hydroxo bridge and further connected with praseodymium metal atoms through bridged two μ_2-methoxy groups, forms boat-shape structure. Of the two types of phosphonates present,

the first type phosphonates chelate to the one antimony atom and two Pr metal atoms in 3.111 coordination mode based on Harris notation.

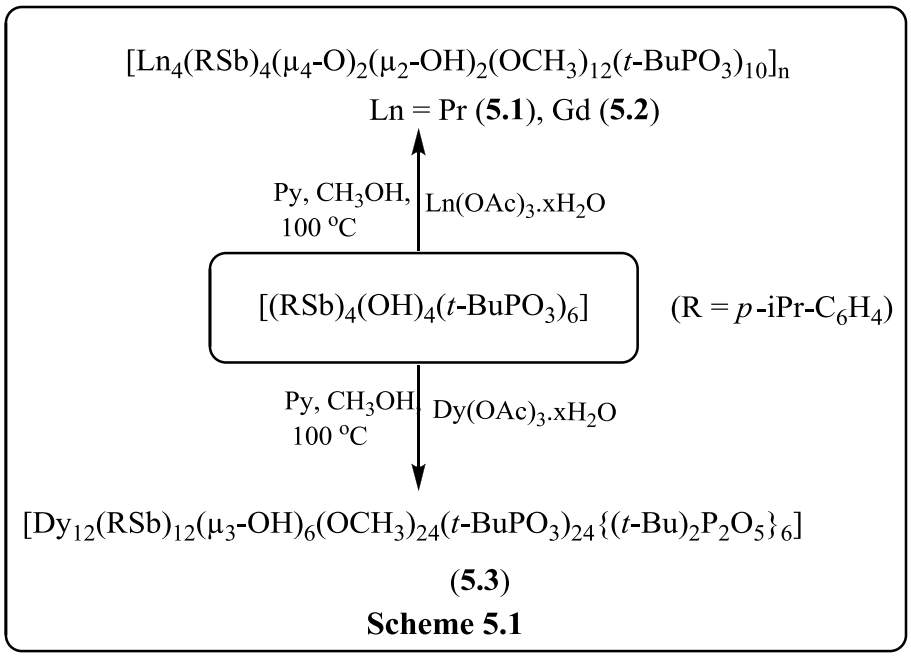

Scheme 5.1

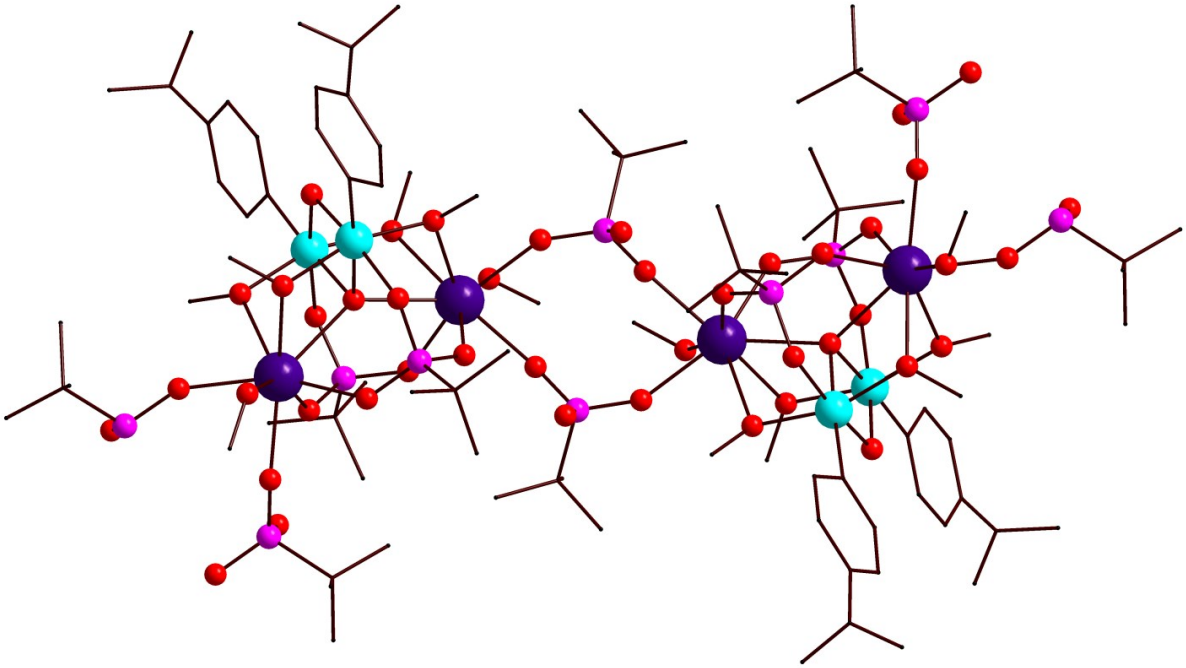

Figure 5.1: Molecular structure of **5.1**. H atoms are omitted for clarity. Color code; Blue: Pr, Cyan: Sb, Pink: P, Red: O, Brown: C

The second type of phosphonates ligands bridges two tetramer units and chelate to two Pr metal atoms in a 2.110 coordination mode. These bridged phosphonates are responsible for the formation of a 1D coordination polymer. Each Sb center is present in an octahedral geometry with the O_5SbC coordination mode. The Sb-O bond lengths involving μ_4-oxido, μ_2-hydroxo and μ_2-OCH_3 bridges are falls in the range of 2.035(8) Å, 1.973(8) Å and 2.009(8) to 2.018(9) Å respectively. The Sb-O bond lengths involving phosphonates falls in the range of 2.019(10) Å which is comparable to literature reported phosphonate bond lengths like organotinphosphonate cage,[28] galliumphosphonate cage[29] and borophosphonate cage.[30] The Sb-O-Sb bond angles fall in the range of 97.9(5) to 102.2(5) °. Each Pr metal center is eight-coordinate, bound to one μ_4-oxido bridge, four phosphonate oxygens and three oxygens from the methoxy group (in which two are bridged and one is terminal). By using SHAPE 2.1 systematic calculations we can conclude the coordination geometries around the all eight-coordinated Pr (III) ions in **5.1** are exhibit the closest similarity to triangular dodecahedron geometry (**Figure 5.2**). The Pr-O bond lengths involving μ_4-oxido, methoxy group and phosphonates falls in the range of 2.639(5) Å, 2.488(9) to 2.584(17) Å and 2.361(9) to 2.409(10) Å respectively. The Pr-O-Pr bond angle is 136.4(5)°. The Pr-O-Sb bond angles are falls in the range of 103.12(8)° to 109.1(4)°.

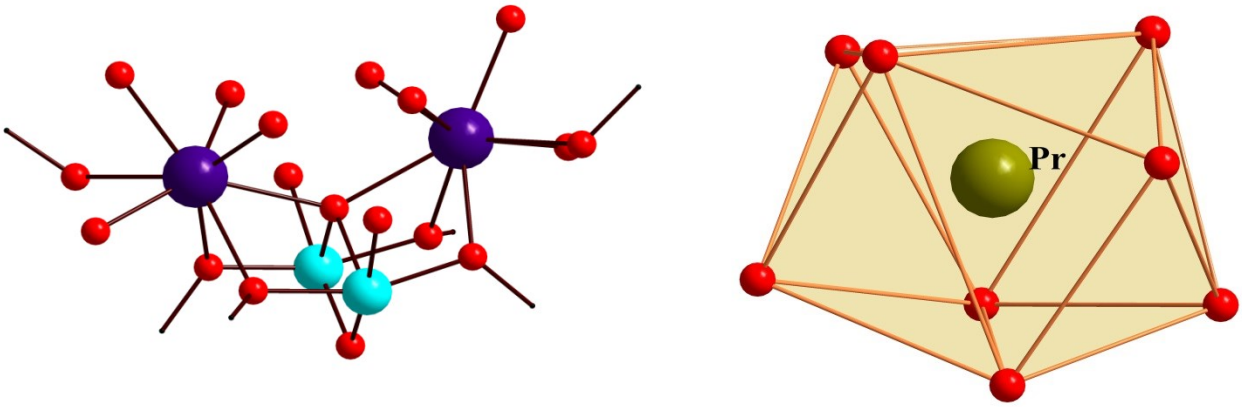

Figure 5.2: (Left) tetramer boat-shape core [Pr_2Sb_2] structure of **5.1** and (Right) Coordination geometry around Pr. Color code; Blue: Pr, Cyan: Sb, Red: O.

Compound **5.2** crystallizes in tetragonal chiral space group P41212. Crystallographic data and bond metric parameters of **5.2** are given in the table 5.4 & 5.5. The overall molecular structures of **5.2** are very similar to **5.1**. Each Sb center is present in an octahedral geometry with the O_5SbC coordination mode. The Sb-O bond lengths involving μ_4-oxido, μ_2-hydroxo and μ_2-OCH_3 bridges are falls in the range of 2.035(8) Å, 1.967(8) Å and 1.996(9) to 2.007(9) Å respectively. The Sb-O bond lengths involving phosphonates are falls in the range of 2.006(10) Å which is comparable to literature reported phosphonate bond lengths like organotinphosphonate cage,[28] galliumphosphonate cage[29] and borophosphonate cage.[30] The Sb-O-Sb bond angles fall in the range of 98.1(5) to 102.7(6) °. Each Gd metal center is in eight-coordinate, bound to one μ_4-oxido bridge, four phosphonate oxygens and three oxygens from methoxy group (in which two are bridged and one is terminal). By using SHAPE 2.1 systematic calculations we can conclude the coordination geometries around the all eight-coordinated Gd(III) ions in **5.2**, exhibit the closest similarity to triangular dodecahedron geometry. The Gd-O bond lengths involving μ_4-oxido, methoxy group and phosphonates are falls in the range of 2.563(5) Å, 2.422(11) to 2.60(2) Å and 2.285(11) to 2.353(10) Å respectively. The Gd-O-Gd bond angle is 136.4(5)°. The Gd-O-Sb bond angles are fall in the range of 103.06(9)° to 109.4(4)°.

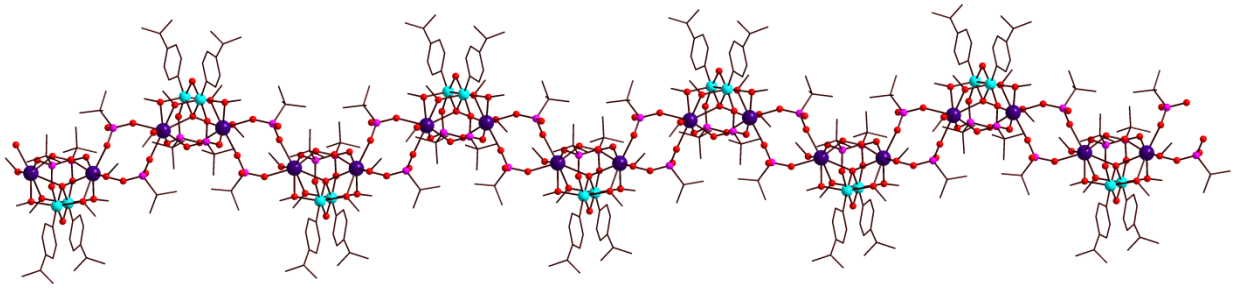

Figure 5.3: 1 D molecular structure of compounds **5.1**

The synthetic procedure for **5.3** is similar to **5.1**. Here change in lanthanide metal precursor from praseodymium acetate hydrate to dysprosium acetate hydrate the molecular structure topology of the resulting cluster changes from 1D coordination polymer to twenty four-membered ring-type architecture. Recently winpenny *et al* reported $\{Ln_{10}\}$ metal cages,[31] in which nine Dy metals atoms form a ring and six-coordinated Dy metal present in the ring center. To date, most of the literature reported metallo-rings have been obtained from the assembly of pure transition metals or lanthanide ions, such as $\{Mo_{176}\}$, $\{Mn_{84}\}$, $\{Ni_{34}\}$, $\{Fe_{18}\}$, $\{Ln_{15}\}$ and $\{Ln_{10}\}$ and so forth. In contrast to hetero metallic 3d-4f rings, the main group metal lanthanide rings are still underdeveloped. Herein we are first time reporting lanthanide metal $\{Dy_{12}\}$ ring-type architecture built with arylstibonic acid-phosphonate pro-ligand (**Figure 5.5**). Compound **5.3** crystallizes in monoclinic space group C2/c with half of the molecule present in the asymmetric unit. Crystallographic data and bond metric parameters of **5.3** are given in the table 5.4 & 5.6. The molecular structure of **5.3** contains twelve Dy metal atoms, twelve Sb atoms thirty-six *t*-butylphosphonates, six μ_3-hydroxo bridges and twenty-four methoxy groups (in which half are bridged and the remaining half are terminal), which combine form a novel $\{Dy_{12}Sb_{12}P_{36}\}$ ring-type architecture (**Figure 5.5**). The ring-type architecture consists of six tetramer units $[Dy_2Sb_2]$. Interestingly rare di *t*-butylphosphonate ligand system $\{(t\text{-}Bu)_2P_2O_5\}$ (**Figure 5.6**) is generated *in situ* by self-condensation of two *t*-butyl phosphonates. This ligand system bridges two tetramer units and placing important role in the formation of ring-type architecture. To the best of our knowledge, this is the first report on self-condensation of arylstibonic acid-phosphonates to stabilize lanthanide molecular cluster assembly. In the tetramer unit surprisingly *in situ* generated Sb_2DyO triangle is present, in which two arylstibonic acid moieties self-condensed through μ_3-hydroxo bridge and further chelate to eight-coordinate Dy atom. The Sb-O-Sb edge is capped by *t*-butyl phosphonate oxygens in 2.110 coordination mode. This triangle is further connected to a six-coordinate Dy atom through *t*-butyl phosphonate oxygens in 3.111 coordination mode. Two types of Dy atoms are present in the structure, first type is eight-coordinate Dy bound to one μ_3-hydroxo bridge, four phosphonate oxygens and three oxygens from the methoxy group (in which two are bridged and one is free). The second type is six-coordinate Dy, bound to one free methoxy group and five phosphonate oxygens. The Dy-O bond lengths involving μ_3-hydroxo, methoxy group and phosphonates falls in the range of 2.431(9) to 2.442(9) Å, 2.375(10) to 2.536(9) Å and 1.976(8) to 2.304(8) Å respectively. The Dy-O-Sb and Sb-O-Sb bond angles are

falls in the range of 106.5(4) to 110.1(4)° and 133.7(2) to 134.1(4)° respectively. Each Sb center is present in an octahedral geometry with the O_5SbC coordination mode. The Sb-O bond lengths involving μ_3-hydroxo, μ_2-methoxy bridges and phosphonates are falls in the range of 1.979(9) to 1.992(9) Å, 1.979(10) to 1.995(9) Å and 1.996(8) to 2.006(8) Å respectively. By using SHAPE 2.1 systematic calculations we can conclude the coordination geometries around the all eight-coordinated Dy(III) ions exhibit the closest similarity to square-antiprism geometry and six coordinated Dy(III) ions exhibit octahedral geometry (**Figure 5.4**).

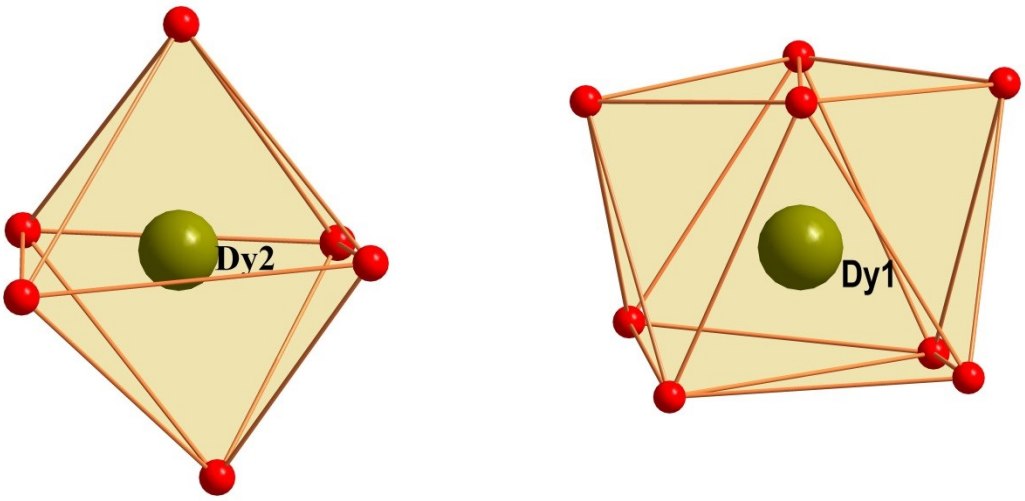

Figure 5.4: (Left) Geometry around six coordinate Dy2 and (Right) Geometry around eight coordinate Dy1.

To the best of our knowledge, these compounds **5.1** to **5.3** represent the first examples of coordination polymers and ring-type architecture of lanthanide ions built with antimonate-phosphonate pro-ligand. Compound **5.1** and **5.2** are 1D coordination polymers whose repeating unit possesses a tetramer motif. Interestingly compound **5.3** possess novel twenty-four membered ring-type architecture $\{Dy_{12}Sb_{12}P_{36}\}$, consist of twelve Dy(III) centers and twelve Sb(V) centers.

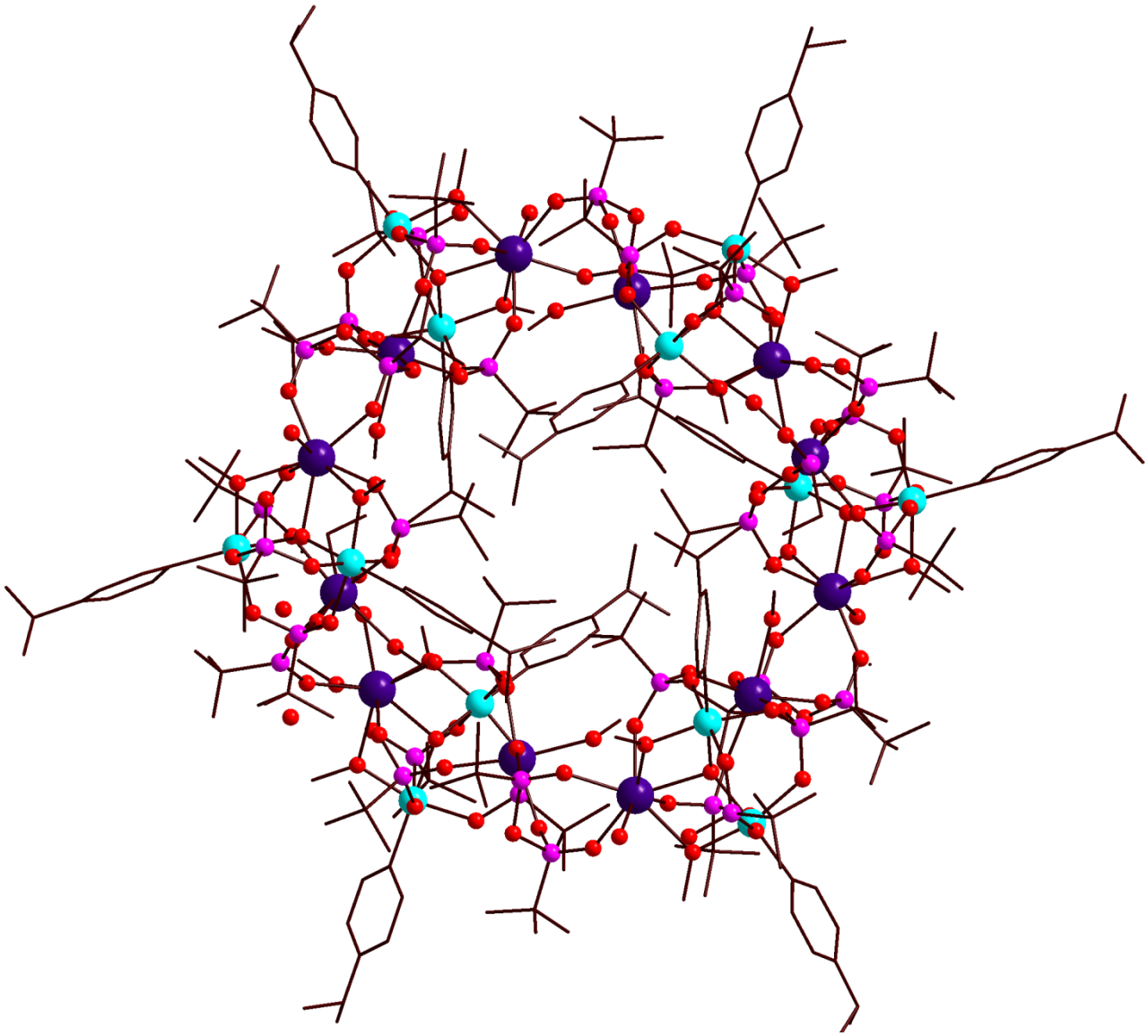

Figure.5.5: Molecular structure of **5.3**. H atoms are removed for clarity. Color code; Blue: Dy, Cyan: Sb, Pink: P, Red: O, Brown: C

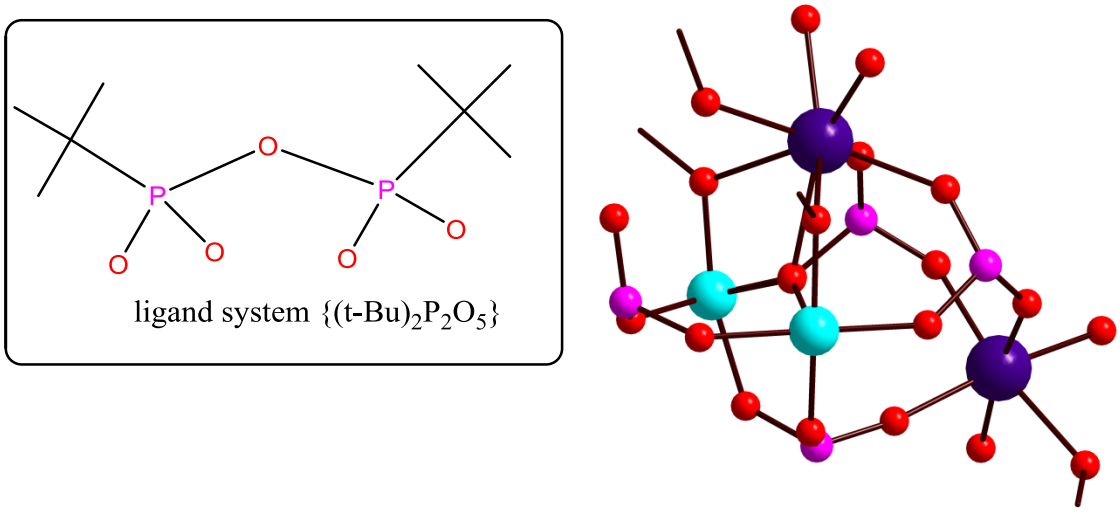

Figure 5.6: (Left) New $\{(t\text{-Bu})_2P_2O_5\}$ ligand system and (Right) Tetramer unit $[Dy_2Sb_2]$ structure. Color code; Blue: Dy, Cyan: Sb, Pink: P, Red: O

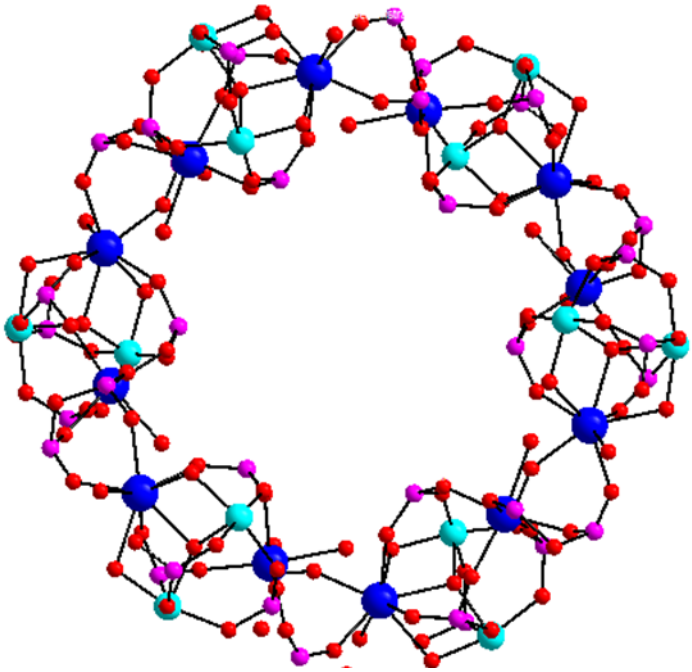

Figure 5.7: Core structure of **5.3**

5.4 Magnetic studies

Temperature-dependent magnetic susceptibility measurements for compounds **5.1** to **5.3** were performed in the temperature range of 300-1.8 K under an applied field of 1000 Oe (**Figure.5.8** to **5.10**). The observed $\chi_m T$ values at 300 K are 0.974, 7.88 and 16.13 cm^3 K mol^{-1} for **5.1**, **5.2**

and **5.3** respectively. Which are in good agreement with expected values for **5.1** and **5.2**. In case of **5.3** the value is slightly larger than the expected value for an isolated Dy(III) ions ($^6H_{15/2}$, S=5/2, L=5, J=15/2, g = 4/3 and C = 14.18 cm^3 K mol^{-1}). In the case of compound **5.1** the $\chi_m T$ value is constant up to 150 K below which it starts decreasing rapidly to a minimum value of 0.04 cm^3 K mol^{-1}. In case of **5.2** as temperature decreases the $\chi_m T$ value increases to 8.22 cm^3 K mol^{-1} up to 100 K, below which it starts decreasing and reaches a minimum value of 6.9 cm^3 K mol^{-1}. Lowering the temperature $\chi_m T$ value decreases steadily and reaches a minimum value of 11.04 cm^3 K mol^{-1} for **5.3**. The low-temperature decrease in $\chi_m T$ values in all the complexes may be attributed to crystal-field effects, intra and intermolecular antiferromagnetic interactions.

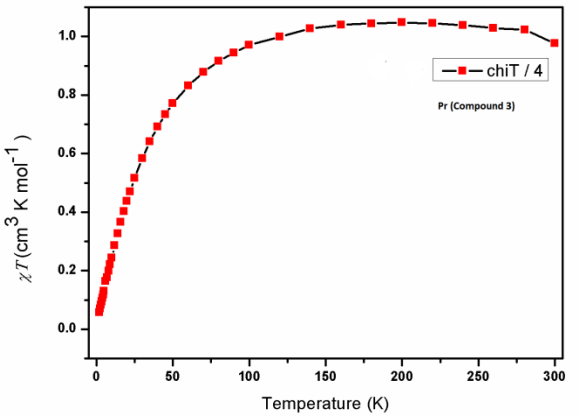

Figure 5.8: $\chi_m T$ vs T plot of compound **5.1**

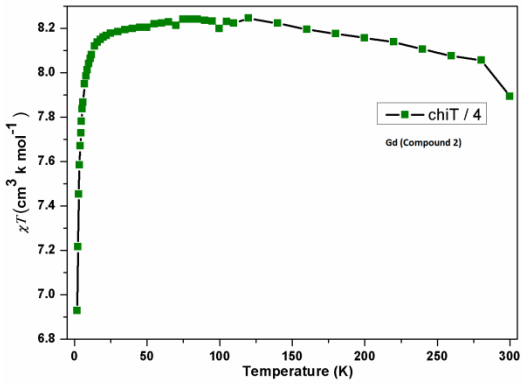

Figure 5.9: $\chi_m T$ vs T plot of compound **5.2**

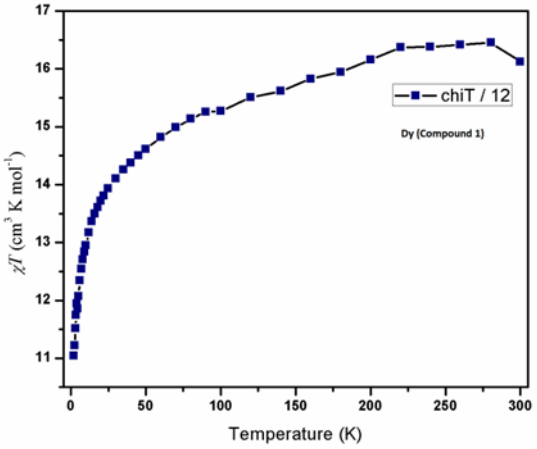

Figure 5.10: $\chi_m T$ vs T plot of compound **5.3**

The field dependence of magnetization plotted as *M vs H* is shown in **Figure5.11** & **5.12** from 0-7 T for **5.1 & 5.3** at low temperatures (1.8 K, 3 K, 5 K and 8 K). It shows that at low field the magnetization increases rapidly and reaches a value of 1.18 (**5.1**) and 77.8 (**5.3**) $N\mu_B$ at 7 T without clear saturation. The values are lower than the expected theoretical values in the case of compound **5.3**, suggesting the anisotropy associated with this complex.

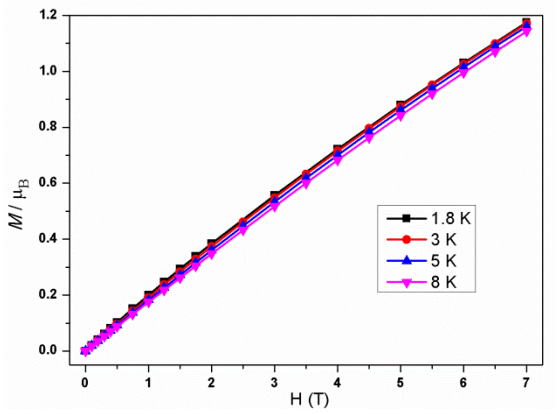

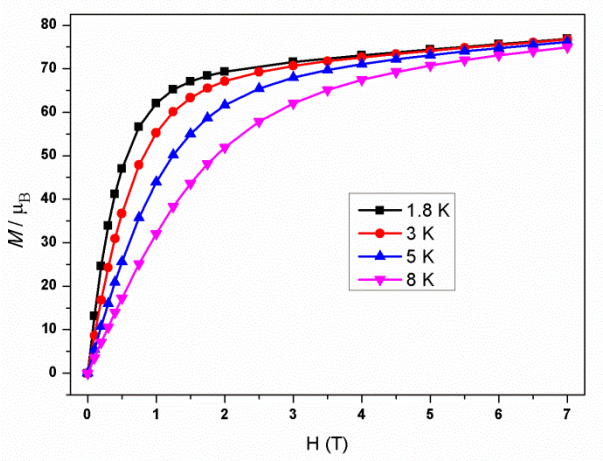

Fig.5.11: Magnetization vs field plot of **5.1** **Fig.5.12**: Magnetization vs field plot of **5.3**

In order to understand the dynamic magnetic behavior of complex **5.3**, ac-susceptibility measurements were performed. It doesn't show any sign of slow relaxation of magnetization under zero-field or under an applied field suggesting the absence of slow relaxation of magnetization

5.5 Conclusion

In summary, we have successfully synthesized and characterized the first examples of arylstibonic acid-lanthanide based metal molecular phosphonates by employing antimonate-phosphonate pro-ligand under solvothermal conditions. Compound **5.1** and **5.2** are 1D coordination polymers, while interestingly compound **5.3** possesses novel twenty-four membered ring-type architecture. Interestingly rare di *t*-butylphosphonate ligand system has been generated *in situ* by self-condensation of two *t*-butyl phosphonic acids which plays important role in the assembling of the macrocyclic cluster. Preliminary magnetic moment studies have been performed and the results are explained in detail.

Table 5.1: Summary of SHAPE calculations of compound **5.1** and **5.2**

S.No	Geometry	Cshm value for **Pr1**	Cshm value for **Gd1**
1	Octagon(D8h)	31.058	31.238
2	Hepatgonal pyramid(C7v)	23.941	24.191
3	Hexagonal bipyramid(D6h)	16.523	16.573
4	Cube(Oh)	10.941	10.836
5	Square antiprism(D4d)	3.084	3.256
6	**Triangular dodecahedron(D2d)**	**0.835**	**0.745**
7	Johnson gyrobifastigium J26 (D2d)	13.011	12.804
8	Johnson elongated triangular bipyramid J14(D3h)	27.626	27.850
9	Biaugmented trigonal prism J50(C2v)	2.431	2.469
10	Biaugmented trigonal prism(C2v)	2.069	2.273
11	Snub diphenoid J84 (D2d)	2.256	2.009
12	Triakis tetrahedron(Td)	11.475	11.264
13	Elongated trigonal bipyramid(D3h)	24.335	24.243

Table 5.2: Summary of SHAPE calculations of compound **5.3** (Dy1)

S.No	Geometry	Cshm value for **Dy1**
1	Octagon(D8h)	31.508
2	Hepatgonal pyramid(C7v)	22.506
3	Hexagonal bipyramid(D6h)	13.695
4	Cube(Oh)	8.898
5	**Square antiprism(D4d)**	**1.033**
6	Triangular dodecahedron(D2d)	2.527
7	Johnson gyrobifastigium J26 (D2d)	13.412
8	Johnson elongated triangular bipyramid J14(D3h)	27.940
9	Biaugmented trigonal prism J50(C2v)	2.718
10	Biaugmented trigonal prism(C2v)	2.018
11	Snub diphenoid J84 (D2d)	4.876
12	Triakis tetrahedron(Td)	9.576
13	Elongated trigonal bipyramid(D3h)	23.218

Table 5.3: Summary of SHAPE calculations of compound **5.3** (Dy2)

S.No	Geometry	Cshm values for **Dy2**
1	Hexagon(D6h)	31.716
2	Pentagonal pyramid(C5v)	25.162
3	**Octahedron(Oh)**	**0.799**
4	Trigonal prism(D3h)	11.499
5	Johnson pentagonal pyramid J2(C5v)	28.857

Table 5.4: Crystallographic tables of compounds **5.1-5.3**

	5.1	**5.2**	**5.3**
Formula	$C_{80}H_{152}O_{40}P_8Pr_4Sb_4$	$C_{80}H_{152}Gd_4O_{40}P_8Sb_4$	$C_{276}H_{528}Dy_{12}O_{134}P_{36}Sb_{12}$
F.wt g/mol^{-1}	3052.41	3117.77	10516.87
T, K	100(2)	100(2)	100(2)
Crystal system	Tetragonal	Tetragonal	Monoclinic
Space group	P 43 21 2	P 41 21 2	C 2/c
Crystal size mm^3			
a, Å	17.515(3)	17.4779(12)	38.8188(17)
b, Å	17.515(3)	17.4779(12)	26.4438(10)
c, Å	19.629(4)	19.326(3)	45.5554(19)
α, deg	90	90	90
β, deg	90	90	108.6010(10)
γ, deg	90	90	90
V, Å3	6022(2)	5903.7(11)	44321(3)
Z	2	2	4
D_{calcd} Mg/m3	1.683	1.754	1.576
μ, mm-1	2.646	3.295	2.914
F(000)	3024	3064	20800
Theta range, deg	1.558 to 26.628	1.571 to 26.425	2.216 to 27.545
Index ranges	-21<=h<=21 -22<=k<=22 -24<=l<=24	-21<=h<=21 -21<=k<=21 -24<=l<=24	-49<=h<=47 -31<=k<=34 -59<=l<=59
Total reflns	64491	63541	216259
Ind. reflns / R(int)	6268/ 0.0972	6075/ 0.0977	49813/0.2163
Data/restraints/parameters	6268 / 3 / 283	6075 / 4 / 296	49813 / 37 / 1978
Completeness to θ_{max}, %	100	100	99.9
GooF(F2)	1.135	1.175	1.063
R_1/wR_2 [I>2σ(I)]	0.0578/ 0.1462	0.0635/ 0.1360	0.0859/ 0.1580
R_1/wR_2 [all data]	0.0674/ 0.1519	0.0701/ 0.1391	0.2269/0.2068
Largest diff peak/hole, e.Å-3	2.396/ -1.603	1.737/ -1.066	2.028/ -2.385

Table 5.5: Bond lengths and Bond angles of compound **5.1** and **5.2**

5.1		**5.2**	
Sb(1)-O(1)#1	2.018(9)	Gd(01)-O(1)	2.507(9)
Sb(1)-O(2)	1.973(8)	Gd(01)-O(2)	2.563(5)
Sb(1)-O(3)	2.035(8)	Gd(01)-O(3)	2.333(10)
Sb(1)-O(4)	2.019(10)	Gd(01)-O(6)	2.422(11)
Sb(1)-O(5)	2.009(8)	Gd(01)-O(7)	2.285(11)
Pr(1)-O(1)	2.488(9)	Gd(01)-O(8)	2.353(10)
Pr(1)-O(3)	2.639(5)	Gd(01)-O(9)	2.301(10)
Pr(1)-O(5)	2.572(9)	Gd(01)-O(11)	2.60(2)
Pr(1)-O(6)	2.406(9)	Sb(1)-O(1)	2.007(9)
Pr(1)-O(7)	2.365(10)	Sb(1)-O(2)	2.035(8)
Pr(1)-O(8)#1	2.361(9)	Sb(1)-O(4)	2.006(10)
Pr(1)-O(9)	2.409(10)	Sb(1)-O(5)	1.967(8)
Pr(1)-O(11)	2.584(17)	Sb(1)-O(6)#1	1.996(9)
O(1)-Sb(1)#1	2.018(9)	O(2)-Sb(1)#1	2.035(8)
O(2)-Sb(1)#1	1.973(7)	O(2)-Gd(01)#1	2.563(5)
O(3)-Sb(1)#1	2.035(8)	O(5)-Sb(1)#1	1.967(8)
O(3)-Pr(1)#1	2.639(5)	O(6)-Sb(1)#1	1.996(9)
O(8)-Pr(1)#1	2.361(9)	Sb(1)-O(2)-Sb(1)#1	98.1(5)
Sb(1)#1-O(1)-Pr(1)	109.1(4)	Sb(1)-O(2)-Gd(01)	105.12(9)
Sb(1)#1-O(2)-Sb(1)	102.2(5)	Sb(1)#1-O(2)-Gd(01)	103.06(9)
Sb(1)#1-O(3)-Sb(1)	97.9(5)	Sb(1)-O(2)-Gd(01)#1	103.06(9)
Sb(1)#1-O(3)-Pr(1)	103.12(8)	Sb(1)#1-O(2)-Gd(01)#1	105.13(9)
Sb(1)-O(3)-Pr(1)	105.07(9)	Gd(01)-O(2)-Gd(01)#1	136.4(5)
Sb(1)#1-O(3)-Pr(1)#1	105.07(9)	Sb(1)#1-O(5)-Sb(1)	102.7(6)
Sb(1)-O(3)-Pr(1)#1	103.13(8)	Sb(1)-O(1)-Gd(01)	108.0(4)
Pr(1)-O(3)-Pr(1)#1	136.4(5)	Sb(1)#1-O(6)-Gd(01)	109.4(4)

Table 5.6: Bond lengths and Bond angles of compound **5.3**

5.3			
Dy(1)-O(12)	2.203(9)	Dy(6)-O(49)	2.304(8)
Dy(1)-O(14)	2.244(8)	Dy(6)-O(51)	2.304(8)
Dy(1)-O(19)	2.369(9)	Dy(6)-O(55)	2.432(10)
Dy(1)-O(62)#1	2.260(13)	Dy(6)-O(56)	2.469(8)
Dy(1)-O(64)#1	2.246(9)	Dy(6)-O(58)	2.386(13)
Dy(2)-O(1)	2.431(9)	Dy(6)-O(63)	2.277(10)
Dy(2)-O(5)	2.449(9)	Dy(6)-O(66)	2.477(10)
Dy(2)-O(9)	2.536(9)	Dy(6)-O(67)	2.278(14)
Dy(2)-O(13)	2.274(10)	Sb(1)-O(1)	1.984(9)
Dy(2)-O(15)	2.310(8)	Sb(1)-O(2)	2.003(9)
Dy(2)-O(16)	2.405(11)	Sb(1)-O(3)	1.999(9)
Dy(2)-O(17)	2.261(9)	Sb(1)-O(4)	1.988(8)
Dy(2)-O(18)	2.304(9)	Sb(1)-O(5)	1.995(9)
Dy(3)-O(21)	2.375(10)	Sb(2)-O(9)	1.979(10)
Dy(3)-O(22)	2.272(9)	Sb(2)-O(1)	1.990(8)
Dy(3)-O(23)	2.284(9)	Sb(2)-O(8)	1.998(9)
Dy(3)-O(24)	2.215(9)	Sb(2)-O(6)	2.002(9)
Dy(3)-O(25)	2.247(9)	Sb(2)-O(7)	2.008(9)
Dy(3)-O(26)	2.245(8)	Sb(3)-O(36)	1.988(9)
Dy(4)-O(41)	2.277(10)	Sb(3)-O(35)	1.992(9)
Dy(4)-O(32)	2.447(9)	Sb(3)-O(34)	1.996(8)
Dy(4)-O(33)	2.424(12)	Sb(3)-O(27)	2.006(8)
Dy(4)-O(35)	2.442(9)	Sb(3)-O(29)	2.006(8)
Dy(4)-O(36)	2.452(10)	Sb(4)-O(35)	1.976(8)
Dy(4)-O(37)	2.305(8)	Sb(4)-O(32)	1.982(10)
Dy(4)-O(38)	2.278(10)	Sb(4)-O(30)	2.007(10)
Dy(4)-O(40)	2.281(9)	Sb(4)-O(39)	2.002(9)
Dy(5)-O(43)	2.247(10)	Sb(4)-O(28)	2.019(9)
Dy(5)-O(44)	2.277(10)	Sb(5)-O(55)	1.979(9)
Dy(5)-O(45)	2.230(9)	Sb(5)-O(66)	1.984(10)
Dy(5)-O(46)	2.252(8)	Sb(5)-O(52)	1.986(10)

Dy(5)-O(47)	2.372(9)	Sb(5)-O(50)	2.001(9)
Dy(5)-O(48)	2.195(9)	Sb(5)-O(60)	2.017(9)
Sb(6)-O(56)	1.979(10)	Sb(3)-O(35)-Dy(4)	108.4(3)
Sb(6)-O(55)	1.990(8)	Sb(5)-O(66)-Dy(6)	107.9(4)
Sb(6)-O(54)	1.998(8)	Sb(5)-O(55)-Sb(6)	133.7(5)
Sb(6)-O(53)	2.002(10)	Sb(5)-O(55)-Dy(6)	109.9(4)
Sb(6)-O(57)	2.021(9)	Sb(6)-O(55)-Dy(6)	108.4(4)
Sb(1)-O(1)-Sb(2)	134.1(4)		
Sb(1)-O(1)-Dy(2)	108.4(4)		
Sb(2)-O(1)-Dy(2)	110.1(4)		
Sb(1)-O(5)-Dy(2)	107.3(4)		
Sb(3)-O(36)-Dy(4)	108.2(4)		
Sb(2)-O(9)-Dy(2)	106.5(4)		
Sb(4)-O(35)-Sb(3)	134.0(5)		

5.6 Analytical and Spectroscopic data

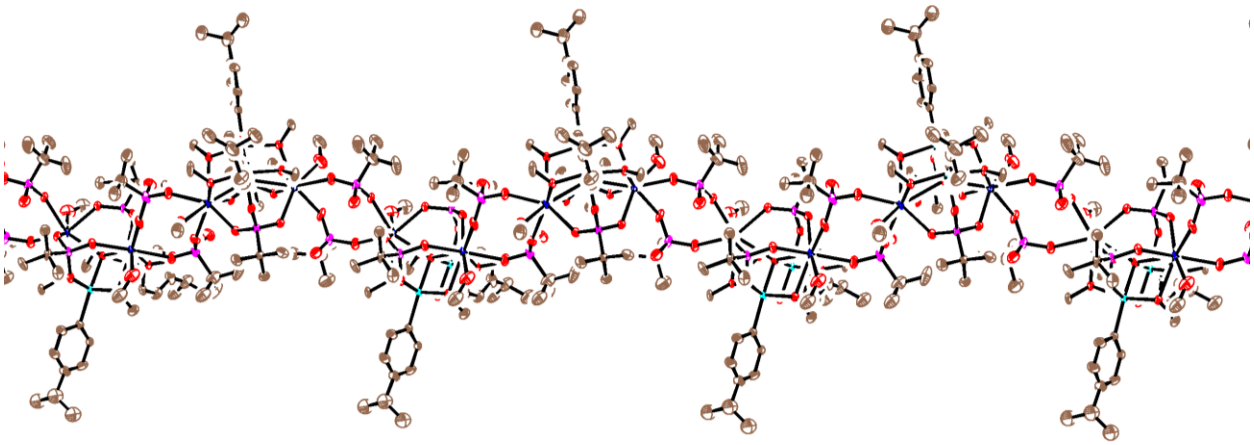

Figure S1: ORTEP view of **5.1** with thermal ellipsoids shown at 30% probability**.**

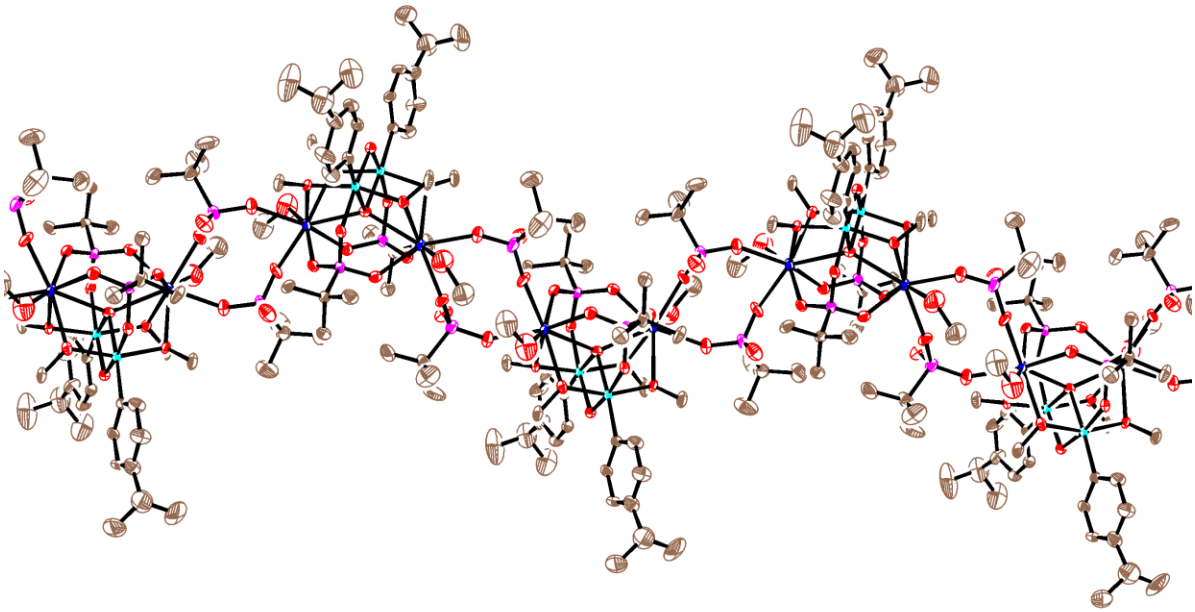

Figure S2: ORTEP view of **5.2** with thermal ellipsoids shown at 30% probability**.**

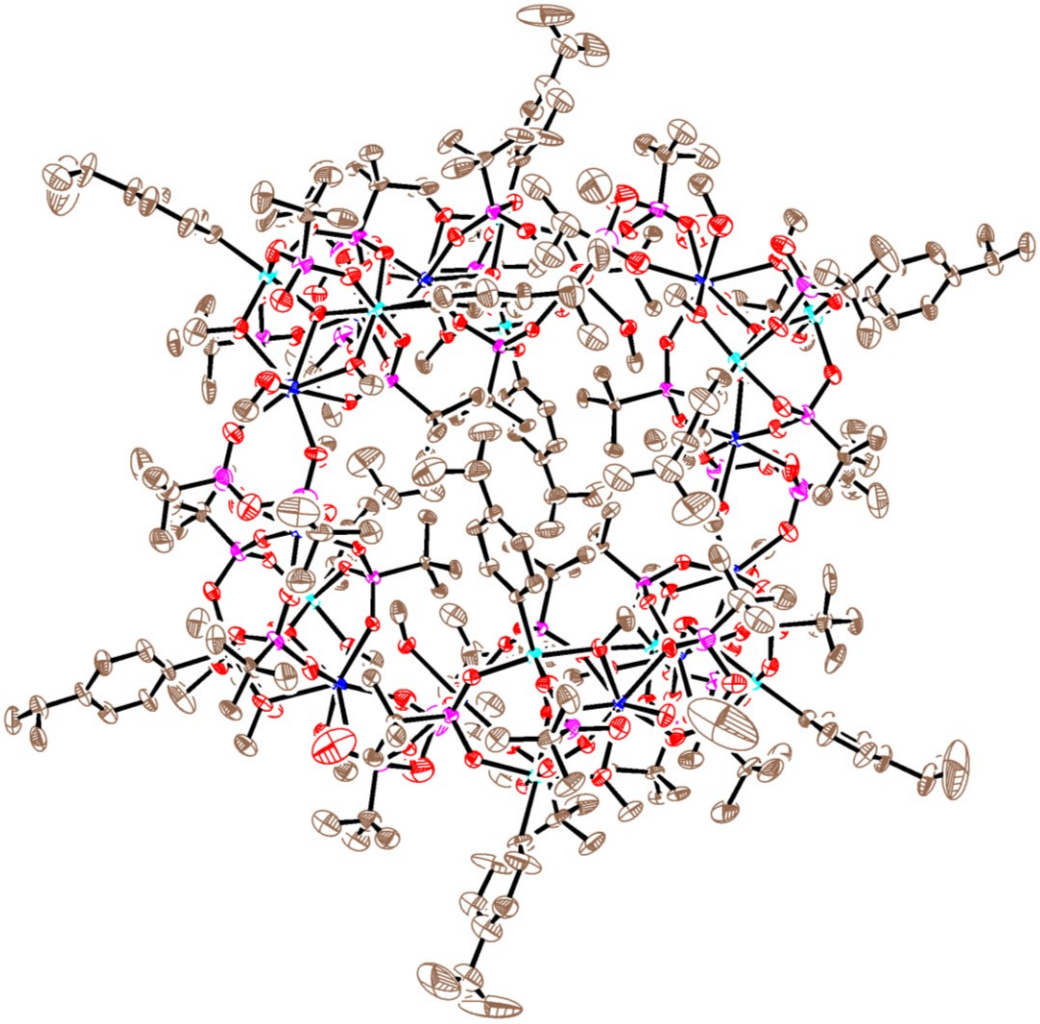

Figure S3: ORTEP view of **5.3** with thermal ellipsoids shown at 30% probability.

5.7 References

1. (a) A. Khan, Y. H. Lan, G. E. Kostakis, C. E. Ansona and A. K. Powell, *Dalton Trans*., 2012, **41**, 8333; (b) S. Schmidt, D. Prodius, G. Novitchi, V. Mereacre, G. E. Kostakisc and A. K. Powell, *Chem. Commun*., 2012, **48**, 9825; (c) V. Mereacre, Y. H. Lan, R. Clérac, A. M. Ako, W. Wernsdorfer, G. Buth, C. E. Anson and A. K. Powell, *Inorg. Chem*., 2011, **50**, 12001; (d) J. Rinck, G. Novitchi, W. V. D. Heuvel, L. Ungur, Y. H. Lan, W. Wernsdorfer, C. E. Anson, L. F. Chibotaru and A. K. Powell, *Angew. Chem., Int. Ed*., 2010, **49**, 7583.
2. P. Wang, J. P. Ma, Y. B. Dong and R. Q. Huang, *J. Am. Chem. Soc*., 2007, **129**, 10620.
3. (a) G. L. Zhuang, W. X. Chen, H. X. Zhao, X. J. Kong, L. S. Long, R. B. Huang and L. S. Zheng, *Inorg. Chem*., 2011, **50**, 3843; (b) G. L. Zhuang, Y. C. Jin, H. X. Zhao, X. J. Kong, L. S. Long, R. B. Huang and L. S. Zheng, *Dalton Trans*., 2010, **39**, 5077; (c) J. J. Zhang, S. M. Hu, S. C. Xiang, T. L. Sheng, X. T. Wu and Y. M. Li, *Inorg. Chem*., 2006, **45**, 7173.
4. (a) T. C. Stamatatos, K. A. Abboud, W. Wernsdorfer and G. Christou, *Angew. Chem., Int. Ed*., 2007, **46**, 884; (b) T. Liu, Y. J. Zhang, Z. M. Wang and S. Gao, *J. Am. Chem. Soc*., 2008, **130**, 10500; (c) D. Gatteschi and R. Sessoli, *Angew. Chem., Int. Ed*., 2003, **42**, 268.
5. (a) M. Romanelli, G. A. Kumar, T. J. Emge, R. E. Riman and J. G. Brennan, *Angew. Chem., Int. Ed*., 2008, **47**, 6049; (b) C. M. Zaleski, E. C. Depperman, J. W. Kampf, M. L. Kirk and V. L. Pecoraro, *Angew. Chem., Int. Ed*., 2004, **43**, 3912.
6. L.-F. Zou, L. Zhao, Y.-N. Guo, G.-M. Yu, Y. Guo, J. Tang and Y.-H. Li, *Chem. Commun*. 2011, **47**, 8659.
7. A. Mishra, A. J. Tasiopoulos, W. Wernsdorfer, K. A. Abboud and G. Christou, *Inorg. Chem*., 2007, **46**, 3105.
8. (a) V. Mereacre, A. M. Ako, R. Clérac, W. Wernsdorfer, I. J. Hewitt, C. E. Anson and A. K. Powell, *Chem.–Eur. J*., 2008, **14**, 3577; (b) Z. Majeed, K. C. Mondal, G. E. Kostakis, Y. H. Lan, C. E. Anson and A. K. Powell, *Dalton Trans*., 2010, **39**, 4740.
9. X. J. Kong, Y. P. Ren, W. X. Chen, L. S. Long, Z. Zheng, R. B. Huang and L. S. Zheng, *Angew. Chem., Int. Ed*., 2008, **47**, 2398.

10. X. Yang, D. Schipper, R. A. Jones, L. A. Lytwak, B. J. Holliday and S. Huang, *J. Am. Chem. Soc*., 2013, **135**, 8468.
11. J.-B. Peng, Q.-C. Zhang, X.-J. Kong, Y.-Z. Zheng, Y.-P. Ren, L.-S. Long, R.-B. Huang, L.-S. Zheng and Z. Zheng, *J. Am. Chem. Soc*., 2012, **134**, 3314.
12. J.-D. Leng, J.-L. Liu and M.-L.Tong, *Chem. Commun*. 2012, **48**, 5286.
13. Y.-Z. Zheng, M. Evangelisti, F. Tuna and R. E. P. Winpenny, *J. Am. Chem. Soc*., 2012, **134**, 1057.
14. (a) K. H. Zangana, E. M. Pineda and R. E. P. Winpenny, *Dalton Trans*., 2014, **43**, 17101; (b) K. H. Zangana, E. M. Pineda, J. Schnack and R. E. P. Winpenny, *Dalton Trans*., 2013, **42**, 14045; (c) K. H. Zangana, E. M. Pineda, E. J. L. McInnes, J. Schnack and R. E. P. Winpenny, *Chem. Commun*., 2014, **50**, 1438; (d) Y.-Z. Zheng, G.-J. Zhou, Z. Zheng and R. E. P. Winpenny, *Chem. Soc. Rev*., 2014, **43**, 1462–1475; (e) T. N. Hooper, J. Schnack, S. Piligkos, M. Evangelisti and E. K. Brechin, *Angew. Chem., Int. Ed*., 2012, **51**, 4633.
15. G. Cao, V. M. Lynch, J. S. Swinnea and T. E. Mallouk, *Inorg. Chem*., 1990, **29**, 2112.
16. (a) V. Baskar, K. Gopal, M. Helliwell, F. Tuna, W. Wernsdorfer and R. E. P. Winpenny, *Dalton Trans*., 2010, **39**, 4747; (b) Y.-Z. Zheng, M. Evangelisti and R. E. P. Winpenny, *Angew. Chem., Int. Ed*., 2011, **50**, 3692; (c) Y.-Z. Zheng, E. Moreno Pineda, M. Helliwell and R. E. P. Winpenny, *Chem.–Eur. J*., 2012, **18**, 4161; (d) Y.-Z. Zheng, M. Evangelisti, F. Tuna and R. E. P. Winpenny, *J. Am. Chem. Soc*., 2012, **134**, 1057; (e) E. M. Pineda, F. Tuna, R. G. Pritchard, A. C. Regan, Y.-Z. Zheng, R. E. P. Winpenny and E. J. L. Mclnnes, *Chem. Commun*., 2013, **49**, 3522; (f) Y.-Z. Zheng, M. Evangelisti and R. E. P. Winpenny, *Chem. Sci*., 2011, **2**, 99.
17. (a) Y. Fujiwara, M. Mitani, S. Yasuike, J. Kurita and T. Kaji, *J. Health Sci*., 2005, **51**, 333; (b) V. Rishi, W. J. Oh, S. L. Heyerdahl, J. Zhao, D. Scudiero, R. H. Shoemaker and C. Vinson, *J. Struct. Biol*., 2010, **170**, 216; (c) S. L. Heyerdahl, J. Rozenberg, L. Jamtgaard, V. Rishi, L. Varticovski, K. Akash, D. Scudiero, R. H. Shoemaker, T. S. Karpova, R. N. Day, J. D. McNally and C. Vinson, *Eur. J. Cell Biol*., 2010, **89**, 564.
18. (a) J. Beckmann, P. Finke, M. Hesse and B. Wettig, *Angew. Chem., Int. Ed*., 2008, **47**, 9982; (b) J. Brunig, E. Hupf, E. Lork, S. Mebs and J. Beckmann, *Dalton Trans*., 2015, **44**, 7105.

19. (a) C. J. Clark, B. K. Nicholson and C. E. Wright, *Chem. Commun*., 2009, 923; (b) B. K. Nicholson, C. J. Clark, C. E. Wright and T. Groutso, *Organometallics*, 2010, **29**, 6518; (c) B. K. Nicholson, C. J. Clark, C. E. Wright, S. G. Telfer and T. Groutso, *Organometallics*, 2011, **30**, 6612; (d) B. K. Nicholson, C. J. Clark, S. G. Telfer and T. Groutso, *Dalton Trans*., 2012, **41**, 9964; (e) B. K. Nicholson, C. J. Clark, G. B. Jameson and S. G. Telfer, *Inorg. Chim. Acta*, 2013, **406**, 53.
20. (a) M. S. R. Prabhu, A. K. Jami and V. Baskar, *Organometallics*, 2009, **28**, 3953; (b) A. K. Jami, M. S. R. Prabhu and V. Baskar, *Organometallics*, 2010, **29**, 1137; (c) A. K. Jami and V. Baskar, *Dalton Trans*., 2012, **41**, 12524; (d) U. Ugandhar and V. Baskar, *Dalton Trans.,* 2016, **45**, 6269; (e) M. S. R. Prabhu, U. Ugandhar and V. Baskar, *Dalton Trans*., 2016, **45**, 6963.
21. N. K. Srungavruksham and V. Baskar, *Dalton Trans*., 2015, **44**, 6358.
22. V. Baskar, M. Shanmugam, M. Helliwell, S. J. Teat and R. E. P. Winpenny, *J. Am. Chem. Soc*., 2007, **129**, 3042.
23. (a) S. Ali, V. Baskar, C. A. Muryn, and R. E. P. Winpenny, *Chem. Commun*., 2008, 6375; (b) S. Ali, C. A. Muryn, F. Tuna and R. E. P. Winpenny, *Dalton Trans*., 2010, **39**, 9588: (c) S. Ali, C. A. Muryn, F. Tuna and R. E. P. Winpenny, *Dalton Trans*., 2010, **39**, 124.
24. (a) H. Schmidt*, Liebigs Ann. Chem*., 1920, **421**, 174; (b) G. O. Doak and H. G. Steinman, *J. Am. Chem. Soc*., 1946, **68,** 1987; (c) G. O. Doak, *J. Am. Chem. Soc.,* 1946, **68**, 1991.
25. (a) R. Rüther, F. Huber and H. Preut, *Z. Anorg. Allg. Chem*., 1986, **539**, 110; (b) P. C. Croft and G. M. Kosolapoff, *J. Am. Chem. Soc*., 1953, **75**, 3379.
26. G. M. Sheldrick, SHELXS-97, Program for Crystal Structure Solution, University of Göttingen, Göttingen, Germany, 1997.
27. (a) G. M. Sheldrick, *Acta Crystallogr., Sec. A: Fundam. Crystallogr*., 2008, **64**, 112; (b) G. M. Sheldrick, *Acta Crystallogr., Sect. C: Cryst. Struct. Commun*., 2015, **71**, 3.
28. V. Chandrasekhar, V. Baskar, A. Steiner and S. Zacchini, *Organometallics*, 2002, **21**, 4528.
29. (a) M. G. Walawalkar, R. Murgavel, A. Voigt, H. W. Roesky and H. G. Schmidt, *J. Am. Chem. Soc*., 1997, **119**, 4656; (b) M. G. Walawalkar, R. Murgavel, H. W. Roesky, I. Uson and R. Kraetzner, *Inorg. Chem*., 1998, **37**, 473.

30. (a) M. G. Walawalkar, R. Murgavel, H. W. Roesky and H. G. Schmidt, *Organometallics*, 1997, **16**, 516; (b) M. G. Walawalkar, R. Murgavel, H. W. Roesky and H. G. Schmidt, *Inorg. Chem*., 1997, **36**, 4202.
31. K. H. Zangana, E. M. Pineda, E. J. L. Mclnnes, J. Schnackb and R. E. P. Winpenny, *Chem. Commun*., 2014, **50**, 1438.

Future Scope of the Thesis

In our lab we have been working on synthesis of organostibonic acids and their reactivity studies towards different ligand systems. Organostibonic acids are amorphous colorless solids mostly insoluble in organic solvents and their structural elucidation have been a challenge for researchers for a long time. We have synthesised a series of soluble stibonic acids and reported a number of their complex with different protic ligands. Few of them are discussed in the introduction part of the thesis. Since, solubility in organic solvents makes it easy to study the biological activities. In addition, there are already literature reports of biological activities of stibonic acids. Anticancer activities of arylstibonic acids and *in vitro* biological activities of these arylstibonic acids can be investigated and they have shown promising potential towards some specific cancer cell lines. The study can be further extended to the mechanistic pathways involved in their course of activity on biological systems. Moreover, these arylstibonic acids can be tested for other pathological conditions.

Arylstibonic acids partial condensation reactions with phosphonic acids lead to formation of tetranuclear organoantimony oxo clusters. This clusters acts as pro-ligands and easily coordinate with transition metal salts in the presence of base under solvothermal conditions. By employing this pro-ligand method we can easily synthesize titanium oxo clusters. These titanium oxo clusters are display interesting electrochemical properties and we can tune easily Ti-O band gap modifications in titanium oxo clusters.

By using similar synthetic strategy we plan to synthesize lanthanide metal clusters with mixed antimonate-phosphonate pro-ligand under hydrothermal conditions. In this way we are successfully synthesized first arylstibonic acid-lanthanides coordination polymers and ring type architecture. These Lanthanide antimonate phosphonate clusters shows weak magnetism and further antimonate-phosphonate pro-ligand can treated with different lanthanide metal ions resulting product may exhibit interesting physical properties.

List of Publications

[1] Monoorganoantimony Phosphonates and Phosphoselininates.
Uppara Ugandhar and V. Baskar, *Dalton Trans*., 2016, **45**, 6269.

[2] In situ generated polysiloxanes stabilizing μ_3-oxo bridged Sb_3 triangles.
M. S. R. Prabhu, **Uppara Ugandhar** and V. Baskar, *Dalton Trans*., 2016, **45**, 6963.

[3] Assembling Homometallic Sb_6 and Heterometallic Ti_4Sb_2 Oxo Clusters.
Uppara Ugandhar, T. Navaneetha, Junaid Ali, S. Mondal, G. Vaitheeswaran and V. Baskar, *Inorg. Chem*., 2020, **59**, 6689.

[4] Stibonate-Phosphonate Cluster Stabilizing Lanthanide ions (Ln = Pr, Gd & Dy).
Uppara Ugandhar, Floriana Tuna and V. Baskar (*Manuscript under preparation*).

Poster Presentations

[1] Presented Poster entitled "Organoantimony (V) Oxo clusters stabilized by Siloxides and Phosphonates" at **Chemfest-2015**, 12th Annual In-House Symposium, February-2015, University of Hyderabad.

[2] Presented Poster entitled "Polyoxostibonates and Titanates" at **Chemfest-2017**, 14th Annual In-House Symposium, February-2017, University of Hyderabad.

Organostibonates: Synthesis, Reactivity Studies and Investigating the Ligating Behavior of Organostibonate Pro-ligands towards Transition Metals and Lanthanides

by Uppara Ugandhar

Organostibonates: Synthesis, Reactivity Studies and Investigating the Ligating Behavior of Organostibonate Pro-ligands towards Transition Metals and Lanthanides

ORIGINALITY REPORT

27%	19%	25%	1%
SIMILARITY INDEX	INTERNET SOURCES	PUBLICATIONS	STUDENT PAPERS

PRIMARY SOURCES

1	pubs.rsc.org Internet Source	16%
2	Uppara Ugandhar, Tokala Navaneetha, Junaid Ali, Subrata Mondal, Ganapathy Vaitheeswaran, Viswanathan Baskar. " Assembling Homometallic Sb and Heterometallic Ti Sb Oxo Clusters ", Inorganic Chemistry, 2020 Publication	5%
3	Pilli V. V. N. Kishore, Viswanathan Baskar. "Hexa- and Trinuclear Organoantimony Oxo Clusters Stabilized by Organosilanols", Inorganic Chemistry, 2014 Publication	<1%
4	Ananda Kumar Jami, M. Santhana Raj Prabhu, Viswanathan Baskar. "Isolation of Tetranuclear Organoantimony Oxo Clusters and Hexa-decanuclear Polyoxostibonates", Organometallics, 2010 Publication	<1%

V. Baskar

V. BASKAR
Professor
School of Chemistry
University of Hyderabad
Hyderabad - 500 046.

V. Baskar

V. BASKAR
Professor
School of Chemistry
University of Hyderabad
Hyderabad - 500 046.

5	Peng Yang, Zhengguo Lin, Gabriela Alfaro-Espinoza, Matthias S. Ullrich, Ciprian I. Raţ, Cristian Silvestru, Ulrich Kortz. "19-Tungstodiarsenate(III) Functionalized by Organoantimony(III) Groups: Tuning the Structure–Bioactivity Relationship", Inorganic Chemistry, 2016 Publication	<1%
6	chemweb.com Internet Source	<1%
7	Uppara Ugandhar, Viswanathan Baskar. " Monoorganoantimony( ) phosphonates and phosphoselininates ", Dalton Trans., 2016 Publication	<1%
8	Min Hong, Han-Dong Yin, Wen-Kuan Li, Xi-Ying You. "Highly symmetrical 24-membered macrocyclic organoantimony(V) complexes constructed from Schiff base ligands possessing two terminal carboxyl groups", Inorganic Chemistry Communications, 2011 Publication	<1%
9	Brian K. Nicholson, Christopher J. Clark, Cody E. Wright, Tania Groutso. " Isopolyoxometalates of Antimony: Arylstibonic Acids [H (RSb) O] and Derived Dodecanuclear Polyoxostibonates [M H (RSb) O] , M = Na or K ", Organometallics, 2010	<1%

V. Baskar
V. BASKAR
Professor
School of Chemistry
University of Hyderabad
Hyderabad - 500 046.

	Publication	
10	www.jove.com Internet Source	<1%
11	Junaid Ali, Tokala Navaneetha, Viswanathan Baskar. "Bismuth and Titanium Phosphinates: Isolation of Tetra-, Hexa- and Octanuclear Clusters", Inorganic Chemistry, 2019 Publication	<1%
12	www.tandfonline.com Internet Source	<1%
13	"Organosilicon Chemistry Set", Wiley, 2005 Publication	<1%
14	publikationen.bibliothek.kit.edu Internet Source	<1%
15	Maria Barsukova-Stuckart, Luis F. Piedra-Garza, Bimersha Gautam, Gabriela Alfaro-Espinoza et al. "Synthesis and Biological Activity of Organoantimony(III)-Containing Heteropolytungstates", Inorganic Chemistry, 2012 Publication	<1%
16	Munendra Yadav, Abhishake Mondal, Valeriu Mereacre, Salil Kumar Jana, Annie K. Powell, Peter W. Roesky. "Tetranuclear and Pentanuclear Compounds of the Rare-Earth Metals: Synthesis and Magnetism", Inorganic	<1%

Chemistry, 2015
Publication

17 Ganglin Xue, Xuemei Liu, Haisheng Xu, Huaiming Hu, Feng Fu, Jiwu Wang. " An Unusual Asymmetric Polyoxomolybdate Containing Mixed-Valence Antimony and Its Derivatives: [Sb Sb Mo O (H O)] and {M(H O) [Sb Sb Mo O (H O)] } (M = Mn , Fe , Cu or Co) ", Inorganic Chemistry, 2008 <1%
Publication

18 Ananda Kumar Jami, Viswanathan Baskar. "Tetranuclear stiboxanes (RSb)4O6, exhibiting an adamantane-type structure", Dalton Transactions, 2012 <1%
Publication

19 Jens Beckmann, Malte Hesse. " Reactivity of the Dinuclear Arylstibonic Acid [2,6-Mes C H Sb(O)(OH)] toward H SO and NaOH ", Organometallics, 2009 <1%
Publication

20 Shu-Bin Zhao, Rui-Yao Wang, Suning Wang. "Intramolecular C−H Activation Directed Self-Assembly of an Organoplatinum(II) Molecular Square", Journal of the American Chemical Society, 2007 <1%
Publication

21 Das, Sourav, Atanu Dey, Sourav Biswas,

Enrique Colacio, and Vadapalli Chandrasekhar. "Hydroxide-Free Cubane-Shaped Tetranuclear [Ln4] Complexes", Inorganic Chemistry
Publication

<1%

---

22 Roxana Haase, Tanja Beschnitt, Ulrich Flörke, Sonja Herres-Pawlis. "Bidentate guanidine ligands with ethylene spacer in copper-dioxygen chemistry: Structural characterization of bis(μ-hydroxo) dicopper complexes", Inorganica Chimica Acta, 2011
Publication

<1%

---

23 Yang, Peng, Bassem S. Bassil, Zhengguo Lin, Ali Haider, Gabriela Alfaro-Espinoza, Matthias S. Ullrich, Cristian Silvestru, and Ulrich Kortz. "Organoantimony(III)-Containing Tungstoarsenates(III): From Controlled Assembly to Biological Activity", Chemistry - A European Journal, 2015.
Publication

<1%

---

24 Jose M. Seco, Itziar Oyarzabal, Sonia Pérez-Yáñez, Javier Cepeda, Antonio Rodríguez-Diéguez. "Designing Multifunctional 5-Cyanoisophthalate-Based Coordination Polymers as Single-Molecule Magnets, Adsorbents, and Luminescent Materials", Inorganic Chemistry, 2016
Publication

<1%

25	H.J Breunig. "Oxidation of tetraaryldistibanes: syntheses and crystal structures of diarylantimony oxides and peroxides, (R2Sb)2O, (R2Sb)4O6 and (R2SbO)4(O2)2 (R=Ph, o-Tol, p-Tol)", Journal of Organometallic Chemistry, 20020401 Publication	<1%
26	Joydeb Goura, Vadapalli Chandrasekhar. "Molecular Metal Phosphonates", Chemical Reviews, 2015 Publication	<1%
27	refubium.fu-berlin.de Internet Source	<1%
28	Tomasz Korzeniak, Dawid Pinkowicz, Wojciech Nitek, Maria Bałanda, Magdalena Fitta, Barbara Sieklucka. "The role of carboxylate ligands in two novel cyanido-bridged 2D coordination networks CuII–WV and MnII–NbIV", Dalton Transactions, 2011 Publication	<1%
29	Srungavruksham, Nagarjuna Kumar, and Viswanathan Baskar. "Assembling anionic Sb(v)/(iii) containing polyoxostibonates stabilized by triphenyltellurium cations", Dalton Transactions, 2014. Publication	<1%
	Kim, H.. "Arylstibonic acids: Novel inhibitors and	

30	activators of human topoisomerase IB", Bioorganic Chemistry, 200808 Publication	<1%
31	pubs.usgs.gov Internet Source	<1%
32	Yun-Shan Zhou, Li-Juan Zhang, Hoong-Kun Fun, Jing-Lin Zuo, Ibrahim Abdul Razak, Suchada Chantrapromma, Xiao-Zeng You. "Synthesis and structures of two novel one-dimensional mixed-valence iron molybdophosphate matrices", New Journal of Chemistry, 2001 Publication	<1%
33	Hong, M.. "Highly symmetrical 24-membered macrocyclic organoantimony(V) complexes constructed from Schiff base ligands possessing two terminal carboxyl groups", Inorganic Chemistry Communications, 201110 Publication	<1%
34	"Recent Development in Clusters of Rare Earths and Actinides: Chemistry and Materials", Springer Science and Business Media LLC, 2017 Publication	<1%
35	Submitted to Higher Education Commission Pakistan Student Paper	<1%

36	Zhu, Jing, Changzheng Wang, Fang Luan, Tianqi Liu, Pengfei Yan, and Guangming Li. "Local Coordination Geometry Perturbed β-Diketone Dysprosium Single-Ion Magnets", Inorganic Chemistry Publication	<1%
37	rd.springer.com Internet Source	<1%
38	Olajuyigbe A. Adebayo, Khalil A. Abboud, George Christou. " Mn Single-Molecule Magnets and Mn /Mn Clusters from the Use of Methyl 2-Pyridyl Ketone Oxime in Manganese Phosphinate and Phosphonate Chemistry ", Inorganic Chemistry, 2017 Publication	<1%
39	open.library.ubc.ca Internet Source	<1%
40	Submitted to University of Hyderabad, Hyderabad Student Paper	<1%
41	Santhana Raj Prabhu, M., Uppara Ugandhar, and Viswanathan Baskar. "In situ generated polysiloxanes stabilizing μ3-oxo bridged Sb3 triangles", Dalton Transactions, 2016. Publication	<1%

V. Baskar

V. BASKAR
Professor
School of Chemistry
University of Hyderabad
Hyderabad - 500 046.